

**Mechanisms of resistance for human respiratory
syncytial virus isolates against anti-fusion agents
in tissue culture**

Wanwarang Hiriote

**Thesis submitted to the University of Newcastle upon Tyne
for the degree of Doctor of Philosophy**

November 2012

Declaration

This thesis contains no material which has been accepted for any other degree in any university. Unless otherwise stated, all of the work presented was performed by me at the University of Newcastle upon Tyne under the supervision of Prof G. L. Toms.

Wanwarang Hiriote

Abstract

Human respiratory syncytial viruses (hRSV) are a major cause of lower respiratory tract disease on primary infection of infants and children. There is no effective vaccine against the virus, but high risk infants can be protected by administration of palivizumab (PZ), a humanised anti-fusion glycoprotein. In previous studies, hRSV isolated from the naso-pharyngeal secretions of infected infants were found to be dominated by slow growing variants which were largely refractory to neutralization by PZ. On further passage in tissue culture, the slow growing variants were replaced by fast growing, neutralization susceptible variants.

The aim of this study was to investigate the mechanism of neutralization phenotype shift between slow-growing neutralization resistant and fast-growing neutralization susceptible clones. Neutralization resistance was found to be cell-line dependent with cell lines varying in their permissiveness to antibody treated virus. Antibody resistant and susceptible viruses showed no differences in the amount of the membrane expressed F glycoprotein or post-translational processing of the F polypeptide. They were also equally susceptible to inhibition by clathrin endocytosis inhibitors (monodansylcadaverine and chlorpromazine) suggesting that endocytosis was required for entry of both. They were further tested for susceptibility to anti-fusion inhibitors. These included a peptide derived from the F glycoprotein heptad repeat 2 and two small molecular weight compounds BMS-433771 and BTA9881. It was found that all three compounds failed to inhibit slow growing PZ resistant virus clones in parallel with PZ, but efficiently blocked fast growing PZ susceptible virus clones. These studies suggest that differences in antibody susceptibility stem from differences in the mechanism of fusion for the two virus clones.

The full genomes of virus clones with resistant and susceptible phenotypes were sequenced to identify mutations which correlate with the difference in antibody susceptibility. The two clones differed at four sites in the SH, G, F and L genes. These mutations were sought in a number of virus clones expressing a range of susceptibility to antibody neutralization. No single mutation was associated with the shift from neutralization resistant to susceptible phenotype in all clones. However, a mutation at

nucleotide 6162 in the L gene was associated with the shift from resistance to susceptibility in one virus lineage.

Acknowledgements

Firstly, I would like to express my heartfelt gratitude to my supervisor, Professor Geoffrey Toms, who provided me invaluable guidance, encouragement and support throughout my study. Thank you for providing me the opportunity to complete my PhD degree and being patient and understanding.

I am very grateful to Fiona Fenwick for her help and invaluable advice on cell culture, virus isolation, neutralization, Western blotting and iodixanol gradient. Also, thank you for helping me improve my English and taking care of me.

Thank you to my co-supervisor, Dr Debbie Bevitt, for her advice in molecular biology and her support. Thank you to my assessors, Professor Andrew Fisher and Professor Colin Harwood, for their encouragement and support during my assessments.

I would especially like to thank all of my colleagues, Cheng Siang, Alison, Sarah, Siti, David, Simon, Dan and Sorren for their friendship and support. Thank you for making my study time very enjoyable.

I am very grateful to the Faculty of Medicine, Thammasat University for the financial support and the opportunity to study in the UK.

Finally, I would like to say thank you to my family and all my friends for your support and words of encouragement. A big thanks to my husband, Sayamchai, for giving me all the support throughout my study and helping me get through some tough times.

List of abbreviations

µm	micron
3D	three-dimensional
5-FU	5-fluorouracil
6HB	six-helix bundles
A	adenine
A	alanine
Aa	amino acid
AAP	American academy of pediatrics
ALRI	acute lower respiratory infection
AMPV	avian metapneumovirus
ANOVA	analysis of variance
AP	adaptor protein
APS	ammonium persulphate
ATCC	American type culture collection
b/hPIV3	bovine/human parainfluenza type 3
BAL	bronchoalveolar lavage
BB	albumin binding
BPD	bronchopulmonary dysplasia
bPIV3	bovine parainfluenza virus type 3
bRSV	bovine respiratory syncytial virus

BSA	bovine serum albumin
C-	carboxyl-
C	cysteine
C	cytosine
Ca	calcium
CARD	caspase activation and recruitment domain
CBP	CREB – binding protein
CC ₅₀	50% cytotoxic concentration
CCA	chimpanzee coryza agent
cDNA	complementary deoxyribonucleic acid
CDRs	complementary determining regions
CHD	congenital heart disease
CLD	chronic lung disease of prematurity
cm ³	cubic centimetre
CO ₂	carbon dioxide
CP	chlorpromazine
<i>cp</i>	cold passage
CPE	cytopathic effect
CREB	cAMP response element-binding
Crm1	chromosome maintenance region 1
CRS	Cambridge reference sequence
CS	chondroitin sulphate

CT	cytoplasmic tail
CTL	cytotoxic T cell
D	aspartic acid
dATP	deoxyadenosine triphosphate
DCs	dendritic cells
dCTP	deoxycytidine triphosphate
DENV	dengue virus
DEPC	diethyl pyrocarbonate
dGTP	deoxyguanosine triphosphate
DMSO	dimethyl sulfoxide
DNA	deoxyribonucleic acid
dNTP	deoxynucleotide triphosphate
dsRNA	double-stranded RNA
dUTP	deoxyuridine triphosphate
E	glutamic acid
EC ₅₀	50% effective concentration
ECL	enhanced chemiluminescence
EDTA	ethylene-diamine-tetra-acetic acid
EGFR	epidermal growth factor receptor
ELISA	enzyme-linked immunosorbent assay
EM	electron microscope
EMEM	Eagle's minimum essential medium

EPS	electrophoresis power supply
EPS15	EGFR pathway substrate 15
ER	endoplasmic reticulum
F	fusion glycoprotein
F	phenylalanine
FCHO	FCH domain only protein
FcRn	neonatal Fc receptor
FCS	foetal calf serum
FDA	food and drug administration
FFU	focus forming unit
FI-RSV	formalin-inactivated hRSV vaccine
FITC	fluorescein isothiocyanate
Fkn	fractalkine
FMDV	foot-and-mouth disease virus
FP	fusion peptide
G	attachment glycoprotein
G	glycine
G	guanine
g	gram
GAG	glycosaminoglycan
GCRR	G cysteine-rich region
GE	gene end

GM	growth medium
GS	gene start
GTP	guanosine-5'-triphosphate
H	histidine
H ₂ O ₂	hydrogen peroxide
H ₂ SO ₄	sulfuric acid
HA	hyaluronic acid
HA	hemagglutinin
HBD	heparin binding domain
HBSS	Hanks' balanced salt solution
HCl	hydrochloric acid
HIV-1	human immunodeficiency virus type 1
hMPV	human metapneumovirus
HN	hemagglutinin-neuraminidase
hPIV3	human parainfluenza type 3
HR	heptad-repeat
hr	hour
hRSV	human respiratory syncytial virus
HS	heparan sulphate
I	isoleucine
ICAM-1	intercellular adhesion molecule 1
IFN	interferon

Ig	immunoglobulin
IKK ϵ	TRAF3 – downstream I κ B kinase ϵ
IL	interleukin
IMP β 1	importin β 1
IRF	IFN regulatory factors
IVIG	intravenous immunoglobulin
K	lysine
KCl	potassium chloride
kDa	kilodalton
KH ₂ PO ₄	potassium phosphate
L	large polymerase protein
L	leucine
L	litre
lbs	pounds
Le	leader
LeC	leader complement
M	matrix protein
M	methionine
M	molar
mA	milliampere
MAb	monoclonal antibody
MAP1B	microtubule-associated protein 1B

MAVs	mitochondrial antiviral-signalling proteins
MBCD	methyl-beta-cyclodextrin
MDC	monodansylcadaverine
MgCl ₂	magnesium chloride
MgSO ₄	magnesium sulphate
min	minute
ml	millilitre
MM	maintenance medium
mm	millimetre
mM	millimolar
M-MuLV	moloney murine leukemia virus
mRNA	messenger ribonucleic acid
MZ	motavizumab
N-	amino-
N	asparagine
N	nucleocapsid protein
N/A	not applicable
NA	neuraminidase
Na ₂ CO ₃	sodium carbonate
Na ₂ HPO ₄	disodium hydrogen phosphate
NaCl	sodium chloride
NaHCO ₃	sodium hydrogen carbonate

NaOH	sodium hydroxide
NDV	Newcastle disease virus
NF- κ B	nuclear factor kappa-light-chain-enhancer of activated B cells
NK	natural killer
nm	nanometre
NPS	nasopharyngeal secretion
NS	non-structural protein
nt	nucleotide
OD	optical density
OPD	o-phenylenediamine dihydrochloride
ORF	open reading frame
oz	ounce
P	passage
P	phosphoprotein
P	proline
PAGE	polyacrylamide gel
PBMC	peripheral blood mononuclear cells
PBS	phosphate buffer saline
PBS/T	phosphate buffer saline/tween
PCR	polymerase chain reaction
pDCs	plasmacytoid dendritic cells
PEG	polyethylene glycol

PFP	purified F protein
PIV5	parainfluenza virus 5
PRRs	pattern recognition receptors
PtdIns(4,5)P ₂	phosphatidylinositol-4,5-bisphosphate
PVDF	polyvinylidene fluoride
PVM	pneumonia virus of mice
PZ	palivizumab
Q	glutamine
R	arginine
RACE	rapid amplification of cDNA ends
RANTES	regulated upon activation, normal T-cell expressed, and secreted
RIG-I	retinoic acid – inducible gene I
RNA	ribonucleic acid
RNAi	RNA interference
RNase	ribonuclease
RNP	ribonucleoprotein
rpm	revolutions per minute
RT-PCR	reverse transcription polymerase chain reaction
rVV	recombinant vaccinia virus
S	serine
SDS	sodium dodecyl sulphate
SH	small hydrophobic protein

siRNA	silencing RNA
<i>sp</i>	small plaque
SP	surfactant protein
ssRNA	single-stranded RNA
STAT2	signal transducer and activator of transcription 2
SV	simian virus
T	threonine
T	thymine
TBE	tris borate EDTA buffer
TCID	tissue culture infective dose
TEMED	tetramethylethylenediamine
Th	T helper
TLR	toll-like receptor
TM	transmembrane domain
TNF	tumor necrosis factor
Tr	trailer
TRAF3	TNF receptor-associated factor 3
TrC	trailer-complement
<i>ts</i>	temperature-sensitive
U	uracil
UTR	untranslated region
UV	ultraviolet

V	valine
V	volt
v/v	volume/volume
VLP	virus-like particle
W	tryptophan
w/v	weight/volume
Y	tyrosine

List of figures

Figure 1.1 Taxonomy of the <i>Mononegavirales</i> order	3
Figure 1.2: The structure of hRSV	4
Figure 1.3: Diagram of hRSV genome	5
Figure 1.4: Scheme of the primary structure of the G glycoprotein based on hRSV A2 strain.....	17
Figure 1.5: Model of the 3-D structure of the hRSV G protein.	18
Figure 1.6: Scheme of the primary structure of F glycoprotein based on hRSV long strain.....	21
Figure 1.7: Model of the 3-D structure of the hRSV F glycoprotein (A) and a full-length F rosette (B).	23
Figure 1.8 Diagram of endocytic pathways used by viruses.....	31
Figure 1.9 Model of membrane fusion process based on the HIV-1 gp41 protein.....	58
Figure 3.1: Schematic diagram for genomic RNA circularization procedure.	104
Figure 3.2: Schematic diagram for 5'RACE procedure from the hRSV anti-genome.	106
Figure 3.3: Schematic diagram for 3'RACE procedure from the hRSV anti-genome.	108
Figure 3.4: Schematic diagram for 3'RACE procedure from the hRSV genome.....	110
Figure 4.1: Immunofluorescent foci of A2 and R17532 clone R3.7.8.3 P3 in HeLa NCL cells at 1, 24, 48 and 72 hours at 100 x magnifications.	119
Figure 4.2: Immunofluorescent foci of A2 and R17532 clone R3.7.8.3 P3 in Vero cells at 1, 24, 48 and 72 hours at 100 x magnifications.	120
Figure 4.3: The percentage virus survival of R17532 clone R11.1.1 P10, clone R3.7.8.3 P3 and A2 after neutralization with PZ using the immunofluorescent focus reduction neutralization assay in Vero cells.....	121
Figure 4.4: The percentage virus survival of R17532 clones R11.1.1 P10 after neutralization with PZ using the immunofluorescent and the immunoperoxidase focus reduction neutralization assay in Vero cells.....	123
Figure 4.5: The percentage virus survival of R17532 clones R11.1.1 P11 and R3.7.8.3 P3 after neutralization with PZ using the immunoperoxidase focus reduction neutralization assay in Vero cells.....	125
Figure 4.6: The percentage virus survival of R17532 clones R11.1.1 P11 and R3.7.8.3 P3 after neutralization with PZ using the immunoperoxidase focus reduction neutralization assay in HeLa NCL79 cells.....	125

Figure 4.7 : Immunoperoxidase foci of R17532 clone R11.1.1 P11 in Vero (A) and HeLa NCL79 cells (B) and clone R3.7.8.3 P3 in Vero (C) and HeLa NCL79 cells (D) at 10x magnifications.	126
Figure 4.8: The percentage virus survival of R17532 clones R11.1.1 P3, P10 and P11 after neutralized by PZ.	127
Figure 4.9: The percentage virus survival of R17532 parental clone R3.7.8 and clones R3.7.8.3 passage 3 to passage 10 after neutralized by PZ in HeLa NCL79 cells.	128
Figure 4.10: Immunoperoxidase foci of R17532 clones R11.1.1 P11 and parental clone R3.7.8 in different HeLa cells at 10x magnifications.	130
Figure 4.11: The percentage virus survival of R17532 clones R11.1.1 P11 and R3.7.8 after neutralization with PZ in HeLa NCL79, JSF, CPV and Lucy cells.	131
Figure 4.12: The percentage virus survival of R17532 clones R11.1.1 P11 and R3.7.8.3 P3 after neutralization with PZ using the immunoperoxidase focus reduction neutralization assay in 16HBE140 cells.	133
Figure 4.13: Immunoperoxidase foci of R17532 clone R11.1.1 P11 (A) and parental clone R3.7.8 (B) in 16HBE140 cells at 10x magnifications.	133
Figure 5.1: The percentage of cell viability and CC ₅₀ of MDC (A) and CP (B).	136
Figure 5.2: The percentage virus survival of clones R11.1.1 P3 and parental clone R3.7.8 after treatment with MDC.	137
Figure 5.3: The percentage virus survival of clone R11.1.1 P3 and parental clone R3.7.8 after treatment with CP.	138
Figure 5.4: Western blot of the F glycoprotein in parental clone R3.7.8 P2 and clone R11.1.1 P3 infected cell lysates stained by the anti-F Mab 1E3.	139
Figure 5.5: Amounts of the F glycoprotein on the surface of cells infected with parental clone R3.7.8 and clone R11.1.1 P3.	140
Figure 5.6: The percentage virus survival of clone R11.1.1 P3 and parental clone R3.7.8 after treatment with R17532-HR2 peptide, BMS-433771, BTA9881 and PZ.	142
Figure 6.1: RT-PCR amplification of the M gene and P-M intergenic region of clones R11.1.1 P8 and R3.7.8.3 P3 using the M1: M2 primer pair.	145
Figure 6.2: RT-PCR amplification of the SH gene and M-SH intergenic region of clones R11.1.1 P8 and R3.7.8.3 P3 using the SH+: SH- primer pair.	146
Figure 6.3: Schematic diagram of primers for amplification and sequencing of the M gene and associated intergenic regions on hRSV antigenome.	147

Figure 6.4: RT-PCR amplification of the G gene and associated intergenic regions in the susceptible and resistant clones of R17532 using the SH292: F164 primer pair.....	150
Figure 6.5: Schematic diagram of primers for amplification and sequencing of the F gene, G gene and associated intergenic regions on hRSV antigenome.	151
Figure 6.6: RT-PCR amplification of the first fragments of the F gene in the susceptible and resistant clones of R17532 using the G886: F1000 primer pairs.	151
Figure 6.7: RT-PCR amplification of the second fragments of the F gene in the susceptible and resistant clones of R17532 using the A2R3: ALW2 primer pairs.	152
Figure 6.8: Lineage of different passage levels of hRSV strain R17532. Clones shown in red colour were used in this study.....	154
Figure 6.9: The percentage virus survival of R17532 (A) clone R2, (B) clone R3, (C) clone R5 and (D) clone R11 after neutralization with PZ in HeLa NCL79 cells.	155
Figure 7.1: Schematic diagram of primers for amplification and sequencing of the NS1, NS2, N genes and associated intergenic regions on hRSV antigenome.	164
Figure 7.2: RT-PCR amplification of the first fragment of the NS1, NS2 genes and associated intergenic regions of clones R11.1.1 P8 and R3.7.8.3 P3 using the NS1: NS2-468 primer pair.	164
Figure 7.3: Optimization of magnesium concentration for the amplification of the second fragment included the NS1 gene, NS2 gene, N gene and associated intergenic regions of R11.1.1 P8 using the NS1_442: N713 primer pair at annealing temperature 55°C.	165
Figure 7.4: Optimization of magnesium concentration for the amplification of the second fragment included the NS1 gene, NS2 gene, N gene and associated intergenic regions of R11.1.1 P8 using the NS1_442: N713 primer pair at annealing temperature 60 °C.	166
Figure 7.5: RT-PCR amplification of the second fragment included the NS1, NS2, N genes and associated intergenic regions of R11.1.1 P8 and R3.7.8.3 P3 using the NS1_442: N713 primer pair.	166
Figure 7.6: Schematic diagram of primers for amplification and sequencing of the NS2, N genes and associated intergenic regions on hRSV antigenome.	168
Figure 7.7: RT-PCR amplification of the N gene and associated intergenic regions of R11.1.1 P8 and R3.7.8.3 P3 using the NP1674: P162 primer pair.	168
Figure 7.8: Schematic diagram of primers for amplification and sequencing of the P gene and associated intergenic regions on hRSV antigenome.....	170

Figure 7.9: RT-PCR amplification of the P gene and associated intergenic regions of clones R11.1.1 P8 and R3.7.8.3 P3 using the P2128: P3459 primer pair.	170
Figure 7.10: Schematic diagram of primers for amplification and sequencing of the F-M2 intergenic region and the M2 gene on hRSV antigenome.	172
Figure 7.11: RT-PCR amplification of the F-M2 intergenic region and the M2 gene of clones R11.1.1 P8 and R3.7.8.3 P3 using the M2F: M2R primer pair.	172
Figure 7.12: Schematic diagram of primers for amplification and sequencing of the M2 and L genes on hRSV antigenome.	174
Figure 7.13: RT-PCR amplification of the LF1 fragments of clones R11.1.1 P8 and R3.7.8.3 P3 using the M2_848: L1307 primer pair.	175
Figure 7.14: RT-PCR amplification of the LF2 fragments of clones R11.1.1 P8 and R3.7.8.3 P3 using the L1116: L2337 primer pair.	176
Figure 7.15: RT-PCR amplification of the LF3 fragments of clones R11.1.1 P8 and R3.7.8.3 P3 using the L3-1: L3-2 primer pair.	176
Figure 7.16: RT-PCR amplification of the LF4 fragments of clones R11.1.1 P8 and R3.7.8.3 P3 using the L4-1: L4-2 primer pair.	177
Figure 7.17: RT-PCR amplification of the LF5.1 fragments of clones R11.1.1 P8 and R3.7.8.3 P3 using the L5-1: L5-3 primer pair.	177
Figure 7.18: RT-PCR amplification of the LF5.2 fragments of clones R11.1.1 P8 and R3.7.8.3 P3 using the L5-2: L5-4 primer pair.	178
Figure 7.19: Schematic diagram of primers for amplification and sequencing of the genomic RNA ligation.	180
Figure 7.20: First round PCR amplification of the genomic RNA ligation of clones R11.1.1 P8 using the Lend: NS1end primer pair.	180
Figure 7.21: Second round PCR amplification of the genomic RNA ligation of clones R11.1.1 P8 using the L5-8R: NS1-134 primer pair.	181
Figure 7.22: Second round PCR amplification of the genomic RNA ligation of clones R11.1.1 P8 using L5-2R: NS1-26 primer pair.	181
Figure 7.23: Sequence data of 5' and 3' termini of the R11.1.1 P8 genome.	182
Figure 7.24: The recovery rate and distribution of clone R11.1.1 P12 infectivity across continuous iodixanol density gradient 1 and 2.	183
Figure 7.25: The recovery rate and distribution of clone R3.7.8.3 P3 infectivity across continuous iodixanol density gradient 1 and 2.	184

Figure 7.26: The percentage virus survival of purified R11.1.1 P12 and R3.7.8.3 P3 after neutralization with PZ.....	185
Figure 7.27: First round PCR amplification of the genomic RNA ligation of purified R11.1.1 P12 using the Lend: NS1end primer pair.	186
Figure 7.28: First round PCR amplification of the genomic RNA ligation of purified R3.7.8.3 P3 using the Lend: NS1end primer pair.	186
Figure 7.29: Second round PCR amplification of the genomic RNA ligation of purified R11.1.1 P12 using the L5-2R: NS1-26 primer pair.	187
Figure 7.30: Second round PCR amplification of the genomic RNA ligation of purified R3.7.8.3 P3 using the L5-2R: NS1-26 primer pair.	187
Figure 7.31: Sequence data of 5'and 3' termini of purified R11.1.1 P12 genome.	188
Figure 7.32: Second round PCR amplification of the genomic RNA ligation of purified R11.1.1 P12 using the L5-2R: NS1.1 primer pair.....	189
Figure 7.33: Sequence data of 5'and 3' termini of purified R11.1.1 P12 genome using the L5-2R: NS1.1 primer pair. The red circle shows multiple peaks at the beginning of 3'end genome.....	189
Figure 7.34: First round PCR amplification of adaptor-ligated cDNA of purified R11.1.1 P12 using the L5-8R: DT89 primer pair.....	190
Figure 7.35: Hemi-nested second round PCR amplification of purified R11.1.1 P12 using the L5-2R: DT89 primer pair.	191
Figure 7.36: Optimization of magnesium concentration for the hemi-nested second round PCR amplification of purified R11.1.1 P12 using the L5-2R: DT89 primer pair.	191
Figure 7.37: Re-amplification of the hemi-nested second round PCR products of purified R11.1.1 P12 using the L5-2R: DT89 primer pair.....	192
Figure 7.38: First round PCR amplification of adaptor-ligated cDNA of clone R3.7.8.3 P3 using the L5-8R: DT89 primer pair.	192
Figure 7.39: Hemi-nested second round PCR amplification of clone R3.7.8.3 P3 using the L5-2R: DT89 primer pair.	193
Figure 7.40: Sequence data of 5'trailer region of clone R3.7.8.3 P3 genome ligated with the adaptor DT88.....	193
Figure 7.41: RT-PCR amplification of the L gene of R3.7.8.3 P3 using the L5-8R: L5-9 primer pair.....	194

Figure 7.42: First round PCR amplification of adaptor-ligated cDNA of parental clone R3.7.8 and clone R11.1.1 P11 using the NS1-206: modified DT89 primer pair.	195
Figure 7.43: Hemi-nested second round PCR amplification of parental clone R3.7.8 and clone R11.1.1 P11 using the NS1-103: modified DT89 primer pair.	196
Figure 7.44: Sequence data of the NS1 gene start of clone R11.1.1 P11 ligated with the adaptor DT88.	196
Figure 7.45: First round PCR amplification of adaptor-ligated genomic RNA of clone R11.1.1 P11 using the modified DT89: NS1-206 primer pair.	197
Figure 7.46: Hemi-nested second round PCR amplification of clone R11.1.1 P11 using the modified DT89: NS1-103 primer pair.	197
Figure 7.47: Re-amplification of the hemi-nested second round PCR of clone R11.1.1 P11 using the modified DT89: NS1-103 primer pair.	198
Figure 7.48: First round PCR amplification of adaptor-ligated genomic RNA of parental clone R3.7.8 using the modified DT89: NS1-206 primer pair.	199
Figure 7.49: Reamplification by hemi-nested second round PCR of parental clone R3.7.8 using the modified DT89: NS1-103 primer pair.	199
Figure 7.50: Sequence data of 3' leader region of parental clone R3.7.8 genome ligated with the adaptor DT88.	199
Figure 7.51: RT-PCR amplification of the L gene of clones R11.2 using the M2_848: L1307 primer pair.	201
Figure 7.52: RT-PCR amplification of the L gene in the susceptible and resistant clones of R17532 using the L5-4: L5-2 primer pair.	203
Figure 7.53: RT-PCR amplification of the L gene in the susceptible and resistant clones of R17532 using the L5-4: L5-2 primer pair.	204
Figure 7.54: Reamplification by nested PCR of R5.3 and R5.14 using the L5-7: L5-8 primer pair.	204
Figure 8.1: Model of the proposed actions of fusion inhibitors and anti-F MAbs in the process of rearrangement in the F glycoprotein.	218
Figure 10.1: Nucleotide sequence comparison of the P-M intergenic region (P-M IR) and 5'UTR of the neutralization resistant and susceptible clones of R17532 and A2 strain.	238
Figure 10.2: Comparison of nucleotide and deduced amino acid sequences of the M gene coding region of the neutralization resistant and susceptible clones of R17532 and A2 strain.	239

Figure 10.3: Nucleotide sequence comparison of the 3'UTR of the M gene of neutralization resistant and susceptible clones of R17532 and A2 strain.	240
Figure 10.4: Nucleotide sequence comparison of the M-SH intergenic region (M-SH IR) and 5'UTR of the neutralization resistant and susceptible clones of R17532 and A2 strain.....	240
Figure 10.5: Comparison of nucleotide and deduced amino acid sequences of the SH gene coding region of the neutralization resistant and susceptible clones of R17532 and A2 strain.	241
Figure 10.6: Nucleotide sequence comparison of the 3'UTR of the SH gene of neutralization resistant and susceptible clones of R17532 and A2 strain.	241
Figure 10.7: Nucleotide sequence comparison of the SH GE sequence, the SH-G intergenic region and 5'UTR of the neutralization resistant and susceptible clones of R17532 and A2 strain.	242
Figure 10.8: Comparison of nucleotide and deduced amino acid sequences of the G gene coding region of the neutralization resistant and susceptible clones of R17532 and A2 strain.	249
Figure 10.9: Nucleotide sequence comparison of the 3'UTR of the G gene and G-F intergenic region of the neutralization resistant and susceptible clones of R17532 and A2 strain.	250
Figure 10.10: Nucleotide sequence comparison of the SH-G intergenic region and 5'UTR of the neutralization resistant and susceptible clones of R17532 and A2 strain.	250
Figure 10.11: Comparison of nucleotide and deduced amino acid sequences of the F gene coding region of the neutralization resistant and susceptible clones of R17532 and A2 strain.	263
Figure 10.12: Nucleotide sequence comparison of the 3'UTR of the F gene of the neutralization resistant and susceptible clones of R17532 and A2 strain.	264
Figure 10.13: Comparison of nucleotide and deduced amino acid sequences of the NS1 gene coding region of the neutralization resistant and susceptible clones of R17532 and A2 strain.	265
Figure 10.14: Nucleotide sequence comparison of the 3'UTR of the NS1 gene of neutralization resistant and susceptible clones of R17532 and A2 strain.	265

Figure 10.15: Nucleotide sequence comparison of the NS1-NS2 intergenic region (NS1-NS2 IR) and 5'UTR of the neutralization resistant and susceptible clones of R17532 and A2 strain.	266
Figure 10.16: Comparison of nucleotide and deduced amino acid sequences of the NS2 gene coding region of the neutralization resistant and susceptible clones of R17532 and A2 strain.	267
Figure 10.17: Nucleotide sequence comparison of the 3'UTR of the NS2 gene of neutralization resistant and susceptible clones of R17532 and A2 strain.	267
Figure 10.18: Nucleotide sequence comparison of the NS2-N intergenic region (NS2-N IR) and 5'UTR of the neutralization resistant and susceptible clones of R17532 and A2 strain.	267
Figure 10.19: Comparison of nucleotide and deduced amino acid sequences of the N gene coding region of the neutralization resistant and susceptible clones of R17532 and A2 strain.	270
Figure 10.20: Nucleotide sequence comparison of the 3'UTR of the N gene and the N-P intergenic region (N-P IR) of neutralization resistant and susceptible clones of R17532 and A2 strain.	270
Figure 10.21: Nucleotide sequence comparison of 5'UTR of the neutralization resistant and susceptible clones of R17532 and A2 strain.	271
Figure 10.22: Comparison of nucleotide and deduced amino acid sequences of the P gene coding region of the neutralization resistant and susceptible clones of R17532 and A2 strain.	272
Figure 10.23: Nucleotide sequence comparison of the 3'UTR of the P gene of neutralization resistant and susceptible clones of R17532 and A2 strain.	273
Figure 10.24: Nucleotide sequence comparison of the F-M2 intergenic region (F-M2 IR) and 5'UTR of the neutralization resistant and susceptible clones of R17532 and A2 strain.	273
Figure 10.25: Comparison of nucleotide and deduced amino acid sequences of the M2 gene coding region of the neutralization resistant and susceptible clones of R17532 and A2 strain.	275
Figure 10.26: Nucleotide sequence comparison of the 3'UTR of the M2 gene and 5'UTR of the L gene of neutralization resistant and susceptible clones of R17532 and A2 strain.	276

Figure 10.27: Comparison of nucleotide and deduced amino acid sequences of the L gene coding region of the neutralization resistant and susceptible clones of R17532 and A2 strain.289

Figure 10.28: Nucleotide sequence comparison of the 3'UTR of the L gene of neutralization resistant and susceptible clones of R17532 and A2 strain.290

Figure 10.29: Nucleotide sequence comparison of the 5'trailer region of neutralization resistant and susceptible clones of R17532 and A2 strain.290

Figure 10.30: Nucleotide sequence comparison of the 3'leader region and 3'UTR of the NS1 gene of neutralization resistant and susceptible clones of R17532 and A2 strain.291

List of tables

Table 3.1: Sources and specificities of immunoreagents	76
Table 3.2: Sources of cell lines.	77
Table 3.3: Preparation of gradient medium for discontinuous iodixanol density gradient	94
Table 3.4: Preparation of gradient medium for continuous iodixanol density gradient..	94
Table 3.5: Sequences and sources of primers.	97
Table 3.6: Summary of RT- PCR and sequencing primers.....	101
Table 3.7: Summary of RT- PCR and sequencing primers for determination of the 5' and 3' terminal sequences.	103
Table 3.8: PCR Reaction for 5'RACE procedure.	107
Table 3.9: PCR condition for 3'RACE procedure from the hRSV anti-genome.....	109
Table 4.1: Neutralization titres of PZ against RSV viruses using the dilution endpoint neutralization test.	118
Table 4.2: The EC ₅₀ values of R17532 clones R11.1.1 P3, P10 and P11 and their p-values.....	127
Table 4.3: The EC ₅₀ values of R17532 parental clone R3.7.8 and clones R3.7.8.3 passage 3 to passage 10 in HeLa NCL79 cells and their p-values.....	128
Table 4.4: Infectivity titres of R17532 clone R11.1.1 P11 and parental clone R3.7.8 in different HeLa cells and their p-values.	129
Table 4.5: The PZ EC ₅₀ values of R17532 clones R11.1.1 P11 and R3.7.8 in different HeLa cells and their p-values compared between the two clones in the same cell lines.	132
Table 4.6: The PZ EC ₅₀ values of R17532 clones R11.1.1 P11 and R3.7.8 in different HeLa cells and their p-values compared each clone to EC ₅₀ values from HeLa NCL79.	132
Table 6.1: Percentage of nucleotide identity in the P-M intergenic region and the M gene of clone R17532 compared to the A2 strain.	147
Table 6.2: Percentage of nucleotide identity in the M-SH intergenic region and the SH gene of clone R17532 compared to the A2 strain.	148
Table 6.3: Percentage of nucleotide identity in the G gene of clone R17532 compared to the A2 strain.	157
Table 6.4: Summary of nucleotides changes of R17532 in the G gene.	157

Table 6.5: Summary of amino acid changes of R17532 in the G glycoprotein.	157
Table 6.6: Percentage of nucleotide identity in the F gene of clone R17532 compared to the A2 strain.	159
Table 6.7: Summary of nucleotides changes of R17532 in the F gene.....	159
Table 6.8: Summary of amino acid changes of R17532 in the F glycoprotein.....	159
Table 6.9: Summary of nucleotide changes of R17532 in the SH GE sequence, G and F genes.....	160
Table 7.1: Percentage of nucleotide identity in the NS1 gene, NS2 gene and associated intergenic regions of clone R17532 compared to the A2 strain.....	167
Table 7.2: Percentage of nucleotide identity in the N gene and associated intergenic regions of clone R17532 compared to the A2 strain.....	169
Table 7.3: Percentage of nucleotide identity in the N-P intergenic region and the P gene of clone R17532 compared to the A2 strain.....	171
Table 7.4: Percentage of nucleotide identity in the F-M2 intergenic region and the M2 gene of clone R17532 compared to the A2 strain.	173
Table 7.5: Percentage of nucleotide identity in the L coding sequence and 3'UTR of the L gene of clone R17532 compared to the A2 strain.....	179
Table 7.6: Summary of densities and viral titres of purified clones R11.1.1 P12 and R3.7.8.3 P3 in continuous iodixanol gradient 1 and 2.	185
Table 7.7: Percentage of nucleotide identity in the 3' leader region, 5'UTR of the NS1 gene and 5' trailer region of clone R17532 compared to the A2 strain.	200
Table 7.8: Summary of nucleotide and amino acid changes in the L gene at position 6162 of different clones of R17532 in the GLT lineage (A) and the AC lineage (B). .	205
Table 7.9: Summary of nucleotide and amino acid changes in the G, F and L genes of R17532 clones considering only the GLT passage arm of Figure 6.8.....	207
Table 7.10: Summary of nucleotide and amino acid changes in the G, F and L genes of R17532 clones considering only the AC passage arm of Figure 6.8	208
Table 8.1: Summary of percent nucleotide identity in all intergenic regions of R17532 and A2 strains.....	225
Table 8.2: Summary of percent nucleotide identity in the 5' untranslated regions (UTR) of all genes of R17532 and A2 strains.	226
Table 8.3: Summary of percent nucleotide identity in the 3' untranslated regions (UTR) of all genes of R17532 and A2 strains.	228

Table 8.4: Summary of percent nucleotide identity in the coding region of the NS1, NS2, N, P, M2 and L gene of R17532 and A2 strains.231

Table of contents

Declaration	ii
Abstract	iii
Acknowledgements	v
List of abbreviations.....	vi
List of figures	xvii
List of tables.....	xxvi
Table of contents	xxix
Chapter 1: Literature review	1
1.1 DISCOVERY.....	2
1.2 CLASSIFICATION AND MORPHOLOGY.....	2
1.3 THE HRSV GENOME	4
1.4 THE HRSV PROTEOME.....	5
1.4.1 <i>The nonstructural proteins 1 and 2</i>	5
1.4.2 <i>The nucleocapsid protein</i>	8
1.4.3 <i>The phosphoprotein</i>	9
1.4.4 <i>The large polymerase protein</i>	10
1.4.5 <i>The M2-1 protein</i>	11
1.4.6 <i>The M2-2 protein</i>	12
1.4.7 <i>The matrix protein</i>	13
1.4.8 <i>The small hydrophobic protein</i>	14
1.4.9 <i>The attachment glycoprotein</i>	15
1.4.10 <i>The fusion glycoprotein</i>	19
1.5 THE HRSV REPLICATIVE CYCLE.....	28
1.5.1 <i>hRSV binding</i>	28
1.5.2 <i>hRSV entry by endocytosis</i>	30
1.5.3 <i>hRSV membrane fusion</i>	34
1.5.4 <i>hRSV transcription</i>	35
1.5.5 <i>hRSV replication</i>	36
1.5.6 <i>hRSV assembly and release</i>	37
1.6 TRANSMISSION AND PATHOGENESIS OF HRSV INFECTION	38
1.7 CLINICAL FEATURES OF HRSV INFECTION	39
1.8 EPIDEMIOLOGY	40
1.8.1 <i>hRSV subgroups</i>	41
1.8.2 <i>hRSV genotypes</i>	42
1.9 IMMUNOLOGY.....	43
1.9.1 <i>Innate immunity</i>	43
1.9.2 <i>Adaptive immunity</i>	46

1.10 TREATMENT AND PREVENTION	52
1.10.1 Treatment.....	52
1.10.2 Vaccines.....	58
1.10.3 Passive immunization	65
Chapter 2: Background of project.....	70
2.1 INTRODUCTION	71
2.2 AIMS.....	73
Chapter 3: Materials and methods	75
3.1 GENERAL REAGENTS	76
3.2 IMMUNOREAGENTS	76
3.3 CELL CULTURES.....	76
3.3.1 Materials.....	76
3.3.2 Routine cell cultures	78
3.4 VIROLOGICAL METHODS	79
3.4.1 Virus stocks.....	79
3.4.2 Growth of hRSV in 4 oz flat glass bottles or 75 cm ³ culture flasks	79
3.4.3 Growth of hRSV in 225 cm ³ culture flasks	79
3.4.4 Biological cloning of hRSV isolates by plaque purification	80
3.4.5 Quantitation of hRSV titres using the fluorescent focus assay	81
3.4.6 Quantitation of hRSV titres using immunoperoxidase focus assay.....	83
3.4.7 Enzyme Linked Immunosorbent Assay (ELISA).....	84
3.4.8 Quantitation of hRSV by the dilution end point method	86
3.4.9 Dilution endpoint neutralization assay.....	86
3.4.10 Focus reduction neutralization assay	87
3.4.11 Focus inhibition assay for the endocytosis inhibitors.....	88
3.4.12 Focus inhibition assay for the antiviral agents directed against the F glycoprotein.....	90
3.4.13 Virus purification methods by iodixanol density gradients ultracentrifugation	92
3.5 DNA ANALYSIS METHODS	95
3.5.1 RNA extraction	95
3.5.2 Reverse transcription (RT).....	95
3.5.3 Polymerase Chain Reaction (PCR)	102
3.5.4 Genomic RNA circularization for determination of the 5' and 3' terminal sequences of the hRSV genome.....	102
3.5.5 5' Rapid amplification of cDNA ends (5'RACE) from the hRSV anti-genome	105
3.5.6 3'Rapid amplification of cDNA ends (3'RACE) from the hRSV anti- genome	107
3.5.7 3'Rapid amplification of cDNA ends (3'RACE) from the hRSV genome.....	109
3.5.8 Agarose gel electrophoresis.....	110
3.5.9 Direct nucleotide sequencing.....	111
3.6 PROTEIN ANALYSIS METHODS	112
3.6.1 SDS Polyacrylamide gel electrophoresis (SDS-PAGE).....	112
3.6.2 Western blotting.....	114

Chapter 4: Neutralization of susceptible and resistant clones of R17532 with palivizumab	116
4.1 PREPARATION OF VIRUS STOCKS	117
4.2 NEUTRALIZATION OF R17532 CLONES WITH PALIVIZUMAB USING DIFFERENT METHODS.....	117
4.2.1 <i>Dilution endpoint neutralization</i>	117
4.2.2 <i>Focus reduction neutralization assay using immunofluorescence staining</i>	118
4.2.3 <i>Focus reduction neutralization assay using immunoperoxidase staining</i>	121
4.3 VARIABILITY OF THE ASSAY	126
4.4 STABILITY OF NEUTRALIZATION PHENOTYPE IN SUSCEPTIBLE AND RESISTANT CLONES OF R17532	126
4.5 NEUTRALIZATION OF SUSCEPTIBLE AND RESISTANT CLONES OF R17532 IN DIFFERENT HELa CELLS	128
4.6 NEUTRALIZATION OF SUSCEPTIBLE AND RESISTANT CLONES OF R17532 IN A HUMAN BRONCHIAL EPITHELIAL CELL LINE	132
Chapter 5: Investigation of the entry mechanism of palivizumab neutralization susceptible and resistant clones of R17532.....	134
5.1 INTRODUCTION	135
5.2 VIRAL ENTRY OF NEUTRALIZATION SUSCEPTIBLE AND RESISTANT CLONES OF R17532 IN HELa NCL79 CELLS	136
5.2.1 <i>Toxicity studies of clathrin endocytosis inhibitors on HeLa NCL79 cells</i>	136
5.2.2 <i>Effect of clathrin endocytosis inhibitors on neutralization susceptible and resistant clones of R17532</i>	137
5.3 ANALYSIS OF F GLYCOPROTEIN POST-TRANSLATIONAL PROCESSING IN NEUTRALIZATION SUSCEPTIBLE AND RESISTANT CLONES OF R17532	138
5.4 COMPARISON OF THE AMOUNTS OF THE FUSION PROTEIN IN NEUTRALIZATION SUSCEPTIBLE AND RESISTANT CLONES OF R17532	139
5.5 EFFECT OF ANTIVIRAL AGENTS DIRECTED AGAINST THE F GLYCOPROTEIN ON NEUTRALIZATION SUSCEPTIBLE AND RESISTANT CLONES OF R17532	141
Chapter 6: Comparison of the membrane associated glycoprotein genes of resistant and susceptible clones of R17532.....	143
6.1 INTRODUCTION	144
6.2 AMPLIFICATION OF THE M GENE AND ASSOCIATED INTERGENIC REGIONS OF PALIVIZUMAB RESISTANT AND SUSCEPTIBLE CLONES OF R17532	144
6.3 AMPLIFICATION OF THE SH GENE AND ASSOCIATED INTERGENIC REGIONS OF NEUTRALIZATION SUSCEPTIBLE AND RESISTANT CLONES OF R17532	145
6.4 SEQUENCE COMPARISON OF THE M AND ASSOCIATED INTERGENIC REGIONS OF NEUTRALIZATION SUSCEPTIBLE AND RESISTANT CLONES OF R17532 AND A2 STRAIN.....	146
6.5 SEQUENCE COMPARISON OF THE SH GENES AND ASSOCIATED INTERGENIC REGIONS OF NEUTRALIZATION SUSCEPTIBLE AND RESISTANT CLONES OF R17532 AND A2 STRAIN	148

6.6	SEQUENCE COMPARISON OF THE G GENE, F GENE AND ASSOCIATED INTERGENIC REGIONS IN NEUTRALIZATION RESISTANT AND SUSCEPTIBLE CLONES OF STRAIN R17532	148
6.6.1	<i>Amplification of the G gene in neutralization resistant and susceptible clones of strain R17532.....</i>	<i>149</i>
6.6.2	<i>Amplification of the F gene in neutralization resistant and susceptible clones of strain R17532</i>	<i>150</i>
6.6.3	<i>Sequence comparison of the G gene, F gene and associated intergenic regions of neutralization resistant clones of R17532 and A2 strain.....</i>	<i>152</i>
6.7	SEQUENCE COMPARISON OF THE G GENE, F GENE AND ASSOCIATED INTERGENIC REGIONS IN DIFFERENT NEUTRALIZATION RESISTANT AND SUSCEPTIBLE CLONES OF R17532.....	152
6.7.1	<i>Neutralization of resistant and susceptible clones of R17532 at different passage levels.</i>	<i>153</i>
6.7.2	<i>Sequence comparison of the G gene and associated intergenic regions of resistant and susceptible clones of R17532 and A2 strain</i>	<i>155</i>
6.7.3	<i>Sequence comparison of the F genes and associated intergenic regions of resistant and susceptible clones of R17532 and A2 strain</i>	<i>158</i>
6.7.4	<i>Summary of nucleotide changes of resistant and susceptible clones of R17532 in the membrane associated protein genes</i>	<i>160</i>
Chapter 7: Comparison of the non-membrane protein genes of resistant and susceptible clones of R17532		162
7.1	INTRODUCTION	163
7.2	PREPARATION OF TOTAL RNA FROM INFECTED CELL LYSATES.....	163
7.3	AMPLIFICATION OF THE NS1, NS2, N GENES AND ASSOCIATED INTERGENIC REGIONS OF RESISTANT AND SUSCEPTIBLE CLONES OF R17532	163
7.4	SEQUENCE COMPARISON OF THE NS1, NS2, N GENES AND ASSOCIATED INTERGENIC REGIONS OF RESISTANT AND SUSCEPTIBLE CLONES OF R17532 AND A2 STRAIN.....	166
7.5	AMPLIFICATION OF THE N GENE AND ASSOCIATED INTERGENIC REGIONS OF RESISTANT AND SUSCEPTIBLE CLONES OF R17532.....	167
7.6	SEQUENCE COMPARISON OF THE N GENE AND ASSOCIATED INTERGENIC REGIONS OF RESISTANT AND SUSCEPTIBLE CLONES OF R17532 AND A2 STRAIN.....	168
7.7	AMPLIFICATION OF THE P GENE AND ASSOCIATED INTERGENIC REGIONS OF RESISTANT AND SUSCEPTIBLE CLONES OF R17532.....	169
7.8	SEQUENCE COMPARISON OF THE P GENE OF RESISTANT AND SUSCEPTIBLE CLONES OF R17532 AND A2 STRAIN	170
7.9	AMPLIFICATION OF THE M2 GENE AND ASSOCIATED INTERGENIC REGIONS OF RESISTANT AND SUSCEPTIBLE CLONES OF R17532.....	171
7.10	SEQUENCE COMPARISON OF THE F-M2 INTERGENIC REGION AND THE M2 GENE OF RESISTANT AND SUSCEPTIBLE CLONES OF R17532 AND A2 STRAIN	172
7.11	AMPLIFICATION OF THE L GENE OF RESISTANT AND SUSCEPTIBLE CLONES OF R17532.....	173
7.12	SEQUENCE COMPARISON OF THE L GENE OF RESISTANT AND SUSCEPTIBLE CLONES OF R17532 AND A2 STRAIN	178

7.13 AMPLIFICATION OF THE 3' LEADER, THE 5'UTR OF THE NS1 GENE AND 5' TRAILER REGIONS OF RESISTANT AND SUSCEPTIBLE CLONES OF R17532	179
7.13.1 <i>Genomic RNA circularization</i>	179
7.13.2 <i>Rapid amplification of cDNA ends (RACE)</i>	189
7.14 IDENTIFICATION OF THE L GENE MUTATION ON THE RESISTANT AND SUSCEPTIBLE CLONES OF DIFFERENT HIGH- AND LOW-PASSAGE OF R17532 CLONES	200
7.14.1 <i>Sequence analysis of the L gene at position 916 in clone R11.2</i>	201
7.14.2 <i>Sequence analysis of the L gene at position 6162 in different clones of R17532</i>	202
7.15 SUMMARY OF NUCLEOTIDE CHANGES OF RESISTANT AND SUSCEPTIBLE CLONES OF R17532 IN THE NON-MEMBRANE GENE REGIONS OF THE GENOME	205
7.16 OVERALL CONCLUSION FROM SEQUENCING DATA	206
Chapter 8: Discussion	209
8.1 NEUTRALIZATION OF LOW PASSAGE RESISTANT AND HIGH PASSAGE SUSCEPTIBLE VIRUSES IN DIFFERENT CELL LINES	210
8.2 NEUTRALIZATION SUSCEPTIBILITY OF LOW PASSAGE VIRUSES AFTER SERIAL PASSAGE IN CELL CULTURES	213
8.3 MECHANISM OF RESISTANCE	214
8.3.1 <i>Binding of neutralizing antibody to resistant and susceptible clones</i>	214
8.3.2 <i>Post-attachment stages of neutralization resistant and susceptible viruses</i>	215
8.4 COMPARISON OF NUCLEOTIDE AND DEDUCED AMINO ACID SEQUENCES OF M AND SH GENES BETWEEN NEUTRALIZATION RESISTANT AND SUSCEPTIBLE VIRUS CLONES.....	219
8.5 COMPARISON OF NUCLEOTIDE AND DEDUCED AMINO ACID SEQUENCES OF G AND F GENES BETWEEN NEUTRALIZATION RESISTANT AND SUSCEPTIBLE VIRUS CLONES.....	221
8.5.1 <i>Variability of the G gene in different clones</i>	221
8.5.2 <i>Variability of the F gene in different clones</i>	222
8.6 COMPARISON OF NUCLEOTIDE SEQUENCES OF ALL INTERGENIC REGIONS BETWEEN NEUTRALIZATION RESISTANT AND SUSCEPTIBLE VIRUS CLONES.....	223
8.7 COMPARISON OF NUCLEOTIDE SEQUENCES OF THE 5' UNTRANSLATED REGIONS (UTR) OF ALL GENES BETWEEN NEUTRALIZATION RESISTANT AND SUSCEPTIBLE VIRUS CLONES.....	226
8.8 COMPARISON OF NUCLEOTIDE SEQUENCES OF THE 3' UNTRANSLATED REGIONS (UTR) OF ALL GENES BETWEEN NEUTRALIZATION RESISTANT AND SUSCEPTIBLE VIRUS CLONES.....	227
8.9 COMPARISON OF NUCLEOTIDE SEQUENCES OF THE 3' LEADER AND 5' TRAILER REGIONS BETWEEN NEUTRALIZATION RESISTANT AND SUSCEPTIBLE VIRUS CLONES.....	229
8.10 COMPARISON OF NUCLEOTIDE AND DEDUCED AMINO ACID SEQUENCES OF NON- MEMBRANE PROTEIN GENES BETWEEN NEUTRALIZATION RESISTANT AND SUSCEPTIBLE VIRUS CLONES	230
Chapter 9: Conclusion and future work	234
Chapter 10:Appendix	237
Chapter 11:References	292

Chapter 1: Literature review

1.1 Discovery

Human respiratory syncytial virus (hRSV) was first discovered in chimpanzees with mild upper respiratory illness and initially named chimpanzee coryza agent (CCA virus). Antibody to the CCA virus was found in a person who had a respiratory infection and worked with infected chimpanzees. An increase of antibody was observed during convalescence (Morris *et al.*, 1956). Thereafter, two strains of a similar virus were recovered from the throat swabs of infants with bronchopneumonia (Long virus) and with laryngotracheobronchitis (Snyder virus). In cell cultures, both isolates produced a cytopathic effect forming a multinucleated mass of cytoplasm, a syncytium, similar to that observed with CCA virus. The antigenic properties of the two human isolates were also indistinguishable from CCA virus and not related to other syncytium – producing viruses or the adenoviruses (Chanock *et al.*, 1957). The three viruses were categorized together and renamed respiratory syncytial virus (Chanock and Finberg, 1957).

1.2 Classification and Morphology

hRSV is a member of the *Paramyxoviridae* family in the *Mononegavirales* order which also includes the *Bornaviridae*, *Filoviridae* and *Rhabdoviridae* (Figure 1.1). All members of the *Mononegavirales* contain linear, non-segmented, negative-strand RNA genomes. The family of *Paramyxoviridae* is divided into two subfamilies: *Paramyxovirinae* and *Pneumovirinae*. The subfamily *Pneumovirinae* is further classified into two genera, *Metapneumovirus* and *Pneumovirus*. The *Metapneumovirus* genus comprises avian metapneumovirus (AMPV) and human metapneumovirus (hMPV). Pneumonia virus of mice (PVM), bovine respiratory syncytial virus (bRSV) and hRSV are grouped together in the *Pneumovirus* genus. The type species of hRSV is the A2 strain (Collins and Crowe, 2007).

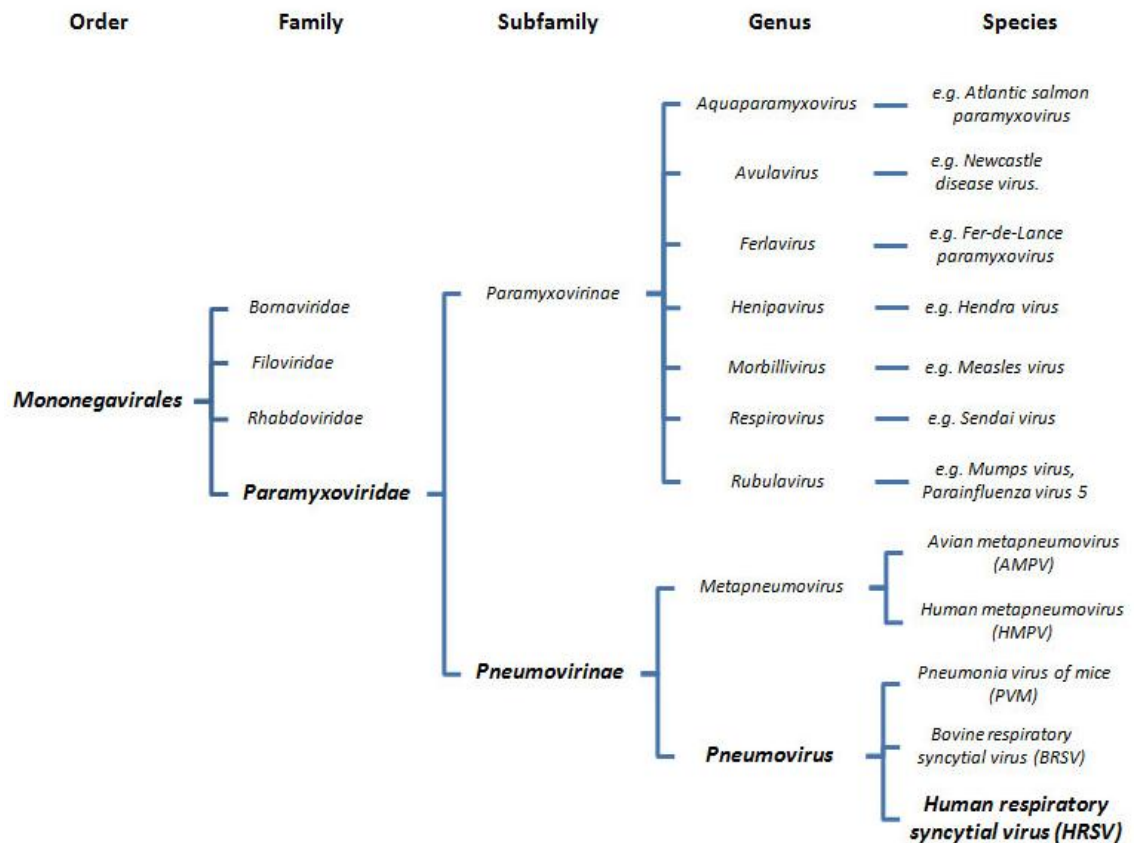


Figure 1.1 Taxonomy of the *Mononegavirales* order

[Modified from original by International Committee on Taxonomy of Viruses (2011)]

hRSV particles are pleomorphic in form varying from kidney-shaped or round (100-300 nm in diameter) to filamentous forms 60-100 nm in diameter and up to 10 µm in length. All forms contain a helical nucleocapsid (11-15 nm in diameter) and have peripheral spikes on the viral envelope (10-12 nm in length). The filamentous morphology is predominant (Norrby *et al.*, 1970; Bachi and Howe, 1973; Roberts *et al.*, 1995). The helical nucleocapsid or ribonucleoprotein (RNP) complex of hRSV consists of the large polymerase protein (L), the phosphoprotein (P), the nucleocapsid protein (N), and the RNA genome (Figure 1.2). The M2-1 protein is also found to associate with nucleocapsids (Collins and Crowe, 2007). All proteins of RNP complex are present in cytoplasmic inclusions and are involved in viral replication and transcription (Garcia *et al.*, 1993; Carromeu *et al.*, 2007).

The nucleocapsid is covered with a lipid envelope derived from the plasma membrane of host cell. The matrix protein (M) forms a layer between the nucleocapsid and the envelope. The envelope carries three viral transmembrane glycoproteins which individually project from the surface as virion spikes. These glycoproteins are the

attachment glycoprotein (G), the fusion glycoprotein (F) and the small hydrophobic protein (SH) (Collins and Crowe, 2007) as shown in Figure 1.2. The G and F glycoproteins are the major neutralization and protective antigens (Taylor *et al.*, 1984; Connors *et al.*, 1991).

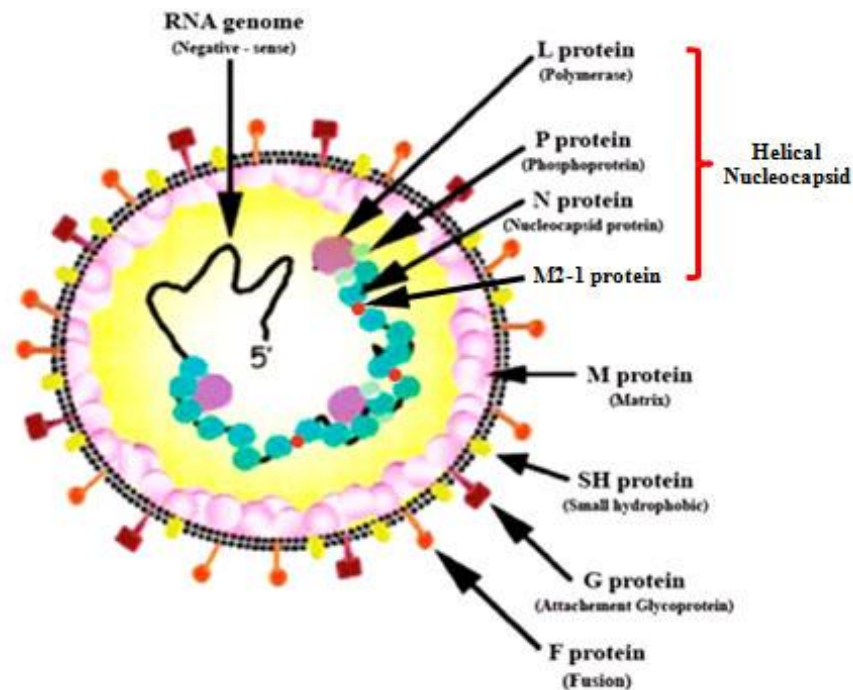


Figure 1.2: The structure of hRSV
[Modified from original by Ghildyal *et al.* (2006)]

1.3 The hRSV Genome

hRSV genome is a single-strand of non-segmented, negative – sense RNA and its size is approximately 15,200 nucleotides. It begins with a 3' leader region (44 nucleotides), followed by 10 viral genes and ends with a 5'trailer region (155 nucleotides) without capping and polyadenylation. Each gene contains a highly conserved gene start (GS) sequence and a semi-conserved gene end (GE) sequence as shown in Figure 1.3 which control the process of transcription (Kuo *et al.*, 1997). In the prototype strain A2, 3'-CCCCGUUUA-5' is the GS sequence for all genes, except the L gene which starts with 3'-CCCUGUUU-5'. The GE sequence of each gene varies between 12 and 13 nucleotides and contains three regions, an upstream conserved sequence 3'...UCAAU...5', a non-conserved central region and a tract of U residues at the end varying from U4 to U7 (Collins and Crowe, 2007). In between the GS and GE sequences, the genes are separated by non-conserved intergenic regions of 1 to 52 nucleotides except M2/L, which overlap by 68 nucleotides. Therefore, the GE of the

M2 gene is in the coding region of the L gene, whereas the GS of the L gene is in the M2 gene as shown in Figure 1.3 (Collins and Crowe, 2007).

In transcription, mRNA synthesis is started from the 3' end of the genome, which has only one promoter, and ten separate mRNAs are sequentially produced. Transcription of each subgenomic mRNA is started at its GS sequence and terminated at its GE sequence. A cap structure and poly(A) tails are added at 5' end and at 3' end of each mRNA, respectively. A different amount of mRNA is produced for each gene. The transcription frequency of the gene at the 3' end is higher than that at the 5' end because a proportion of polymerase molecule “falls off” the genome at each gene end sequentially reducing the efficiency of translation at each succeeding gene (Collins and Wertz, 1983; Krempl *et al.*, 2002). The mRNAs generated are the templates for translating 11 proteins. Each mRNA contains a single open reading frames (ORF) coding for a unique protein, except for the M2 mRNA which contains 2 ORFs (Collins and Crowe, 2007). The first ORF, encoding the M2-1 protein, is upstream and overlaps with the second ORF, encoding the M2-2 protein, by 32 nucleotides. Translation of the M2-2 ORF initiates after the translation of the M2-1 ORF has terminated (Ahmadian *et al.*, 2000).

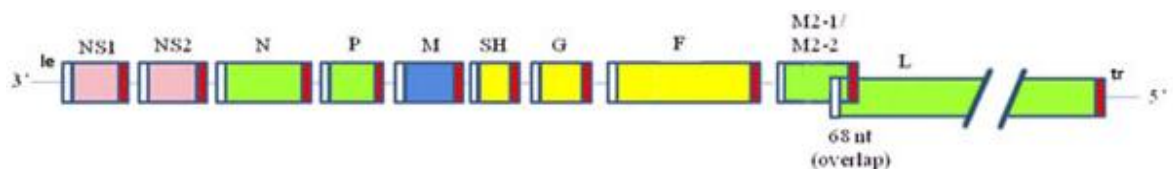


Figure 1.3: Diagram of hRSV genome

[Modified from original by Collins and Melero (2011)]

Viral genes are depicted as rectangles (not to scale) which have the gene start (white boxes) and gene end (red boxes). The genome has a 3' leader (le) and 5' trailer (tr) regions with 10 viral genes between the two ends arranged as follows: non-structural protein 1 gene (NS1), non-structural protein 2 gene (NS2), nucleocapsid protein gene (N), phosphoprotein gene (P), matrix protein gene (M), small hydrophobic protein gene (SH), attachment glycoprotein gene (G), fusion glycoprotein gene (F), M2 gene containing two ORF for encoding M2-1 and M2-2 proteins and large polymerase protein gene (L). The genes encoding the non-structural protein, the matrix proteins, the viral glycoproteins and the RNA-dependent RNA polymerase complex are shown as pink, blue, yellow and green, respectively.

1.4 The hRSV Proteome

1.4.1 The nonstructural proteins 1 and 2

The hRSV non-structural protein 1 (NS1) and non-structural protein 2 (NS2) (formerly known as 1C and 1B, respectively) are 139 and 124 amino acids in length, respectively.

They have molecular weights of approximately 14,000 for the NS1 protein and 11,000 for the NS2 protein measured by gel electrophoresis (Collins and Wertz, 1985). There are four identical amino acids (DLNP) in the carboxyl-terminus of both proteins, but other sequences are not similar. This feature may account for the cross-reaction when both proteins have been investigated by a rabbit antibody against a synthetic peptide containing 12 amino acids of the C-terminus of the NS2 protein (Collins and Wertz, 1985; Johnson and Collins, 1989).

NS1 and NS2 proteins are expected to be expressed in infected cells at high levels because of their promoter-proximal location, but only a low amount of NS1 and NS2 proteins is detectable using monoclonal antibodies. Connors *et al.* (1991) demonstrated that mice immunized with recombinant vaccinia virus expressing NS1 and NS2 proteins were not resistant to hRSV challenge. These results suggested that neither NS1 nor NS2 proteins are the protective antigens.

The NS1 protein was shown to be co-precipitated by a murine monoclonal antibody against the M protein, suggesting that the NS1 protein is associated with the M protein in infected cells. Whereas no viral structural protein is associated with the NS2 protein (Evans *et al.*, 1996), it has been suggested that there is an interaction between the NS2 protein and host cell cytoskeletal intermediate filaments (Weber *et al.*, 1995). Recently, recombinant NS1 and NS2 proteins have been reported to form homomers and heteromers (NS1-NS2). When recombinant NS1 or NS2 proteins were expressed alone, high amounts of the NS1 protein appeared in the nucleus and of the NS2 protein in the mitochondria. However, when the NS1 protein was co-expressed with the NS2 protein, the NS1 was also observed in the mitochondria, indicating that the localization of the NS1-NS2 heteromer was in the mitochondria (Swedan *et al.*, 2011).

Neither NS1 nor NS2 proteins are essential for viral replication; therefore, they are defined as accessory proteins (Teng and Collins, 1998). However, virus growth can be attenuated *in vitro* and *in vivo* by gene deletion of NS1 or NS2 genes from recombinant hRSV (Teng and Collins, 1999; Whitehead *et al.*, 1999a; Teng *et al.*, 2000). The NS1 protein has been found to have a negative regulatory effect on transcription and RNA replication in a minigenome replication system (Atreya *et al.*, 1998). Also, NS proteins

are capable of suppressing premature apoptosis via an IFN- and NF- κ B dependent pathway, thereby facilitating viral growth (Bitko *et al.*, 2007).

NS proteins are vital inhibitors of the innate immune response through the inhibition of one or multiple signalling factors of the type I IFN induction and/or response pathway. Recent studies have shown that NS proteins suppress IFN induction by reducing levels of TNF receptor-associated factor 3 (TRAF3). TRAF3 acts as an integrator of IFN-inducing signals from both the retinoic acid – inducible gene I (RIG-I) and Toll – like receptor (TLR) pathways. Swedan *et al.* (2009) showed the TRAF3 levels were sharply decreased by recombinant NS1 and NS2 proteins together, by the NS1 protein alone, but weakly by the NS2 protein alone. Levels of TRAF3 – downstream I κ B kinase ϵ (IKK ϵ), which plays a role in activation of the IFN regulatory factors (IRF), was also reduced by the recombinant NS1 protein, but increased by the NS2 protein. The N-terminal of the NS1 protein is found to be necessary for the reduction of IKK ϵ (Swedan *et al.*, 2011). NS2 protein can bind to the N-terminal caspase activation and recruitment domain (CARD) sequence of RIG-I and inhibit the interaction between RIG-I and the downstream of mitochondrial antiviral-signalling proteins (MAVs) blocking the activation of the IFN promoter (Ling *et al.*, 2009). NS1 protein was not able to interact with RIG-I.

NS1 and NS2 proteins have also been shown to suppress the activation of interferon regulatory factor 3 (IRF3) which is one of the transcription factors for IFN- β and IFN- α 1 genes. In wild-type hRSV infected cells containing substantial amounts of NS1 and NS2 proteins, the activation and nuclear translocation of IRF3 was suppressed. Correspondingly, recombinant hRSV lacking NS1 and NS2 genes increased the level of IRF3 activation (Spann *et al.*, 2005). Although the NS1 protein is unable to associate with RIG-I, a recent study has shown that the NS1 protein can directly interact with IRF-3 and its coactivator CBP (CREB – binding protein). Consequently, the formation of IRF-3 associated with CBP is inhibited preventing binding of IRF-3 with the IFN promoter (Ren *et al.*, 2011).

Lo *et al.* (2005) has demonstrated that recombinant NS1 plus NS2 proteins and NS2 expressed alone in human pulmonary epithelial cells (A549) also suppress the IFN response pathway by decreasing the level of signal transducer and activator of

transcription 2 (STAT2). Ramaswamy *et al.* (2004) has reported that the loss of STAT2 expression likely occurs due to the proteasome-mediated degradation of STAT2. STAT2 levels are restored after adding a proteasome inhibitor in hRSV infected cells. Whilst recombinant hRSV lacking NS1 and NS2 genes increased the STAT2 level in A549 and monocyte derived macrophage (Spann *et al.*, 2004; Lo *et al.*, 2005), recombinant NS1 protein alone had little effect on the STAT2 suppression and NS2 protein alone and the combination of NS1 and NS2 proteins produced a significant reduction (Lo *et al.*, 2005). Although these results suggest that reduction of the STAT2 level is predominantly caused by NS2 function, the C-terminal DLNP tetrapeptide, the four amino acids identical in both NS1 and NS2, is reported to be important for the reduction of STAT2 levels by binding with the cellular microtubule-associated protein 1B (MAP1B) (Swedan *et al.*, 2011). Also, the NS1 protein has been shown to form Elongin-Cullin E3 ligase complexes leading to proteasome-mediated STAT2 degradation (Elliott *et al.*, 2007).

1.4.2 The nucleocapsid protein

The hRSV nucleocapsid protein (N) contains 391 amino acids which is smaller than that of other paramyxoviruses (489 – 553 amino acids) (Collins *et al.*, 1985). However, the structure and function of the N protein are likely to be similar to those of other mononegaviruses.

Evidence from deletion mutation, yeast two-hybrid experiments and recent three-dimensional (3D) modelling of recombinant hRSV N/RNA complexes indicate that the N protein contains two functional domains which are N- and C- terminal domains. The N-terminus is essential for binding to the L polymerase, whilst the C-terminus contains the P binding region (Krishnamurthy and Samal, 1998; Tawar *et al.*, 2009). The C-terminus of the P protein is reported to bind this region of the N protein (Garcia-Barreno *et al.*, 1996; Mallipeddi *et al.*, 1996). In the 3D crystal structure of a recombinant hRSV N protein, it has been shown that each N monomer associates with seven nucleotides of bound RNA. The RNA binding is in the groove between the C- and N-terminus of the N protein (Tawar *et al.*, 2009).

The encapsidation of viral RNA with the N protein is necessary for viral replication and transcription because the viral polymerase only recognizes the N-RNA complex and

also the N-RNA complex is resistant to nuclease treatment (Murphy *et al.*, 2003). The N-terminus of the N protein is demonstrated to be required for nucleocapsid formation and RNA synthesis using a minigenome system (Khattar *et al.*, 2000). Therefore, the N protein can be an important target for producing an effective antiviral compound. One such is RSV604, an anti-hRSV compound, exhibiting potent antiviral activity against hRSV isolates of both subgroup A and B. The resistant mutations of RSV604 have been mapped to the conserved N-terminus of the N protein (residues 105 – 139) (Chapman *et al.*, 2007).

1.4.3 The phosphoprotein

The hRSV phosphoprotein (P), which is 241 amino acids in length, is shorter than that of other paramyxoviruses (391 – 602 amino acids), but its activities are similar. The P protein associates with N, L and M2-1 proteins for RNA synthesis (Garcia-Barreno *et al.*, 1996; Khattar *et al.*, 2000). The C-terminal of the P protein binds to the C-terminal of the N protein opening the ribonucleoprotein structure. Subsequently, the L protein can interact with the N-RNA template. In addition, the P protein interacts with newly synthesized soluble N (N⁰) to prevent illegitimate polymerization before the latter binds to the nascent RNA chain during viral replication (Curran *et al.*, 1995).

The P protein is able to form a homotetramer oligomerizing via a coiled-coil motif which contains a repeated pattern of hydrophobic and hydrophilic amino acids. The P oligomerization domain is located between residues 120 – 150 in the central region of the P protein (Asenjo and Villanueva, 2000; Castagne *et al.*, 2004).

The phosphorylation of the P protein occurs at several serines (S) and threonines (T) residues by cellular casein kinase II (Mazumder and Barik, 1994; Dupuy *et al.*, 1999). The S232 is the major phosphorylation site, but other minor phosphorylation sites are S116, S117, S119, S237 and T108 (Barik *et al.*, 1995; Sanchez-Seco *et al.*, 1995; Asenjo *et al.*, 2006). Site-directed mutagenesis studies have indicated that phosphorylation of S232 and S237 is essential for the transcriptional activity of the P protein (Mazumder and Barik, 1994; Barik *et al.*, 1995). The former is also important for the elongation activity of the P-L complex during RNA transcription (Dupuy *et al.*, 1999). Moreover, the phosphorylation at T108 is involved in the control of the P-M2-1 interaction and facilitates the incorporation of the M2-1 protein into a viral polymerase

complex during viral transcription (Asenjo *et al.*, 2006). However, it has been shown that the phosphorylation of the P protein is not compulsory for the interaction of the P-P, P-N (Castagne *et al.*, 2004) and P-M2-1 complexes (Mason *et al.*, 2003), but it is necessary for efficient virus budding and replication *in vitro* and *in vivo* (Lu *et al.*, 2002).

1.4.4 The large polymerase protein

The hRSV large polymerase protein (L) is a component of the viral RNA dependent RNA polymerase complex which also includes P, N and M2 proteins. It is 2,165 amino acids in length which is similar to the L protein of other paramyxoviruses. The localization of the L protein in infected cells appears to be near the viral membrane associated with N and P proteins (Carroneu *et al.*, 2007). The L protein plays a major role in all enzymatic activities during viral replication and transcription, including capping, methylation and polyadenylation. After alignment analysis of the *Mononegavirales* L proteins, six discrete segments (region I to VI) containing highly conserved residues have been revealed (Poch *et al.*, 1990). The central region of the L protein (II to V) contains the most highly conserved amino acid sequences and has an area of highly positive charged protein residues in region II. This area is likely to be involved in the recognition of template.

Furthermore, it has been found that mutation of the GDNQ motif, lying in region III of all the *Mononegavirales* L proteins and at residues 810-813 of the hRSV Long strain L protein, inactivated the polymerase activity (Jin and Elliott, 1992; Sleat and Banerjee, 1993; Schnell and Conzelmann, 1995; Fix *et al.*, 2011). Therefore, the GDNQ motif has been proposed as the polymerase active site. In addition, a single amino acid change in region IV of the hRSV L protein caused the production of high levels of polycistronic readthrough RNAs due to a lower ability to terminate at gene end sequence (Cartee *et al.*, 2003). The guanylation and methylation activity involved in a cap structure synthesis have been located in the regions V and VI respectively of the *Mononegavirales* L protein (Ferron *et al.*, 2002; Liuzzi *et al.*, 2005; Ogino *et al.*, 2005).

1.4.5 *The M2-1 protein*

The M2-1 protein, or 22kDa protein, is encoded by the 5'-proximal ORF of the M2 gene (Collins *et al.*, 1990). The M2 gene is only found in the subfamily *Pneumovirinae*, while the subfamily *Paramyxovirinae* lacks this gene. The M2-1 protein is 194 amino acids in length and forms a homotetramer (Tran *et al.*, 2009). The M2-1 protein is located in cytoplasmic inclusions (Garcia *et al.*, 1993) and also in the nucleus of infected cells (Reimers *et al.*, 2005). It has been thought that the M2-1 protein may be translocated into the nucleus following interaction with the Rel A protein leading the induction of NF- κ B activation.

The M2-1 protein is involved in elongation or anti-termination activity during RNA transcription. High amounts of incomplete mRNAs were produced in a minigenome system lacking the M2-1 ORF plasmid due to the premature termination of transcription, whilst there was a substantial change to the efficient full-length mRNAs synthesis when an M2-1 ORF plasmid was added. However, this activity of the M2-1 protein depends on the position of the target gene. The synthesis of full-length NS1 and NS2 mRNAs is not associated with M2-1 protein expression. In contrast, the M2-1 protein is very important in producing complete mRNAs from the other, downstream genes. In addition, it was found that there was no difference in genome synthesis in the presence or absence of the M2-1 protein suggesting that the M2-1 protein is not involved in RNA replication (Collins *et al.*, 1996; Fearn and Collins, 1999b).

Besides intragenic anti-termination, the M2-1 protein also acts as a transcriptional anti-terminator at gene end sequences (GE-anti-termination activity). It has been reported the synthesis of polycistronic mRNAs increased when whole M2 plasmid containing M2-1 and M2-2 ORF and M2-1 ORF alone were expressed. (Hardy and Wertz, 1998; Fearn and Collins, 1999b; Hardy *et al.*, 1999).

The M2-1 protein carries a conserved C₃-H₁ motif (C-X₇-C-X₅-C-X₃-H) at the N-terminus. This motif in other proteins has been reported to bind zinc ions (Worthington *et al.*, 1996). When the predicted zinc-coordinating residues in this motif were mutated, the ability of both transcriptional readthrough and the interaction with the N protein were inhibited. However, a mutation in a non-coordinating residue increased readthrough transcription, but still blocked the association with the N protein (Hardy

and Wertz, 2000). These findings suggest that the anti-termination activity of the M2-1 protein requires the zinc binding motif, but not the interaction between the M2-1 protein and the N protein.

Two forms of the M2-1 protein are present in infected cells and can be demonstrated in reducing sodium dodecyl sulphate-polyacrylamide gels (SDS-PAGE). It has been shown that the slower migrating form is phosphorylated, whereas the faster form is unphosphorylated. The mutation in the predicted zinc-coordinating residues caused a shift from the slower migrating form to the faster form, suggesting that this motif is also important for phosphorylation. Together these results indicate that the predicted zinc coordinating residues of the C₃-H₁ motif in the M2-1 protein are necessary for the maintenance of protein integrity, efficient transcriptional readthrough at gene junctions and efficient phosphorylation (Hardy and Wertz, 2000). The serine residues 58 and 61 of the M2-1 protein have been found to be the sites of phosphorylation (Cartee and Wertz, 2001) instead of threonine 56 and serine 58 as previously reported by Cuesta *et al.* (2000). Mutation of S58 and S61 resulted in the reduction of antitermination activity, indicating that the phosphorylation of the M2-1 protein is important for hRSV transcription, but had no effect on the association with N protein (Cartee and Wertz, 2001). It has been reported that the M2-1 protein has RNA binding capacity and the M2-1/N interaction is mediated by viral RNA (Cuesta *et al.*, 2000; Cartee and Wertz, 2001).

1.4.6 The M2-2 protein

An 11kDa M2-2 protein (90 amino acids) is encoded by the 3'-proximal ORF of the M2 mRNA that is located slightly upstream of the M2-1 gene end (Collins *et al.*, 1990). A low level of the M2-2 protein is expressed and found to be localized in cytoplasmic inclusion bodies (Ahmadian *et al.*, 2000). It has been reported that the removal of the M2-2 protein does not affect the replication in cell culture; therefore, the M2-2 protein is defined as an accessory protein. However, recombinant hRSV with an M2-2 deletion can be attenuated *in vivo* (Jin *et al.*, 2000a).

The amount of genomic RNA and antigenomic RNA in hRSV lacking the M2-2 protein is less than hRSV wild-type, whereas the level of mRNA is significantly increased. It has thus been suggested that the M2-2 protein is a regulator of the switch from viral

transcription to RNA replication (Bermingham and Collins, 1999; Jin *et al.*, 2000a). Overexpression of the M2-2 protein blocks viral replication (Cheng *et al.*, 2005).

1.4.7 The matrix protein

The hRSV matrix protein (M) is a non-glycosylated protein of 256 amino acids in length that has no homologous sequence with the M protein of other paramyxoviruses and is smaller than them (335 – 375 amino acids). The hRSV M protein comprises two domains connected by a linker region (Money *et al.*, 2009). The C and N-terminal domains have high and low hydrophobicity, respectively. The C-terminal domain of the M protein is thought to interact with the plasma membrane (Ghildyal *et al.*, 2006). In addition, positively-charged patches are found on the surface of both domains and the linker, suggesting an ability of the M protein to interact with negatively-charged host membrane or viral nucleocapsid (Money *et al.*, 2009).

The function of the M protein in other mononegaviruses is to inhibit viral transcription prior to assembly and to bring the envelope complex together with the nucleocapsid in the formation of viral particles (Kaptur *et al.*, 1991; Lenard, 1996; Coronel *et al.*, 2001). The hRSV M protein has been shown to be an essential structural protein for viral replication and passage (Teng and Collins, 1998). It can be associated with the RNP, an association mediated by the M2-1 protein, and is localised in cytoplasmic inclusions in the late phase of infection. The M protein has viral transcription inhibition activity (Ghildyal *et al.*, 2002; Li *et al.*, 2008). Also, in the early infection, the M protein is detected in the nucleus of the infected cells and inhibits transcription of host cell which may conceivably facilitate viral replication (Ghildyal *et al.*, 2003).

The M protein is associated with the cytoplasmic side of the plasma membrane co-ordinating all components of virus in the step of budding (Marty *et al.*, 2004). It is able to bind with the plasma membrane without viral glycoprotein expression. However, its co-expression with the F glycoprotein results in M protein sorting into lipid rafts (Henderson *et al.*, 2002). It has been reported that lipid rafts are used for packaging and budding of hRSV and that the M, G and N proteins are all present in them (Marty *et al.*, 2004). The M protein has also been shown to interact with the amino terminus of the G protein (Ghildyal *et al.*, 2005). Furthermore, the M protein has a capacity for RNA binding which is not sequence specific. The function of M protein-RNA interaction is

unknown, but it may relate to transcription inhibition of the host cell during early infection (Rodriguez *et al.*, 2004).

1.4.8 The small hydrophobic protein

The small hydrophobic protein of hRSV (SH) is a surface, type II transmembrane protein (Collins and Mottet, 1993). The integral membrane proteins are divided into 4 topological classes: types I, II and III have single, membrane – spanning, hydrophobic segments and type IV have multiple transmembrane segments. Type I transmembrane proteins contain a signal sequence and an extracellular region at the N-terminus and have a transmembrane anchor domain at the C-terminus. Type III proteins have the same orientation as type I proteins, but do not have a signal sequence. Type II proteins, including, the hRSV SH, also lack a signal sequence but are anchored into the membrane via a hydrophobic, N-terminal anchor with an extracellular C-terminal region (Harvey, 2007).

The length of the polypeptide chain in the SH protein is slightly different between subgroups A and B being composed of 64 and 65 amino acids, respectively. It has been shown that the amino acid sequence of the SH protein among hRSV clinical isolates is relatively highly conserved within the subgroups (Chen *et al.*, 2000).

During infection, SH protein is produced in several forms comprising two non-glycosylated and two glycosylated forms. All four forms are integral membrane proteins which are produced and processed on intracellular membranes. SHo (full-length 7.5kDa, most abundant species) and SHt (4.5kDa, N-terminally truncated form) are non-glycosylated species. SHt is possibly synthesized by translational initiation at the second start codon (AUG), while SHo is originated from the first AUG. SHg (13-15kDa) is an N-linked glycosylated form modified from SHo. SHp (21 - 30kDa) is a modified species synthesized by adding polylactosaminoglycan to the N-linked carbohydrate of SHg. The SHo, SHg and SHp forms are transported to the cell surface; however, only SHo and SHp are incorporated into virions.

The function of the SH protein is still unclear. It has been observed that it induces a permeability change in the *Escherichia coli* membrane when it is expressed in the bacterial cell, suggesting that it has an ion-channel function (Perez *et al.*, 1997).

Recently, the transmembrane domain of the SH protein has been found to form α -helical pentamers which have cation-selective ion channel activity (Gan *et al.*, 2008). Furthermore, SH protein may be essential for infectivity *in vivo* as the recombinant hRSV lacking the SH gene is attenuated in mice and chimpanzees; however, deletion of the SH gene from recombinant hRSV does not affect viral replication in tissue culture (Bukreyev *et al.*, 1997; Whitehead *et al.*, 1999a).

Expression of a recombinant parainfluenza virus 5 (PIV5) in which the PIV5 SH is replaced with hRSV SH (PIV5 Δ SH-RSV-SH) and study of hRSV with a deleted SH gene (RSV Δ SH) suggest that the SH protein of hRSV is able to inhibit TNF- α mediated NF- κ B activation and is similar in this respect to the SH protein in PIV5. hRSV SH protein can also inhibit apoptosis (Wilson *et al.*, 2006; Fuentes *et al.*, 2007).

1.4.9 The attachment glycoprotein

The hRSV attachment glycoprotein (G) is a type II glycoprotein which contributes to virus binding (Levine *et al.*, 1987), but for which the full role in virus replication remains uncertain. The amino acid sequence and structural features of the hRSV G glycoprotein are significantly different from those of other paramyxovirus attachment proteins (HN or HA proteins) (Wertz *et al.*, 1985; Johnson *et al.*, 1987). There are two different forms of the G glycoprotein observed in the infected cell. One is a membrane-bound form (G_m) which is full-length containing 289 to 319 amino acids depending on the virus strain (Collins and Crowe, 2007). The other is a soluble form (G_s) that is secreted into the culture medium before virus release (Hendricks *et al.*, 1987; Hendricks *et al.*, 1988). The G_s protein is produced from an alternative translation initiation at the third AUG (residue 48) located in the middle of the G ORF and further trimmed by N-terminal proteolytic cleavage following residue 65. Therefore, the soluble G glycoprotein lacks 65 amino acids including the entire signal and the hydrophobic transmembrane region (Roberts *et al.*, 1994).

The G_m glycoprotein is synthesized as a 32kDa precursor by transcriptional initiation at the second AUG of the mRNA. Only a short peptide of 15 amino acids residues is encoded from the first AUG. The G_m precursor is then modified by the addition of high-mannose N-linked sugars to asparagine residues leading to an increase in the mass of the protein to 45 - 50kDa (Wertz *et al.*, 1989; Collins and Mottet, 1992). These

intermediate proteins form homo-oligomers (trimers or tetramers) probably in the endoplasmic reticulum and O-linked sugars are added to serines (S) and threonines (T) on the surface of the oligomers. The mature form of the G glycoprotein is produced in the trans-Golgi compartment with a monomeric molecular weight of approximately 80 – 90kDa as estimated by SDS-PAGE (Collins and Mottet, 1992) and then transported into the cell surface.

The Gm glycoprotein consists of three major parts - the N-terminal cytoplasmic domain (residues 1 – 37), the hydrophobic transmembrane domain (residues 38 – 63) and the C-terminal ectodomain (residues 64 – 298 based on strain A2) as shown in Figure 1.4 (Satake *et al.*, 1985; Wertz *et al.*, 1985). The ectodomain consists of a central region which is largely conserved among different virus isolates flanked by two mucin-like variable regions, resembling the structure of the 55kDa tumor necrosis factor receptor (Langedijk *et al.*, 1998). The mucin-like regions have a high amount of potential acceptor sites for O-linked sugar (S/T) and N-linked sugar and also have a high proline (P) and serine content (Melero *et al.*, 1997). The amino acid compositions of these regions are similar to the mucins produced by many epithelial tissues (Apostolopoulos and McKenzie, 1994).

As shown in Figure 1.4, the central region segment lacks potential glycosylation sites and contains a 13-amino acid completely conserved segment (residue 164 – 176 based on strain A2) which overlaps a sequence with four cysteine (C) residues (position 173, 176, 182 and 186) which form a cystine noose by two disulfide bridges occurring between C173 and C186, and between C176 and C182 (Gorman *et al.*, 1997). The C182 to C186 segment is a CX3C motif similar to that of the CX3C chemokine fractalkine (Fkn) which binds to cells via CX3CR1 and glycosaminoglycans (GAGs) (Tripp *et al.*, 2001). It has been reported that GAGs are required for hRSV infection (Feldman *et al.*, 1999; Hallak *et al.*, 2000a; Hallak *et al.*, 2000b) and a major heparin binding domain (HBD) maps to amino acid position 184-198 of the G protein (Feldman *et al.*, 1999).

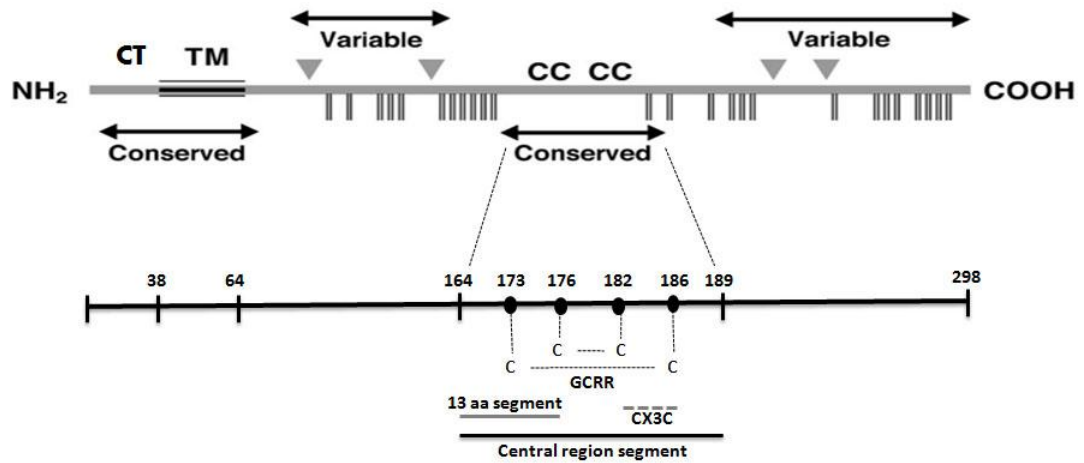


Figure 1.4: Scheme of the primary structure of the G glycoprotein based on hRSV A2 strain.

[Modified from original by Polack *et al.* (2005) and Wertz and Moudy (2004)]

Areas of mucin-like variable region, conserved region, the 13-amino acid (aa) segment and the CX3C chemokine fractalkine are denoted. Positions of N- and O-linked carbohydrate are depicted as triangles (▼) and rods (▮), respectively. Cysteine residues are shown with filled ovals and the disulfide bridges with dotted lines. NH₂: N-terminal domain; COOH: C-terminal domain; CT: cytoplasmic domain; TM: transmembrane domain; C: conserved cysteine; GCRR: cysteine rich region.

Melero *et al.* (1997) described the 3D structure of the G_m molecule (homotrimer). The cytoplasmic tail at the N-terminus, followed by the transmembrane region and then the first hypervariable region form a rod-like feature (Figure 1.5). The cysteine noose containing conserved and group specific epitopes sits at the loop of the rod-like shape. The second carboxyl-terminal hypervariable region which follows the cluster of cysteine at the end of molecule and carries strain-specific epitopes loops back on itself to sit at the top of the rod giving the whole structure of the appearance of a lollipop.

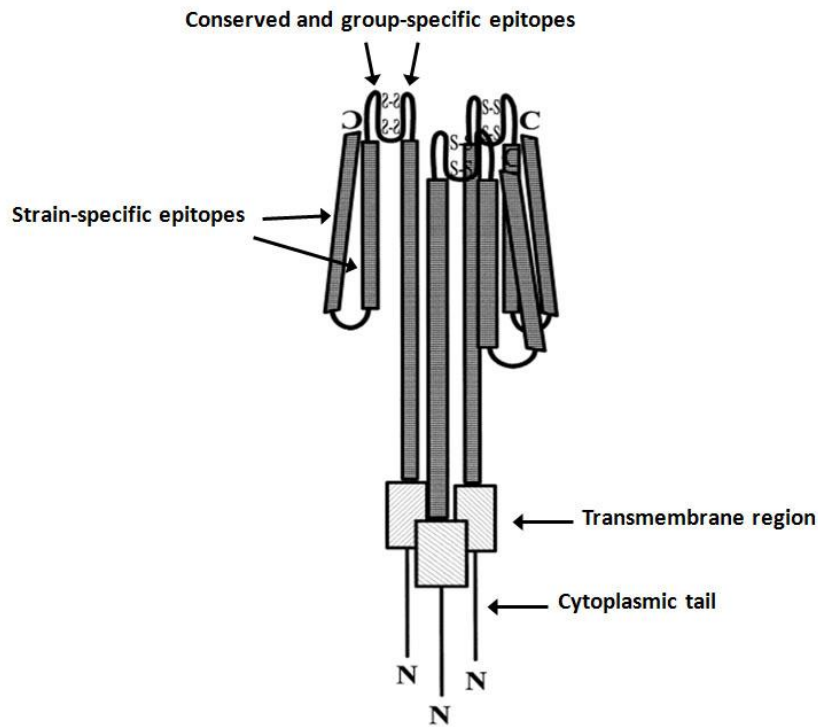


Figure 1.5: Model of the 3-D structure of the hRSV G protein.

[Modified from original by Melero (2007) and Melero *et al.* (1997)]

A proposed homotrimer is modified from the model of Langedijk *et al.* (1996). Hatched and shaded rectangles are depicted as the transmembrane domains and the mucin-like variable regions, respectively. Areas of several structural motifs are indicated. Disulphide bonds (S-S) and the N- and C-terminal domain are denoted.

A cold-passaged candidate hRSV vaccine (*cp-52*) lacking the G and SH genes (Karron *et al.*, 1997) or recombinant virus lacking the G gene alone (Teng *et al.*, 2001) replicate as well as wild type *in vitro* depending on cell types. However, both viruses exhibit reduced efficiency of the viral replication in mice suggesting that the G glycoprotein is necessary for viral replication *in vivo*. In addition, the Gs protein is found to be sufficient for the virus growth both *in vivo* and *in vitro*, indicating that both cytoplasmic and transmembrane forms are not required for the viral replication (Teng *et al.*, 2001).

The conserved regions in the ectodomain of G_m are believed to be the putative receptor binding site for attachment activity (Johnson *et al.*, 1987). Nevertheless, the deletion of this conserved region including the cysteine noose and part or all of the 13- amino acid conserved segment from the G protein has no effect on hRSV replication either *in vivo* or *in vitro* (Teng and Collins, 2002). The removal of the heparin-binding domain in the recombinant hRSV also does not decrease the efficiency of viral growth *in vitro*, although there is a slight reduction *in vivo* (Teng *et al.*, 2001).

Polack *et al.* (2005) have demonstrated that the cysteine noose or G cysteine-rich region (GCRR) is involved in modulating the innate inflammatory response. Recombinant hRSV lacking the GCRR or with the disulfide bridges in the GCRR disrupted have enhanced production of IL-6 in human monocytes and inhibited nuclear translocation of the NF- κ B transcription factor. Moreover, the GCRR can block the production of proinflammatory cytokines elicited via TLR2, 4 and 9 agonists. The expression of the full-length G protein or the CX3C motif of the G protein in CX3CR1⁺ cytotoxic T cells also decreases the pulmonary influx of immune cells associated with innate and adaptive immune response (Harcourt *et al.*, 2006). Therefore, the GCRR and CX3C motifs appear to inhibit inflammatory responses.

It has been found that the recombinant hRSV producing only the G_m protein has higher susceptibility to neutralizing antibodies than wild-type hRSV in tissue culture cells and mice suggesting that the G_s protein serves as an antigen decoy to escape antibody neutralization (Bukreyev *et al.*, 2008). Infection of human lung epithelial cells (A549) by a spontaneous hRSV mutant which cannot produce the G_s protein (RSV- Δ S_G) resulted in the enhancement of the host cell inflammatory response when compared to wild type virus infection (Arnold *et al.*, 2004). Similarly, RSV- Δ S_G infection in mice stimulated a high amount of eosinophils and macrophages and a high concentration of IFN- γ and IL-10 (Schwarze and Schauer, 2004). The G_s protein appears to be important in blocking chemokine release. It seems likely that G_s protein acts as a soluble factor inhibiting inflammatory responses.

1.4.10 The fusion glycoprotein

Primary structure of the fusion protein

The hRSV fusion glycoprotein (F) is a type I membrane protein which is initially synthesized as an inactive pre-F₀ precursor protein (574 amino acids). This precursor contains a hydrophobic signal peptide at the N-terminus and a hydrophobic transmembrane anchor domain at the C-terminus. The signal peptide is thought to initiate transport of the nascent pre-F₀ protein across the plasma membrane and into the lumen of the endoplasmic reticulum. F₀ (~ 70kDa) is synthesized by removal of the signal peptide using a signal peptidase (Collins *et al.*, 1984), followed by N-glycosylation and homo-oligomerization (into trimers) in the endoplasmic reticulum

(Collins and Mottet, 1991; Anderson *et al.*, 1992). The F₀ is then cleaved twice at residue 109 and 136 as shown in Figure 1.6 (Gonzalez-Reyes *et al.*, 2001) by furin-like proteases in the trans-Golgi to generate the F2 (~ 20kDa) and F1 (~ 50kDa) subunits, respectively. The two subunits are held together by a disulfide bond between conserved cysteines (Collins and Mottet, 1991; Bolt *et al.*, 2000).

The primary structure of the F glycoprotein in all paramyxoviruses comprises an F1 subunit with hydrophobic domains at both ends which are the trans-membrane anchor (TM) at the C-terminus and a fusion peptide (FP) at the N-terminus as shown in Figure 1.6. The fusion peptide is believed to have the same function as other fusion peptides that penetrate into the target membrane during the membrane fusion process (Durrer *et al.*, 1996). Each hydrophobic domain is adjacent to a heptad-repeat (HR), HR1 for the fusion peptide and HR2 for the transmembrane domain (Chambers *et al.*, 1990). A HR3 has been identified within the F2 protein by a computer search strategy, but its function has not yet been established (Matthews *et al.*, 2000). The F1 subunit contains one site for N-linked glycosylation, while two N-linked glycosylation sites are found in the F2 subunit (Rixon *et al.*, 2002). The cytoplasmic tail (CT) extends from transmembrane anchoring domain of F1 at the C-terminus (Colman and Lawrence, 2003).

The orientation of the F₀ precursor is NH₂-F₂-FP-HR1-F₁-HR2-TM-CT-COOH (Collins *et al.*, 1984). Cleavage at both residues 109 and 136 upstream of the fusion peptide is necessary for the formation of syncytia in the hRSV infection. The cleavage site I is RARR at residues 106-109 and the cleavage site II is KKRKRR at residues 131-136 (Gonzalez-Reyes *et al.*, 2001; Zimmer *et al.*, 2001). Cleavage site II is conserved in all hRSV and bRSV isolates, but differs from the cleavage sites of all other paramyxovirus F glycoproteins which usually contain one site only of three or four basic amino acids (Klenk and Garten, 1994). A short peptide of 27 amino acids (p27) is released after the endoproteolytic cleavage at both sites of F₀. The hRSV p27 peptide contains two to three N-glycosylation sites depending of the hRSV subtype, whereas the p27 peptide of the bRSV contains only one N-glycosylation motif.

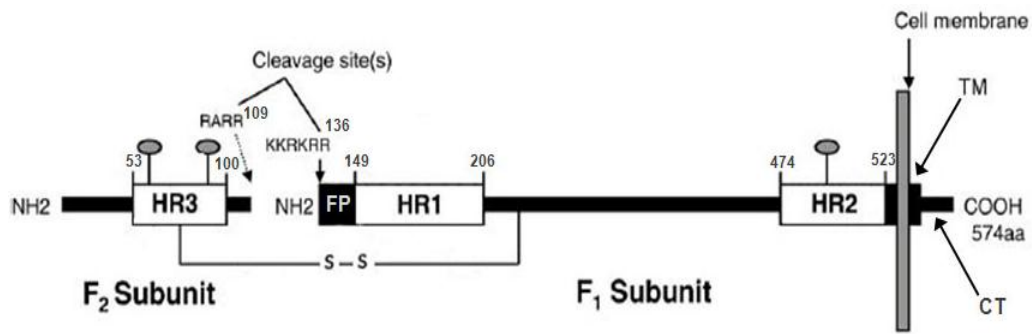


Figure 1.6: Scheme of the primary structure of F glycoprotein based on hRSV long strain.

[Modified from original by Yunus *et al.* (2010)]

The F glycoprotein contains two subunits, F1 and F2. The F1 subunit has two heptad-repeat (HR) domains, HR1 and HR2 depicted as unfilled rectangles, and two hydrophobic regions, the fusion peptide (FP) and the transmembrane domain (TM) shown as filled rectangles. In the F2 subunit, the location of an additional predicted HR3 is shown. The N-terminal (NH₂) domain, furin cleavage site I (RARR), site II (KKRKRR), the disulfide (-S-S-) bond, C-terminal domain (COOH) and the cytoplasmic tail (CT) are also denoted. The conserved N-glycosylation sites are represented as the lollipop-shaped structure in the F1 and F2 subunits. The numbering of amino acids is based on the F0 precursor.

Secondary and tertiary structure of the fusion protein

Virus membrane-fusion proteins are divided into two classes based on structural features; class I and class II. Class I viral fusion proteins are synthesized as inactive single-chain precursors assembling into trimers. They are proteolytically cleaved by host proteases to generate two subunits and fold to a pre-fusion form with a metastable conformation (Chen *et al.*, 1998). Their structures are trimeric spikes perpendicularly projecting from the viral membrane and have primarily secondary structures of α -helix. After exposure to low pH or binding to the cell receptor, the fusion protein is activated to form an extended structure (pre-hairpin intermediate form) and the N-terminal fusion peptide is inserted into the target membrane. A trimer of hairpins containing a central α -helical coiled-coil (six-helix bundles, 6HB) is then formed, the post-fusion structure. In this 6HB motif, three N-terminal regions of the fusion protein (HR1) form an inner trimeric coiled-coil core and three C-terminal regions (HR2) pack against the coiled-coil in an antiparallel orientation (Carr and Kim, 1993; Bullough *et al.*, 1994). The examples of class I fusion proteins are the influenza virus hemagglutinin protein (HA), HIV-1 gp41 protein, parainfluenza virus 5 (PIV5; formerly known as Simian virus 5, SV5) F glycoprotein and hRSV F glycoprotein.

The structures of class II fusion proteins found in flavivirus and alphavirus are different from class I proteins. These fusion proteins are synthesized by proteolytic processing of

an accessory protein and β -sheet is the predominant secondary structure of the fusion subunit. They orientate in parallel to the viral membrane. Their internal hydrophobic loops are thought to be inserted into the target membrane during fusion and a trimer of hairpins containing a β structure (non-coiled-coil) is the post-fusion form (Earp *et al.*, 2005; Kielian, 2006; Kielian and Rey, 2006).

The hRSV F glycoprotein is not triggered by low pH and not by the attachment of the G glycoprotein to the host cell receptor (see details in section 1.5.3). It is still unclear what triggers this F glycoprotein. However, the structure of hRSV F glycoprotein is similar to other class I fusion proteins. In pre-fusion form, the hRSV F glycoprotein is a trimer of heterodimers containing three N-terminal F2 proteins linked to three F1 transmembrane proteins by disulphide bonds. After activation, the fusion peptide inserts into the host cytoplasmic membrane, followed by subsequent conformational changes and the formation of a 6HB structure which is the interaction of the HR1 and HR2 domains. In this structure, an inner trimeric coiled-coil core containing highly α -helical contents formed by three HR1 peptides organizes along the central axis of the F glycoprotein and three HR2 peptides interact along the grooves of the HR1 trimer in an antiparallel arrangement to construct the 6HB (Lawless-Delmedico *et al.*, 2000; Matthews *et al.*, 2000; Zhao *et al.*, 2000). Peptides derived from the HR2 region can block the viral infection likely due to the inhibition of the 6HB formation (Lambert *et al.*, 1996). This hexameric form of the F glycoprotein probably brings the viral membrane and the host cell membrane into close apposition (Zhao *et al.*, 2000). The HR3 located in the F2 polypeptide has not been shown to associate with HR1, HR2 or the 6HB motif (Matthews *et al.*, 2000).

The 3D structure of the hRSV F glycoprotein has been modelled from its homology with the F glycoprotein of Newcastle disease virus (NDV-F) as shown in Figure 1.7. Although the percentage of sequence homology between both viruses is low, several features are the same in the hRSV-F and NDV-F glycoprotein such as the morphology, the function and key sequences in identical positions (Smith *et al.*, 2002). As shown in NDV-F (Chen *et al.*, 2001), the trimeric F molecule is divided into three parts that are head, neck and stalk (core). There is a large channel in the head region running through the axis and three symmetrical radial channels intersecting the axial channel between the head and neck regions. The F1 and F2 polypeptides form the head and neck, whilst

the stalk region contains HR1 and HR2 of the F1 polypeptides forming a six-membered antiparallel helical coiled-coil as mentioned above. The three fusion peptides and three viral transmembrane domains are present at the base of the stalk, indicating that this model represents the post-fusion form of the hRSV-F glycoprotein (Morton *et al.*, 2003).

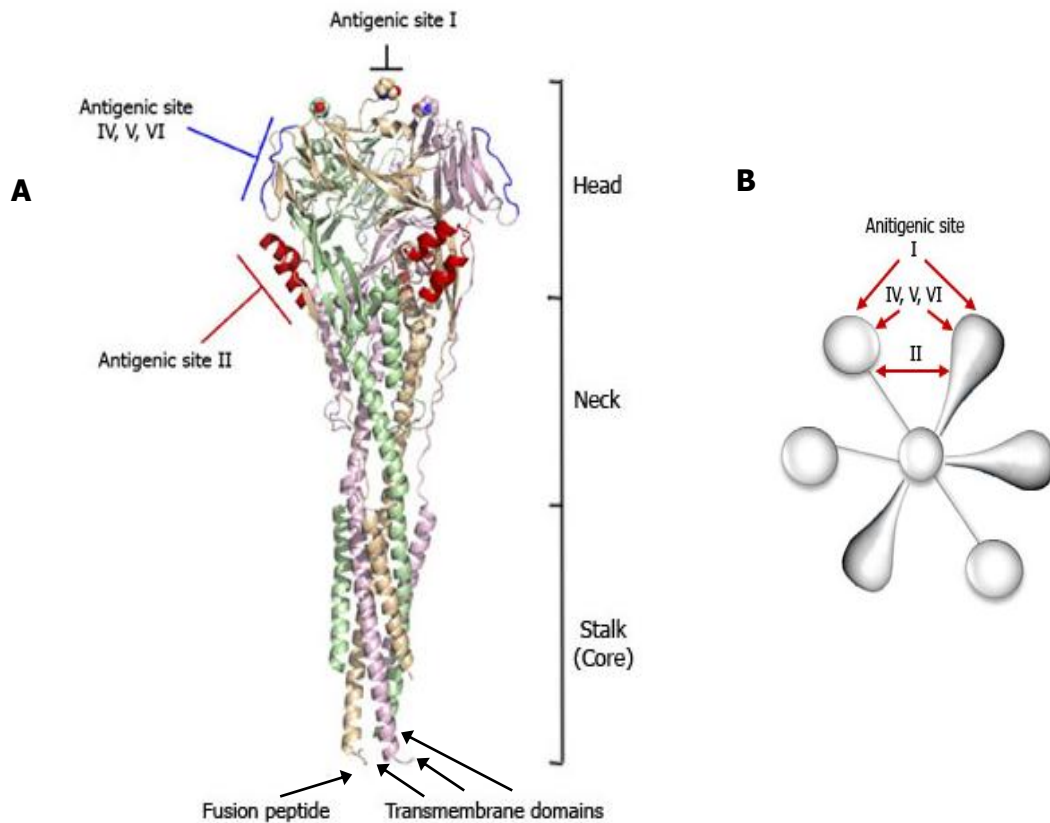


Figure 1.7: Model of the 3-D structure of the hRSV F glycoprotein (A) and a full-length F rosette (B).

[Modified from original by Calder *et al.* (2000), Morton *et al.* (2003) and McLellan *et al.* (2011)]

(A) The trimeric F glycoprotein, depicted as polypeptide ribbons with each F2/F1 monomer in a different color, is divided into head, neck and stalk (core) regions. The base of the stalk contains the three transmembrane domains and three fusion peptides. Antigenic site II and antigenic sites IV, V, VI are colored in red and blue, respectively. Antigenic site I is at the top of the head. (B) The full-length F rosette consists of three lollipop-shaped rods and three cone-shaped. The locations of all antigenic sites are shown.

Morphology of the hRSV fusion glycoprotein

The morphology of the full-length F glycoproteins of hRSV (F_{WT}) has been studied by the electron microscope (EM). F_{WT} was purified from recombinant vaccinia viruses infected cells expressing F_{WT} by immunoaffinity chromatography, followed by sucrose gradient centrifugation. The EM studies of F_{WT} revealed rosettes of rods which contain both inverted cone-shaped and lollipop-shaped rods (Figure 1.7B). However, the rods are mainly cone-shaped (70%) with only a minority lollipop-shaped. The wider ends of

both rod types project from the centre of the rosette, suggesting that the inner ends are hydrophobic membrane anchors which facilitate aggregation. The size of both rods is 19 nm in length and 6 nm in width. The length of the stem is 10 nm for the lollipop-shaped rods. The end views of both types is triangular which is consistent with the full-length F glycoprotein which usually forms a trimer (Calder *et al.*, 2000).

Conversely, preparations of a mutated F glycoprotein lacking the transmembrane region and cytoplasmic tail or a mutant anchorless F glycoprotein (F_{TM-}) mainly contained unaggregated cone-shaped rods the end views of which were the same as the F_{WT} molecules (triangular), suggesting that aggregation of the cones is dependent on the membrane anchor. The anchorless F glycoprotein was sometimes found in rosettes which contained predominantly lollipop-shaped rods in contrast to the full-length F glycoprotein rosettes which were mostly cone-shaped rods (Calder *et al.*, 2000). The anchorless F glycoprotein completely cleaved with trypsin at both site I and II also formed rosettes with a high amount of lollipop-shaped rods. A high proportion of unaggregated cone-shaped rods observed in the untreated anchorless F glycoprotein was predominantly uncleaved F_0 and $F_{\Delta 1-109}$, an intermediate cleaved only at cleavage site I (after residue 109). Trypsin treatment resulted in the formation of rosettes and it was suggested that this was due to exposure of the fusion peptides in the anchorless F glycoprotein. In line with this, the removal of the first portion of the fusion peptide leads to inhibition of the anchorless F molecule aggregation (Ruiz-Arguello *et al.*, 2004).

Inhibition of cleavage at site I, by two amino acids substitution (R108N/R109N), results in a low proportion of aggregated molecules and an increase of unaggregated (uncleaved) F_0 molecule. Inhibition of cleavage at site II, by the deletion of four amino acids (residues 131-134), results in the appearance of individual cone-shaped rods, indicating that the site II is necessary to aggregate the anchorless F molecules (Ruiz-Arguello *et al.*, 2002).

From these findings, it is suggested that the cone-shaped molecule represent the pre-activated (uncleaved) F glycoprotein which, in the full length form, aggregate into rosettes via their hydrophobic transmembrane anchors. Cone-shaped forms of molecules lacking the transmembrane region are thus found only as monomers.

Lollipop shaped molecules are the post-activated (cleaved) structures in which the hydrophobic fusion peptide is exposed. Lollipop shaped forms of anchorless F may form rosettes aggregated via the fusion peptide (Gonzalez-Reyes *et al.*, 2001; Ruiz-Arguello *et al.*, 2002).

Taken together, these observations suggest that the activation of the F glycoprotein by cleavage at both sites might be important in exposure of the fusion peptide which plays a particular role in fusion process. The inhibition of cleavage at either site I or II of the F glycoprotein has been found to block the formation of syncytia, suggesting that membrane fusion has to be promoted by cleavage at both sites (Gonzalez-Reyes *et al.*, 2001).

Epitope mapping of the fusion protein

Several anti-F monoclonal antibodies (MAbs) have been used in identifying and mapping epitopes on the F molecule. There are three types of the epitopes identified according to their biological activity: neutralizing and fusion-inhibiting epitopes, neutralizing epitopes and non-neutralizing epitopes (Walsh *et al.*, 1986). Using competitive binding assays with 15 MAbs, four antigenic domains (A, B, C, and D) were identified. Antigenic site A and B are recognized by MAbs with potent neutralizing and fusion activities. MAbs with only neutralizing activity is bound to antigenic site C, whilst antigenic site D is recognized by MAbs without neutralizing and fusion-inhibiting activity (Trudel *et al.*, 1987b).

Similar studies by Beeler and van Wyke Coelingh (1989) were largely in agreement with that of Walsh *et al.* (1986) and Trudel *et al.* (1987b) recognizing antigenic domains (A, B and C) and a potential bridge site (AB). Garcia-Barreno *et al.* (1989) reported five non-overlapping antigenic areas (Ia, Ib, II, III and IV) from 14 anti-F MAbs. The antigenic site II and IV correspond with site A (Trudel *et al.*, 1987b) and C (Arbiza *et al.*, 1992), respectively. Lopez *et al.* (1998) identified further antigenic sites V and VI from 12 neutralizing anti-F Mabs.

The location of each antigenic site is mapped on the primary structure of the F molecule by

(i) Testing the reactivity of monoclonal antibodies (Trudel *et al.*, 1987a; Bourgeois *et al.*, 1991; Arbiza *et al.*, 1992) or polyclonal antibodies (Scopes *et al.*, 1990) with synthetic peptides or with protein fragments expressed in bacteria (Martin-Gallardo *et al.*, 1991; Naval *et al.*, 1997). This first method has the limitation of mapping only linear epitopes.

(ii) Identifying amino acid residues which are important for epitope integrity from virus mutants which escape neutralization selected by growing and passaging viruses in the presence of individual anti-F MAbs (Lopez *et al.*, 1990; Arbiza *et al.*, 1992; Lopez *et al.*, 1998).

(iii) The two complementary procedures have been combined identifying epitopes initially by sequencing escape mutants selected by anti-F MAbs and confirming the position of the antigenic sites by binding to synthetic peptides which contain the same mutation as the resistant viruses (Arbiza *et al.*, 1992).

Using identification of escape mutants, epitopes in antigenic site I are located in the centre of the cysteine rich-region (Lopez *et al.*, 1998). Epitopes in antigenic site II involve residues 255 – 275 which contain a helix-loop-helix structure (Arbiza *et al.*, 1992; Lopez *et al.*, 1993; Toiron *et al.*, 1996). In mapping of antigenic site II by synthetic peptides, it was found that antibody reactivities were dependent on the length of peptide. The antigenicity of a 61 residue peptide (aa 215-275) of the F1 subunit was higher than a shorter 41 (aa 235-275) and 21 (aa 255-275) residue peptides. F215-275 peptide contains a high content of ordered structures with two predicted α -helices and a high resistance to trypsin digestion compared to peptides F235-275 and F255-275. Taken together, these observations suggest that a particular folded conformation was required for efficient antibody binding in this region (Arbiza *et al.*, 1992; Lopez *et al.*, 1993). Antigenic sites IV, V and VI clustered near the carboxy-terminal end of the cysteine rich-region (Arbiza *et al.*, 1992; Lopez *et al.*, 1998).

These antigenic regions were not only mapped to the primary structure of F molecule, but they were also located on the 3D structure of F glycoprotein by two methods. Firstly, the binding of antibodies to the anchorless F glycoprotein (soluble rod) and full-length F glycoprotein (rosettes) was studied by the EM. The binding of antibody in the rosettes showed the same position as in the cone-shaped soluble rods (Calder *et al.*, 2000). Secondly, the antigenic sites were located by sequence on the RSV-F model

(Smith *et al.*, 2002; Morton *et al.*, 2003). The data from both methods agreed (Figure 1.7). Antigenic site I is at the top of the head in the 3D structure or at the distal end of the rods in the rosettes. Antigenic site II is at the base of the head in the F model or the base of the head region of rods under the EM. Antigenic sites IV, V and VI are located on the side of the head in the model or the side of the rods in the aggregated of lollipop- and cone-shaped rods.

Function of the F glycoprotein

The hRSV F glycoprotein is thought to play a major role in allowing the penetration of the virus nucleocapsid into the host cell by membrane fusion. This conclusion is supported by similarities of the sequences and structures of hRSV F glycoprotein related to the fusion proteins of other paramyxoviruses (Collins *et al.*, 1984; Spriggs *et al.*, 1986), the ability of monoclonal antibodies against the hRSV F glycoprotein to neutralize infectivity and block the cell-cell fusion in tissue culture (Walsh and Hruska, 1983) and the ability of HR2 peptides and small molecular weight inhibitors of fusion to block infectivity (Lambert *et al.*, 1996; Cianci *et al.*, 2004a; Cianci *et al.*, 2004c; Douglas *et al.*, 2005; Bond *et al.*, 2007; Luttick *et al.*, 2007; Bonfanti *et al.*, 2008).

The F glycoprotein is not only responsible for the viral entry into a host cell by fusion, but it also mediates the syncytial formation which is the major characteristic of hRSV cytopathic effect (CPE) and is a route for viral spread (Merz *et al.*, 1980). The hRSV F glycoprotein is able to form syncytia without other proteins (Kahn *et al.*, 1999), whereas most paramyxoviruses require both F glycoprotein and the attachment of the HN for fusion. However, studies have shown that there is an increase of syncytial formation efficiency when G and SH proteins are coexpressed with the F glycoprotein (Heminway *et al.*, 1994).

Besides fusion and the syncytium formation, it has been suggested that F glycoprotein is able to facilitate viral attachment. hRSV subgroup B strain (hRSV B1/cp-52) lacking both G and SH proteins due to a large deletion is able to infect tissue culture cells and attach to cells via cell surface glycosaminoglycan (GAG) (Feldman *et al.*, 2000). In addition, soluble heparin has been shown to block the attachment of the hRSV- F glycoprotein as well as the G glycoprotein (Karger *et al.*, 2001). These studies indicate that the F glycoprotein could be a mediator of both attachment and infectivity.

1.5 The hRSV replicative cycle

1.5.1 hRSV binding

The G and F glycoproteins have been shown to be involved in the binding of virus to the host cells; however, the cellular receptor (s) involved has not been characterized. Several methods (Dimmock *et al.*, 2007) have been used to identify proposed receptors for the hRSV attachment as follows.

- (i) Competition by soluble candidate receptors incubated with hRSV before inoculation, leading to inhibition of the viral infection.
- (ii) Inhibition of viral growth by antibodies against candidate receptors applied to cells before viral exposure.
- (iii) Silencing of candidate receptor expression by RNA interference (RNAi).
- (iv) Expression of candidate receptors in nonpermissive cells, leading to susceptibility to hRSV infection.

Glycosaminoglycans (GAGs) have been identified as receptors for binding of G and F glycoproteins (Hallak *et al.*, 2000b; Techaarpornkul *et al.*, 2001). GAGs are unbranched polysaccharide chains consisting of repeating disaccharide units of hexuronic acid and hexosamine with different post-synthetic modifications such as sulphation. Hexuronic acid may be either glucuronic acid or iduronic acid and hexosamine may be either glucosamine or galactosamine depending on the GAG types (Hallak *et al.*, 2000a; Hallak *et al.*, 2000b).

There are seven types of GAGs, five of which are present on the surface of most cells. These are heparan sulphate (HS), hyaluronic acid (HA) and chondroitin sulphate A, B and C (CS-A, B, and C). The other two types are heparin and keratan sulphate present only on mast cells and keratinocytes, respectively (Hallak *et al.*, 2000a). All of GAGs are connected to transmembrane core proteins, except HA which is secreted and may be bound to the cell surface mediated by CD44 (Knudson and Knudson, 1993). The functions of CD44 are involved in cell – cell interaction, adhesion and migration (Pasonen-Seppanen *et al.*, 2012).

The composition of HS is glucuronic acid or iduronic acid connected to *N*-acetylglucosamine resembling heparin, although heparin contains a higher degree of

sulphation than HS (Powell *et al.*, 2004). CS-B also contains iduronic acid, but is linked to *N*-acetylgalactosamine and modified by sulphation at carbon 4. CS-A and CS-C consist of glucuronic acid linked to *N*-acetylgalactosamine. The sulphation of CS-A and CS-C occur on carbon 4 and carbon 6, respectively.

Several studies have reported that preincubation of hRSV with heparin inhibits viral infection *in vitro* (Krusat and Streckert, 1997; Bourgeois *et al.*, 1998; Martinez and Melero, 2000). In addition, HS and CS-B also block hRSV infection, indicating that GAGs containing iduronic acid are required for hRSV infection (Hallak *et al.*, 2000a). Apart from the composition of iduronic acid, N-sulphate and a minimum length of 10 saccharides in the structure are necessary for the interaction between hRSV and GAGs (Hallak *et al.*, 2000b). Although interaction of hRSV with GAGs has been shown to be important for the viral infection, hRSV replication in GAG-deficient cells is not completely inhibited, being reduced by only 80%. This suggests that not only GAGs are involved in virus binding and that other cellular receptors may play a role (Hallak *et al.*, 2000a).

CX3CR1, a receptor of the CX3C chemokine fractalkine Fkn, has also been found to facilitate hRSV infection via the G glycoprotein. Both the G and Fkn proteins contain heparin-binding domains and a CX3C motif and both are large glycoproteins consisting of an intracellular, transmembrane and extracellular domain. The G glycoprotein binds to CX3CR1 via its CX3C motif and to heparin through heparin-binding domains. hRSV infection in cells expressing CX3CR1 has been reported to be inhibited by the addition of heparin or antibodies to CX3CR1 or peptide containing a CX3C motif, suggesting that the CX3CR1 and GAGs are receptors for hRSV infection (Tripp *et al.*, 2001).

Surfactant protein A (SP-A) present in the epithelial lining of the lung has been shown to attach G glycoprotein. SP-A is a member of the C-type lectin family called collectins which are multimeric glycoproteins with carbohydrate recognition domains connected to collagen stalks. Collectins function as immune system molecules that bind to surface carbohydrates of inhaled pathogens (Haagsman, 1998). The carbohydrate recognition region of the SP-A has been shown to bind to a carbohydrate moiety of the G glycoprotein. Enhanced hRSV replication correlates with increased concentration of the

SP-A in Hep-2C cells, indicating that binding of hRSV may be augmented by SP-A (Hickling *et al.*, 2000). However, the SP-A has also been found to be involved in viral clearance (see details in 1.9.1).

In addition to the candidate receptors bound by the G glycoprotein, the F glycoprotein can bind to RhoA (a small GTP binding protein), which is important for the formation of syncytia (Gower *et al.*, 2001), and also attaches to intercellular adhesion molecule-1 (ICAM-1) which is found on the surface of epithelial cells (Behera *et al.*, 2001). Likewise, nucleolin expressed on the surface of many cell types has been recently shown to be a receptor for hRSV binding via the F glycoprotein (Tayyari *et al.*, 2011). The significance of these multiple receptors in entry and infection of hRSV remains to be determined.

1.5.2 hRSV entry by endocytosis

There are several different mechanisms of internalization by endocytosis involved in virus entry as shown in Figure 1.8. Phagocytosis is involved in the uptake of large particles and is used by specialized cells such as macrophages and amoeba. Pinocytosis, the internalization of fluid and solutes, is further categorised into 2 subgroups: dynamin-independent and dynamin-dependent entry. Macropinocytosis, lipid raft-mediated endocytosis, non-clathrin/non-caveolar-mediated endocytosis are dynamin-independent. Caveolar endocytosis and clathrin-mediated endocytosis require dynamins (Mercer and Helenius, 2009).

Once inside the cell, material internalized within endocytic vesicles progresses through the endosome network. Early endosomes are located in the periphery of the cytoplasm. These firstly develop into maturing endosomes and then into late endosomes, which fuse with lysosomes to generate endolysosomes in which degradation processes occur. Dense core lysosomes form the end point of degradation and await fusion with further incoming late endosomes. Incoming membrane components are recycled back to the plasma membrane (Mercer *et al.*, 2010).

Endocytosis is a process which depends on energy; therefore, it can be interrupted by the inhibition of energy production, for instance, exposure to metabolic inhibitors (e.g. sodium azide) or to low temperatures (Punnonen *et al.*, 1998; Atkinson *et al.*, 2002).

Sodium azide has been reported to interfere with the entry of adenovirus (Svensson and Persson, 1984) and influenza A virus (Nussbaum and Loyer, 1987) into cultured cells, but there is not any effect on that of hRSV (Srinivasakumar *et al.*, 1991). These early findings suggested that endocytosis is not involved in the entry of hRSV, whereas both adenovirus and influenza require endocytosis for penetration through the plasma membrane. However, more recently, caveolar (Werling *et al.*, 1999) and clathrin-mediated endocytosis (Kolokoltsov *et al.*, 2007; Gutierrez-Ortega *et al.*, 2008) has been found to be involved in the entry of hRSV in dendritic cells and HeLa cells, respectively.

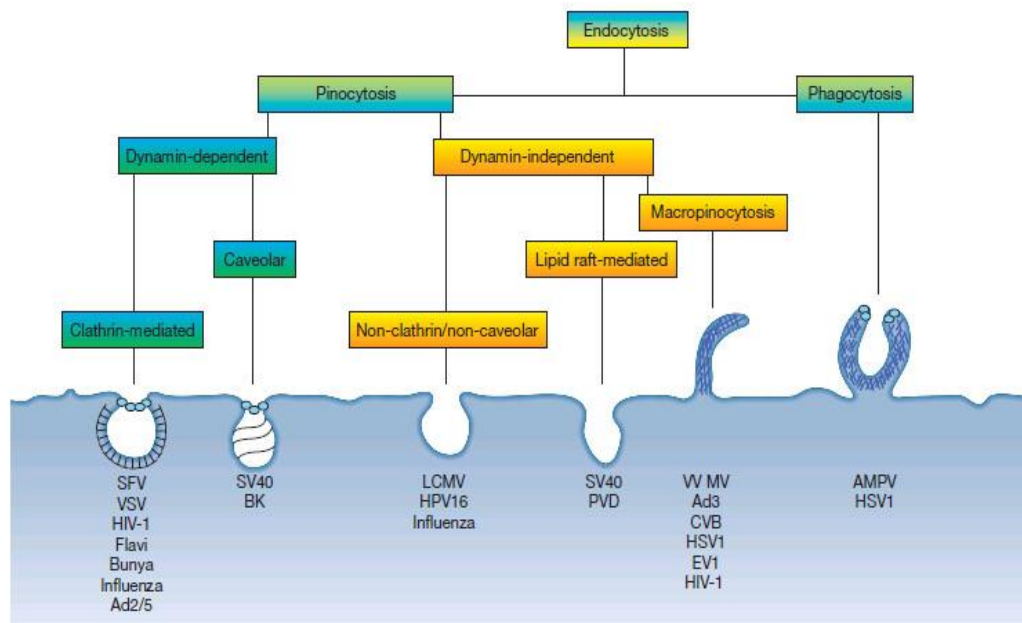


Figure 1.8 Diagram of endocytic pathways used by viruses

[Taken from Mercer and Helenius (2009)]

Viruses shown in this diagram are semliki forest virus (SFV); vesicular stomatis virus (VSV); human immunodeficiency virus 1(HIV-1); flaviviruses (Flavi); bunyaviruses (Bunya); influenza virus (Influenza); adenovirus 2/5 (Ad2/5); simian virus 40 (SV40); BK virus (BK); human papilloma virus 16(HPV16); lymphocytic choriomeningitis virus (LCMV); polyomavirus (PVD); vaccinia virus mature virion (VV MV); adenovirus 3 (Ad3); coxsackievirus B (CVB); herpes simplex virus 1 (HSV1); echovirus 1(EV1) and Acanthamoeba polyphaga mimivirus (AMPV). Dynamins are indicated as small blue circles at the neck of forming endocytic vesicles. The blue lines represent actin.

Caveolar endocytosis (Caveolae)

Caveolae contain oligomerized caveolin molecules associated with cholesterol and sphingolipids. These form spherical or flask-shaped vesicles of approximately 70 nm in diameter by invagination of the plasma membrane with a neck region composed of dynamin (Stan, 2002; Nichols, 2003). Dynamin is a GTPase responsible for scission of newly formed vesicles from the membrane (Henley *et al.*, 1999). Hence, budding of caveolae into the cytoplasm is believed to occur at the plasma membrane.

Caveolae are found on the surface of many mammalian cell types, but are highly abundant in specific cell types such as adipocytes, endothelial cells, fibroblasts and smooth muscle cells (Parton and Simons, 2007). Their composition, appearance, and function depend on cell type. For example, caveolae appear as grape-like structures or single indentations in epithelial cells, but form clusters or linear rows of multiple units in muscle cells (Parton *et al.*, 1997; Pelkmans and Helenius, 2002).

The involvement of caveolae in the uptake of hRSV in dendritic cells has been reported. The inhibition of caveolae using phorbol myristate acetate and filipin has been shown to block the presentation of the hRSV antigen by dendritic cells, indicating that the uptake of hRSV is mediated by caveolae in these cells. These findings have been confirmed in the same cells by investigating the co-localization of hRSV and caveolae using mAbs against hRSV F glycoprotein and caveolin-1, respectively. Both hRSV and caveolae co-localized at the cellular surface 5 minutes after infection and in the cytoplasm after 30 minutes. The additions of inhibitors involved in blocking other mechanisms of endosome formation such as the mannose receptor (mannan), macropinocytosis (cytochalasin D) and clathrin-mediated endocytosis (amiloride) had no effect in the hRSV uptake of dendritic cells, suggesting that dendritic cells require caveolae in uptake of hRSV (Werling *et al.*, 1999).

Clathrin-mediated endocytosis

Clathrin-mediated endocytosis is a process involving the formation of clathrin-coated pits and vesicles on the cytoplasmic side of the plasma membrane which are found in all eukaryotic cells. This process mainly mediates the internalization of extracellular fluid, receptors and ligands (Mellman, 1996).

Clathrin occurs in the cytoplasm and is divided into two types, clathrin heavy and light chains. It forms a soluble clathrin triskelion which consists of three clathrin heavy and three clathrin light chains. The structure of the triskelion contains three bent limbs radiating from a centre. Triskelions do not directly interact with cargo receptors or with membrane. They bind to adaptor proteins (e.g. AP2) and cargo adaptors (e.g. epsin) which are produced in the cytoplasm and recruited to clathrin-coated vesicle formation sites. The process of this formation consists of five stages (McMahon and Boucrot, 2011).

(1) Initiation is the formation of a membrane invagination called a clathrin-coated pit. FCH domain only proteins (FCHO) bind to phosphatidylinositol-4,5-bisphosphate (PtdIns(4,5)P₂)-rich zones of the plasma membrane, EGFR pathway substrate 15 (EPS15) and intersectins to initiate the pit formation.

(2) Cargo selection is the recruitment of adaptor protein 2 (AP2), transmembrane receptors and cargo-specific adaptor proteins. The AP2 is an heterotetrameric complex which contains α , β 2, μ 2 and σ 2 subunits and plays a role in binding to PtdIns(4,5)P₂, receptors, cargo, cargo-specific adaptor proteins and clathrin (Collins et al., 2002; Kelly et al., 2008). Different cargo-specific adaptor proteins are recruited by different receptors.

(3) Clathrin coat assembly is the recruitment of clathrin triskelia by the AP2 and by cargo-specific adaptor proteins to polymerize in hexagons and pentagons and form a clathrin coat around the pit (a clathrin-coated vesicle).

(4) Vesicle scission is budding of vesicles mediated by the GTPase dynamin recruited at the vesicle neck. The GTP hydrolysis induces membrane scission.

(5) Uncoating and clathrin component recycling is the disassembly of the clathrin coat. The uncoated vesicles fuse with their target endosome and components of the clathrin machinery are released back into the cytoplasm for recycling.

Clathrin-mediated endocytosis has been implicated in the entry of hRSV into HeLa cells by RNA silencing techniques (siRNA). The inhibition of genes related to clathrin-mediated endocytosis, such as the light chain subunit of clathrin and the alpha subunit of the AP2, significantly blocks hRSV infection. These results have been confirmed by expression of dominant-negative mutants for EPS15 and treatment with chlorpromazine, both of which result in the inhibition of the hRSV infection (Kolokoltsov *et al.*, 2007). Chlorpromazine has been reported to cause the loss of clathrin and the AP2 at the cell surface and their reappearance on endosomal membranes (Wang *et al.*, 1993).

Monodansylcadaverine (MDC) inhibits the polymerization of clathrin (Nandi *et al.*, 1981). In human epithelial cells, localization of hRSV antigens in the presence of MDC was observed on the surface of infected cells after incubation with anti-RSV antibodies for 0, 30 and 60 min using indirect immunofluorescence and confocal laser scanning microscopy. In contrast, hRSV antigens were located inside the cells after incubation

for 30 and 60 min when infected cells were treated with caveolae inhibitor (methyl-beta-cyclodextrin, MBCD). These results suggest that caveolae are not involved in hRSV uptake in non-dendritic cells, whereas clathrin-mediated endocytosis is.

1.5.3 hRSV membrane fusion

In line with other members of the *Paramyxoviridae*, hRSV membrane fusion has been found to occur through a pH-independent mechanism being resistant to treatment with lysosomotropic agents ammonium chloride and chloroquine which increase pH in the endosome (Srinivasakumar *et al.*, 1991; Kolokoltsov *et al.*, 2007). In contrast, the fusion of Vesicular Stomatitis Virus was fully inhibited by both drugs (Kolokoltsov *et al.*, 2007). Ammonium chloride also significantly reduced infection of Influenza A virus (Nussbaum and Loyter, 1987) and adenovirus (Svensson and Persson, 1984). These findings suggest that, unlike the paramyxoviruses, these three viruses enter host cells via a pH-dependent process.

F glycoproteins of most paramyxoviruses expressed on the cell surface at neutral pH induce cell-cell fusion and syncytium formation (Smith *et al.*, 2009). Triggering of membrane fusion, however, requires a homotypic attachment protein. This is so for measles virus, Newcastle disease virus and Hendra (Stone-Hulslander and Morrison, 1997; Bishop *et al.*, 2008; Corey and Iorio, 2009). For hRSV, membrane fusion, both virus-cell and cell-cell, is mediated by the F glycoprotein without the G glycoprotein. Several studies have reported that recombinant hRSV lacking SH and G genes retain infectivity and syncytium formation in certain cell lines (Karron *et al.*, 1997; Techaarpornkul *et al.*, 2002).

Despite differences in triggering, the process of hRSV fusion is thought to be similar to that of other paramyxoviruses. The activation of the F glycoprotein involves a shift from the pre-fusion form to the post-fusion form. This process has been proposed to occur in proximity to the cell membrane starting with the exposure of the hydrophobic fusion peptide at the N-terminus of the F1 polypeptide and resulting in its insertion into the host cell membrane and the formation of a prehairpin intermediate. This forms a protein bridge between the two membranes, the C-terminus being embedded in the viral membrane. Then, a conformational change occurs by refolding of the pre-fusion F glycoprotein to form the 6HB structure as described in section 1.4.10 (Lawless-

Delmedico *et al.*, 2000; Matthews *et al.*, 2000). As a result, the viral membrane and the host cell membrane are brought close to each other. The two membranes eventually fuse by mixing of lipid components and the nucleocapsid is released into the cytoplasm (Melero, 2007).

1.5.4 hRSV transcription

The template for hRSV transcription is the RNA genome encapsidated with N protein. There is a single promoter located at the 3' terminus which is 44 nucleotides in length and includes the leader region (Dickens *et al.*, 1984; Collins *et al.*, 1991). The RNA-dependent RNA polymerase complex composed of N, P, L and M2-1 proteins mediate viral transcription and replication both of which occur in the cytoplasm of infected cells. Three proteins (N, P and L) are required for sequential transcription of the genes on the monopartite genomic RNA guided by the GS and GE sequences (Kuo *et al.*, 1996b; Kuo *et al.*, 1997). The M2-1 is involved in the elongation and antitermination activity (Collins *et al.*, 1995; Collins *et al.*, 1996; Hardy and Wertz, 1998; Fearn and Collins, 1999b; Hardy *et al.*, 1999).

The polymerase is thought to comprise the large protein (L) and phosphoprotein (P) in a minimal complex. The functions of this complex are promoter recognition, RNA synthesis and mRNA processing (Mazumder and Barik, 1994). The L-P complex has been shown to be sufficient for the activity of RNA synthesis *in vitro*; nevertheless, within host cells actin and profilin are also important in viral RNA transcription (Burke *et al.*, 1998; Burke *et al.*, 2000). Actin binds to the RNA template via its divalent-cation-binding domain and recruits profilin which acts as a transcriptional cofactor (Harpen *et al.*, 2009).

Initiation of hRSV transcription requires 11-nt at the 3' terminus of the leader (polymerase binding site), a U-rich region at the end of the leader and the gene start sequence (GS) (Cowton *et al.*, 2006). The correct spacing among the three regions has been reported to be important in viral transcription (Fearn *et al.*, 2000; McGivern *et al.*, 2005). After initiation, the mRNA is capped and methylated at the 5' end (Liuzzi *et al.*, 2005) and the polymerase continues to transcribe along the genome, elongates to the end of the gene and polyadenylates the 3' end of mRNA when its active site is positioned on the U tract of GE sequence. Then, the nascent mRNA is released.

After termination of transcription at the GE sequence, the polymerase is believed to scan the intergenic region to locate the next GS sequence. Extending the length of the intergenic regions located between the GS and GE sequences has been shown to have no effect on the efficient scanning activity of polymerase (Bukreyev *et al.*, 2000). For the overlapping region of the M2 and L genes, the polymerase has been reported to transcribe to the GE sequence of the M2 gene and then scan backwards to reinitiate at the GS sequence of the L gene (Fearn and Collins, 1999a).

Differences in the intergenic junctions have been reported to regulate the termination of hRSV transcription. It has been shown that the gene junctions of the NS1/NS2, NS2/N, M2/L and L/trailer inefficiently terminate transcription, whereas the intergenic region of the N/P, P/M, M/SH, SH/G and G/F effectively terminate. The most efficient termination was at the SH/G gene junction. Terminations at gene junctions are independent of the absence or presence of the M2 protein, except for the F/M2 gene junction. In the absence of the M2 protein, efficient termination occurs at F/M2; however, the levels of readthrough transcripts are higher in the presence of the M2 protein. As only F glycoprotein will be translated from the readthrough. This indicates that the M2 protein may be responsible for negative feedback regulation of its own expression (Hardy *et al.*, 1999).

The polymerase tends to dissociate from the template at intergenic regions and can only re-initiate transcription at the 3' end of genome due to the location of promoter. Consequently, there is a 3' to 5' gradient of gene expression with the number of transcripts from 3' end of genome being higher than that of genes located towards the 5' end (Kuo *et al.*, 1996a; Hardy and Wertz, 1998; Krempf *et al.*, 2002). When complete, hRSV transcription results in ten mono-cistronic mRNAs with 5' cap structures and 3' poly (A) tails which are then translated by the machinery of host cell.

1.5.5 hRSV replication

RNA replication involves the synthesis of a full-length positive-sense RNA (anti-genome) which is complementary to the genome. The anti-genome serves as the template for the production of progeny genomes. hRSV RNA replication is controlled by the M2-2 protein which is responsible for the transition from transcription to replication (Birmingham and Collins, 1999; Jin *et al.*, 2000a).

During replication, the anti-genome is synthesized without guiding by the GS and GE sequences. However, it contains the trailer-complement (TrC) promoter of 155 nucleotides in length at its 3' end and acts as a promoter for synthesis of new full-length negative-sense genomes. The replication level from the TrC promoter is higher than that from the genomic leader, resulting in an imbalance between antigenome and genome in infected cells (Mink *et al.*, 1991; Fearn *et al.*, 2000).

It has been recently shown that the complete trailer increases promoter activity, facilitates virus growth by enabling optimal genome production and subverts stress granule formation when comparing with mutant recombinant viruses containing truncated trailer sequences or with leader-complement sequence substituted for the trailer region (Hanley *et al.*, 2010).

Both the anti-genome and genome are encapsidated with N proteins during synthesis. It is thought that the encapsidation reduces the activation of host anti-viral defense and also protects these RNAs, which lack stabilization by 5' cap and 3' poly (A) tails, from degradation (Collins and Melero, 2011).

1.5.6 hRSV assembly and release

Following production of viral proteins and genomic RNA, assembly of new virions occurs in the cytoplasm of target cell without the involvement of the nucleus. The M protein facilitates viral assembly by interacting at the plasma membrane with both the nucleocapsids in cytoplasm (Ghildyal *et al.*, 2002; Marty *et al.*, 2004; Li *et al.*, 2008) and the envelope glycoproteins on plasma membrane (Henderson *et al.*, 2002; Ghildyal *et al.*, 2005). In polarized cells, assembly and budding of hRSV occurs at the apical surface (Roberts *et al.*, 1995; Zhang *et al.*, 2002).

It has been reported that G, F and SH glycoproteins are not involved in viral release (Batonick *et al.*, 2008). There is no any effect on the release of hRSV from polarized epithelial cells when individual G, F, SH glycoproteins or pairs of these genes are deleted. However, recombinant hRSV lacking the F glycoprotein has recently been shown to reduce the co-localization between the G and N proteins and between the SH and N proteins at the plasma membrane. Furthermore, the G glycoprotein is not localized at the surface of cells infected with recombinant hRSV lacking the F

glycoprotein gene. These findings fit with those of Oomens *et al.* (2006) who found no the G glycoprotein localized to viral filaments at the plasma membrane in cells infected with recombinant hRSV lacking the cytoplasmic tail of the F glycoprotein (FACT), whereas it was present in wildtype hRSV. Filamentous structures were rarely present in the cells infected with FACT. Deletion of the F glycoprotein gene also resulted in a decrease in the incorporation of the G and SH proteins into budded virions and the removal of the G glycoprotein gene reduced the amount of SH protein incorporated into released virions (Batonick and Wertz, 2011). Taken together, these results suggest that the F glycoprotein may be involved in protein sorting at the plasma membrane and that hRSV assembly requires expression of both the F and G genes.

Several studies have shown that host cell cytoskeletal elements are involved in hRSV assembly and egress (Kallewaard *et al.*, 2005). Knockdown of profilin and vasodilator-stimulated phosphoprotein (a regulator of profilin and actin) with siRNAs inhibited hRSV release (Bitko *et al.*, 2003; Musiyenko *et al.*, 2007).

1.6 Transmission and pathogenesis of hRSV infection

Transmission of hRSV mainly occurs through close contact with infected patients or by contact with environment surfaces contaminated with respiratory secretions (fomites). Small aerosol particles are not a major route for the spread of hRSV infection. Families are thought to be the major cause of nosocomial hRSV infections. It has been reported hRSV can survive on skin for up to 20 minutes, on rubber gloves for 90 minutes and on countertops for 6 hours and can entry to the body by nose or eye (Hall *et al.*, 1975; Hall and Douglas, 1981).

Strict compliance with gown and glove precautions significantly reduces the spread of viral infections in hospital (Leclair *et al.*, 1987). Furthermore, careful hand washing and contact precautions may also limit the transmission of hRSV infection, especially during the seasonal epidemic. Hand washing agents reported to effective kill hRSV are 70% isopropanol and chlorhexidine-detergent solutions (Platt and Bucknall, 1985).

Infection of hRSV in humans has an incubation period of 4 – 5 days (Collins and Crowe, 2007). After entry, hRSV initially replicates in the nasopharyngeal epithelium and can spread to the lower respiratory tract within 1 – 3 days. Spread from upper to

lower respiratory tract is believed to occur by aspiration of secretion or cell-cell fusion along the respiratory epithelium lining the airways (Hoffman *et al.*, 2004; Johnson *et al.*, 2007). Besides airways and lung tissues, hRSV has been found to spread in circulating inflammatory cells and cells from blood (Domurat *et al.*, 1985; Krilov *et al.*, 1987; Panuska *et al.*, 1992).

After viral replication in the human respiratory epithelium, viral cytotoxicity and the immune response lead to manifestations of bronchiolitis and pneumonia. For bronchiolitis, there is obstruction of the bronchioles and alveoli caused by a combination of mucus, cell debris and inflammatory cells leading to air trapping. During pneumonia, the interalveolar walls thicken, resulting in infiltrating mononuclear cells and fluid into the alveolar spaces (Aherne *et al.*, 1970; Neilson and Yunis, 1990).

hRSV shedding in children with primary infection has been found to be longer than that in children experiencing secondary infection (Okiro *et al.*, 2010). hRSV was shed in children less than 2 years for an average of 9 days compared to 3.9 days in children aged 2-16 years (Hall *et al.*, 1976). In addition, viral shedding has been shown to be prolonged in immunocompromised individuals for weeks and even several months (Hall *et al.*, 1986; Cheng *et al.*, 2008).

1.7 Clinical features of hRSV infection

The clinical manifestations of hRSV infection range from mild to serious illness based on age. Mild illness or upper respiratory tract infection is a frequent presentation in healthy adults and older children with rhinorrhea, nasal congestion, pharyngitis, cough, low grade fever and acute otitis media. Chest X ray of this stage is normal. Severe symptoms usually occur only in primary hRSV infection among infants younger than 24 months, elderly patients, immunocompromised patients, or patients with chronic underlying diseases. The most serious lower respiratory tract diseases are life-threatening bronchiolitis and pneumonia (Ogra, 2004; O'Donnell, 2009).

Children with bronchiolitis firstly have mild symptoms followed by lower respiratory symptoms such as wheezing, dyspnea, tachypnea and poor feeding (Ruuskanen and Ogra, 1993; Hall, 2001). Radiographic manifestations of bronchiolitis are hyperexpansion with diffuse interstitial shadow and peribronchial thickening. Fine

crackles and a chest X ray of alveolar, segmental, or lobar consolidation occur in pneumonia patients (Simoes, 1999).

Late preterm infants (born between 34 – 36 weeks gestation) have been shown to be at greater risk of severe lower respiratory symptoms than full term babies due to immaturity of both humoral and cell-mediated immunity and also to incomplete lung development such as reduced expiratory air flow and diminished gas exchange (Friedrich *et al.*, 2006; Friedrich *et al.*, 2007). Both morbidity and mortality are substantially increased in late preterm infants compared with full term infants (Resch and Paes, 2011).

1.8 Epidemiology

hRSV is a major cause of respiratory tract infection in infants and children under 2 years of age with worldwide distribution. The highest incidence of serious illness (bronchiolitis or pneumonia) occurs between 6 weeks and 9 months of age (Simoes, 1999). Children with underlying risk factors are in a high-risk group of hRSV infection, for example, children with bronchopulmonary dysplasia (BPD) (Groothuis *et al.*, 1988), cardiac abnormalities (MacDonald *et al.*, 1982), and premature birth (Navas *et al.*, 1992). There are other risk factors which also may be involved in more severe illness including low socioeconomic status, crowding, exposure to smoking and family history of atopy and asthma (Simoes, 1999).

The prevalence of hRSV infection varies with season and region. In temperate zones outbreaks appear annually in the cold season, peaking in February – March (Kim *et al.*, 1973; Mufson *et al.*, 1973). In tropical and subtropical regions, hRSV epidemics occur year round, but peak during the rainy season (Spence and Barratt, 1968; Huq *et al.*, 1990; Vardas *et al.*, 1999). Recently, a systematic review and meta-analysis (1995 – 2009) has reported the incidence of hRSV infection caused acute lower respiratory infection (ALRI) in children younger than 5 years commonly occurs worldwide, but the incidence in developing countries is more than twice that of industrialised countries. Furthermore, hRSV is a major cause of mortality associated with ALRI after hospital admission (66,000 – 199,000 deaths in children in 2005), especially in developing countries (Nair *et al.*, 2010).

Reinfection with hRSV is common not only in children younger than 24 months, but also in healthy older children and adults. Studies have shown that healthy adults with recent natural hRSV infection can be re-infected by intranasal challenging repeatedly (Hall *et al.*, 1991). Nevertheless, the symptoms of reinfection are usually less severe than the previous infection. hRSV is also a cause of morbidity in elderly people (Fleming and Cross, 1993; Han *et al.*, 1999) and immunocompromised patients such as patients undergoing chemotherapy with underlying disorders of cellular immunity or following a bone-marrow or solid-organ transplantation (Englund *et al.*, 1988; Whimbey *et al.*, 1995).

1.8.1 hRSV subgroups

hRSV is comprised of two major subgroups (A and B) based on antigenic and genetic differences. Initially, hRSV was divided into three groups identified by monoclonal antibodies (MAbs) against the F, G and N proteins. They were group 1 (Long strain), group 2 (18537 strain) and group 3 (A2 strain) (Anderson *et al.*, 1985). Subsequently, group 1 and 3 were found to be similar and group 2 viruses were distinct (Anderson *et al.*, 1985). Based on neutralization studies and reactivity with anti-P, N, M, G and F MAbs, isolates similar to Long and A2 strains formed the A subgroup. Isolates similar to the 18537 strain formed the B subgroup (Gimenez *et al.*, 1984; Mufson *et al.*, 1985; Gimenez *et al.*, 1986; Morgan *et al.*, 1987). Using MAbs recognizing different viral proteins, several studies found the greatest variation between subgroups A and B was found in the G glycoprotein.

Subsequently, the nucleotide sequences of individual proteins in both subgroups were analysed confirming the split of isolates into two distinct subgroups. The hRSV Long and A2 strains are regarded as the prototype subgroup A viruses, whereas the hRSV 18537 and 8/60 strain are regarded as subgroup B prototypes (Sullender, 2000). The amino acid sequences of the NS1, NS2, N and F glycoproteins are highly conserved between subgroup A (A2 strain) and B (18537 strain) with 87 – 96% identity. The sequences of the G glycoprotein in Long strain share 94% identity with the A2 strain. Likewise, the sequence comparisons of the G glycoprotein within subgroup B (8/60 and 18537) showed only 2% amino acid differences (Sullender *et al.*, 1990).

In contrast, the ectodomain of the G glycoprotein shared only 53% amino acid identity between subgroups (A2 = subgroup A and 18537 = subgroup B) (Johnson *et al.*, 1987). Nonetheless, all isolates share a single highly conserved region in the G ectodomain (residues 164 - 174) which is proposed to be a functional domain for the attachment activity of the G glycoprotein (Johnson *et al.*, 1987; Johnson and Collins, 1988; Johnson and Collins, 1989). Similarly, A2 (A) and 8/60 (B) were divergent by 44% amino acid differences (Sullender *et al.*, 1990).

1.8.2 hRSV genotypes

Besides the major variation between subgroups A and B, antigenic and genetic variation has been reported to exist within each sub-group. Among a large panel of isolates of subgroup A viruses, Cane *et al.* (1994) observed 20% genetic diversity in the G gene with a high level of coding changes. The variability of the G gene has also been reported among subgroup B viruses with 9% amino acid differences occurring in the domains of the G glycoproteins flanking either side of the conserved region. The types of mutations were single amino acid substitutions, frameshifts and alterations of termination codons, resulting in different protein lengths (Sullender *et al.*, 1991). It has been thought that the genetic variability of the G glycoprotein may be caused by immunologic pressure likely from the host response. Genetic diversity of the G glycoproteins may contribute to the ease of hRSV reinfection (Sullender *et al.*, 1991). Prevalence studies of hRSV in several countries have shown fluctuation of the predominant strain between subgroup A and B. However, hRSV subgroup A was found to be more frequently predominant in most countries than subgroup B (Cane, 2001). Multiple genotypes, generally with representatives from both subgroups have been found to co-circulate in a single epidemic and different genotypes are predominant in each hRSV season (Cane *et al.*, 1994). In addition, a displacement of the predominant circulating genotypes (lineages) has been observed in consecutive hRSV epidemics, suggesting that this may help the viruses to escape from pre-existing immunity (Peret *et al.*, 2000).

In North America, the distribution of hRSV genotypes was evaluated during a single epidemic in 5 different communities from 1994 – 1995 (Peret *et al.*, 2000) using nucleotide sequencing of the G glycoprotein gene in both subgroups A and B viruses. Six genotypes of subgroup A (GA1 – GA3 and GA5 – GA7) and two genotypes of

subgroup B (GB3 and GB4) were detected. Subgroup A strains was predominant in four of five communities. Within each community, there were different predominant genotypes circulating. Genotypes GA5 and GA7 predominated in Winnipeg, GA1 and GB4 in Rochester, GA5 in Houston and GA1 in St. Louis.

In South Africa, the variability of the G glycoprotein gene was determined in 4 successive seasons from 1997 – 2000 (Venter *et al.*, 2001). Subgroup A strains was predominant in two epidemics, whereas subgroups A and B were equally co-circulated in other epidemics. There were four genotypes of subgroup A (GA5, GA7, GA2 and SAA1) and five genotypes of subgroup B (GB3, GB4, SAB1, SAB2 and SAB3) identified from isolates. One new subgroup A (SAA1 or South Africa A1) and three new subgroup B viruses (SAB1 – SAB3) were detected. Co-circulating with different genotypes was identified in each epidemic. Genotypes GA5, GB3 and SAB3 were detected over 4 seasons. In addition, a shift of genotypes and more variability were determined in subgroup A strains, whilst subgroup B strains was more stable.

Recently, the most prevalent genotypes in subgroup A are the genotypes GA2 and GA5 identified in most European countries and other geographic areas (Frabasile *et al.*, 2003; Sato *et al.*, 2005; Parveen *et al.*, 2006; Ostlund *et al.*, 2008; Reiche and Schweiger, 2009).

1.9 Immunology

The host immunological response to hRSV infection consists of innate and adaptive immunity. These responses may ameliorate or exacerbate the severity of infections.

1.9.1 Innate immunity

Innate immunity is a non - pathogen specific rapid host response which is initiated by recognition of pathogens via pattern recognition receptors (PRRs), including Toll-like receptors (TLRs), and other molecules such as surfactant protein (SP) in the lung. Up to 15 TLRs have been identified in mammals and recognize various pathogen molecules. For example, TLR3 and 7 recognize dsRNA and ssRNA, respectively (Alexopoulou *et al.*, 2001; Lund *et al.*, 2004). Some TLRs are present on the cell surface of monocytes (TLR4 and 5), whilst some of them are found in endosomes (TLR3, 7, 8 and 9). However, all TLRs can activate IFN induction leading to production of type I

interferons (IFN- α/β). IFN stimulates of the Jak-Stat signalling cascade, resulting in the expression of many different genes which are necessary for biological effects. Furthermore, type I IFNs induce the production of proinflammatory cytokines such as TNF- α , IL-1 and IL-6. In the lung airways, these cytokines stimulate alveolar macrophages and dendritic cells (DCs) to produce chemokines, leading to a recruitment of neutrophils and NK cells from the circulation to the site of infection. The release of cytokines and the influx of innate immune cells limit virus replication. Stimulation of dendritic cells facilitates the initiation of antigen specific T cell and B cell responses (Kohlmeier and Woodland, 2009).

For hRSV, the F glycoprotein has been found to be recognized by TLR4 and CD14 in human monocytes resulting in the production of proinflammatory cytokines including TNF- α , IL-6 and IL-12. Deficiency of TLR4 in mice is associated with persistence of hRSV infection when compared to controls (Kurt-Jones *et al.*, 2000). Both G and F glycoproteins of hRSV are also recognized by human surfactant proteins-A (SP-A) and only G glycoproteins by human SP-D (Ghildyal *et al.*, 1999; Hickling *et al.*, 1999). These surfactant proteins can be produced from the respiratory epithelium. Binding between the SP and viral proteins increases the uptake of hRSV by human peripheral blood mononuclear cells (PBMC) and human macrophages cell lines expressing SP-A receptors (Barr *et al.*, 2000).

Despite this, poor induction of type I interferons in human has been reported in the infection of hRSV compared to those of other respiratory viruses (Hall *et al.*, 1978; Roberts *et al.*, 1992). The NS1 and NS2 proteins have been shown to be involved in suppression of the IFN production (see details in section 1.4.1). The efficacy of IFN- α/β in hRSV infection remains uncertain. hRSV has been shown to be variably resistant to the effect of IFN- α/β in cell culture (Atreya and Kulkarni, 1999) and in mice (Merolla *et al.*, 1995; Guerrero-Plata *et al.*, 2005). There have also been conflicting reports of treatment with IFN- α in humans. For instance, Chipps *et al.* (1993) reported no differences of bronchiolitis symptoms or the duration of oxygen requirement between IFN- α treated children and untreated control groups. Whereas, Sung *et al.* (1993) found that IFN- α treatment improved the clinical course.

Secreted cytokines and chemokines are the important signals in activation of alveolar macrophages, NK cells and maturation of dendritic cells. Human alveolar macrophages have been reported to stimulate the production of TNF- α , IL-1 β , IL-6, IL-8, IL-10 and IL-12 following hRSV infection (Becker *et al.*, 1991; Panuska *et al.*, 1995). These cytokines subsequently modulate the activation and recruitment of other inflammatory cells such as neutrophils, natural killer (NK) cells and lymphocytes (McNamara and Smyth, 2002). The depletion of macrophages in mice has inhibited the stimulation and recruitment of NK cells and increased viral loads (Pribul *et al.*, 2008).

In the mouse model, NK cells activated by alveolar macrophages have been found to be primary sources for production of IFN- γ (Hussell and Openshaw, 1998). Natural killer T (NKT) cells, which are a subset of CD1d-restricted T cells co-expressing semi-invariant T-cell receptor and NK-cell markers (Brutkiewicz *et al.*, 2003), have been implicated in viral clearance, IFN- γ production and effective expansion of CD8⁺ T cells during hRSV infection (Johnson *et al.*, 2002).

DCs, the major antigen presenting cells, are present in the respiratory epithelium. They are activated by cytokines and migrate to the draining lymph nodes preceding the adaptive immune response. They are divided into two subsets, conventional DCs and plasmacytoid DCs (pDCs). The balance between the two DCs is essential for determining the outcome of hRSV infection. In mice, increased amounts of pDC have been shown to increase the levels of IFN- α and Th1 cytokines and also reduce pathophysiology of hRSV infection with a decrease of airway inflammation and mucus overexpression. In contrast, depletion of pDC has resulted in an increase of viral loads, Th2 cytokines production, airway inflammation and hyperresponsiveness (Smit *et al.*, 2006; Wang *et al.*, 2006; Smit *et al.*, 2008).

Innate immune response can be significant determinants of hRSV severity. In the nasopharyngeal aspirate of human infants, levels of IL-8, a potent neutrophil chemoattractant, has been associated with the severity of bronchiolitis (Smyth *et al.*, 2002). High levels of neutrophils have been found in bronchoalveolar lavage (BAL) fluids from hRSV infected infants with bronchiolitis (Everard *et al.*, 1994). A genetic polymorphism close to the IL-8 gene and associated with increased production of IL-8 is also correlated with disease severity (Hull *et al.*, 2000). In several studies,

polymorphisms involved in the recognition stage including TLR4, SP-A and SP-D genes have also been linked to susceptibility to severe hRSV infection (Lahti *et al.*, 2002; Lofgren *et al.*, 2002; Tal *et al.*, 2004; Mandelberg *et al.*, 2006; Lofgren *et al.*, 2010). Severe hRSV disease was found in mice lacking SP-A when compared to those with normal levels, suggesting SP-A is necessary for hRSV clearance (LeVine *et al.*, 1999).

1.9.2 Adaptive immunity

The adaptive immunological responses develop after primary infection requiring several days for production of immune effectors including antiviral cytokines, cytotoxic T cells and specific antibodies. Furthermore, immunological memory is also formed for rapid immune response when reinfections occur. Adaptive immunity can be divided into humoral and cell-mediated immunity (Welliver, 2008). The cell-mediated response predominantly functions in the clearance of viral infection, whereas the humoral response is principally associated with protective immunity in hRSV infection (McNamara and Smyth, 2002).

Cell-mediated immunity

Prolonged hRSV shedding for weeks to several months occurs in patients with defective cell mediated immune responses suggesting that cell-mediated immunity functions in the clearance of hRSV. There are two types of T lymphocytes involved in the cellular immune response, CD8⁺ cytotoxic T cells (CTL) and CD4⁺ T helper cells, and both play a role in both the protective and the immunopathogenic responses after hRSV infection. The CD4⁺ T helper cells can be categorised into two types based on functions, CD4⁺ regulatory T cells (Treg) and CD4⁺ T effector cells. Treg cells are necessary for controlling immune response to hRSV infection. In both humans and mice, Treg cells have been found to be increased in peripheral blood or lung after hRSV infection. The reduction of Treg cells resulted in enhanced disease severity in mice, suggesting that Treg cells play a role in modulating inflammation (Cusi *et al.*, 2010; Fulton *et al.*, 2010; Lee *et al.*, 2010). The CD4⁺ T effector cells consist of type 1 CD4⁺ T effector cells (Th1 cells) secreting IFN- γ , TNF- α and IL-2 which promote vigorous cytotoxic T cell responses. Type 2 CD4⁺ T effector cells (Th2 cells), characterized by secretion of IL-4, IL-5, IL-10 and IL-13, induce the production of IgE and eosinophilia (Romagnani, 1992; McNamara and Smyth, 2002). In addition to the Th1/Th2 paradigm, Th17 cells

are novel CD4⁺ T effector cells that secrete the IL-17 family cytokine involved in activating granulocytes and macrophages (Kurts, 2008). Increased numbers of Th17 cells were found in peripheral blood from human infants with hRSV bronchiolitis (Li *et al.*, 2012). CD4⁺ T cell responses to formalin-inactivated hRSV vaccine (FI-RSV) have been extensively studied, see details in section 1.10.2.

A number of studies have sought to establish the relative role of CD4⁺ and CD8⁺ cells in the mouse model of hRSV infection. In immunodeficient mice with persistent hRSV infections, the transfer of hRSV specific CTLs has been shown to clear viruses in the lung (Cannon *et al.*, 1987). Passive transfer of hRSV specific CD8⁺ or CD4⁺ lymphocytes into normal mice infected with hRSV has also been shown to reduce the shedding of hRSV, but pulmonary damage was exacerbated. Both antiviral and immunopathogenic effects were more pronounced with CD4⁺ compared to CD8⁺ cells (Cannon *et al.*, 1988; Munoz *et al.*, 1991; Alwan *et al.*, 1992). Depletion of both CD8⁺ and CD4⁺ lymphocytes in mice has prolonged hRSV replication, but with no evidence of illness. Together these studies suggest that, at least in mice, the host immune response is the main determinant of disease rather than viral cytotoxic effect (Graham *et al.*, 1991).

Immunization of mice with the recombinant virus expressing only the F glycoprotein activates a Th1 type response, whilst a Th2 type response is promoted by the immunization with recombinant G protein, suggesting that the G epitope may be responsible for vaccine-augmented disease (see section 1.10.2) (Alwan *et al.*, 1994; Hancock *et al.*, 1996). Moreover, the secreted form of the G protein has been found to be much more capable of promoting eosinophilia compared to the membrane-bound G protein, increasing IL-5, IL-13 (Johnson and Graham, 1999). The secreted F glycoprotein can also induce an intermediate Th2-like phenotype resulting in the release of IL-4 and IL-5; however, in this case the development of pulmonary eosinophilia is less than that in mice induced by secreted G proteins and is accompanied by high levels of IFN- γ and the production of hRSV F specific CTL (Bembridge *et al.*, 1999).

In man, blood CTL responses vary between 7 days and 3 months after hRSV infection depending on the age of the patients. They are detectable in 65% of older infants (6-24 months) compared to 35-38% in infants less than 5 month old after 5 - 6 days of

infection (Chiba *et al.*, 1989). Poor responses in younger infants may be because of the immunological immaturity or suppression by maternal antibody. In patients with severe hRSV infections, blood CTL peaked between days 9 and 12 after the onset of symptoms (Heidema *et al.*, 2007). However, in nasal aspirates and BAL, the viral load has been reported to usually decrease during 3 – 6 days after the onset of symptom (Malley *et al.*, 2000; Buckingham *et al.*, 2002; Perkins *et al.*, 2005; Campanini *et al.*, 2007). The severity of disease has not been correlated with the amounts of hRSV specific CTLs (Heidema *et al.*, 2007). Human CTLs have been shown to significantly recognize the NS2, N, M, SH, F and M2-1 proteins of hRSV. However, the G, P and NS1 proteins were not recognized (Cherrie *et al.*, 1992). In a post mortem study, low amounts of lymphocytes were found in lung tissue of children with severe hRSV diseases (Welliver *et al.*, 2007). However, hRSV specific CTLs have been detected in BAL of infants with severe hRSV disease (Heidema *et al.*, 2007). Taken together, these findings suggest that CTL responses do not correlate well with recovery.

It has been reported that there was no difference between Th-1 and Th-2 cytokines detected in plasma samples from patients with severe hRSV disease and Th-1 type immune responses was predominant in stimulated T-cell cultures based on high levels of IFN- γ and low levels of IL-4 and IL-10 (Brandenburg *et al.*, 2000; Tripp *et al.*, 2002). However, a body of evidence suggests that Th-2 type responses are associated with severe hRSV infection. Blood CD4⁺ cells were detected at high levels in infected infants with severe disease compared to control groups, whereas CD8⁺ cells were decreased (Roman *et al.*, 1997). Levels of IL-4, IL-4/IFN- γ and IL-10/IL-12 detected in infected patients with hRSV bronchiolitis were significantly higher than those in the control infants (Roman *et al.*, 1997; Legg *et al.*, 2003; Hassan *et al.*, 2008). Likewise, low levels of IFN- γ mRNA in the acute phase were observed in PBMC from infants with severe disease, whilst there were higher levels in infants with moderate illness (Aberle *et al.*, 1999; Legg *et al.*, 2003).

Humoral immunity

Several studies have demonstrated that antibodies can protect against hRSV infection. The F and G glycoproteins are the major protective antigens (Elango *et al.*, 1986; Olmsted *et al.*, 1986) and provide a relatively long-term protection (Connors *et al.*, 1991). Mice immunized with recombinant vaccinia viruses (rVV) encoding only the F

or G protein were fully resistant to hRSV challenge on both day 9 and 28 compared to mice immunized with rVV expressing the M2 and N proteins which exhibited incomplete resistance on day 9. Resistance in mice immunized with other viral proteins (P, SH, M, NS1 and NS2) was undetectable (Connors *et al.*, 1991). Similarly, rVV encoding the bRSV F, G or N proteins induced resistance to hRSV challenge in calves (Taylor *et al.*, 1997). MAbs directed against F or G were able to protect both mice and cotton rats against hRSV challenge (Taylor *et al.*, 1984; Walsh *et al.*, 1984).

Human infants receive antibodies from their mothers, transplacentally and in breast milk, and also make their own humoral responses to infection. Any of these may contribute to protection against hRSV. Higher levels of maternally derived antibodies are associated with a lower incidence of hRSV infection in young infants (Roca *et al.*, 2002; Stensballe *et al.*, 2009). Furthermore, levels of antibody from infants hospitalized with hRSV were lower than those from randomly selected infants born during the same period, indicating that the level of maternal antibody is related to prevention of hRSV infection in infants less than 6 months of age (Glezen *et al.*, 1981). However, no difference between maternal antibody levels to either F or G glycoproteins has been found in infants hospitalized with severe hRSV infection (Toms *et al.*, 1989). Breast-fed infants have been reported to receive maternal antibody in the form colostrum in which hRSV specific IgA and IgG antibodies and neutralizing activity can be detected (Downham *et al.*, 1976; Scott *et al.*, 1981) and it may be for this reason that breast feeding is significantly correlated with protection of lower respiratory tract illness from hRSV infection (Holberg *et al.*, 1991).

Serum antibodies of IgM, IgG and IgA isotypes can be produced in infants and children after primary hRSV infection. The serum IgM specific antibody normally presents a few days after infection and antibodies persist for 2 – 10 weeks (Welliver *et al.*, 1980). The virus-specific IgG response occurs in the second week, peaks in the fourth week beginning to decline after 1 – 2 months (Hall, 1998). All three immunoglobulin can be boosted and detected within 5 – 7 days after reinfection (Welliver *et al.*, 1980).

Older infants and children tend to produce greater hRSV-specific IgG, IgM, and IgA antibody responses than young infants (Welliver *et al.*, 1980; Meurman *et al.*, 1984). Poor responses in infants are attributed both to immunological immaturity and the

suppressing effect of pre-existing maternal antibody in infant sera (Murphy *et al.*, 1986). Passively acquired hRSV antibodies in cotton rats and mice have been shown to reduce antibody responses (Murphy *et al.*, 1988).

Besides serum antibodies, specific anti-hRSV antibodies of IgM, IgG and IgA isotypes in both free and cell-bound forms are detectable in the secretions of infants (McIntosh *et al.*, 1978; Kaul *et al.*, 1981; Wright *et al.*, 2002). It has been shown the higher levels of nasal neutralizing antibodies correlate with reduced hRSV replication; however, patients possessing secretory IgA anti-hRSV antibodies may still be infected with the virus (Mills *et al.*, 1971; Hall *et al.*, 1991).

Increasing levels of hRSV specific IgE and histamine have been detected in the nasopharyngeal secretions of infants with acute bronchiolitis, suggesting that secretion IgE antibody might play a role in the pathogenesis of hRSV infection (Welliver *et al.*, 1981; Bui *et al.*, 1987). Leukotriene C₄, a potent mediator of obstructive airway disease, has been shown to be directly related with the levels of specific IgE in infected infants (Volovitz *et al.*, 1988). Therefore, it has been postulated that IgE-mediated hypersensitivity may be the cause of severe illness. However, another study failed to demonstrate secretory or serum IgE antibodies in either acute or convalescent samples from infants with hRSV infection (Toms *et al.*, 1996).

Anti-hRSV neutralizing antibodies

Antibody responses induced by hRSV infection can recognize several viral proteins; nevertheless, only the F and G protein induce neutralizing antibodies (Groothuis, 1994). Neutralizing antibodies against the F glycoprotein tend to be cross-reactive among subgroup A, subgroup B, and bRSV (Taylor *et al.*, 1992). In contrast, antibodies recognizing the G glycoprotein are either subgroup specific or strain specific. Antibodies reacting with the cysteine noose of the hRSV or bRSV are cross-reactive or subgroup specific, but individually do not neutralize efficiently. However, pooling MAbs recognizing strain specific, group specific and conserved epitope increases the level of neutralization (Langedijk *et al.*, 1997; Martinez *et al.*, 1997; Martinez and Melero, 1998).

MAbs against the fusion glycoprotein with both neutralizing and fusion inhibiting activity have been shown to be highly protective in mice. These recognize antigenic site B (Taylor *et al.*, 1992) or site A (site II) (Trudel *et al.*, 1987b), whereas MAbs with only neutralizing activity recognize antigenic site C (site IV) (Trudel *et al.*, 1987b). Limited studies suggest that neutralizing antibodies may be important in protection against severe disease in human infants. Glezen *et al.* (1981) have demonstrated that titres of neutralizing antibodies in infants with severe illness are lower than those from randomly selected healthy infants born in the same period of time. Similarly, infants with high neutralizing maternal antibodies were protected from hRSV infection, whereas infants with low levels of antibodies became infected (Ogilvie *et al.*, 1981).

The mechanism of viral neutralization by antibodies has been suggested to involve interference at different stages of viral infection including:

(i) Aggregation of virions by antibodies to reduce the number of available infectious units (Dimmock, 1993). This has been demonstrated by an electron microscope study of influenza virus with influenza-specific IgM, IgG and IgA. Aggregation did not occur at high antibody:virus ratios due to lack of free epitopes (Armstrong *et al.*, 1990; Outlaw and Dimmock, 1990; Armstrong and Dimmock, 1992).

(ii) Inhibition of viral attachment to cells by binding to glycoproteins mediating attachment such as antibodies to the hemagglutinin (HA) protein of influenza virus.

(iii) Inhibition of endocytosis for some viruses entering to the cells via endocytosis. For example, IgM has been reported to neutralize influenza virus by interfering the ability of virus to bind a sufficient number of cell receptors involving in initiation of endocytosis (Taylor and Dimmock, 1985; Outlaw and Dimmock, 1990).

(iv) Inhibition of fusion between virus and host cell membranes by interrupting fusion process at cellular membranes at neutral pH such as antibodies against the F glycoproteins of PIV3 or in endosomal vesicles at low pH. Antibodies may affect conformational changes in the fusion process or block the contact between viral and cellular membranes (Klasse and Sattentau, 2002).

(v) Post-entry mechanisms where interference with further replicative steps occur after the viral capsid enters into the cytoplasm of the host cell. Antibody to the HA of influenza virus has been shown to block virion transcriptase activity (Possee *et al.*, 1982).

A body of evidence suggests that viruses are inactivated by multi-hit events rather than by a single-hit. In a multi-hit model, more than one antibody molecule is required to neutralize one virion, whereas in a single-hit model the binding of one antibody molecule to a virus particle is sufficient (Burton *et al.*, 2001). Each virus needs a different amount of antibody molecule in order to neutralize. For instance, 10-20 antibody molecules per virion are required to neutralize rhinovirus by 90% (Smith *et al.*, 1993), whilst influenza virus requires over 100 antibody molecules per virion for 90% neutralization (Taylor *et al.*, 1987).

The degree of neutralization may relate to antibody occupancy on the virion. Increasing occupancy of antibody on HIV-1 results in increased neutralization level, irrespective of epitope recognized. In these occupancy theories of neutralization, viruses has been proposed to be neutralized when they are bound with antibody and rendered incapable of attachment or fusion to the host cell membrane (Burton *et al.*, 2000). Factors influencing antibody occupancy are the number of antigens on the virus surface, the proximity of the viral antigens to each other on the surface of the virion, the number of antibody binding sites on the virion and the size of the virion (Klasse and Sattentau, 2002).

Conversely, viral neutralization may occur by steric or direct inhibition of a proportion of the virion surface, resulting in prevention of necessary interactions between virus particle and target cell membrane. This is termed the coating theory of virus neutralization. This theory can explain the neutralization by antibodies to antigens on the particle surface which do not participate in viral entry. For example, antibodies against influenza NA proteins, which function at virus release rather than entry, would become neutralizing when a high level of NA proteins are present on the surface (Klasse and Sattentau, 2002).

1.10 Treatment and prevention

1.10.1 Treatment

The management of hRSV infection depends on the severity of disease. Most cases of mild lower respiratory tract disease are usually self-limiting conditions and may not require hospital admission. There are no specific drug treatments; therefore, patients with severe illness are managed by the supportive care such as secretion removal,

oxygen administration and mechanical ventilation. The use of anti-inflammatory agents has been studied in treatment of severe disease because the effects of immune response on severity are greater than those of viral replication. However, there is no evidence that anti-inflammatory agents alone are of benefit for hRSV patients (Simoes, 1999; Patel *et al.*, 2004).

Small molecule anti-hRSV compounds

Several small molecule anti-hRSV compounds have been discovered. Many compounds pass through animal testing and a few are in the early-phase of clinical trials. Most of them belong to a series of benzimidazole derivatives and are synthesized to inhibit the formation of the six helix bundle in the F molecule during the fusion process which is a crucial stage in the life cycle of hRSV (Collins and Melero, 2011).

Ribavirin

Ribavirin (1- β -D-ribofuranosyl-1,2,4-triazole-3-carboxamide) is a guanosine analog which functions on incorporation into the viral genome. It has been evaluated for hRSV treatment since the 1980s (Hall *et al.*, 1983). Its use, however, remains controversial. Some studies have demonstrated that ribavirin administration is able to decrease the duration of mechanical ventilation and the length of hospital stay (Ventre and Randolph, 2004). In contrast, other studies have shown that the mortality rate of hRSV infected patients does not differ between treatment with and without ribavirin (Moler *et al.*, 1996; Randolph and Wang, 1996).

The use of ribavirin in hRSV infected patients “may be considered” according to the recommendation of the American Academy of Pediatrics (AAP) (Committee on infectious disease, 1996). Patients with hRSV infection have to be given a small-particle aerosol of ribavirin (Hall *et al.*, 1983). At present, ribavirin is not recommended for use in the routine for treatment of hRSV infection; however, it can be considered in high risk patients for severe disease such as those who are immunocompromised or who have haemodynamically significant cardiopulmonary disease (Subcommittee on diagnosis and management of bronchiolitis, 2006).

BTA9881

BTA9881 (Biota, AstraZeneca, London, UK) is a derivative of imidazoisoindolone which has antiviral activity by inhibiting the F glycoprotein (Bond *et al.*, 2007). It has been successfully tested in rodents with promising oral bioavailability and efficacy (Luttick *et al.*, 2007). In 2007, it completed phase I clinical trials having been evaluated in 72 healthy adult volunteers (Biota Scientific Management Pty Ltd, 2007) and the results showed this drug was a long-lasting in plasma of humans and also displayed approximately 100% oral bioavailability. However, its safety profile was unsatisfactory; therefore, the development of this drug has been discontinued (Biota Holdings Limited, 2009).

BMS-433771

BMS-433771 (Bristol-Myers Squibb, Wallingford, USA) is a radiolabelled analogue of benzimidazole and is an oral fusion inhibitor containing a photoreactive diazirine group. Studies using photoactivated affinity probes have shown that BMS-433771 binds within the hydrophobic pocket of the HR1 associated with the HR2 in a trimer-of-hairpins structure (Cianci *et al.*, 2004b).

The binding site of BMS-433771 was also mapped by generating the resistant viruses in the presence of several analogs of BMS-43771 and analysing their sequences. Although the compounds used for isolating the escape mutants were either the early synthetic analogs (BMS-233675 and BMS-243458) or structurally related compound (BABIM), all selected mutants were cross-resistant to BMS-433771, indicating that there was a common or overlapping site of action among these compounds. The molecular targets of BMS-433771 analysed from the escape mutants were located within the F1 domain of the F glycoprotein, including the fusion peptide (F140I, V144A), the cysteine-rich region (D392G, K394R) and the HR2 (D489Y). Furthermore, it was found that a rescued transfectant virus with a mutation at K394R produced by reverse genetics was resistant to BMS-433771, showing that a single-residue substitution in the F1 subunit alone can generate resistance to BMS-433771 (Cianci *et al.*, 2004c).

In *in vitro* studies, BMS-433771 was found to protect Hep-2 cell from the hRSV clinical isolates of both subgroup A and B induced CPE with a 50% effective concentration of 20 nM (12 nM obtained from testing with Long strain) and did not have cell protection

for infection with other viruses (Cianci *et al.*, 2004c). The compound blocked virus-cell fusion early in infection during viral entry and cell-cell fusion mediated by the F glycoprotein, but had no effect upon the viral attachment (Cianci *et al.*, 2004c; Magro *et al.*, 2010).

In animal models, lungs of BALB/c mice given with BMS-433771 orally before inoculation of hRSV had reduced virus titres compared to control groups (Cianci *et al.*, 2004c). BMS-433771, given in either single or multiple doses, was able to reduce virus titres in both BALB/c mice and cotton rats, although effects were greater in mice than in cotton rats. These results were confirmed by a pharmacodynamic analysis that showed the EAUC₅₀ (a value that determines the potency of compounds *in vivo* achieving 50% of the maximum response) of mice was higher than that of cotton rats. Moreover, the escape mutant (K394R) was resistant to BMS-433771 in mice, confirming the *in vitro* studies (Cianci *et al.*, 2004a). The development of this compound has recently been discontinued by Bristol-Myers Squibb (Olszewska and Openshaw, 2009).

TMC353121

TMC353121 (Tibotec Pharmaceuticals, Mechelen, Belgium) is a benzimidazole derivative which has been reported to block both virus-cell and cell-cell fusion. The binding site was mapped by generating resistant mutants and located in the cysteine-rich region (K394R and S398L) and the HR2 region (D486N) of the F1 polypeptide. However, it has been reported that this inhibitor binds both HR1 (Y198) and HR2 (D486) within a hydrophobic pocket of the six helix bundle complex (Roymans *et al.*, 2010). TMC353121 exhibited antiviral activity *in vitro* for viruses of both subgroups A and B. In cotton rats, this inhibitor produced a high reduction of hRSV titre when administered shortly before virus challenge, suggesting that it has to be present before fusion (Bonfanti *et al.*, 2008). TMC353121 is currently in preclinical evaluation by Tibotec (Olszewska and Openshaw, 2009).

JNJ-2408068

JNJ-2408068 is a benzimidazole derivative which has been shown to inhibit hRSV infection in both subgroup A and B in *in vitro* studies and which does not have antiviral activity to other paramyxoviruses such as HPIV2, Mumps virus or hPIV3. Its mechanism of action is similar to that of TMC35321 and it binds both the HR1 and

HR2 within a hydrophobic pocket of the six helix bundle in the F glycoprotein. In addition, JNJ-2408068 is able to block both virus-cell fusion (early stage) and also cell-cell fusion at the end of the infection cycle (Douglas *et al.*, 2005). Two resistant mutants have been characterised with changes in the F gene, S398L and D486N. JNJ-2408068 has been reported to block the release of proinflammatory cytokines from infected cells (IL-6, IL-8 and RANTES) (Andries *et al.*, 2003). This compound remains to be completely evaluated in humans.

YM-53403

YM-53403 (Yamanouchi Pharmaceutical Co., Ltd., Ibaraki, Japan) is a benzazepine derivative which is able to inhibit hRSV replication in both subgroup A and B ($EC_{50} = 0.2-0.4 \mu\text{M}$) and there is no antiviral activity to measles virus, influenza A virus or HSV-1. Unlike BMS-433771, it has been shown to reduce the virus titre when added up to 8 hours post-infection similar to ribavirin which blocks RNA synthesis during the viral replication. The mapping of YM-53403 by sequencing mutant viruses has revealed changes in the L protein (Y1631H) (Sudo *et al.*, 2005). This compound has not yet been fully tested in human.

RSV-604

RSV-604 (Novartis, Basel, Switzerland) is a benzodiazepine derivative which has been reported to have submicromolar antiviral activity ($EC_{50} = 0.5-0.9 \mu\text{M}$) against several isolates of both subgroup A and B in *in vitro* studies. This inhibitor is active up to 6 hour after hRSV inoculation, like YM-53403, suggesting that RSV604 functions at late stage of the replication cycle. Resistant mutations of RSV604 have been shown to have changes in the highly conserved N protein. Currently, RSV604 is testing in phase II clinical trials (Chapman *et al.*, 2007).

Heptad-repeat peptide

In HIV-1, it has been reported that synthetic peptides based on the sequences of the highly conserved regions in the transmembrane (TM) protein gp41 (fusion protein) have potent antiviral activity (Wild *et al.*, 1992; Wild *et al.*, 1993). Those regions are the leucine zipper region at residue 558-595 (peptide DP-107) and an extended amphipathic α -helix region at residue 643-678 (peptide DP-178) which were predicted to form a helical structure in fusogenic viral proteins (Gallaher *et al.*, 1989; Delwart *et al.*, 1990).

From sequence analysis, the hRSV F1 protein motifs HR1 and HR2 presented a high level of homology to DP-107 and DP-178 in gp41 (Gallaher, 1987).

Therefore, it is seemed likely that peptides synthesized from the sequences of HR1 and HR2 would inhibit hRSV induced membrane fusion. The location of the HR1 (residues 149-206) and HR2 (residues 474-523) domains was identified in the F glycoprotein of the Long strain hRSV and sequential overlapping peptides of 35 amino acids in length shifting by 1 amino acid from the N-terminus were synthesized to scan across the entire HR1 and HR2 domains. The abilities of these peptides in protecting cell monolayers from hRSV infection were analysed. It was found that overlapping peptides scanned across the HR2 domains presented substantially more potent antiviral activity than those of the HR1 domains, especially peptide based on residues 488 – 522, namely T-118. Its sequence is FDASISQVNEKINQSLAFIRKSDELLHNVNAGKST (Lambert *et al.*, 1996). T-118 was acetylated at the N-terminal region and amidated at the C-terminal region to enhance the biological half-life (Powell, 1993). It had the submicromolar antiviral activity ($EC_{50} = 0.05 \mu\text{M}$) against hRSV induced fusion. Similarly, in a separate study, a 39-amino acid HR2 peptide based on residue 478 – 516 of the F1 protein, namely F478-516, also inhibited the viral antigen production and neutralized hRSV when present during the active process of viral entry (Magro *et al.*, 2010).

The inhibiting mechanism of hRSV fusion by HR2 peptides is likely to be similar to that of DP178 inhibition of HIV-1 gp41-mediated membrane fusion (Figure 1.9) (Zhao *et al.*, 2000). After activation of the gp41, a prehairpin intermediate is formed by the projection of the fusion peptide (red lines) into the host cell membrane, forming a trimeric coiled coil of the HR1 domain (grey). At this stage, the HR2 region has not yet associated with the HR1 coiled coil. Therefore, HR2 peptides (orange box) can bind to the HR1 region of the fusion protein, resulting in the inhibition of 6HB formation (hairpin) and the blocking of membrane fusion.

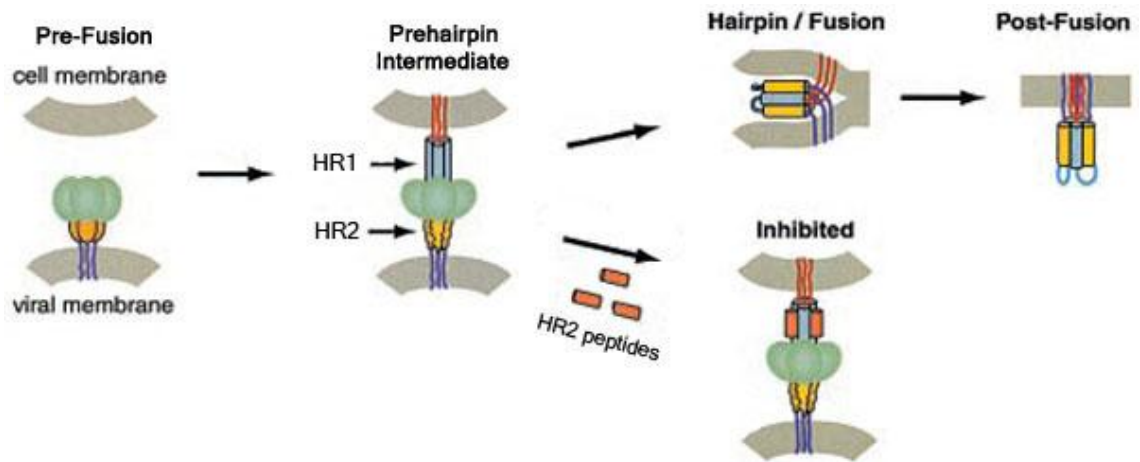


Figure 1.9 Model of membrane fusion process based on the HIV-1 gp41 protein
 [Modified from original by Zhao *et al.* (2000) and Chan and Kim (1998)].

1.10.2 Vaccines

The development of effective RSV vaccines presents many difficulties. As severe RSV disease usually occurs in young infants (2-6 months), a vaccine would need to be administered during the first weeks of life for efficient protection (Collins and Crowe, 2007). Infants of this age have low immune responses compared to older children and adults due to their immaturity and the immunosuppressive effect of maternal antibodies (Crowe, 1999; Crowe *et al.*, 2001). It has been difficult to achieve sufficient attenuation of potential live virus vaccines, especially for seronegative infants (Wright *et al.*, 2000) and formalin-inactivated vaccines have been found to augment rather than ameliorate disease severity.

Formalin-inactivated RSV vaccines

Formalin-inactivated RSV vaccines (FI-RSV) were first developed using a similar process to that for other, successful, vaccines for polio and influenza. After propagation, hRSV was formalin – inactivated, ultracentrifuged and alum-precipitated (FI-RSV). FI-RSV vaccines were tested by intramuscular administration to infants and young children in four separate trials during 1965 – 1966 (Chin *et al.*, 1969; Fulginiti *et al.*, 1969; Kapikian *et al.*, 1969; Kim *et al.*, 1969). In these clinical trials, FI-RSV was poorly protective and was associated with severe disease after subsequent natural infection with hRSV. In epidemics, the hospitalization rate of infants immunized with FI-RSV vaccines (80%) was higher than that of children vaccinated with FI-parainfluenza virus vaccine (5%) and two infants died due to FI-RSV vaccine.

The induction of severe disease in mice induced by the inoculation of anti-RSV CD4⁺ and CD8⁺ T cells suggested the hypothesis is that FI-RSV stimulates a CD4⁺ response in the absence of neutralizing antibody which leads to inflammation, but not protection. More recently however, it has been proposed that enhancement of severe illness by FI-RSV may involve an imbalance between the Th1 and Th2 CD4⁺ T cell response and this has been studied in both animal models and using specimens from hRSV infected patients, nasopharyngeal secretions and peripheral blood mononuclear cells. Together, these studies suggest that Th2 responses induce eosinophilic infiltrates in lung and an increasing ratio of IL-4/IFN- γ as compared with the Th1 responses which promote a strong CTL response with undetectable IL-4 (Graham *et al.*, 1993; Roman *et al.*, 1997; Bont *et al.*, 2001; Legg *et al.*, 2003; Semple *et al.*, 2007; Byeon *et al.*, 2009).

Live attenuated vaccine

Several live, attenuated hRSV vaccines have been developed since the 1960s. It has been reported that these vaccines do not result in augmented disease in animal models and in clinical trials (Wright *et al.*, 2007). Furthermore, intranasal administration of these vaccines induces both local and systemic immune responses and also escapes from immunosuppressive effect of maternal antibodies (Crowe *et al.*, 1995).

Live attenuated vaccines by conventional methods

Initially, hRSV was attenuated by 52 serial passages at the suboptimal temperature of 26°C (cold-passage, *cp*-RSV) in bovine tissue culture (Friedewald *et al.*, 1968). This virus was completely attenuated in hRSV-seropositive children and adults, but still remained of unacceptable virulence in young infants (Kim *et al.*, 1971).

The chemical mutagen (5-fluorouracil, 5-FU) was used to generate temperature-sensitive (*ts*) mutants of the virus unable to replicate at 37-39°C. These mutants are presumed incapable of infecting the lower respiratory tract which has a temperature of 37°C (Gharpure *et al.*, 1969). The infectivity of RSV *ts* mutants (*ts-1* and *ts-2*) has been shown to be poor in adults and children, but they are still not satisfactory when intranasally administered to hRSV-seronegative children (Wright *et al.*, 1976; Wright *et al.*, 1982).

Therefore, these approaches were continued by mutagenizing a *cp*-RSV mutant with 5-FU, screening for either small plaque (*sp*) or temperature sensitive (*ts*) phenotypes by plaque titration at 32°C or 38°C, respectively. Two *ts* mutants, *cpts*-248 and *cpts*-530, were the most of restricted in replication in mice when compared to wild-type virus. Both the *cpts*-248 and *cpts*-530 had a more stable *ts* phenotype than the *ts*-1 virus. In addition, the *cpts*-248 was highly immunogenic and attenuated in seronegative chimpanzees (Crowe *et al.*, 1994b).

The *cpts*-248 was additionally attenuated by a second round of mutagenesis with 5-FU, selecting progeny for either *ts* or *sp* phenotypes. The resultant *cpts*-248/404 mutant has been reported to be fully restricted in replication in chimpanzees and to have a stable *ts* phenotype. Moreover, chimpanzees immunized with the *cpts*-248/404 mutant produced a high level of antibody and were completely protected against wild-type virus challenge, indicating that this vaccine has a favourable balance between attenuation and immunogenicity (Crowe *et al.*, 1994a). The *cpts*-248/404 vaccine was tested in phase I clinical trials in children and infants less than 2 months of age. It was highly attenuated in these infants; however, it caused mild nasal congestion (Wright *et al.*, 2000). Therefore, this vaccine was unacceptable for immunization in very young infants. Additional attenuating mutations are required and may be introduced in the *cpts*-248/404 vaccine using reverse genetics.

Live attenuated vaccines by reverse genetics

The production of live attenuated vaccines by conventional methods has subsequently been replaced by reverse genetics which is able to produce viruses containing a combination of desirable attenuating mutations and has led to the generation of “designer” vaccines (Collins and Murphy, 2005). In this method, infectious RSV is constructed in tissue cultures in which five viral components involved in transcription and replication are co-expressed. These are cDNAs encoding the full length RSV antigenome with a ribozyme at the downstream end which generates a correct 3' end after cleavage and four cDNAs encoding the proteins of the polymerase complex (N, P, L and M2-1 proteins). All cDNAs are expressed from a T7 RNA polymerase promoter and transfected into Vero cells which are safe for human use (Collins *et al.*, 1995).

Identification of the mutations involved in RSV attenuation is required to develop live attenuated vaccines using reverse genetics. Deletion of accessory hRSV proteins has been found to be associated with attenuation. Recombinant hRSV mutants lacking either the NS2 or SH gene were attenuated in chimpanzees (Whitehead *et al.*, 1999a). Using reverse genetics, a recombinant vaccine candidate has been generated by deletion of the SH gene of *cpts-248/404* resulting in the production of rA2cp248/404 Δ SH. On examination of the levels of attenuation of this vaccine in adults, seropositive- and seronegative- children, it was found there was no difference between rA2cp248/404 Δ SH and *cpts-248/404*. The development of rA2cp248/404 Δ SH virus was continued by adding the 1030 mutation, generating rA2cp248/404/1030 Δ SH virus or MEDI-559. rA2cp248/404/1030 was reported to be more temperature sensitive *in vitro* and more attenuated *in vivo* than *cpts-248/404* (Whitehead *et al.*, 1999b). rA2cp248/404/1030 Δ SH virus was more attenuated in seronegative children and produced more protective immunity compared to rA2cp248/404 Δ SH virus (Karron *et al.*, 2005). At present, MEDI-559 is in phase I/IIa clinical trials which are recruiting healthy children between 1 and 24 months old to test its viral shedding, immunogenicity, tolerability and safety (MedImmune LLC, 2008a).

Mutants with NS1, NS2, SH and M2-2 genes removed individually or in different combination from the genome also showed a reduction in replication in the lungs of cotton rats compared to the wild-type A2 strain (Jin *et al.*, 2000b). Moreover, the deletions of the NS1 or NS2 increased the immunogenicity due to the loss of their functions involved in blocking the IFN α / β system which led to enhanced induction of both innate and adaptive immunity (Valarcher *et al.*, 2003). Immunogenicity could also be enhanced by the removal of M2-2 gene. This gene correlated with shifts between transcription and replication. The absence of M2-2 gene results in an increase in viral gene expression, including that of the F and G glycoproteins (Bermingham and Collins, 1999). It has been reported that recombinant hRSV viruses lacking either NS1 (rA2 Δ NS1) or M2-2 (rA2 Δ M2-2) administered to seronegative chimpanzees were limited in replication in both the upper and lower respiratory tract, but that the level of neutralizing antibody induced by these mutant viruses was only slightly less than that induced by wild-type hRSV. Chimpanzees immunized with either rA2 Δ NS1 or rA2 Δ M2-2 were protected from challenge with wild-type hRSV (Teng *et al.*, 2000). These constructs remain to be completely evaluated in humans.

A number of alternative mechanisms for attenuation of hRSV have been tried, but have yet to be fully explored. The replacement of charged amino acids in the L protein with alanine, a non-charged amino acid, has been found to facilitate attenuation producing recombinant hRSV virus which is more temperature sensitive and is capable of only limited replication in the lung of cotton rats (Tang *et al.*, 2002). Another strategy is the modification at the cleavage sites of the F glycoprotein at the two positions digested by cellular protease. These sites have been reported to be important in activation of membrane fusion (Gonzalez-Reyes *et al.*, 2001). Therefore, it is possible to attenuate hRSV by changing the sequences at these sites; however, this method has yet to be fully evaluated (Collins and Murphy, 2005). Alteration of the gene order also may lead to increase in immunogenicity. Changing the position of the F and G gene so that they are in a more promoter proximal position in recombinant hRSV virus enhances the expression of both genes, resulting in an increase in the level of serum F glycoprotein specific IgG antibody, but not IgG antibody specific to G glycoprotein (Krempl *et al.*, 2002).

Recombinant animal viruses

Recombinant animal viruses engineered to express genes encoding hRSV proteins using reverse genetics are also promising anti-hRSV candidate vaccines. The advantage of this strategy that is efficient restriction of replication in humans is not dependent upon a temperature sensitive phenotype. One such candidate is a chimeric bRSV/hRSV expressing the hRSV F and G protein. However, this construct has been found to be over-attenuated in chimpanzees and did not induce resistance to wild-type hRSV challenge. It may be that replacing more bRSV genes with hRSV genes may increase the immunogenicity in primates (Buchholz *et al.*, 2000).

Bovine parainfluenza virus type 3 (bPIV3) has also been widely studied as a potential vaccine vector for hRSV genes. A chimeric bPIV3 in which the wild type fusion (F) and hemagglutinin-neuraminidase (HN) genes were replaced with genes from human parainfluenza virus type 3 (hPIV3) was found to be attenuated in the lungs of hamsters and fully protected them against hPIV3 challenge (Haller *et al.*, 2000). In addition, this virus has been shown to be immunogenic and safe for administration to young infants and children (Karron *et al.*, 1996; Lee *et al.*, 2001).

Chimeric b/h PIV3 has been further modified by the insertion of the hRSV F or G proteins. Hamsters immunized with either chimeric virus were protected from challenge with both hRSV and hPIV3 (Tang *et al.*, 2003). Furthermore, African green monkeys immunized with the b/h PIV3/RSV (MEDI-534) harbouring either the native or soluble hRSV F glycoprotein were resistant to wild-type hRSV challenge and released neutralizing F-protein specific IgG antibody (Tang *et al.*, 2004). MEDI-534 is currently in phase I/IIa clinical trials testing in infants and children between 1 and 24 months of age who are seronegative to both hPIV3 and hRSV (MedImmune LLC, 2008b).

Subunit vaccines

Subunit vaccines are an alternative strategy for immunization against hRSV consisting of viral glycoproteins either purified from infected cell culture or produced by recombinant vectors. F glycoprotein has been developed as a candidate vaccine following purification by affinity chromatography, PFP-1, (90% F and 5% G proteins) or by ion exchange chromatography, PFP-2 (>99.9% F and <0.1% G proteins). Both PFP-1 and PFP-2 were adsorbed to alum and evaluated in hRSV-seropositive children, children with cystic fibrosis, healthy elderly people and pregnant women. It was found that these vaccines did not enhance disease severity on subsequent natural infection and induced the production of neutralizing antibodies (Tristram *et al.*, 1993; Paradiso *et al.*, 1994; Piedra *et al.*, 1995; Falsey and Walsh, 1996; Piedra *et al.*, 1996; Groothuis *et al.*, 1998; Munoz *et al.*, 2003). However, PFP-1 did not protect against recurrent hRSV infection (Belshe *et al.*, 1993). PFP-3 vaccine was subsequently developed from highly purified cold passaged and temperature sensitive mutant strains. In a phase II trial performed in children with cystic fibrosis, anti-F neutralizing and binding antibodies were maintained for 28 days post-vaccination (Piedra *et al.*, 2003).

Using recombinant technology it has been possible to link the hRSV glycoproteins to molecules which may enhance the immune response. A G protein fragment (residue 130 – 230, designated G2Na) has been fused to an albumin binding region (BB) of streptococcal protein G, generating BBG2Na vaccine (Power *et al.*, 1997). BB domain was selected to be a fusion partner because it can increase the half-life of fused peptides, resulting in extended exposure of the immunogens to the immune responses (Makrides *et al.*, 1996). BB domain also has carrier-related properties which facilitate

antibody response to weak immunogens (peptides) (Sjolander *et al.*, 1997). Moreover, the BB domain can be effectively purified by affinity chromatography on albumin-Sepharose (Nygren *et al.*, 1988).

Seropositive adults given BBG2Na vaccine produced high neutralizing antibodies and did not present enhanced disease after hRSV infection (Power *et al.*, 2001). Nevertheless, infant macaques immunized with BBG2Na and challenged with hRSV were found to produce IL-13 which is involved in Th2 responses similar to the effect of FI-RSV vaccine. Low levels of eosinophilia were also present in the lungs of animals on subsequent hRSV challenge (de Waal *et al.*, 2004). BBG2Na reached clinical phase III, but it was terminated due to evidence of adverse reactions in vaccinees (Nguyen *et al.*, 2012).

By recombinant expression of the F glycoprotein, it has been possibly developed to a subunit vaccine that is composed of the post-fusion form of the F glycoprotein (trimer) lacking the fusion peptide, transmembrane and cytoplasmic region, resulting in no aggregation. This vaccine has been reported to protect cotton rat from hRSV challenge and induce the high levels of neutralizing antibody. It was found that the post-fusion form presents the neutralizing binding site recognized by several antibodies such as palivizumab (PZ), motavizumab and 101F (McLellan *et al.*, 2011; Swanson *et al.*, 2011).

The immunogenicity of viral proteins may be enhanced by presentation within virus-like particle (VLP) (Noad and Roy, 2003). VLPs resemble viral particles containing structural proteins and lipid with no genetic materials which are incapable of replication. Hence, the VLP vaccine is safe and also highly immunogenic because antigens on its surface and core can potentially stimulate both humoral and cell-mediated immune response. (Sedlik *et al.*, 1999; Lechmann *et al.*, 2001; Liu *et al.*, 2002; Swenson *et al.*, 2005).

The VLP vaccines which are allowed for human use have been successfully developed against papillomavirus and hepatitis B viruses. hRSV VLPs have been generated by connecting the ectodomain of hRSV G protein to the cytoplasmic tail and transmembrane domain of the NDV HN (VLP-H/G). This chimeric protein is

incorporated into the VLP containing NDV N and M proteins. It was found that the ND VLP with hRSV G protein (ND VLP-H/G) protected mice from hRSV challenge and did not cause enhanced disease in lungs on subsequent hRSV challenge (Murawski *et al.*, 2010). ND VLP-H/G assembled with a chimeric RSV F/NDV F glycoprotein (F/F) has been subsequently generated (ND VLP-H/G+F/F). Anti-hRSV F and G protein antibody responses and neutralizing antibodies were stimulated in mice immunized with ND VLP-H/G+F/F. On subsequent hRSV challenge, no enhanced lung pathology was detected in ND VLP-H/G+F/F - immunized mice, suggesting that these VLP vaccines can efficiently protect mice against hRSV infection (McGinnes *et al.*, 2011). However, this vaccine remains to be completely evaluated in humans.

1.10.3 Passive immunization

RSV intravenous immunoglobulin

RSV intravenous immunoglobulin licensed in 1996 (RS-IVIG, RespiGam™, MedImmune, Inc, Gaithersburg, MD) is purified human polyclonal IgG containing high hRSV-neutralizing activity. Cotton rats treated with the RS-IVIG were resistant to wild-type hRSV challenge by 99% (Siber *et al.*, 1994). Two doses of the RS-IVIG (750 and 150 mg/kg) was evaluated in high risk children with chronic lung disease of prematurity (CLD) and congenital heart disease (CHD). There were significantly fewer lower respiratory tract infections and lower levels of hospitalization in the high-dose group compared to those in the low-dose group.

The evaluation of the RS-IVIG with a high dose was confirmed in children with CLD compared to placebo controls with a reduction of hospitalization related to hRSV. However, there was a problem in some children caused by infusion of a large volume of fluid (The PREVENT Study Group, 1997). Children with CHD receiving the RS-IVIG suffered a higher frequency of unanticipated cyanotic episodes with an unsatisfactory outcome after surgery for children with cyanotic CHD. Therefore, the RS-IVIG has not been further developed because of low efficiency and safety concerns (Simoes *et al.*, 1998). RS-IVIG may also interfere with subsequent vaccination with other viruses such as measles, mumps and rubella (Wu *et al.*, 2008).

Anti-F monoclonal antibodies

Palivizumab

Palivizumab (MEDI-493, Synagis™, MedImmune, Inc, Gaithersburg, MD) or PZ is a humanized monoclonal antibody against a conserved region of hRSV F glycoprotein which binds antigenic site II (or site A) in the N-terminal region of F1 in both pre- and post-fusion forms of the glycoprotein (Swanson *et al.*, 2011; Magro *et al.*, 2012). It has been shown that PZ is 20-30 fold more effective than RS-IVIG. PZ was synthesized by transplanting six complementarity determining regions (CDRs) of anti-hRSV F glycoprotein MAb 1129 (3 CDRs of light chain and 3 CDRs of heavy chain) into a human IgG1/κ antibody in the corresponding light and heavy chain regions (Johnson *et al.*, 1997). The MAb 1129 was secreted from the 1129 hybridoma constructed by fusion of murine myeloma cell lines with mouse splenic lymphocytes. These lymphocytes were derived from mice intravenously injected with hRSV A2 strain and subsequently intranasally inoculated with recombinant F glycoprotein (Beeler and van Wyke Coelingh, 1989). Hence, PZ consists of immunoglobulin sequences of both human (95%) and murine (5%) origin (Johnson *et al.*, 1997).

The antigenic site of PZ was mapped by the production of escape mutants in the presence of PZ. These were MP4, MS412 and F212. The MP4 and MS412 mutants were fully resistant to PZ both *in vitro* and *in vivo* and had point mutations in the region encoding the F1 chain at nucleotide 828 (A→T, K272M) and 827 (A→C, K272Q), respectively. Mutant F212 was partially neutralized by PZ *in vitro*, but was completely susceptible to PZ *in vivo*. The mutation of the F212 was also found in the region encoding the F1 subunit at nucleotide 816 (A→T, N268I). The locations of all escape mutants were in antigenic site II, suggesting that this site was specific for the binding of PZ (Zhao *et al.*, 2004a; Zhao *et al.*, 2004b).

Mutation of hRSV isolates collected from NPS of infants receiving a high dose of PZ also occurred at residue 272 which changed from lysine (K) to glutamate (E) (Boivin *et al.*, 2008). Similarly, in a separate study, mutations in the F gene of isolates derived from patients given PZ were found at residues 272 (K272E and K272Q) and 275 (S275F and S275L). However, there were only a low frequency of variants with amino

acid changes in antigenic site II and the resistant phenotype disappeared after passaging mixtures of wild-type and mutant variants (Zhu *et al.*, 2011).

In *in vitro* studies, PZ was able to neutralize all hRSV from clinical isolates of both subgroups A and B tested (Johnson *et al.*, 1997). The neutralization to hRSV by PZ has been studied and it has been found that PZ does not inhibit viral attachment or budding, but blocks viral transcription. It was suggested that PZ is active at the stage of fusion. This study also showed PZ inhibited cell-to-cell fusion mediated by the F glycoproteins. It has been suggested that this antibody acts by preventing the conformational change of the F glycoprotein involved in the fusion process (Huang *et al.*, 2010).

In *in vivo* studies, a 99% reduction of hRSV titres in the lungs of cotton rats was found with serum levels of PZ of 40 µg/ml. There was no enhancement of pathology or viral infection after hRSV challenge (Johnson *et al.*, 1997). In 1,502 high-risk children, intramuscular injection of PZ at 15 mg/kg decreased hRSV hospitalizations by 55%. Premature children with and without bronchopulmonary dysplasia (BPD) injected with PZ had a reduction in hRSV hospitalization of 39% and 78%, respectively. Furthermore, PZ was revealed to be safe in all studies and patients given PZ had the same side effects as the placebo groups (The IMPact-RSV Study Group, 1998). After this trial, PZ was approved by the Food and Drug Administration (FDA) in 1998.

PZ was also evaluated for protective effect in young children with hemodynamically significant congenital heart disease and showed a 45% reduction in the length of hRSV hospitalization. Moreover, patients who required supplemental oxygen had a 73% reduction in hRSV hospitalization. At present, according to the recommendation of the American Academy of Pediatrics (AAP) (Committee on infectious disease, 2009) PZ is recommended for use in young children (≤ 2 years of age) with hemodynamically significant congenital heart disease, chronic lung disease of prematurity, premature infants (≤ 32 weeks' gestation) and high-risk infants (32 - 35 weeks' gestation). The latter group is limited to infants born within 3 months before the start of hRSV season or at any time during the hRSV season.

Motavizumab

Motavizumab (MEDI-524, MedImmune, Inc, Gaithersburg, MD) has been developed from PZ by mutagenization of the PZ immunoglobulin gene. There were only 13 amino acids of motavizumab that differ from PZ. The modifications improve binding affinity and *in vitro* neutralization which are reported to be approximately 70-fold and 20-fold greater than those for PZ, respectively. The mechanism of neutralization has been reported to be the same as PZ. Motavizumab was not associated with the stage of viral attachment and budding; however, it inhibited both the virus-cell and cell-cell fusion (Huang *et al.*, 2010). In addition, it has been confirmed that motavizumab can bind to antigenic site II of the F glycoprotein in the pre-fusion, intermediate and post-fusion states (McLellan *et al.*, 2011).

Motavizumab can reduce virus titres in cotton rats 10 – 100 fold more than PZ at the same concentration and block viral growth in the upper respiratory tract (Wu *et al.*, 2005; Wu *et al.*, 2007). In phase III clinical trials, motavizumab decreased the percentage of hospitalization (26%) compared to PZ; however, antidrug antibodies were detected by 1.8% of patients receiving motavizumab and the incidence of hypersensitivity reactions in motavizumab recipients (0.4%) was slightly increased from patients treated with PZ (0.1%) (Carbonell-Estrany *et al.*, 2010). Recently, it has been reported that the US FDA Antiviral Drugs Advisory Committee has not approved the license application for motavizumab due to concern about the increase of hypersensitivity reactions and have requested additional clinical data about frequency and severity of these reactions (The antiviral drug advisory committee of the Food and Drug Administration, 2010). Subsequently, MedImmune has decided to discontinue further development of motavizumab (MedImmune, 2010).

Numax-YTE

Numax-YTE (MEDI-557, MedImmune, Inc, Gaithersburg, MD) was developed from motavizumab by improving its circulation half-life. The neonatal Fc receptor (FcRn) is responsible for maintaining the levels of serum IgG. The IgG pathway is initiated by the uptake of circulating IgGs into cells by pinocytosis and IgGs then bind to FcRn located in the wall of the acidic endosomes. This binding depends on the pH with a tight binding occurring at pH 6.0, but no binding at pH 7.4. After binding in the

endosome, bound IgGs are recycled back to the cell surface and easily released into circulation (Junghans, 1997).

The Fc region of motavizumab was modified for higher affinity binding to FcRn, resulting in a better recycling step and thus longer circulation half-life. The Fc domain of Motavizumab was engineered by three substitution mutations, M252Y/S254T/T256E (YTE), and this antibody was named NuMax-YTE. This modification resulted in an increased (10-fold) binding affinity of NuMax-YTE for cynomolgus monkey and human FcRn at pH 6.0 and also effective dissociation from FcRn at pH 7.4. NuMax-YTE has been shown to have a 4-fold increased circulation half-life compared to the original motavizumab, but still maintains its activities in binding to antigen and blocking hRSV replication (Dall'Acqua *et al.*, 2006). This product is currently in clinical testing for human.

Chapter 2: Background of project

2.1 Introduction

hRSV is the major cause of severe respiratory disease in infants and young children leading to hospitalization and death worldwide. It has been reported that there are approximately 64 million cases and 160,000 deaths caused by hRSV disease every year (WHO, 2009). Prevention of this disease in high risk infants has only been accomplished by the administration of palivizumab (PZ) which is a humanized monoclonal antibody (MAb) directed against the F glycoprotein. However, PZ has only reduced hRSV hospitalization by 55% (Fenton *et al.*, 2004).

Previous studies have reported that all hRSV isolates are susceptible to neutralization by PZ (Johnson *et al.*, 1997; DeVincenzo *et al.*, 2004). hRSV resistant to PZ have been isolated from nasopharyngeal secretions of infants receiving PZ, suggesting that PZ exerts selective pressure for resistance to develop. Their sequence analysis revealed the mutation at residue 272, 275 and 276 (K272E/Q, S275F/L and N276S) which are in the PZ epitope (Boivin *et al.*, 2008; Adams *et al.*, 2010; Zhu *et al.*, 2011). None of these studies have ever shown resistant hRSV in infants without PZ treatment.

Against this background it was surprising that Marsh *et al.* (2007) reported that the predominant hRSV variants isolated from untreated infants are slow growing and resistant to neutralization by anti-F glycoprotein MAbs. These isolates did not carry mutations in known anti-F MAb epitopes. Similar isolates were subsequently found to be additionally resistant to neutralization by PZ and to hRSV immune human serum (Gias, 2006; Welsh, 2010). However, on further passage in culture these isolates rapidly lost their resistance and fast growing, neutralization susceptible variants came to predominate in the cultures (Gias, 2006; Marsh *et al.*, 2007; Welsh, 2010).

This may indicate that virus present in the respiratory tract is less susceptible to neutralization by anti-F antibodies than had been thought hitherto. However, it is unclear whether it is the early resistance in the Newcastle studies or the susceptibility found by others which represents the true state of virus in the respiratory tract. Whichever, this phenomenon is worth elucidating as it presents a complicating factor in assessing the results of neutralization studies on clinical isolates.

In order to locate the genetic changes responsible for this loss of resistance on passage, one such isolate, hRSV R17532, was passaged repeatedly in culture. The virus retained resistance to neutralization up to passage 9, but thereafter resistance was variably lost after a further one or two passages. Sequence comparison of R17532 virus stocks comprising two neutralization resistant cultures at passage 1 and 10 (10a) and one susceptible culture also at passage 10 (10b) revealed no nucleotide changes in the M, SH genes or associated intergenic regions (Gias, 2006; Marsh *et al.*, 2007). A single nucleotide change (T → C) was observed in the G gene between resistant passage 1 and susceptible 10b at position 884, resulting in change from isoleucine to threonine in the residue 295. Both T and C were detected in chromatogram of the resistant passage 10a. For the F gene, four changes occurred between passage 1 and 10b. Two changes occurred (C → T) at nucleotide positions 1802 and 1833 in the 5' untranslated region and two changes were detected in the F coding region shifting residue 20 from phenylalanine to leucine in the signal peptide region and residue 152 from isoleucine to methionine in the HR1 region. However, these changes in the susceptible 10b virus were shared with the still resistant 10a virus (Marsh *et al.*, 2007).

In similar studies by Gias (2006), resistant and susceptible variants of two virus isolates, N5843 and R17532, were cloned and their F genes sequenced. For R17532, neutralization resistant clone R3 and susceptible clone R11 differed with a change from isoleucine to methionine at amino acid 152, the same change as that observed by Marsh *et al.* (2007) in uncloned cultures. They further differed at amino acid 386 in the cysteine-rich domain, with a leucine in the resistant and an isoleucine in the susceptible clone. Neither of these residues varied between resistant and susceptible N5843 clones. Resistant N5843 clone N1 and susceptible clone N10a differed only by a single nucleotide change from proline in clones N1 to serine in clone N10a at amino acid 101 in the F2 subunit.

These studies, therefore, whilst demonstrating that point mutations tend to accumulate in F and G glycoprotein genes on passage found that none were correlated unequivocally with changes in neutralization phenotype. Whilst it is possible that the observed phenotype changes are the result of different, possibly multiple mutations in different cultures and clones, it is also possible that mutations in regions of the genome encoding the non-membrane associated proteins and controlling replication and

transcription may be responsible. In an attempt to investigate the possibility that differences in susceptibility to neutralization result from differences in the efficiency of transcription of the F gene with consequent differences in the concentration of F glycoprotein in the virion, Gias (2006) assessed the F glycoprotein content of virus cultures and purified virions from resistant and susceptible clones. Resistant clones R3 and N1 had higher amount of the F glycoprotein per infectious particle than the susceptible clones R11 and N10a. However, the F glycoprotein per genome copy of purified virions was significantly higher in only clone R3 compared to clone R11. The amount of the F glycoprotein genome in purified clone N1 was similar to that in purified clone N10a (Gias, 2006).

Welsh (2010) initiated studies of the early stages of virus binding and entry of resistant and susceptible clones in the hope of determining differences which might account for changes in the efficacy of antibody neutralization. PZ was found to bind equally to the F glycoprotein of either purified resistant or susceptible hRSV clones. Resistant clones were independent on cell surface heparan sulphate (HS) in binding, whereas susceptible clones required HS. In addition, resistant clones bound to the cells faster than susceptible clones. These results suggested that the neutralization susceptibility to PZ of low and high passage viruses may be affected by differences in receptor usage for cell binding.

In previous studies, Huang *et al.* (2010) found that PZ did not inhibit viral attachment and suggested that neutralization by PZ occurs after the attachment step. In agreement with this Welsh (2010) demonstrated that PZ did not block viral attachment of either neutralization resistant or susceptible R17532 virus clones. It therefore seems that differences between the two clones in susceptibility to neutralization by PZ most likely occur at post-attachment steps.

2.2 Aims

This study seeks to further investigate the genetic and phenotypic differences between slow growing, neutralization resistant and fast growing, neutralization susceptible clones of hRSV with the aim of elucidating the mechanism of resistance and its possible significance in the pathogenesis of human hRSV infection.

The specific aims of this project are:

1. To reclone and verify the neutralization susceptibilities of multiple independent R17532 clones.
2. To compare neutralization resistant and susceptible clones at post-attachment stages of entry.
3. To compare F protein expression levels on the surface of cells infected with resistant and susceptible R17532 clone.
4. To test the conclusion of previous studies that the genetic changes in the membrane associated protein genes are not correlated with neutralization phenotype conversion.
5. To identify the mutations in the full genome of virus clones with resistant and susceptible phenotypes that are associated with the differences in replication rate and antibody susceptibility.

Chapter 3: Materials and methods

3.1 General Reagents

All chemicals were obtained from Sigma-Aldrich (Poole, UK) or Fisher Scientific (Leicestershire, UK) unless stated otherwise. Sterilisation of reagents was carried out by autoclaving at 15 lbs for 15 minutes at 121°C. Distilled water was produced by the Aquatron A4S distillation system (J, Bibby Science Products Ltd., UK) and this water was treated with diethyl pyrocarbonate (DEPC) for use in molecular biology. The DEPC-treated water was prepared by incubating with 0.1% (v/v) DEPC at 37°C overnight before autoclaving.

3.2 Immunoreagents

Table 3.1: Sources and specificities of immunoreagents

Immunoreagents	Specificity	Source
Palivizumab (PZ)	hRSV F glycoprotein	Abbott Laboratories Ltd., Kent, UK (The IMPact-RSV Study Group, 1998)
MAb 1E3	hRSV F glycoprotein	Kindly supplied by Prof. G.L.Toms (West <i>et al.</i> , 1994)
Mouse anti-hRSV MAb pool	hRSV N, P, F and M2 proteins	Novocastra Leica, Leica Biosystems Newcastle Ltd., Newcastle upon Tyne, UK.
Polyclonal rabbit anti-mouse fluorescein isothiocyanate (FITC) conjugated immunoglobulin	Mouse immunoglobulin	DakoCytomation Glostrup, Denmark
Polyclonal goat anti-mouse peroxidase conjugated immunoglobulin (NCL-GAMP)	Mouse immunoglobulin	Novocastra Leica, Leica Biosystems Newcastle Ltd., Newcastle upon Tyne, UK.

3.3 Cell cultures

3.3.1 Materials

Cell lines

Table 3.2: Sources of cell lines.

Cell line	Source	Reference
HeLa NCL	Human cervical carcinoma	Kindly supplied by F. Fenwick (University of Newcastle upon Tyne).
HeLa NCL79 [†]	Human cervical carcinoma	Kindly supplied by Prof G. L. Toms (University of Newcastle upon Tyne).
HeLa Lucy	Human cervical carcinoma	Kindly supplied by Dr J. Hiscox (University of Leeds).
HeLa JSF	Human cervical carcinoma	Kindly supplied by Prof G. E. Blair (University of Leeds).
HeLa CPV	Human cervical carcinoma	Kindly supplied by Prof D. Rowlands (University of Leeds).
16HBE140	Human bronchial epithelial cell	Kindly supplied by Dr D. Grunert (University of Vermont, Burlington, VT; (Cozens <i>et al.</i> , 1994)).
Vero	African green monkey kidney	Clinical Virology unit, Royal Victoria Infirmary, Newcastle upon Tyne.

[†]The HeLa cell, HeLa NCL79, was selected from available lines circulating in the virus diagnostic community in the 1970s following screening for its ability to isolate hRSV from clinical specimens (R. McGuckin personal communication) and was preserved in liquid nitrogen until resuscitated for this study.

Phosphate Buffered Saline (PBS)

Two PBS A tablets (Oxoid, Basingstoke, Hampshire, UK) were dissolved in 200 ml of distilled water, autoclaved and stored at room temperature.

Heat-inactivated foetal calf serum (FCS)

FCS (Biosera, Biosera Ltd, East Sussex, UK) was heat-inactivated in a water bath at 56°C for 30 minutes, then aliquoted in 20 ml volumes and stored at -20°C.

0.4% (w/v) Phenol red indicator solution

Phenol red was diluted in PBS to a final concentration of 0.4% and the pH was adjusted with 1 M NaOH until the solution turned red in colour.

Gassed sodium bicarbonate buffer

44 g of NaHCO₃ and 2.5 ml of 0.4% (w/v) phenol red solution were dissolved in 1 litre of distilled water. The solution was gassed by bubbling 5% CO₂ through it until a peach

coloured solution was produced. It was then aliquoted in 5 ml volumes, autoclaved and stored at room temperature.

Growth Medium (GM)

GM was prepared in 500 ml volumes containing Eagle's Minimum Essential Medium (EMEM) (BioWhittaker, Cambrex BioScience Verviers, Belgium), 10% (v/v) of heat-inactivated FCS, 1% (v/v) of 10 mg/ml Penicillin-Streptomycin (PAA Laboratories, Austria), 1% (v/v) of 200 mM L-glutamine (PAA Laboratories, Austria) and 5% (v/v) of gassed sodium bicarbonate buffer. Media for 16HBE140 cell had the addition of non-essential amino acids (PAA Laboratories, Austria).

Maintenance Medium (MM)

MM was prepared in 500 ml volumes containing Eagle's Minimum Essential Medium (EMEM), 2% (v/v) of heat-inactivated FCS, 1% (v/v) of 10 mg/ml Penicillin-Streptomycin, 1% (v/v) of 200 mM L-glutamine and 5% (v/v) of gassed sodium bicarbonate buffer. Media for 16HBE140 cell had the addition of non-essential amino acids (PAA Laboratories, Austria).

Versene/Trypsin solution

0.25 g of ethylene-diamine-tetra-acetic acid (EDTA) were dissolved in 1 litre of PBS, aliquoted in 100 ml volumes, autoclaved and stored at 4°C. Versene (EDTA) solution had the addition of 2.5% of sterile trypsin solution (PAA Laboratories, Austria) to a final concentration of 0.025% (v/v) prior to use.

3.3.2 Routine cell cultures

Cells were either cultured in 4 oz flat glass bottles or plastic tissue culture flasks. When the cells were confluent, the monolayers were routinely subcultured as follows. The GM was removed and the cells were gently washed with 5 ml of PBS followed by 5 ml of versene/trypsin solution. After discarding versene/trypsin, the cells were then incubated at 37°C in 5% CO₂ for 5 – 10 minutes until the cells were dissociated. The cells were re-suspended in 3 ml of GM and split into three sterile bottles or flasks. The GM was added to each bottle or flasks and incubated at 37°C in 5% CO₂. The cells were routinely passaged every 3 days.

3.4 Virological methods

3.4.1 Virus stocks

hRSV strain R17532 (subgroup A) stocks at passage level 2 (P2-GLT_24/09/98) and level 5 (P5-AC_10/04/98 and P5-RM_23/05/09) and R17532 clones at passage level 3 (R3.2_7/05/04 and R3.7.8_7/05/04) and level 11 (R11.2_5/04/04 and R11.1.1_20/11/09) and strain A2 were kindly provided by Prof G.L. Toms.

3.4.2 Growth of hRSV in 4 oz flat glass bottles or 75 cm³ culture flasks

After rapidly thawing in a 37°C water bath, virus stock was diluted 1/10 in cold MM and then held on ice. The GM was discarded from 80 – 90% confluent HeLa cells in 4 oz flat glass bottle or plastic tissue culture flasks (section 3.3.2) and 300 µl of virus suspension were inoculated onto a monolayer of cells. An equal volume of MM was added to another HeLa cell bottle or flask as a negative control. The HeLa cells were incubated for an hour at 37°C in 5% CO₂ with rocking every 15 minutes before 12 ml of MM were added and then re-incubated at 37°C in 5% CO₂. The media were replaced after 24 hours and every 48 hours. The cultures were examined daily for cytopathic effect and scored on a subjective four counting scoring system 1 – 4+, where 1+ represents just discernible CPE and 4+ complete involvement of the whole monolayer. When 3+ to 4+ cytopathic effect (CPE) developed, hRSV was harvested by scraping the remaining cells into the media using a cell scraper. Virus cultures were aliquoted into 2 ml vials, snap frozen in liquid nitrogen and stored at -80 °C. Infected cells used in RNA extraction were aliquoted into 1.5 ml centrifuge tubes and centrifuged at 500 x g for 5 minutes. The supernatants were aspirated and cell pellets were stored at -80 °C.

3.4.3 Growth of hRSV in 225 cm³ culture flasks

Confluent HeLa cells were stripped with versene/trypsin as described in section 3.3.2. Cell lysate was re-suspended in 10 ml of GM, transferred to 225 cm³ culture flask and 40 ml of GM were added. The flask was incubated at 37°C in 5% CO₂ for 3 days until the monolayer displayed approximately 80 – 90% confluence. Virus stock was rapidly thawed in a 37°C water bath and diluted 1/10 in cold MM. The GM was discarded from HeLa culture flask and 5 ml of virus suspension were inoculated onto the monolayer. Five millilitres of MM were added to another HeLa cell flask as a negative control.

Both flasks were incubated for an hour at 37°C in 5% CO₂ with rocking every 15 minutes. Following incubation, 45 ml of MM were added and the monolayers were treated thereafter as described in section 3.4.2.

3.4.4 Biological cloning of hRSV isolates by plaque purification

The procedure for plaque purification of hRSV was modified from a protocol based on that of Herlocher et al (1999).

Materials

Neutral red solution

Neutral red solution (3 g/L) was diluted 1/3 in PBS.

Overlay media

3.2 g of low gelling temperature Agarose Type VII (Sigma, St Louis, MO, USA) were melted in 200 ml of distilled water in a boiling water bath. The 1.6% (w/v) agarose solution was aliquoted in 12 ml volumes, autoclaved and stored at room temperature. For the nutrient first overlay, 1.6% (w/v) agarose was melted at 100°C and cooled to 37°C before mixing with an equal volume of double strength growth medium pre-warmed to 37°C. For the second overlay, an aliquot of 1.6% (w/v) agarose was melted, cooled to 37°C and 1.5 ml of 1 g/L neutral red were added.

Method

Confluent Vero cells were stripped from 4 oz flat glass bottle or plastic tissue culture flasks as described in section 3.3.2 and re-suspended in 20 ml of GM. Cell suspension was then seeded into 6-wells plates at 3 ml per well and the plates were incubated at 37°C under 5% CO₂ in a moist box (a plastic lunchbox containing a wad of moisture paper towel to ensure high humidity) overnight. When the cells reached 80 – 90% confluence, the GM was discarded from each well and the cells were washed once with 4 ml of PBS per well. Virus stocks were rapidly thawed and ten-fold serial dilutions from 10⁻¹ to 10⁻⁵ were prepared in cold MM. 500 µl of each viral dilution were inoculated onto a cell culture well and 500 µl of MM were added to a further well as a negative control. The virus was allowed to adsorb for 1 hour at 37°C under 5% CO₂ in a moist box with rocking every 15 minutes. The inocula were then removed and the

monolayers were washed 3 times with PBS. Three millilitres of the first nutrient overlay medium were gently added to each well and the agarose was allowed to solidify. The plate was then incubated at 37°C with 5% CO₂ in a moist box until early CPE had developed as determined by examination under the microscope.

When virus plaques were visible and ready to be picked, 2 ml of the second overlay containing 0.01% neutral red solution were gently added to each well. The agarose was allowed to solidify as above and the plate was then incubated at 37°C with 5% CO₂ in a moist box overnight. On the same day, HeLa cell culture tubes were prepared as follows. Confluent HeLa cells were stripped from 4 oz flat glass bottle or culture flasks as described in section 3.3.2 and re-suspended in 30 ml of GM. Cell suspension was then seeded into 30 glass tissue culture tubes with 1 ml per tube and the tubes were incubated overnight at 37°C under 5% CO₂ at a 25° angle. The following day, the monolayers in tubes displayed 80 - 90% confluence.

The plaques were visible as light areas against a dark background. Plaques were carefully marked on the base of the plates under the stereomicroscope. Isolated plaques were then picked with sterile 200 µl pipette tips and emulsified in 200 µl of cold MM by pipetting up and down. Two hundred microlitres of each emulsified plaque were inoculated into a HeLa cell culture tube after discarding the media. A similar volume of MM was added additional tubes to act as negative controls. The tubes were then incubated in a roller drum at 37 °C for 1 hour. After incubation, 800 µl of MM were added to each tube and tubes were re-incubated as above. The CPE in each tube was observed every day and the media were replaced after 24 hours and every 48 hours until 4+ CPE was observed. Virus clones were harvested by scraping the remaining cells into the media using a Pasteur pipette and aliquoted into 2 ml vials. The vials were snap frozen in liquid nitrogen and stored at -80 °C.

3.4.5 Quantitation of hRSV titres using the fluorescent focus assay

Materials

75% (v/v) Acetone/PBS

25 ml of PBS were added to 75 ml of acetone and allowed to equilibrate overnight at 4°C.

0.0033% (w/v) Naphthalene black

0.2 g of naphthalene black were dissolved in 6 L of PBS, aliquoted into volumes of 500 ml, autoclaved and stored at room temperature.

Methods

Plate preparation and infection

Confluent monolayers of cells were dissociated and re-suspended in GM to obtain 3×10^5 cells/ml. 96-well plates were seeded with 200 μ l per well of cell suspension and incubated at 37 °C under 5% CO₂ overnight in a moist box. The following day, the cells were 80 – 90% confluent. Ten- fold dilutions of virus samples were prepared in cold MM from 10^{-1} to 10^{-6} . The GM was discarded from the cell culture plate and then 25 μ l of each virus dilution were inoculated onto triplicate wells. Twenty-five microlitres of MM were added a further well as a negative control and the plate was incubated at 37°C under 5% CO₂ for 1 hour in a moist box. After incubation, the inocula were discarded and the wells were washed with 200 μ l of Hanks' balance salt solution (HBSS). Two hundred microlitres of MM were added to each well and the culture plate was incubated at 37°C in 5% CO₂ for 18 hours in a moist box.

Fixing and immunofluorescent staining

After 18 hours, the MM was discarded and the cells were fixed in 200 μ l of cold 75% (v/v) acetone in PBS for 10 minutes at 4°C. After fixation, the acetone was discarded and then 25 μ l of mouse anti-hRSV MAb pool diluted to 1/5 in PBS were added to each well. The plate was incubated at 37°C for 30 minutes in a moist box and then washed twice with 200 μ l of PBS. Twenty-five microlitres of polyclonal rabbit anti-mouse fluorescein isothiocyanate (FITC) conjugated immunoglobulin diluted to 1/20 in PBS were added into each well and the plate was re-incubated as above. After incubation, the plate was washed twice with 200 μ l of PBS and 200 μ l of 0.0033% (v/v) naphthalene black were added in each well and left at room temperature for 10 minutes. Then, the plate was washed once with 200 μ l of PBS for 5 minutes and followed by distilled water for 1 minute. The plate was air dried at room temperature and examined under a fluorescence microscope (Nikon Eclipse E400, Tokyo, Japan) using a 10x objective lenses. The number of fluorescent foci per well were counted in wells containing between 20 and 60 foci and the virus titre (focus forming units per ml or FFU/ml) was calculated using the following formula:

Virus titre = Average number of fluorescent foci per well \times dilution factor \times 40

3.4.6 Quantitation of hRSV titres using immunoperoxidase focus assay

Materials

0.4% Nutrient agarose overlay medium

1.6 g of low gelling temperature Agarose Type VII (Sigma, St Louis, MO, USA) were melted in 200 ml of distilled water in a boiling water bath. The 0.8% (w/v) agarose solution was aliquoted in 12 ml volumes, autoclaved and stored at room temperature. For the 0.4% nutrient agarose overlay medium, 0.8% (w/v) agarose was melted at 100°C and cooled to 37°C before mixing with an equal volume of double strength growth medium pre-warmed to 37°C.

0.025% (v/v) Eosin solution

0.5% (v/v) Eosin solution was diluted 1/20 in distilled water.

10 x PBS/T

80 g of NaCl, 2 g of KH₂PO₄, 29 g of Na₂HPO₄ and 2 g of KCl were dissolved in 800 ml of distilled water. 5 ml of Tween 20 were added and followed by distilled water to a final volume of 1 litre. The solution was aliquoted in 500 ml volumes, autoclaved and stored at room temperature.

PTF buffer

10 ml of heat-inactivated FCS were added to 90 ml 1xPBS/T and stored at -20°C.

NT buffer

8.76 g of NaCl and 6.06 g of Trizma base were dissolved in 800 ml of distilled water and adjusted to pH 7.5 with concentrated HCl. The solution was made up to 1 litre with distilled water, autoclaved and stored at 4°C.

4-chloronaphthol substrate

4-chloronaphthol substrate was freshly prepared by adding 30 μ l of 30% (v/v) H₂O₂ to 50 ml of NT buffer for the solution 1. The solution 2 contained 30 mg of 4-chloronaphthol

dissolved in 10 ml of cold methanol and two solutions were then mixed immediately prior to use.

Method

This assay was performed as the quantitation of hRSV using fluorescent focus assay in section 3.4.5, except the addition of media after washing with HBSS. Two hundred microlitres of 0.4% nutrient agarose overlay medium were added to each well and the culture plate was incubated at 37°C in 5% CO₂ for 10 minutes at 4°C for gel solidification. The plate was re-incubated at 37°C with 5% CO₂ in a moist box for 72 hours. After incubation, the media was discarded and the cells were fixed in 200 µl of cold 75% (v/v) acetone in PBS for 10 minutes at 4°C. After fixation, the acetone was discarded and then 25 µl of mouse anti-hRSV MAb pool diluted to 1/5 in PTF buffer were added to each well. The plate was incubated at 37°C for 1 hour in a moist box and then washed three times with 200 µl of 1x PBS/T.

Twenty-five microlitres of polyclonal goat anti-mouse peroxidase conjugated immunoglobulin (NCL-GAMP) diluted to 1/1000 in PTF buffer were added into each well. The plate was incubated at 37°C for 1 hour in a moist box and then washed with 1x PBS/T as above. One hundred microlitres of 4-chloronaphthol substrate were added to each well and the plate was incubated at 37°C for 1 hour. After incubation, the substrate was discarded and the plate was rinsed with tap water. Forty microlitres of 0.025% eosin were added to each well and left for approximately one minute. The plate was then rinsed with distilled water, air dried at room temperature and the multicellular foci of infection were counted under the stereomicroscope. The virus titre was calculated using the same formula as section 3.4.5.

3.4.7 Enzyme Linked Immunosorbent Assay (ELISA)

Materials

Substrate buffer

5.1 g of citric acid and 18.4 g of anhydrous Na₂HPO₄ were dissolved in 1 litre of distilled water and adjusted to pH 5.0. The solution was aliquoted in 200 ml volumes, autoclaved and stored at room temperature.

62.5 mg/ml O-phenyldiamine dihydrochloride (OPD) stock solution

1.25 g OPD were dissolved in 20 ml of substrate buffer, aliquoted of 0.4 ml volumes and stored at -20°C.

OPD substrate solution

Immediately before use, 0.4 ml of OPD were thawed and mixed with 24.6 ml of substrate buffer and 10 µl of 30% (v/v) H₂O₂ solution.

3 M H₂SO₄

420 ml of distilled water were placed on ice and 80 ml of concentrated H₂SO₄ was slowly added to the water and mixed.

Washing buffer (10x PBS containing 0.5% (v/v) Tween 20)

160 g of NaCl, 4 g of KH₂PO₄, 23 g of anhydrous Na₂HPO₄ and 4 g of KCl were dissolved in 2 litres of distilled water and 10 ml of Tween 20 were added in the solution. The pH was adjusted to 7.4 and the solution was autoclaved.

Method

A 96-well plate was seeded with HeLa cells as described in section 3.4.5. Virus stocks were adjusted in cold MM to a final titre of 5 x 10⁵ FFU/ml and held on ice. The GM was discarded from the cell culture plate and then 25 µl of each virus were inoculated onto HeLa monolayer. Twenty-five microlitres of MM were added as negative controls. The plate was incubated at 37 °C under 5% CO₂ for 1 hour in a moist box. After incubation, the inocula were discarded and the wells were washed with 200 µl of Hanks' balance salt solution (HBSS). Two hundred microlitres of MM were added to each well and the culture plate was incubated at 37 °C in 5% CO₂ for 18 hours in a moist box.

After 18 hours, the MM was discarded and the cells were fixed with acetone/PBS as described in section 3.4.5. Anti-F MAb 1E3 was serially four-fold diluted from 1/100 to 1/102400 in PTF buffer and then 50 µl of each dilution were added to duplicate wells of each viral dilution and control. The plate was incubated at 37°C for 90 minutes in a moist box and then washed three times with 1x PBS/T at 3 minute interval. Fifty five microlitres of polyclonal goat anti-mouse peroxidase conjugated immunoglobulin

(NCL-GAMP) diluted to 1/1000 in PTF buffer were added into each well. The plate was incubated at 37°C for 1 hour in a moist box and then washed with 1x PBS/T as above. After washing, 50 µl of OPD substrate solution was added to each well and incubated as above for 20 minutes. The reaction was stopped by adding 50 µl of 3M H₂SO₄ in each well and the plate was read at an optical density of 492 nm using an MRX II Microplate reader (Dynex Technologies, UK).

3.4.8 Quantitation of hRSV by the dilution end point method

HeLa cell culture tubes were prepared as described in section 3.4.4 and ten-fold dilutions of virus samples, up to 10⁻⁶, were made in cold MM and held on ice. The GM was discarded from 80 – 90% confluent tissue culture tubes. Two hundred microlitres of each virus dilution were inoculated into triplicate cell culture tubes and 100 µl of MM were added to an additional tube as a negative control. The tubes were then incubated in a roller drum at 37°C for 1 hour. After incubation, 800 µl of MM were added to each tube and tubes were incubated at 37°C in a roller drum. The cytopathic effect (CPE) was observed in each tube every day. Using separate pipettes for each tube to ensure no cross-contamination, the media were replaced after 24 hours and every 48 hours until all positive tubes exhibited 4+CPE. Observation was terminated at 15 days postinoculation. The endpoint dilution was calculated by the Reed-Muench method and expressed as TCID₅₀/ml (Reed and Muench, 1938).

3.4.9 Dilution endpoint neutralization assay

Material

1 mg/ml PZ stock

PZ (Abbott Laboratories Ltd., Kent, UK) was prepared to a final concentration of 50 mg/ml in distilled water according to the manufacturer's instructions and then diluted 1/50 with MM.

Method

HeLa cell culture tubes were prepared (section 3.4.4) and monolayers incubated until approximately 80% confluent. PZ stock was serially four-fold diluted from 1/16 to 1/4096 in cold MM. The diluted PZ solutions were added to an equal volume of MM containing approximately 100 TCID₅₀ (50% tissue culture infective dose) of the virus

under test in a clean 96-well round bottom plate. The plate was incubated at 37°C under 5% CO₂ for 1 hour in a moist box. After incubation, 240 µl of the virus/PZ mixture was inoculated onto triplicate cell culture tubes and the MM was added to an additional tube as a negative control. The tubes were then incubated in a roller drum at 37°C. After 1 hour, 800 µl of MM was added to each tube and tubes were then re-incubated at 37°C in a roller drum. The CPE in each tube was observed every day and the media were replaced after 24 hours and every 48 hours until 15 days. This assay was performed three times for each virus and the neutralization titres were calculated by the Reed-Muench method (Reed and Muench, 1938).

3.4.10 Focus reduction neutralization assay

Mock neutralization assay

For each virus under test, a mock neutralization assay was performed to establish a viral working dilution for use in a focus neutralization assay. A 96-well plate was seeded with Vero or HeLa cells as described in section 3.4.5. Five-fold dilutions of virus stock were prepared in cold MM from 1/5 to 1/625. In a clean 96-well round bottom plate, 50 µl of MM were added to each well to mimic antibody and 50 µl of each virus dilution were added. 100 µl of MM were added to a further well as a negative control. The plate was incubated at 37 °C under 5% CO₂ for 1 hour in a moist box. After incubation, the GM was discarded from the 96-well tissue culture plate containing confluent cells. 25 µl of virus/MM mixtures were inoculated onto triplicate wells of tissue culture plate and the culture plate was incubated at 37 °C under 5% CO₂ for 1 hour in a moist box. The inocula were removed and the cells were washed with 200 µl of HBSS. For assays to be read at 18 hours, two hundred microlitres of MM were added in each well. For the plates to be read at 24 to 72 hours, 200 µl of 0.4% nutrient agarose overlay medium (section 3.4.6) was added to each well and the plate was incubated for 10 minutes at 4°C for gel solidification. The plate was re-incubated at 37°C with 5% CO₂ in a moist box for the requisite time (24 to 72 hours), then fixed and stained either for immunofluorescent foci (section 3.4.5) or immunoperoxidase foci (section 3.4.6). The number of foci determined as described in section 3.4.5. Virus dilutions, which gave a focus number between 40 and 160 FFU per well, were used in the focus neutralization assay.

Neutralization assay

A 96-well plate was seeded with HeLa or Vero cells as described in section 3.4.5. Serial four-fold dilutions of PZ were prepared in cold MM from 1/4 to 1/4096 and held on ice. Virus stock was diluted in cold MM to contain 40 – 160 FFU/25 µl as determined by the mock neutralization test (see above). Fifty microlitres of virus dilution were then mixed with 50 µl of each PZ dilution in a clean 96-well round bottom plate. For a virus control, 50 µl of virus dilution were mixed with 50 µl of MM and 100 µl of MM were added to a further well as a negative control. The plate was incubated at 37 °C under 5% CO₂ for 1 hour in a moist box. After incubation, the GM was discarded from the 96-well plate tissue culture plate containing confluent cells prepared as described in section 3.4.5. Twenty-five microlitres of each virus/PZ mixture and controls in the 96-well round bottom plate were inoculated onto the triplicate wells of tissue culture plate. Thereafter, the plate was cultured and stained as described for the mock neutralization test above. The 50% effective concentration (EC₅₀) of PZ for each virus was that antibody concentration reducing the virus focus count by 50% compared to the virus control and was calculated using a nonlinear regression equation with the Prism™ Graphpad programme. Comparison of neutralization among virus clones was compared by two-way ANOVA.

3.4.11 Focus inhibition assay for the endocytosis inhibitors

Trypan blue exclusion test of cell viability for endocytosis inhibitors

Materials

0.4% (v/v) trypan blue

Trypan blue stock (10%) was diluted in sterile PBS to a final concentration of 0.4%.

Monodansylcadaverine (MDC) stock

Monodansylcadaverine stock was freshly prepared by dissolving 600 µg MDC in 50 µl DMSO and adding MM to a final concentration of 1 mM.

Chlorpromazine (CP) stock

Chlorpromazine stock was freshly prepared by dissolving 800 µg CP in 50µl DMSO and adding MM to a final concentration of 40 µg/ml.

Method

A 96-well plate was seeded with HeLa cells as describe in section 3.4.5. For the MDC test, the MDC stock was diluted to 150, 100, 75, 50 and 25 μM with MM. The GM was removed from the plate and 100 μl of the diluted MDC solutions were added into each well. In a control well, 100 μl of MM were added and the plate was incubated at 37 °C under 5% CO_2 in a moist box for 2 hours. After incubation, the MDC solutions were discarded and the wells were washed with 200 μl of Hanks' balance salt solution (BioWhittaker, Cambrex BioScience Verviers, Belgium). Then, 150 μl of 0.4% nutrient agarose (section 3.4.6) containing the MDC solutions at concentrations corresponding to those above were added into each well. The plate was incubated for 10 minutes at 4°C for gel solidification and then re-incubated at 37°C with 5% CO_2 in a moist box for 72 hours. For the CP test, the CP stock was diluted with MM to 20, 15, 10, 5 and 2.5 $\mu\text{g/ml}$. After discarding the GM, 100 μl of the diluted CP solutions were each added in a well and 100 μl of MM were added to a control well. The plate was incubated at 37°C with 5% CO_2 in a moist box for 6 hours and washed as above. After washing, 200 μl of MM was added to each well and the plate was then re-incubated at 37°C with 5% CO_2 in a moist box for up to 72 hours.

After 72 hours, the media in both tests were discarded from the plate and washed twice with PBS. Twenty five microlitres of versene solution were added into each well and incubated at 37°C for 5-10 minutes until the cells were dissociated. The cells were re-suspended in 25 μl of PBS and 10 μl of cell suspension were mixed with 10 μl of 0.4% trypan blue. Cell/trypan blue mixture was incubated for 3 minutes at room temperature. One drop of mixture was applied to an improved Neubauer hemocytometer and the unstained (viable cell) and stained (nonviable) cells were separately counted. The percentage of viable cell was calculated using the following formula:

$$\% \text{ cell viability} = (\text{the number of viable cells} / \text{total number of cells}) \times 100$$

The 50% cytotoxic concentration (CC_{50}) of endocytosis inhibitors was that the concentration reducing the cell viability by 50% and was calculated using a nonlinear regression equation with the PrismTM Graphpad programme.

Focus inhibition assay using the endocytosis inhibitors

A 96-well plate was seeded with HeLa cells (section 3.4.5) and the endocytosis inhibitors (MDC and CP) were diluted at concentrations which were found to be non-toxic for the cells (see above). The cells were treated with each inhibitor (100 µl/well) in triplicate wells for 1 hour at 37°C under 5% CO₂ in a moist box. The virus stock was diluted in MM to contain 40 – 160 FFU/25 µl as determined by a mock neutralization assay (see section 3.4.10). After 1 hour treatment, 50 µl of each inhibitor was mixed with 50 µl of diluted virus in a clean 96-well round bottom plate. For a virus control, 50 µl of each virus dilution was mixed with 50 µl of MM and 100 µl of MM were added to a further well as a negative control. Twenty-five microlitres of each virus/inhibitor mixture and controls in the 96-well round bottom plate were inoculated onto the triplicate wells of tissue culture plate in the same concentration of inhibitors treated.

After inoculation, the plate for MDC test was incubated at 37°C under 5% CO₂ for 1 hour and the inocula were removed from tissue culture plate after incubation. The cells were washed with 200 µl of HBSS and 200 µl of 0.4% nutrient agarose overlay medium (section 3.4.6) containing the MDC at concentrations corresponding to those in the inoculum were added to each well. The plate was incubated for 10 minutes at 4°C for gel solidification and then incubated at 37°C with 5% CO₂ in a moist box for 72 hours. For the CP test, the plate was incubated for 5 hours at 37 °C under 5% CO₂ after inoculation. The inocula were discarded and the wells were washed with 200 µl of HBSS. Two hundred microlitres of 0.4% nutrient agarose overlay medium (section 3.4.6) without the CP were added to each well and the culture plate was incubated at 37 °C in 5% CO₂ for 72 hours. Following incubation, all plates were fixed, stained and the number of foci in each well was determined as described in section 3.4.6. The 50% effective concentration (EC₅₀) for each drug, that concentration which reduced the focus count by 50% when compared to the virus controls, was determined by nonlinear regression equation using the PrismTM Graphpad programme. Comparison of inhibition among virus clones was compared by two-way ANOVA.

3.4.12 Focus inhibition assay for the antiviral agents directed against the F glycoprotein

Materials

R17532-Heptad repeat 2 (HR2) peptide

- Peptide formulation

The hRSV inhibitory HR2 peptide was formulated based upon the study of Lambert *et al.* (1996) (see section 1.10.1) in which the HR2 domain was identified in the F glycoprotein of the hRSV Long strain with a computer search strategy recognizing sequences predicted to form helical structures in fusogenic viral proteins. The amino acid sequence of the R17532 strain F glycoprotein was identical to that of the Long strain in this region, except at residue 518 which was A in the Long strain, but V in both R17532 clones R11 and R3 (Gias, 2006). Therefore, the sequence of the peptide used in this study, R17532-HR2, was

“FDASISQVNEKINQSLAFIRKSDELLHNVNVGKST”.

- Peptide synthesis

The R17532-HR2 peptide was manufactured as lyophilized crude peptides by GenScript, New Jersey, USA. It was modified with acetylation at N-terminus and amidation at C-terminus to enhance biological half-life (Powell, 1993).

- Peptide preparation

4 mg of the peptide were dissolved in 100 µl DMSO and diluted with distilled water to a final concentration of 1 mM. Diluted solution was aliquoted in 100 µl volumes and stored at -80 °C.

The BTA9881 and BMS-433771 stocks

The BTA9881 was kindly supplied by Laura Wood (Biota Holdings Limited, Notting Hill, Australia) and BMS-433771 was kindly provided by Mark Krystal (Bristol-Myers Squibb, Wallingford, USA). The BTA9881 and BMS-433771 were prepared by dissolving in 100 µl DMSO and diluted with distilled water to a final concentration of 2 mM. Stock solutions were aliquoted in 100 µl volumes and stored at -80 °C.

Methods

The HR2 peptide and BTA9881 were diluted to 80, 20, 5, 1.25, 0.312 and 0.078 µM in MM and the BMS-433771 was diluted to 20, 5, 1.25, 0.312, 0.078 and 0.0195 µM. The assay was carried out as for the focus reduction neutralization assay and read at 72

hours as described in section 3.4.10, except that virus/PZ mixture was immediately added to HeLa cell monolayers without a 1 hour pre-incubation and the antiviral agents at concentrations corresponding to those in the inocula were incorporated in the nutrient agarose overlay medium. The immunoperoxidase method was used to stain the plate as described in section 3.4.6. The 50% effective concentration (EC₅₀) was calculated as described in section 3.4.10.

3.4.13 Virus purification methods by iodixanol density gradients ultracentrifugation

This protocol for purification of hRSV by ultracentrifugation in iodixanol density gradient was performed as described by Gias et al. (2008).

Materials

500 mM Tris-HCL

30.29 g of Tris base (Melford, Suffolk, UK) were dissolved in distilled water and the pH was adjusted to 7.5 with concentrated HCl. The buffer was made up to a final volume of 500 ml with distilled water, autoclaved and stored at 4°C.

1 M MgSO₄ solution

24.65 g of MgSO₄·7H₂O were dissolved in 100 ml distilled water, autoclaved and stored at 4°C.

0.25 M Sucrose solution

8.56 g of sucrose were dissolved in 100 ml distilled water, sterilized by filtering through 0.22 µm filter (Corning Incorporated, USA) and stored at 4°C.

50% (w/v) PEG 6000

250 g of PEG 6000 were dissolved in 40 ml of NT buffer (prepared in section 3.4.6) in a 56°C water bath, brought to a final volume of 500 ml, sterilized by filtering through 0.22 µm filter and stored at 4°C.

OptiPrep™ iodixanol solution

Iodixanol solution was supplied as a 60% (w/v) solution by Axis-Shield PoC AS, Oslo, Norway and was wrapped in aluminium foil and stored at 4°C.

0.5 M EDTA

93.06 g of EDTA and 10 g NaOH were dissolved in 350 ml distilled water and the pH was adjusted to 8.0 with NaOH. The solution was made up to a final volume of 500 ml, autoclaved and stored at room temperature.

Methods

Clarification of virus clone stocks

Virus cell lysate was harvested at 4+ CPE from 225 cm³ flasks (see section 3.4.3) and aliquoted in 25 ml volumes. Lysate were then sonicated on ice using a SANYO MSE Soniprep sonicator at amplitude of 5 microns for 1 minute repeated three times with a 1 minute rest between each. Sonicated virus material was then pooled together and centrifuged in sterile 50 ml centrifuge tubes in a MSE Coolspin centrifuge at 3,250 g (4,000 rpm) for 20 minutes at 4°C. The clarified viral supernatants were transferred to a sterile 250 ml Schott bottle and 500 µl of supernatant were taken for subsequent infectious focus and neutralization assays. The clarified viral supernatant was then adjusted to 0.1 M MgSO₄ and 50 mM Tris-HCl (pH 7.5) (Ferne and Gerin, 1980).

PEG precipitation

50% (w/v) PEG 6000 was added to the clarified viral supernatant to a final concentration of 10% (v/v) and allowed to precipitate overnight at 4°C with moderate stirring. After overnight precipitation, the PEG solution was centrifuged at 3,250 g (4,000 rpm) for 20 minutes at 4°C in a MSE Coolspin centrifuge. The supernatant was carefully removed and the pellet was re-centrifuged as above. The pellet was then re-suspended in 1 ml of cold NT and held on ice. 1 M MgSO₄ was added to the PEG viral suspension to a final concentration of 100 mM MgSO₄. The suspension was collected in 10 µl volumes and combined with EDTA to a final concentration of 1 mM EDTA and infectivity was quantified by the immunoperoxidase focus assay (section 3.4.6).

Rate zonal ultracentrifugation: discontinuous iodixanol density gradient

Gradient medium containing 20%, 36% and 52% (v/v) of iodixanol, 10 mM Tris-HCl pH 7.5, 100 mM MgSO₄ and 0.25 M sucrose added up to 10 ml were individually prepared as described in Table 3.3.

Table 3.3: Preparation of gradient medium for discontinuous iodixanol density gradient

Solution	Gradient medium with Iodixanol		
	20%	36%	52%
60% iodixanol	3.30 ml	6.00 ml	8.70 ml
500 mM Tris-HCl pH 7.5	0.20 ml	0.20 ml	0.20 ml
1 M MgSO ₄	1.00 ml	1.00 ml	1.00 ml
0.25 M sucrose	5.50 ml	2.80 ml	0.10 ml
Total volume	10.00 ml	10.00 ml	10.00 ml

Two discontinuous gradients were immediately prepared in 14 ml Ultraclear centrifuge tubes (Beckman, USA) before use by sequentially adding 4 ml of 52%, 36% and 20% iodixanol medium. The PEG-concentrated virus sample was then added on the top of each gradient in equal volumes (approximately 0.5 ml each). The gradients were centrifuged in a SW-40 rotor for 90 minutes at 154,693 g (35,000 rpm) at 4°C. After centrifugation, visible virus bands locating the interface between the 20% and 36% iodixanol medium were collected from each gradient using pipette tips and held on ice. The fraction samples containing 1mM EDTA were carried out the immunoperoxidase focus assay as described in section 3.4.6.

Buoyant density ultracentrifugation: continuous iodixanol density gradient

Gradient medium containing 20%, 32%, 42% and 52% (v/v) of iodixanol, 10 mM Tris-HCl pH 7.5, 100 mM MgSO₄ and 0.25 M sucrose added up to 9 ml were individually prepared as described in Table 3.4.

Table 3.4: Preparation of gradient medium for continuous iodixanol density gradient

Solution	Gradient medium with Iodixanol			
	20%	32%	42%	52%
60% iodixanol	3.00 ml	4.80 ml	6.30 ml	7.80 ml
500 mM Tris-HCl pH 7.5	0.18 ml	0.18 ml	0.18 ml	0.18 ml
1 M MgSO ₄	0.90 ml	0.90 ml	0.90 ml	0.90 ml
0.25 M sucrose	4.92 ml	3.12 ml	1.62 ml	0.12 ml
Total volume	9.00 ml	9.00 ml	9.00 ml	9.00 ml

Two continuous gradients were prepared in 14 ml Ultraclear centrifuge tubes (Beckman, USA) by sequentially layering 4 ml of 52%, 42%, 32% and 20% iodixanol medium. The tubes were wrapped in aluminium foil and stored overnight at 4°C to allow the gradient to diffuse. The virus bands collected from each discontinuous gradient were diluted 1/2 in cold NT buffer containing 100 mM MgSO₄ and layered on the top of each continuous gradient. The gradients were centrifuged in a SW-40 rotor for 18 hours at 154,693 g (35,000 rpm) at 4°C. After 18 hours, the gradient fractions were harvested in approximately 700 µl volumes and the density was measured using a refractometer (ATACO, USA). Each fraction was aliquoted in 200 µl volumes for RNA extraction and the rest aliquoted for virus assay. All fractions were snap-frozen in liquid nitrogen and stored at -80 °C. The fraction samples with 1 mM EDTA were subsequently used in immunoperoxidase focus assay and neutralization assay.

3.5 DNA analysis methods

3.5.1 RNA extraction

Total RNA extraction from hRSV virus stock

Total RNA was extracted from infected cells using the RNeasy Mini Kit (QIAGEN, Crawley, W. Sussex, UK) according to the manufacturer's instructions. The RNA was eluted in the DEPC treated water and stored at -20°C or used immediately. The amount of RNA was determined using a ND-1000 Nanodrop spectrophotometer (NanoDrop products, Wilmington).

RNA extraction from purified hRSV virus

Two hundred microlitres of iodixanol gradient fractions containing purified virus (section 3.4.13) were thawed rapidly at 37°C. RNA extraction was carried out using QIAamp[®] MinElute Virus Spin Kit (QIAGEN, Crawley, W. Sussex, UK) according to manufacturer's instruction. Carrier RNA in the kit reagent precluded direct determination of the concentration of hRSV RNA recovered.

3.5.2 Reverse transcription (RT)

Reverse transcription was carried out in 20 µl volumes containing 0.5 – 1 µg RNA (or 10 µl of RNA from purified virus), 1 mM dNTPs (Thermo Scientific Fermentas, UK),

20 pmol RT primer (Table 3.5 and 3.6), 20 units RNasin ribonuclease inhibitor (Promega, Madison, UK), 1x RevertAidTM H Minus M-MuLV reverse transcription buffer, 200 units RevertAidTM H Minus M-MuLV Reverse transcriptase (Thermo Scientific Fermentas, UK) and DEPC-treated water. Synthesis of cDNA was carried out in a PTC-200 Thermal Cycler (MJ Research, now Bio-Rad, Hemel Hempstead, UK) at 42°C for 60 minutes and 70°C for 10 minutes. The reaction was then cooled at 4°C and either used immediately or stored at -20°C.

Table 3.5: Sequences and sources of primers.

Name	Sequence (5'→3')	Nucleotide*	Source†
NS1	CGCGAAAAAATGCGTACAAC	2-20	In house
NS1.1	ATTTTTTTGGTTTACGCAAGTTTG	44-21	In house
NS1-26	CCAAAGGAGTTGAATTTAAGTGG	92-70	In house
NS1-103	CAATGCTACTTCATCATTGTCAAA	170-147	In house
NS1-134	TCAATTTGTCAGTATAGCAGGTTA	201-178	In house
NS1end	CTGCCTTAGCCAAAGCATTAA	231-212	In house
NS1-206	GCACAAATACAATGCCATTCA	270-250	In house
NS1-442	TCTGAATTACTTGGATTTGATCTTAA	486-511	In house
NS2-358	AGCCTACAAAGCATACTCCATAA	953-976	In house
NS2-468	TACTATAATTTTCAGGCTCCATCTGGAC	1,090-1,063	In house
NP1674	CTTACAGCCGTGATTAGGAGAGC	1,674-1,696	In house
N713	CTTCAACTCTACTGCCACCTCTGG	1,860-1,837	In house
P2128	GCCTAGGCATAATGGGAGAGTA	2,128-2,149	In house
P162	TATAGGGCTTTCTTTGGTTACTTC	2,513-2,490	In house
PS3	CAGACAAACGATAATATAACAGCAAGAT	2,720-2,748	In house
PS4	TCTTTTGCCATCTTTTCACTTTCCTCAT	2,971-2,944	In house
P3459	CCTTGGGTGTGGATATTTGTTTC	3,459-3,437	In house
M1	GCCAA[A/C]AAAACAAC[C/T]AGCCAATCC	3,174-3,197	(Gias, 2006)
M2	GTGTAAAGTAAGGCCAGAATTTGCTTGAG	4,360-4,332	(Gias, 2006)

Name	Sequence (5'→3')	Nucleotide*	Source†
SH+	CAGCTACACG[A/T]TTT[G/T]CAATCAAAC	3,994-4,017	(Marsh, 2002)
SH-	GTTGAGATTATCATTGCC	4,842-4,825	(Marsh, 2002)
SH292	TGATGGCTCAAAACAGTAACCT	4,510-4,531	In house
G713	TTTTGGTGGTGTGATGGTTGGCT	5,408-5,385	In house
GC1	GCAGCATATGCAGCAACA	5,205-5,222	(Roca <i>et al.</i> , 2001)
G886	TCTCCATCCAACATAACAAACCTG	5,558-5,581	In house
F164	GTTATGACACTGGTATACCAACC	5,855-5,833	(Sullender <i>et al.</i> , 1993)
F400	CTTGTTTGTGGATAGTAGAGC	6,188-6,168	(Marsh, 2002)
F1000	GCAGAGATTTACTTCACTTGG	6,806-6,786	(Marsh, 2002)
ALW1	ATAACCATGGAGTTGC[C/T][A/G]ATCC	5,655-5,676	(Connor, 1998)
A2R2	TAGTGTCTTAACCAGCAAAG	6,215-6,234	(Connor, 1998)
A2R3	GTGACACAATGAACAGTTTA	6,760-6,779	(Connor, 1998)
ALW2	TTGCAAGGATTCCTTCGTGAC	7,668-7,628	(Connor, 1998)
M2F	TTACAATGGTTTACTATCTGCTCA	7,411-7,434	In house
M2R	GTTCTATTAATGGATTTTGTCTAC	8,669-8,646	In house
M2-848	ACACTCACCACATCGTTAC	8,444-8,462	In house
L589	TGTGTTTCGATGCAACATCCT	9,078-9,097	In house
L662	CCTCATTTGATCGATACTGTGTT	9,173-9,151	In house
L716	TTGGAATCCATTGAGAGTATGA	9,226-9,205	In house

Name	Sequence (5'→3')	Nucleotide*	Source†
L1307	TGGCTTGTCTTTCATCTACC	9,796-9,815	In house
L1116	AAAGCTCAGAAAAATCTGCTATCAA	9,605-9,629	In house
L2337	TTTTGACACCACCCTTCGAT	10,845-10,826	In house
L3-1	CTCAGCAAATTCAATCAAGCA	10,598-10,618	In house
L3-2	CCTCATCATCTCAGTGGCTCT	12,007-11,987	In house
L3-3	GAGGTGAAAGTCTATTATGCAGTTTA	11,250-11,275	In house
L3-4	GGGATCACCACCACCAAATA	11,467-11,448	In house
L4-1	GCAAAATATAGAACCTACATATCCTCA	11,830-11,856	In house
L4-2	CCCTCTCCCAATCTTTTTTC	13,059-13,040	In house
L5-1	CACTCAAATCTGGATCTCATGTTA	12,891-12,914	In house
L5-2	GGGTTTAAATTTATTCTCCAAGA	15,153-15,130	In house
L5-3	ACAGACAATTCGGCATCACA	14,319-14,300	In house
L5-4	TGAGTTTTTAAGGCTGTACAATGG	14,161-14,184	In house
L5-5	AGATCTTGTTAGAATGGGATTGAT	13,426-13,449	In house
L5-6	TTCAGAATTAGCAATCCTTATATGTTT	13,588-13,562	In house
L5-7	GACCATTCCCGCTACAGATG	14,215-14,234	In house
L5-8	TGTTAGTGTGTAGATGTGGGAATTT	15,041-15,017	In house
L5-8R	AAATTCCCACATCTACACACTAACA	15,017-15,041	In house
L5-9	ACGAGAAAAAAAGTGCAAAAAC	15,222-15,199	In house

Name	Sequence (5'→3')	Nucleotide*	Source†
Lend	CATCTTAAAGTGGTTCAATCATGT	14,812-14,825	In house
L5-2R	TCTAGGAGGTATAAATTTAAATCC	15,130-15,153	In house
Adaptor DT88	GAAGAGAAGGTGGAAATGGCGTTTTGG (Modification: 5'-Phosphate & 2',3'dideoxyC)	-	(Li <i>et al.</i> , 2005)
DT89	CCAAAACGCCATTTCCACCTTCTCTTC	-	(Li <i>et al.</i> , 2005)
Modified DT89	CCAAAACGCCATTTCCAC	-	Modified from (Li <i>et al.</i> , 2005)

*Nucleotide numbering is based on hRSV A2 genome, GenBank accession number M74568.

†Primers were designed according to the guidelines described in Dieffenbach and Dveksler (2003) and using the Primer3 program (Rozen and Skaletsky, 2000). All primers were manufactured by Sigma-Aldrich (Poole, UK) or Eurofins MWG Operon (Ebersber, Germany). Freeze dried primers were re-suspended in DEPC-treated water to a final concentration of 100 µM and 30 µM of working primer solutions was prepared in DEPC-treated water.

Table 3.6: Summary of RT- PCR and sequencing primers.

Gene	RT primer	PCR primer pair	PCR product size	Sequencing primer
NS1 NS1-NS2 IR ^a NS2	NS1	NS1: NS2-468	1,089nt	NS1, NS1-134, NS2-468
NS1-NS2 IR NS2 NS2-N IR N	NS1-442	NS1-442: N713	1,375nt	NS1-442, NS2-358, N713
N N-P IR	NP1674	NP1674: P162	840nt	NP1674, P162
M M-SH IR	M1	M1: M2	1,184nt	M1, M2
M-SH IR SH SH-G IR	SH+	SH+: SH-	849nt	SH+, SH-
N-P IR P P-M IR	P2128	P2128: P3459	1,332nt	P2128, P3459, PS3, PS4,
SH-G IR G G-F IR	SH292	SH292: F164	1,326nt	SH292, GC1, G713, F164
G-F IR F	G886	G886: F1000	1,249nt	G886, F400, A2R2,F1000
F F-M2 IR	G886	A2R3: ALW2	869nt	A2R3, ALW2
F-M2 IR M2	M2F	M2F: M2R	1,259nt	M2F, M2R
M2, LF1 ^b	M2-848	M2-848 : L1307	1,372nt	M2-848, L1307, L589, L662, L716
LF2	M2-848	L1116: L2337	1,241nt	L1116, L2337
LF3	M2-848	L3-1: L3-2	1,410nt	L3-1, L3-2, L3-3, L3-4
LF4	L4	L4-1: L4-2	1,230nt	L4-1, L4-2
LF5.1	L5-1	L5-1: L5-3	1,429nt	L5-1, L5-3, L5-5, L5-6
LF5.2	L5-1	L5-4: L5-2	993nt	L5-4, L5-2
LF5.2	L5-1	L5-7: L5-8 (Nested primers for R5.3, R5.14,)	827nt	L5-7, L5-8
LF5.2	L5-1	L5-8R: L5-9 (Used only with R3)	206nt	L5-8R, L5-9

^aIR: Intergenic regions; ^b L gene was separated into 6 fragments as follows; LF1 (nt 8,444 to nt 9,815), LF2 (nt 9,605 to nt 10,845), LF3 (nt 10,598 to nt 12,007), LF4 (nt 11,830 to nt 13,059), LF5.1 (nt 12,891 to nt 14,319) and LF5.2 (nt 14,161 to nt 15,153) including 5' terminal sequence.

3.5.3 Polymerase Chain Reaction (PCR)

PCR reactions were carried out in 100 µl volumes containing 4 µl of cDNA, 5 mM of MgCl₂, 1x ImmoBuffer, 0.25 mM mixture of dATP, dCTP and dGTP, 0.5 mM dUTP, 0.3 µM of each forward and reverse primer (Table 3.5 and 3.6), 5 units of IMMOLASE™ DNA polymerase and DEPC-treated distilled water. PCR was carried out in a PTC-200 Thermal Cycler (MJ Research, now Bio-Rad, Hemel Hempstead, UK) with the following conditions: an initial denaturation at 95°C for 10 minutes, followed by 35 cycles of reactions consisting of a denaturation step at 95°C for 1 minute, an annealing step at 55°C for 30 seconds and an elongation step at 72°C for 2 minutes and a final elongation at 72°C for 7 minutes. The reaction was then cooled at 4°C and either used immediately or stored at -20°C. The PCR amplification of all hRSV genes was conducted using the reaction and condition as above, except PCR using N1674:P162 and NS1-442: N713 primer pair. The first primer pair was carried out at annealing temperature of 50°C. Reactions with the latter primer pair were performed with 3.75 mM MgCl₂ and an annealing temperature of 60°C.

3.5.4 Genomic RNA circularization for determination of the 5' and 3' terminal sequences of the hRSV genome

Genomic RNA circularization protocols were modified from Krempl *et al.* (2005) as shown in Figure 3.1. All primers utilised were presented in Table 3.5 and 3.7. The circularization of RNA genome was performed in a reaction mix containing 1 µg of total RNA extracted from virus stock or 10 µl of viral RNA isolated from purified virus (section 3.5.1), 1x T4 RNA ligase buffer, 10 units of T4 RNA ligase (Ambion, Life Technologies Ltd, Paisley, UK) and DEPC treated water to a final volume of 20 µl. The reaction mixtures were incubated overnight at 4°C for RNA circularization and cDNA synthesis was then performed as described in section 3.5.2 using the Lend primer that bound to the position near the end of L gene. This was followed by the first round of a nested PCR reaction carried out as described in section 3.5.3 using Lend:NS1end. Three alternative sets of primers were used for the second round as follows: L5-8R: NS1-134, L5-2R:NS1-26 or L5-2R:NS1.1.

Table 3.7: Summary of RT- PCR and sequencing primers for determination of the 5' and 3' terminal sequences.

Procedure	RT primer	1st round PCR primers (PCR product size)	2nd round PCR and sequencing primers (PCR product size)
Genomic RNA circularization	Lend	Lend:NS1end (642nt)	L5-8R:NS1-134 (383nt) L5-2R:NS1-26 (185nt) L5-2R:NS1.1 (137nt)
5'RACE	L5-8R	L5-8R:DT89 (233nt)	L5-2R:DT89 (120nt)
3'RACE from the anti-genome	NS1-206	NS1-206:modified DT89 (297nt)	NS1-103:modified DT89 (197nt)
3'RACE from the genome	DT89	modified DT89:NS1-206 (297nt)	modified DT89:NS1-103 (197nt)

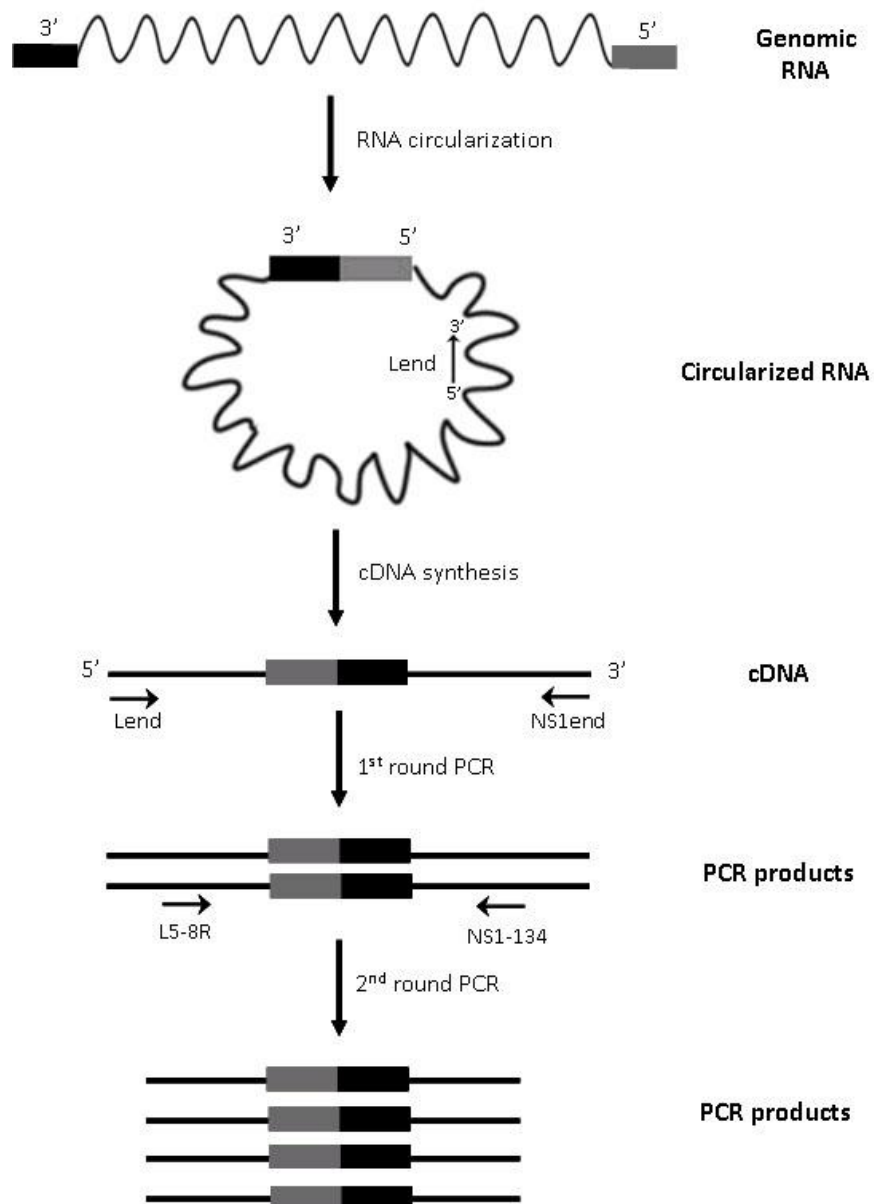


Figure 3.1: Schematic diagram for genomic RNA circularization procedure.

The viral RNA genome oriented 3' to 5' was circularized using T4 RNA ligase, followed by cDNA synthesis using the Lend primer. After cDNA containing 3'-5'-ligated RNA end production, two rounds of PCR amplification were conducted using the Lend: NS1end primer pair for the first round PCR and the L5-8R: NS1-134 primer pair for the second round. The RNA genome is indicated by a wavy line; cDNA and PCR products are straight lines; 3'end is a black box; 5'end is a grey box and primers are arrows.

3.5.5 5' Rapid amplification of cDNA ends (5'RACE) from the hRSV anti-genome

5'RACE was performed following Figure 3.2 using procedures based upon those described by Tillett *et al.* (2000) and Li *et al.* (2005). All primers used in these methods are shown in Table 3.5 and 3.7. The cDNA was synthesized from 1 µg of total RNA or 10 µl of viral RNA (section 3.5.1) using the L5-8R primer by reverse transcription (section 3.5.2) followed by treatment with 2 units of RNase H (Thermo Scientific Fermentas, UK) at 37°C for 20 minutes. The resulting cDNA was purified using a GeneJET™ PCR purification kit (Thermo Scientific Fermentas, UK) according to the manufacturer's instructions and then ligated with the adaptor DT88 overnight at room temperature using 10 µl of cDNA, 0.4 µM of adaptor DT88, 1x T4 RNA ligase buffer, 3 units of T4 RNA ligase (Ambion, Life Technologies Ltd, Paisley, UK) and DEPC treated water to a final volume of 13 µl. Another ligation reaction without T4 RNA ligase was carried out as a negative control.

The adaptor-ligated cDNA was then subjected to two hemi-nested rounds of PCR amplification. The first and second round PCRs were performed using the virus-specific primers (L5-8R and L5-2R primers used for 1st and 2nd round PCR, respectively) and the DT89 primer, complementary with the adaptor DT88 for both rounds, in a PTC-200 Thermal Cycler (MJ Research, now Bio-Rad, Hemel Hempstead, UK) with reaction mixes as described in Table 3.8 and with the following conditions: 95°C for 10 minutes, followed by 35 cycles of 95°C for 20 seconds, 55°C for 20 seconds, 72°C for 30 seconds and a final elongation at 72°C for 7 minutes.

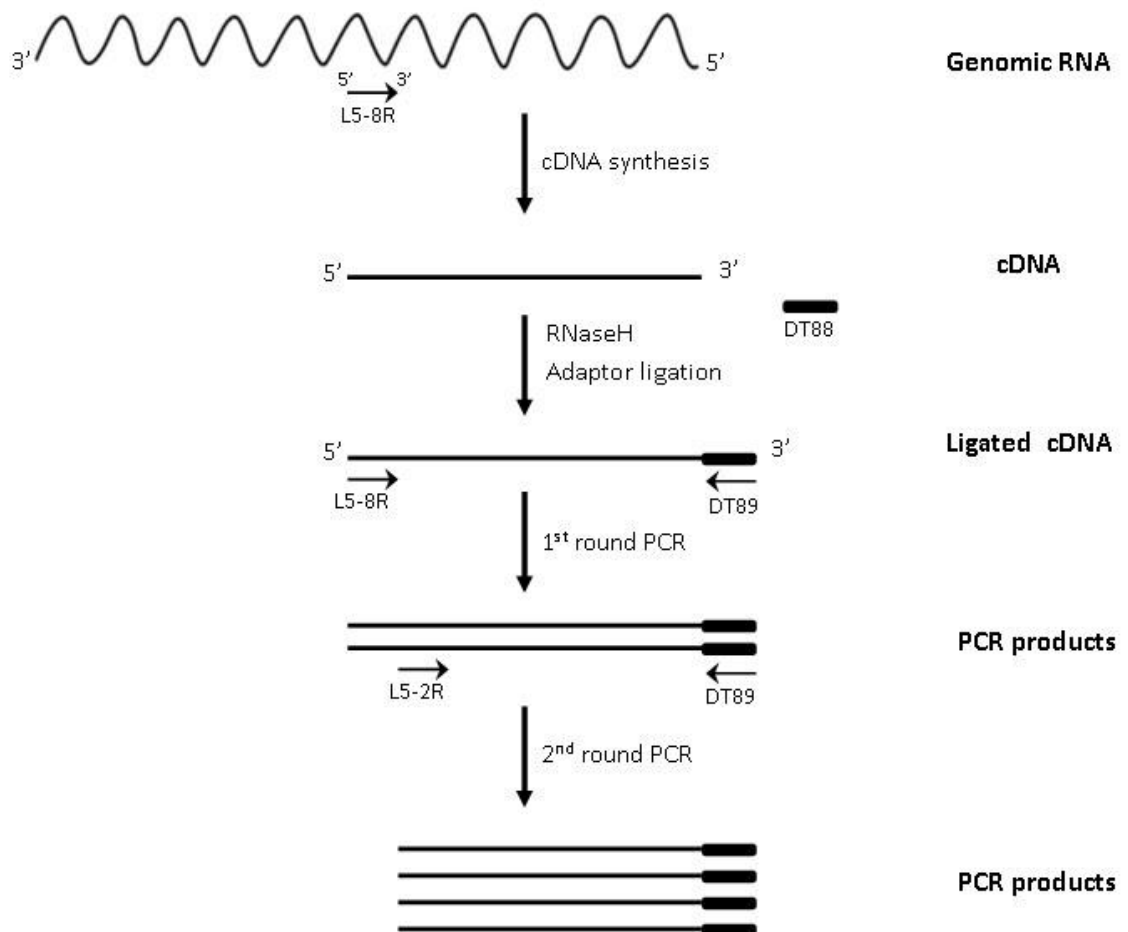


Figure 3.2: Schematic diagram for 5'RACE procedure from the hRSV anti-genome.

[Modified from original by Hsieh *et al.* (1997) and Li *et al.* (2005)]

The cDNA synthesis was first synthesized from the virus genome using the L5-8R primer. The cDNA was then treated with RNaseH, followed by ligation to adaptor DT88 using T4 RNA ligase. Then, a first round PCR was carried out using the L5-8R primer and the DT89 primer, complementary to the adaptor DT88, followed by a hemi-nested second round PCR using the L5-2R and DT89 primers. The RNA genome is indicated by a wavy line; cDNA and PCR products are straight lines; adaptors are black boxes; primers are arrows.

Table 3.8: PCR Reaction for 5'RACE procedure.

Procedure	PCR reaction*
1 st round PCR	0.8 µM L5-8R
	0.8 µM DT89
	5 mM MgCl ₂
	250 µM dNTPs mix
	1.25 U IMMOLASE™ DNA polymerase
	1x ImmoBuffer
	4 µl cDNA
2 nd round PCR	0.8 µM L5-2R
	0.8 µM DT89
	5 mM MgCl ₂
	250 µM dNTPs mix
	1.25 U IMMOLASE™ DNA polymerase
	1x ImmoBuffer
	4 µl 1:100 diluted 1 st round PCR product
2 nd round PCR after optimization	0.3 µM L5-2R
	0.3 µM DT89
	7.5 mM MgCl ₂
	250 µM dNTPs mix
	1.25U IMMOLASE™ DNA polymerase
	1x ImmoBuffer
	4 µl 1:100 diluted 1 st round PCR product

*DEPC treated water was added in all procedures to a final volume of 100 µl.

3.5.6 3'Rapid amplification of cDNA ends (3'RACE) from the hRSV anti- genome

The procedure for 3'RACE (Figure 3.3) was modified from a protocol based on that of Li *et al.* (2005) and all primers used in this method are presented in Table 3.5 and 3.7. Antigenome cDNA was synthesized from 1 µg of total RNA or 10 µl of viral RNA (section 3.5.1) using the NS206 primer by reverse transcription (section 3.5.2) and the cDNA was then treated with RNase H (Thermo Scientific Fermentas, UK) as described in section 3.5.5. The adaptor DT88 was ligated to the cDNA overnight at room temperature after purification using the GeneJET™ PCR purification kit (Thermo Scientific Fermentas, UK). Ligation reaction contained 10 µl of cDNA, 0.4 µM of adaptor DT88, 1x T4 RNA ligase buffer, 3 units of T4 RNA ligase (Ambion, Life

Technologies Ltd, Paisley, UK) and DEPC treated water to a final volume of 13 μ l. As a negative control, another set of ligation reaction was performed without T4 RNA ligase in the solution. The adaptor-ligated cDNA was then amplified by hemi-nested PCR in a PTC-200 Thermal Cycler (MJ Research, now Bio-Rad, Hemel Hempstead, UK) using the NS206 and modified DT89 primers in the first round. The length of modified DT89 primer was shorter than unmodified DT89 primer (Li *et al.*, 2005) in order to match the T_m with that of NS206 and NS103. The second round PCR was then conducted using the NS103 and modified DT89 primers. Both PCR reactions were performed as described in section 3.5.5 with conditions as described in Table 3.9, but with the primers described above.

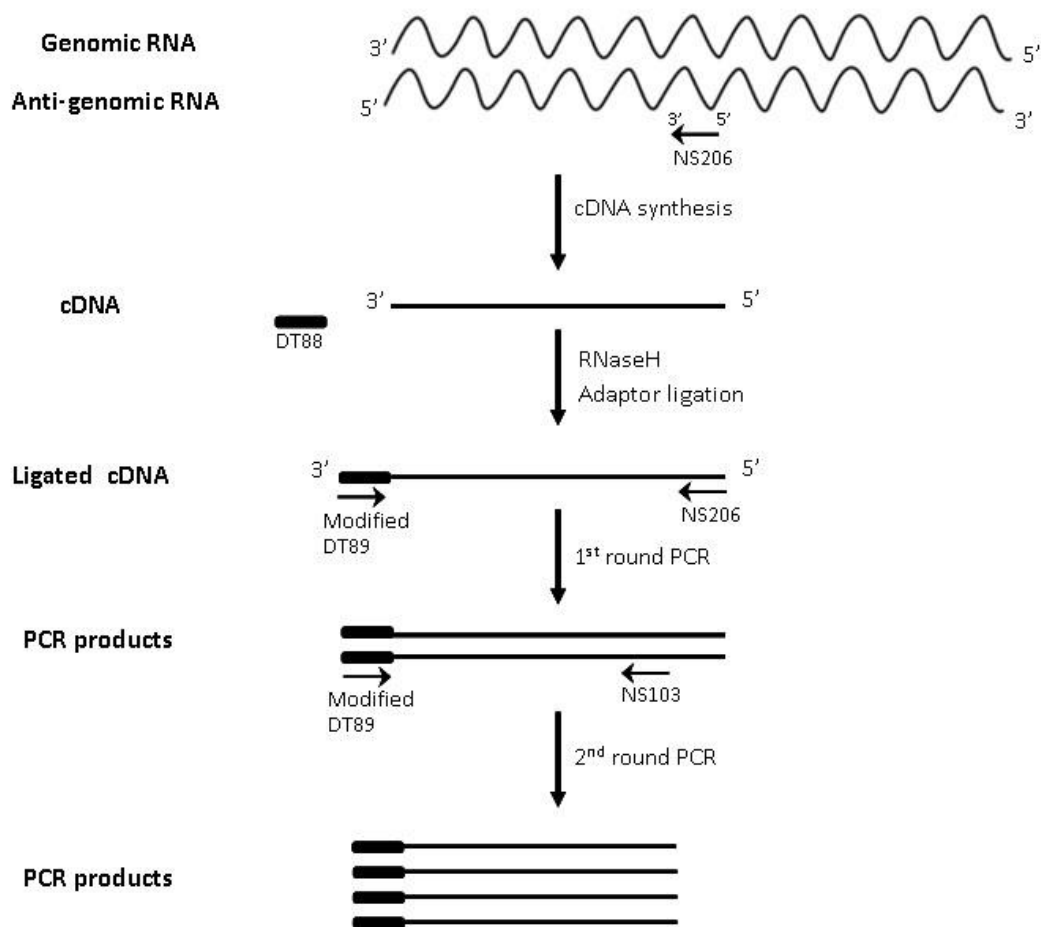


Figure 3.3: Schematic diagram for 3'RACE procedure from the hRSV anti-genome.

[Modified from original by Hsieh *et al.* (1997) and Li *et al.* (2005)]

cDNA was firstly synthesized from the antigenome using the NS206 primer, followed by RNaseH treatment. Adaptor (DT88) ligation was then performed using T4 RNA ligase and followed by hemi-nested of PCR. The first round PCR was carried out using the NS206 and modified DT89 primers. The NS103 and modified DT89 primers were used for the second round of the PCR. The RNA genome/antigenome is indicated by a wavy line; cDNA and PCR products are straight lines; adaptors are black boxes; primers are arrows.

Table 3.9: PCR condition for 3'RACE procedure from the hRSV anti-genome.

Procedure	PCR Condition
1 st round PCR	Initial denaturation: 95°C for 10 mins
	Denaturation: 95°C for 20 secs
	Annealing: 48°C for 20 secs
	Extension: 72°C for 30 secs
	Final extension: 72°C for 7 mins.
	Cooled: 4°C
	} 35 cycles
2 nd round PCR	Initial denaturation: 95°C for 10 mins
	Denaturation: 95°C for 20 secs
	Annealing: 55°C for 20 secs
	Extension: 72°C for 30 secs
	Final extension: 72°C for 7 mins.
	Cooled: 4°C
	} 35 cycles

3.5.7 3'Rapid amplification of cDNA ends (3'RACE) from the hRSV genome

These methods were performed following Li et al. (2005) as illustrated in Figure 3.4 and are similar to 3'RACE protocols in section 3.5.6, except that DT88 was ligated directly onto the virus RNA genome rather than to genomic sense cDNA. All primers used in this method are presented in Table 3.5 and 3.7. The adaptor DT88 was firstly ligated to the viral RNA overnight at 4°C in a ligation reaction mixed containing 1 µg of hRSV clone R11 RNA, 3 µg of hRSV clone R3 RNA or 1 µg of uninfected control HeLa cell RNA plus 1 µM of adaptor DT88, 1x T4 RNA ligase buffer, 15 units of T4 RNA ligase (Ambion, Life Technologies Ltd, Paisley, UK) and DEPC treated water to a final volume of 20 µl. Another ligation reaction without T4 RNA ligase was carried out as a negative control. After ligation, cDNA synthesis was conducted using the DT89 primer (section 3.5.2) and treatment of RNase H was then performed as described in section 3.5.5. The adaptor-ligated RNA was then amplified by hemi-nested PCR in a PTC-200 Thermal Cycler (MJ Research, now Bio-Rad, Hemel Hempstead, UK) using the NS206: modified DT89 in the first round and the NS103: modified DT89 primer pair in the second round. The reaction and conditions of both PCRs were described in section 3.5.6.

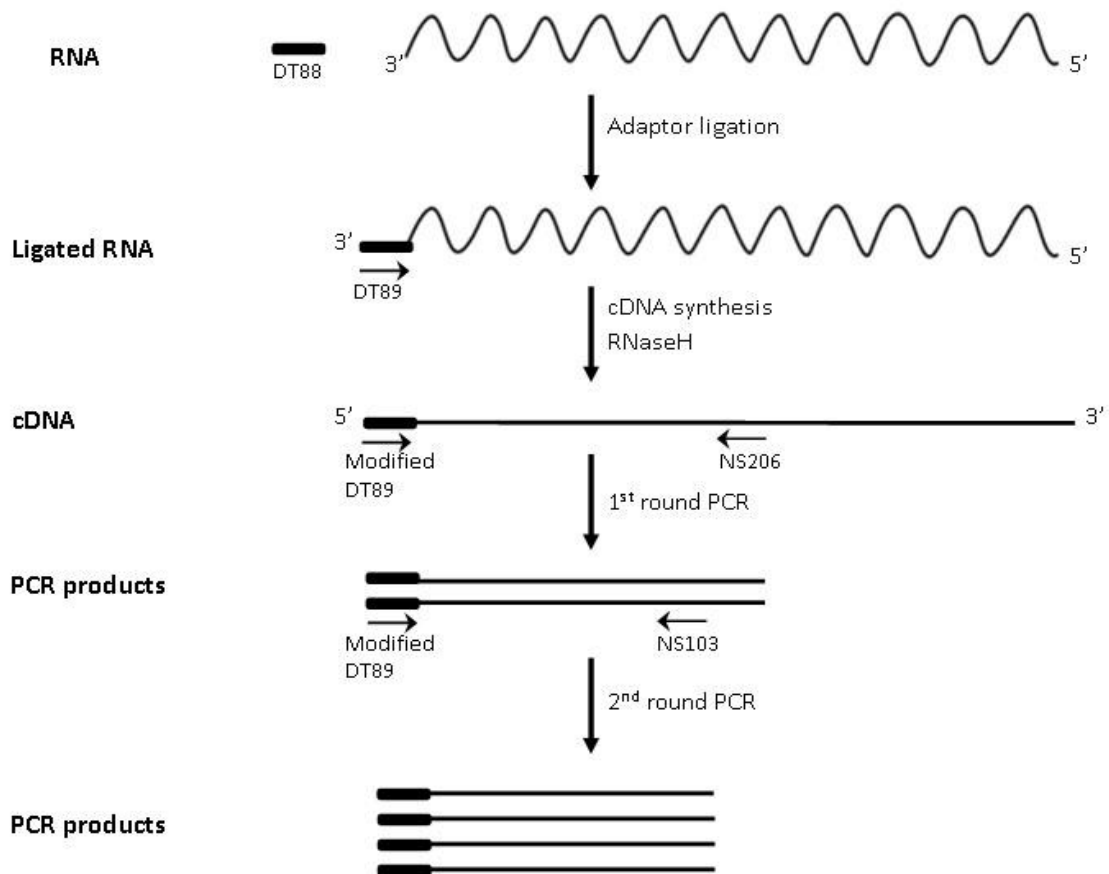


Figure 3.4: Schematic diagram for 3'RACE procedure from the hRSV genome.

[Modified from original by Li *et al.* (2005) and Hsieh *et al.* (1997)]

The adaptor (DT88) was firstly ligated with the genome using T4 RNA ligase, followed by cDNA synthesis using the DT89 primer. The ligated RNA was then treated with RNaseH, followed by the first round PCR using the modified DT89 and NS206 primers. The hemi-nested PCR was then performed using the modified DT89 and NS103 primers. The RNA genome is indicated by a wavy line; cDNA and PCR products are straight lines; adaptors are black box; primers are arrows.

3.5.8 Agarose gel electrophoresis

Materials

10x TBE buffer

108 g of Tris base (Melford, Suffolk, UK) and 55 g of boric acid were dissolved in 800 ml of distilled water. 40 ml of 0.5 M EDTA were then added and made up to a final volume of 1 litre. The solution was autoclaved and store at room temperature.

6x Gel loading buffer

25 mg of bromophenol blue and 25 mg of xylene cyanol FF were dissolved in 5 ml of distilled water to which was added 3 ml of glycerol. The solution was made up to a

final volume of 10 ml with distilled water, aliquoted in 1 ml volumes and stored at -20°C.

1% (w/v) Agarose

0.5 g LE agarose (Lonza, Rockland, USA) were melted in 50 ml of 1x TBE buffer in a boiling water bath. After melting, gel was mixed with 10 µl of 5 mg/ml ethidium bromide, poured into a horizontal submarine agarose slab gel mould (Northumbria Biological, UK) and allowed to solidify at room temperature.

Methods

PCR products were analysed by agarose gel electrophoresis as described by Sambrook J (1989). The PCR products to which were added one fifth volume of 6x loading buffer were loaded into wells of the 1% (w/v) agarose gel. “100bp DNA ladder plus” (Thermo Scientific Fermentas, UK) standard DNA molecular weights markers were also loaded into a well. Electrophoresis was carried out in 1x TBE buffer at 100 V using a Bio-Rad power pack (Bio-Rad Laboratories Ltd, Hemel Hempstead) until the dye front had migrated approximately 80% of the length of the gel. PCR product bands in the gel were viewed using a gel ultraviolet transilluminator (Bio-Rad Fluor-S Multimager).

3.5.9 Direct nucleotide sequencing

Extraction of PCR products from agarose gel

PCR product bands were excised from agarose gel with sterile scalpel blades under a UV transilluminator. The products were then purified from agarose gel using the QIAquick Gel Extraction Kit (Qiagen, Crawley, W. Sussex, UK) according to the manufacturer’s instructions and eluted with Buffer EB (10mM Tris-Cl, pH 8.5) and either stored at -20°C or used immediately.

Nucleotide sequencing

The concentration of DNA was determined using a ND-1000 Nanodrop spectrophotometer (NanoDrop products, Wilmington). Sequences were determined by GATC biotech AG (Konstanz, Germany) or Genevision (Newcastle Upon Tyne, UK). Apart from the ends, all sequences were determined in both directions with appropriate sequencing primers (Table 3.5, 3.6 and 3.7). Discrepancies were resolved by

resequencing a both directions from alternative primers. For the genome ends, sequences obtained in one direction by RACE, were confirmed by sequencing from terminal primers designed from published sequences of the A2 strain (GenBank accession number M74568). The regions corresponding to the primers were therefore determined in only one direction.

The sequence data were assembled into a single gene contiguous gene sequence (contig) using the CAP3 sequence assembly program (Huang and Madan, 1999) and aligned using ClustalW and ClustalX version 2 (Larkin *et al.*, 2007) compared to the A2 strain obtained from the GenBank database (M74568). The coding region was translated using the ExPasy server (Gasteiger *et al.*, 2003) and the percentage of nucleotide identity was obtained from ClustalW program.

3.6 Protein analysis methods

3.6.1 SDS Polyacrylamide gel electrophoresis (SDS-PAGE)

Materials

8x Stacking gel buffer

6.05 g Tris base (Melford, Suffolk, UK) were dissolved in 40 ml distilled water. The pH was adjusted to 6.8 using concentrated HCl and made up to a final volume of 50 ml with distilled water.

6x Sample buffer

15 g of glycerol, 3 mg of bromophenol blue, 2.4 g of sodium dodecyl sulphate (SDS), 7.5 ml of 8x stacking gel buffer and distilled water to a final volume of 20 ml were mixed, aliquoted in 500 μ l volumes and stored at -20°C . 40 μ l of β -mercaptoethanol were immediately added to 500 μ l aliquots prior to use.

2x Resolving gel buffer

45.4 g Tris base (Melford, Suffolk, UK) and 0.8 g SDS were dissolved in 400 ml of distilled water. The pH was adjusted to 8.8 using concentrated HCl and made up to a final volume of 500 ml with distilled water.

10% (w/v) Ammonium persulphate (APS)

1 g of APS was dissolved in 9 ml of distilled water and stored at 4°C for only 7 days.

12% Acrylamide solution

9 ml of 40% bis-acrylamide, 15 ml of resolving gel buffer and 6 ml of distilled water were mixed well and then degassed for 5 minutes using vacuum equipment (Aerosol Products Ltd, London, UK). Immediately before pouring, 240 µl of 10% (w/v) APS and 15 µl of Tetramethylethylenediamine (TEMED) were added and gently mixed.

18% Acrylamide solution

11.7 ml of 40% bis-acrylamide, 13 ml of 2x resolving gel buffer and 3.9 g of sucrose were mixed and then degassed for 5 minutes using vacuum equipment (Aerosol Products Ltd, London, UK). Immediately before pouring, 180 µl of 10% (w/v) APS and 10 µl of TEMED were added and gently mixed.

SDS Running buffer

6.05 g Tris base (Melford, Suffolk, UK), 2 g of SDS and 28.8 g glycine were dissolved in 2 litres of distilled water.

Methods

SDS-PAGE gel preparation

An 18% to 12% gradient gel was poured in a Protean II xi gel mould (Bio-Rad Laboratories Ltd, Hemel Hempstead, UK) according to the manufacturer's instructions. A 15-well comb was then gently inserted into the mould and the gel was allowed to set for 2 hours at room temperature. The wells were then rinsed three times with distilled water and once with 1x stacking gel buffer. Gels were either used immediately or kept for up to 1 week by storing at 4°C with stacking gel buffer in each well.

SDS-PAGE gel electrophoresis

Gel wells were rinsed twice with running buffer before mounting onto the Protean II xi gel chamber (Bio-Rad Laboratories Ltd, Hemel Hempstead, UK) which was filled with SDS running buffer. Five microlitres of protease inhibitor (Roche, UK) were added into 500 µl of frozen sample and then rapidly thawed. The samples were mixed with 6x sample buffer to a final concentration of 1x and heated at 100°C for 3 minutes to break

disulphide bonds. Sixty microlitres of samples were loaded into wells alongside with 10 µl of PAGE Prestained molecular weight markers (Thermo Scientific Fermentas, UK). A magnetic stirrer was placed into a chamber connected to a Grant cooling system (Grant Instruments Ltd, Cambridge, UK) and an electrophoresis power supply (EPS) 600 (Pharmacia Biotech, now Amersham Biosciences, Buckinghamshire, UK). The cooling system was set at 0.5°C and the current for 1 gel was determined by the following formula:

$$\text{Current (mA)} = 16,000 \text{ mins} / (\text{expected running time (hr.)} \times 60)$$

3.6.2 Western blotting

Materials

Tris-glycine protein transfer buffer

3.03 g of Tris base (Melford, Suffolk, UK), 14.4 g of glycine and 200 ml of methanol were dissolved in 650 ml of distilled water, made up to a final volume of 1 litre and stored at 4°C.

10x phosphate buffered saline (PBS)

160 g of NaCl, 4 g of KH₂PO₄, 23 g of anhydrous Na₂HPO₄ and 4 g of KCl were dissolved in 2 litres of distilled water and adjusted to pH 6.8.

Blocking buffer 1

200 ml of PBS containing 0.1% (v/v) Tween 20 (PBS/T), 20 g of Marvel Milk powder (Boots, Newcastle upon Tyne) and 2 g of bovine serum albumin (BSA) were mixed and filtered through a glass microfiber filter (Whatman plc, Middlesex, UK) before storage at 4°C.

Blocking buffer 3

360 ml of PBS/T, 40 ml of heat inactivated foetal calf serum and 4 g of bovine serum albumin Cohn fraction V powder pH 7.0 (VWR International, Leicestershire, UK) were combined, filtered through a 0.2 µm vacuum filter and store at -20°C.

Methods

Protein transfer from SDS-PAGE gels

After completion of electrophoresis, the gel orientation was marked and it was washed three times in the tris-glycine protein transfer buffer at 20 minute intervals. A sheet of polyvinylidene fluoride (PVDF) membrane (Hybond-P, Amersham Biosciences Buckinghamshire, UK) and 8 sheets of 3 mm Whatman filter paper (Whatman plc, Middlesex, UK) were cut to the same size as the gel. The membrane was initially soaked in methanol for 5 minutes. Whatman papers and sponges were then soaked in the tris-glycine protein transfer buffer for 20 minutes. The gel and membrane were sandwiched together in a holder cassette (Bio-Rad, UK) with 4 sheets of 3 mm Whatman filter paper and one sponge either side of them. The cassette was submerged entirely under the protein transfer buffer in Bio-Rad transfer apparatus connected to the Grant cooling system and a BIO-Rad 200 power pack. The cooling system was set at 0.5°C and the power supply was adjusted to 120 V and run for 5 hours. After transfer, the PDVF membrane was washed 3 times in distilled water and blocked overnight in the blocking buffer 1 at room temperature.

Immunostaining of blot membranes with Enhanced Chemiluminescence (ECL) kit

The PVDF membrane was washed twice for 5 minutes each in PBS/T and incubated in 50 ml of primary antibody 1E3 diluted 1/10,000 in blocking buffer 3 with moderate shaking for 90 minutes. The membrane was then washed in PBS/T three times, 15 minute each wash, and once for 30 minutes followed by 5 minutes in blocking buffer 3. Polyclonal goat anti-mouse peroxidase conjugated immunoglobulin (NCL-GAMP) was diluted to 1/1000 in blocking solution 3 and incubated on the membrane for 90 minutes with moderate shaking. The membrane was then washed for 15 minutes three times in PBS/T and blotted on Whatman filter paper before incubation in ECL detection reagent (Amersham Biosciences, Buckinghamshire, UK) for 5 minute. The membrane was then blotted again, wrapped in clingfilm and placed in an X-ray cassette. Under the safe-light conditions, the membrane was exposed to photographic film (Hyperfilm ECL, Amersham Biosciences, Buckinghamshire, UK) for between 10 seconds and 1 minutes, depending on the intensity of the protein bands. The films were developed in the automatic developer (Konica Minolta, Tokyo, Japan) using X-ray developing and fixing solutions (Tetenal, Leicester, UK).

**Chapter 4: Neutralization of susceptible and resistant clones of
R17532 with palivizumab**

4.1 Preparation of virus stocks

In previous studies, the anti-F MAb neutralization resistant hRSV strain R17532 was isolated from the nasopharyngeal secretions (NPS) of an infected infant. After repeated passaging in HeLa cells, the virus became susceptible to neutralization (Gias, 2006; Marsh *et al.*, 2007). To facilitate study of the resistance mechanism of this virus, an attempt was made to produce stable stocks of both resistant and susceptible virus variants by plaque purification (Gias *et al.*, 2008). Whilst clones of the high passage, susceptible variant maintained a stable phenotype on further passage, clones of the low passage resistant virus remained unstable usually losing resistance after four passages unless recloned.

The low passage resistant clone R3.7.8 and high passage susceptible clone R11.1.1 stocks were prepared in the previous study (Gias *et al.*, 2008). Clones R3.7.8 and R11.1.1 were produced by the 2-fold purification of plaque from a stock of R17532 at passage level 3 and 11, respectively. In the production of clone R3.7.8, clone 7 was chosen from the first purification (R3.7) and then clone 8 was selected from the second purification (R3.7.8). For clone R11.1.1, clone 1 was chosen from both the first (R11.1) and second purification (R11.1.1). In this study, the low passage resistant clone was produced by the plaque purification once from clone R3.7.8 (section 3.4.1 and 3.4.4). Clone 3 was selected (R3.7.8.3) and passaged 3 times further in HeLa NCL cells (R3.7.8.3 P3). The high passage susceptible clone R11.1.1 was passaged 8 times further in HeLa NCL cells (R11.1.1 P8).

4.2 Neutralization of R17532 clones with palivizumab using different methods

To ensure that the observed difference in phenotype were robust using methodologies for neutralization, both clones and A2, the type species of hRSV, were tested for their susceptibility to neutralization by palivizumab (PZ) using three neutralization techniques – the dilution endpoint neutralization assay, the immunofluorescent focus reduction neutralization assay and the immunoperoxidase focus reduction neutralization assay.

4.2.1 Dilution endpoint neutralization

Viral infectivity of the R17532 clone R11.1.1 P8, clone R3.7.8.3 P3 and A2 were quantitated in HeLa NCL cell culture tubes and read 15 days after inoculation (section

3.4.8). The concentration of all three viruses was adjusted to 100 TCID₅₀ /ml and used in the neutralization test against PZ as in section 3.4.9. The infectivity and neutralization titres are shown in Table 4.1.

Table 4.1: Neutralization titres of PZ against RSV viruses using the dilution endpoint neutralization test.

Type	Infectivity titres (TCID ₅₀ /ml)	Neutralization titres [†] (µg/ml)	Neutralization phenotype
A2	1.58 x 10 ⁶	0.79	Susceptible
R11.1.1 P8	3.16 x 10 ⁴	0.39	Susceptible
R3.7.8.3 P3	7.41 x 10 ³	9.52	Resistant

[†]PZ concentration that neutralized virus in 50% of the inoculated tubes obtained from triplicate determinations.

The high passage clone R11.1.1 P8 and A2 exhibited a susceptible phenotype with neutralization titres of 0.39 and 0.79 µg/ml, respectively. The low passage resistant clone R3.7.8.3 P3 had a higher neutralization titre than A2 and clone R11.1.1 P8 with the titre of 9.52 µg/ml, confirming the difference in susceptibility of these viruses reported by Gias (2006) and Welsh (2010). The dilution endpoint neutralization assay is a time-consuming test (4 weeks per determination) and requires large volumes of antibody and reagents and is thus cumbersome for the routine quantitation of virus stocks.

4.2.2 Focus reduction neutralization assay using immunofluorescence staining

i) Assay optimization

This assay was firstly optimized using Vero and HeLa NCL cells infected with A2 (susceptible strain) and clone R3.7.8.3 P3 (resistant strain). The infected plates were incubated for 1, 24, 48 or 72 hours before fixing and staining as in section 3.4.10. The A2 foci could be easily counted in both HeLa NCL (Figure 4.1) and Vero cells (Figure 4.2) for all incubation times. For clone R3.7.8.3 P3 foci were only clearly discernible on Vero cells at 72 hours (Figure 4.2). At earlier time points in Vero and throughout the experiment in HeLa NCL, the putative infectious foci remained small and could not be reliably distinguished from debris which was observed at 1 hour after incubation.

Figure 4.1: Immunofluorescent foci of A2 and R17532 clone R3.7.8.3 P3 in HeLa NCL cells at 1, 24, 48 and 72 hours at 100 x magnifications.

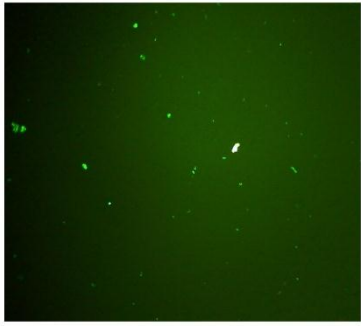
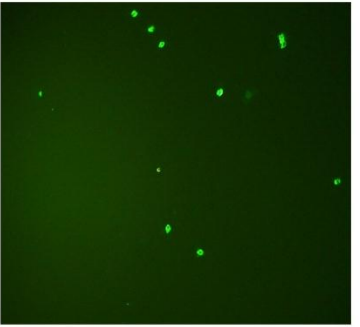
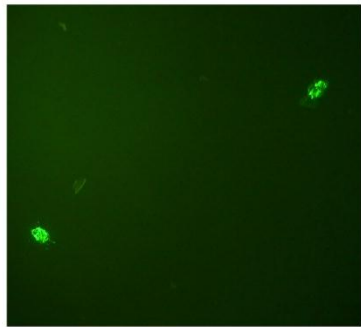

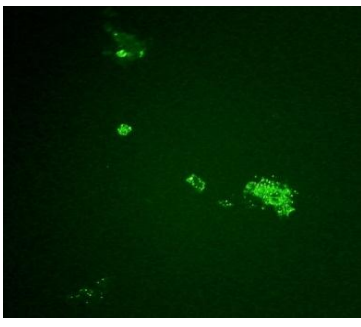
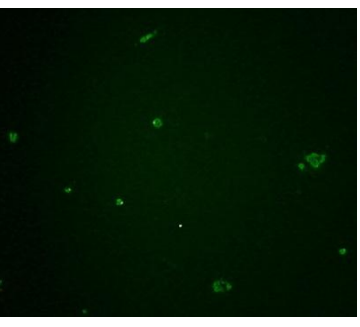
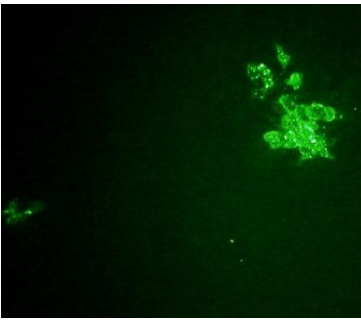
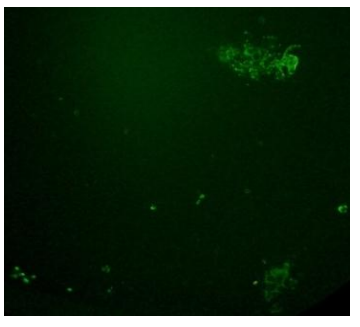
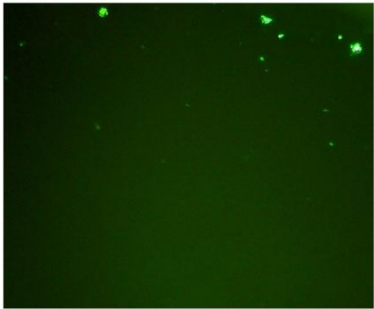
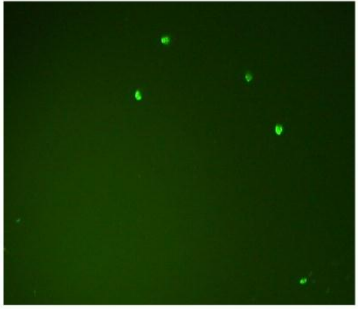

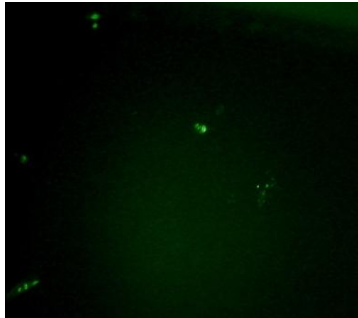
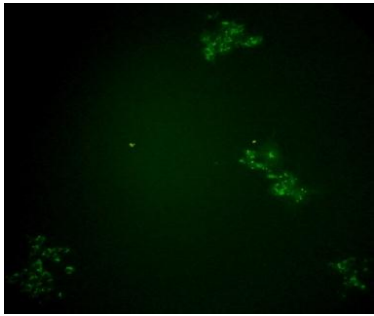
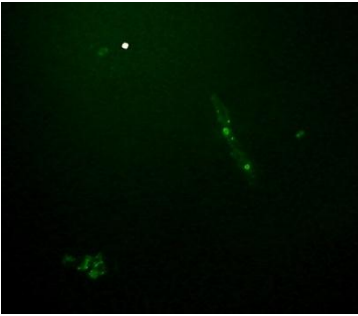
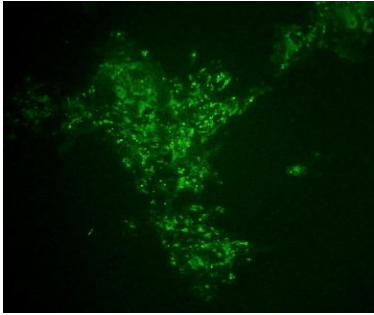
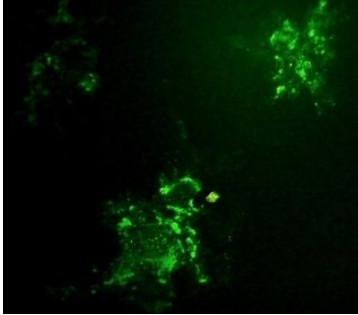
Virus	A2	R3.7.8.3 P3
1 hour		
24 hours		
48 hours		
72 hours		

Figure 4.2: Immunofluorescent foci of A2 and R17532 clone R3.7.8.3 P3 in Vero cells at 1, 24, 48 and 72 hours at 100 x magnifications.

Virus	A2	R3.7.8.3 P3
1 hour		
24 hours		
48 hours		
72 hours		

ii) Determination of EC₅₀ for three viruses

Three viruses, A2, R17532 clone R3.7.8.3 P3 and clone R11.1.1 P10, were titrated in the immunofluorescence focus reduction neutralization test on Vero cells and read at 72 hours. Clone R11.1.1 P10 was used to be representative for a high passage susceptible strain instead of clone R11.1.1 P8 which was of low volume. The results are presented in Figure 4.3. The EC₅₀ values of PZ on A2 and clone R11.1.1 P10 were 6.23 and 1.08 µg/ml, respectively. The EC₅₀ of PZ for clone R3.7.8.3 P3 (> 125 µg/ml) was higher than those of both susceptible virus strains (Figure 4.3). Clone R3.7.8.3 P3 was significantly different from clone R11.1.1 P10 and A2 (P<0.0001) after statistical analysis by two-way ANOVA.

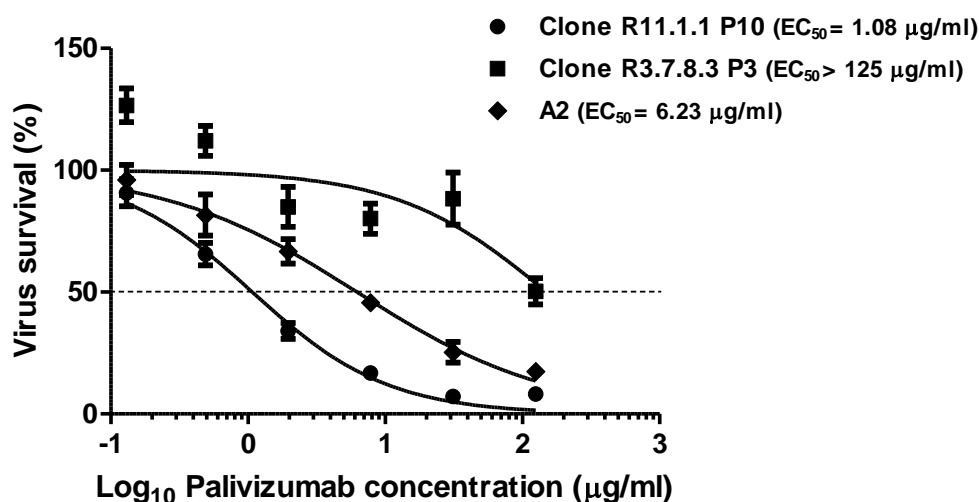


Figure 4.3: The percentage virus survival of R17532 clone R11.1.1 P10, clone R3.7.8.3 P3 and A2 after neutralization with PZ using the immunofluorescent focus reduction neutralization assay in Vero cells.

Plots were prepared from duplicate values and error bars show the standard error. The 50% reduction level is indicated by (...).

4.2.3 Focus reduction neutralization assay using immunoperoxidase staining

i) Comparison of immunofluorescent and immunoperoxidase methods of the high passage susceptible clone of R17532

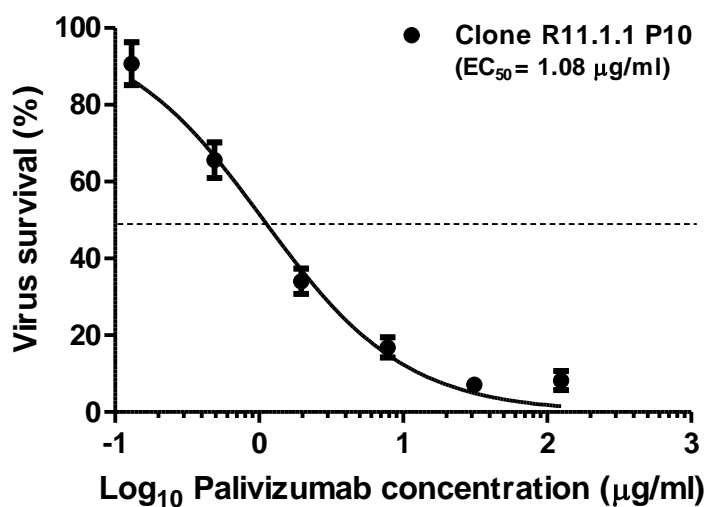
As the secondary antibody labelled with FITC was expensive and immunofluorescent foci must be read immediately. A further modification of the assay using a secondary antibody labelled with peroxidase was evaluated.

In order to compare the efficiency of the two methods in titration of hRSV, clone R11.1.1 P10 were quantitated 4 times using the immunofluorescent and the immunoperoxidase focus assay on Vero cells and read at 72 hours as described in section 3.4.5 and 3.4.6. The mean of infectivity titres was $3.45 \times 10^5 \pm 1.19 \times 10^5$ in the immunofluorescent method and $4.32 \times 10^5 \pm 1.10 \times 10^5$ in the immunoperoxidase methods. Statistical analysis by student t-test shows that titres from both methods were not significantly different with p-value of 0.34.

The focus reduction neutralization assays using the two methods (section 3.4.10) were also compared on Vero cells against the same stock of clone R11.1.1 P10. The results are presented in Figure 4.4. The EC_{50} of PZ for clone R11.1.1 P10 in the immunofluorescent assay (1.08 $\mu\text{g/ml}$) was not significantly different from that of the immunoperoxidase assay (0.82 $\mu\text{g/ml}$) with a p-value of 0.25 (Two-way ANOVA). This suggests that the two methods have the same effectiveness for the determination of neutralization titres of PZ.

However, the focus reduction neutralization assay stained using the immunoperoxidase method was chosen to determine the neutralization of further virus clones because the secondary antibody labelled with peroxidase (NCL-GAMP) could be used at a dilution of 1:1000 compared to the FITC conjugated antibody which worked only at a dilution of 1:20. Also, the immunoperoxidase stained foci were easier to count under the stereomicroscope and stained infectious foci remained countable for more than 6 months.

Immunofluorescent method



Immunoperoxidase method

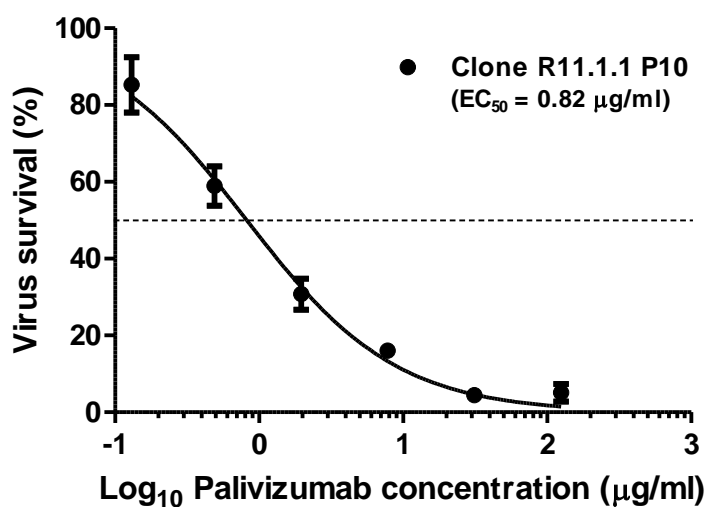


Figure 4.4: The percentage virus survival of R17532 clones R11.1.1 P10 after neutralization with PZ using the immunofluorescent and the immunoperoxidase focus reduction neutralization assay in Vero cells.

Plots were prepared from triplicate values and error bars show the standard error. The 50% reduction level is indicated by (...).

ii) Re-determination of EC₅₀ for the high and low passage clones of R17532 on Vero and HeLa NCL79 cells

Clone R11.1.1 P10 was passaged once in HeLa NCL cells generating clone R11.1.1 P11. Clones R11.1.1 P11 and R3.7.8.3 P3 were tested for neutralization by PZ in the focus reduction assay in Vero incubated for 72 hours and stained by the immunoperoxidase method (section 3.4.6). In parallel both clones were tested against PZ in HeLa NCL79 cells which were used for the original isolation of hRSV R17532 and which were resuscitated from stocks stored in liquid nitrogen in 1979.

On Vero cells, the EC₅₀ values of PZ for clone R11.1.1 P11 and clone R3.7.8.3 P3 were 4.19 and 67.34 µg/ml, respectively (P<0.0001) (Figure 4.5). On HeLa NCL79 the PZ EC₅₀ values were 4.84 and 48.46 µg/ml, respectively (P<0.0001) (Figure 4.6). For clone R11.1.1 P11, the EC₅₀ values in Vero were not significantly different from those in HeLa NCL79 (P=0.45). In contrast, the EC₅₀ values for clone R3.7.8.3 P3 in Vero was significantly higher than those in HeLa NCL79 (P<0.0001). In addition, low concentrations of antibody enhanced the infectivity of the resistant clone in Vero cells but not HeLa NCL79 cells.

Nonetheless, R3.7.8.3 P3 remained an order of magnitude more resistant than R11.1.1 P11 using HeLa NCL79. As foci of both clones in HeLa NCL79 cells were larger and more clearly defined compared to those in Vero cells (Figure 4.7), the immunoperoxidase focus reduction neutralization assay on HeLa NCL79 was selected for determination of the neutralization for other virus clones.

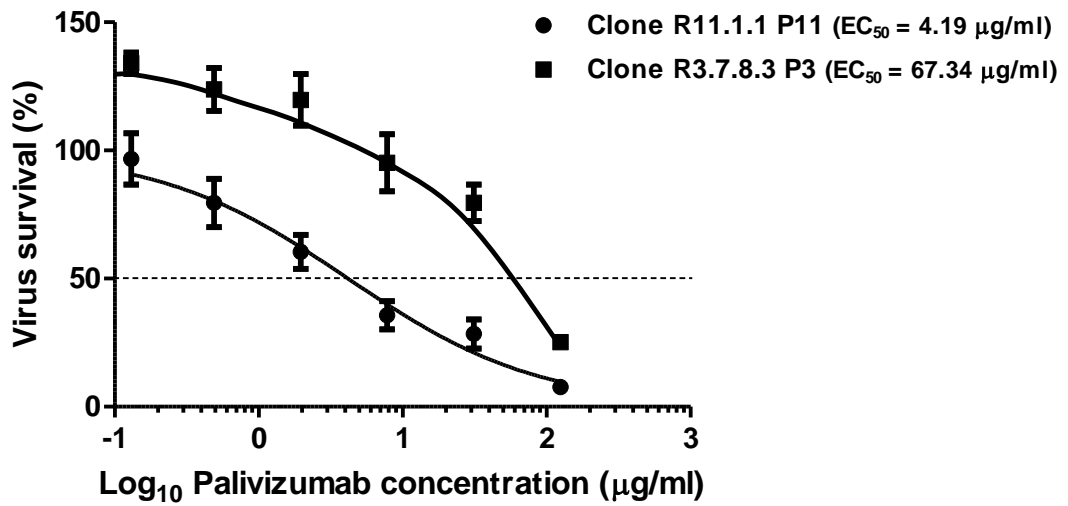


Figure 4.5: The percentage virus survival of R17532 clones R11.1.1 P11 and R3.7.8.3 P3 after neutralization with PZ using the immunoperoxidase focus reduction neutralization assay in Vero cells.

Plots were prepared from triplicate values and error bars show the standard error. The 50% reduction level is indicated by (...).

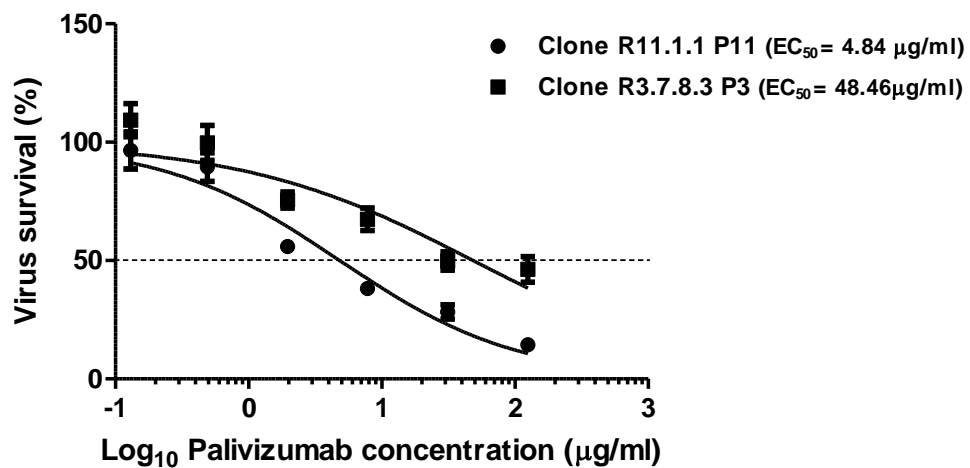


Figure 4.6: The percentage virus survival of R17532 clones R11.1.1 P11 and R3.7.8.3 P3 after neutralization with PZ using the immunoperoxidase focus reduction neutralization assay in HeLa NCL79 cells.

Plots were prepared from triplicate values and error bars show the standard error. The 50% reduction level is indicated by (...).

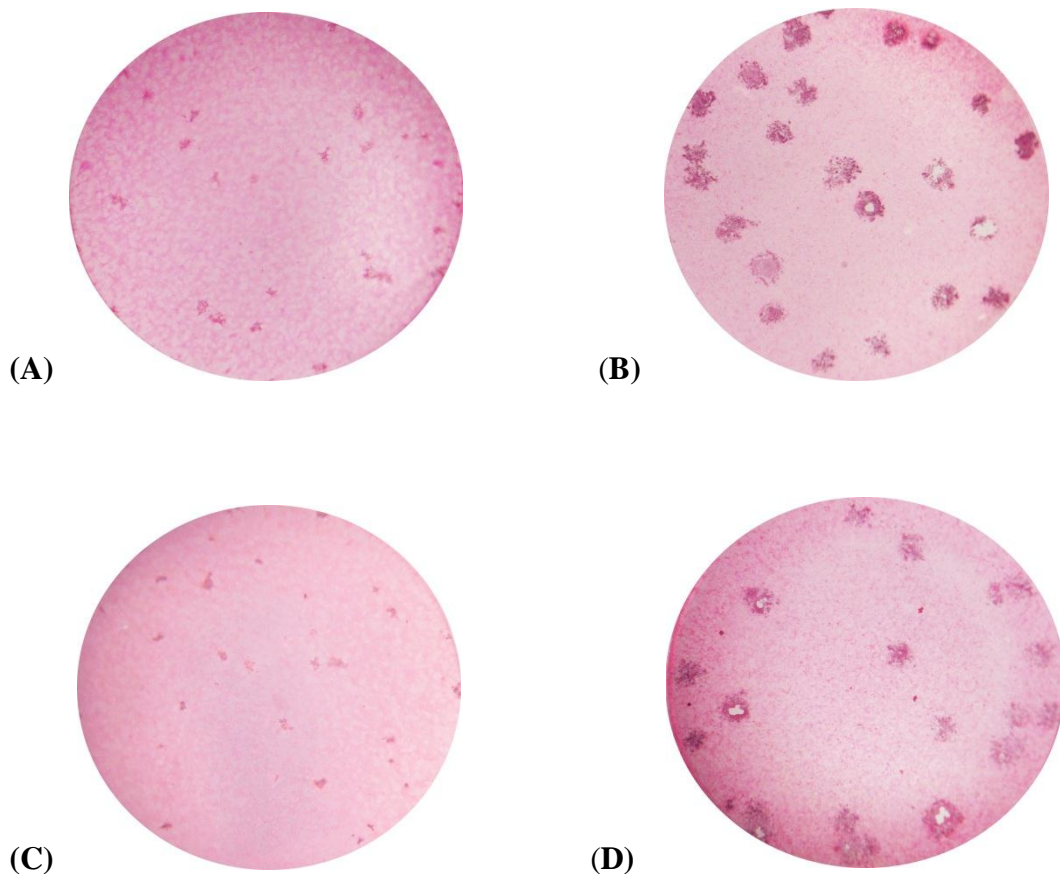


Figure 4.7 : Immunoperoxidase foci of R17532 clone R11.1.1 P11 in Vero (A) and HeLa NCL79 cells (B) and clone R3.7.8.3 P3 in Vero (C) and HeLa NCL79 cells (D) at 10x magnifications.

4.3 Variability of the assay

In order to determine the variability of the immunoperoxidase focus reduction neutralization test. PZ was titrated 9 times against the same stock of clone R11.1.1 P11 and 3 times against the same stock of clone R3.7.8.3 P3. The mean of EC_{50} of the antibody for clones R11.1.1 P11 and R3.7.8.3 P3 was 5.88 ± 3.51 and 32.87 ± 10.16 , respectively (student t test, $t = 1.046$, $P < 0.0001$).

4.4 Stability of neutralization phenotype in susceptible and resistant clones of R17532

hRSV R17532 clone R11.1.1 was passaged in HeLa NCL cells from passage 3 to 11. The PZ EC_{50} values of clone R11.1.1 passage 3, 10 and 11 were determined by focus reduction titration in HeLa NCL79 cells with immunoperoxidase staining and were found to be 2.38, 1.62 and 7.45 $\mu\text{g/ml}$, respectively (Figure 4.8 and Table 4.2). These values indicated that they all were susceptible to PZ and relatively stable even though

they were passaged several times. Clone R11.1.1 at passage 3 was not significantly different from clone R11.1.1 at passage 10 or 11 (Table 4.2).

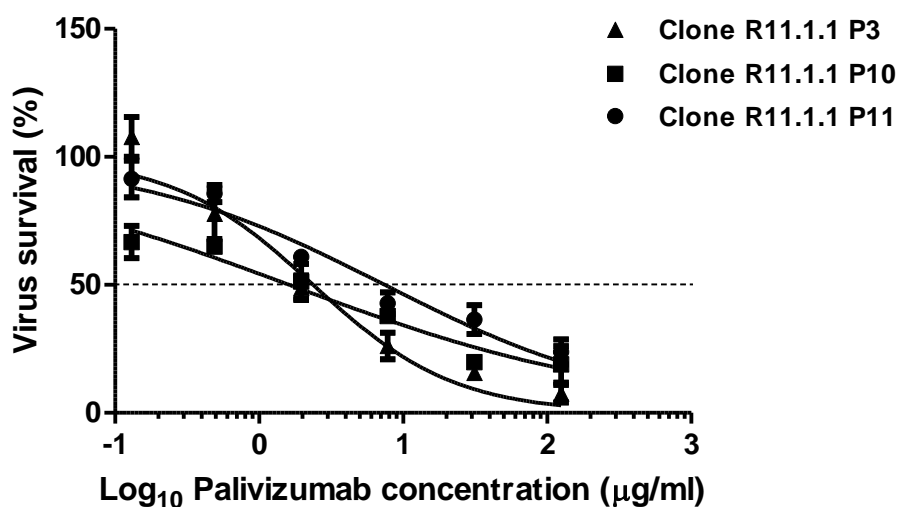


Figure 4.8: The percentage virus survival of R17532 clones R11.1.1 P3, P10 and P11 after neutralized by PZ.

Plots were prepared from triplicate values and error bars show the standard error. The 50% reduction level is indicated by (...).

Table 4.2: The EC₅₀ values of R17532 clones R11.1.1 P3, P10 and P11 and their p-values.

Virus	EC ₅₀ (µg/ml)	Two way ANOVA
		P-value
Clone R11.1.1 P3	2.38	vs. Clone R11.1.1 P3
Clone R11.1.1 P10	1.62	0.32
Clone R11.1.1 P11	7.45	0.10

R17532 clone R3.7.8.3 was passaged in HeLa NCL cells from passage 3 to passage 10 and the PZ EC₅₀ values determined as above of each passage levels. In addition, the parental clone R3.7.8 (section 3.4.1) from which R3.7.8.3 was derived and was titrated in parallel. The parental R3.7.8 clone was over three fold more resistant than clone R3.7.8.3 at passage 3 although this was not significantly different (Table 4.3). Furthermore, the phenotype of clone 3.7.8.3 was not stable after further passaged in HeLa NCL cells. From passage 3 to 10, there was a shift of resistant to susceptible phenotype (Figure 4.9 and Table 4.3). Subsequent to a major fall in resistance between passage 3 and 4, there was a fluctuation of neutralization phenotype trending downward

to passage 10. Between passage 8 and 10, the level and variability of resistance of R3.7.8.3 paralleled that of clone R11.1.1.

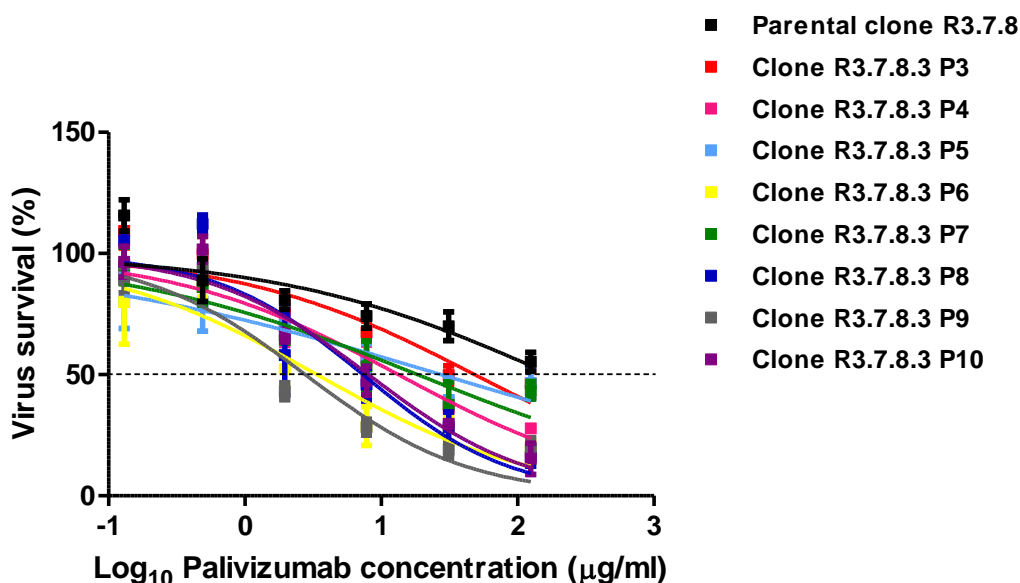


Figure 4.9: The percentage virus survival of R17532 parental clone R3.7.8 and clones R3.7.8.3 passage 3 to passage 10 after neutralized by PZ in HeLa NCL79 cells. Plots were prepared from triplicate values and error bars show the standard error. The 50% reduction level is indicated by (...).

Table 4.3: The EC₅₀ values of R17532 parental clone R3.7.8 and clones R3.7.8.3 passage 3 to passage 10 in HeLa NCL79 cells and their p-values.

Virus	EC ₅₀ (µg/ml)	Two way ANOVA
		P-value
Parental clone R3.7.8	>125	0.0742
Clone R3.7.8.3 P3	48.46	
Clone R3.7.8.3 P4	13.32	0.0036
Clone R3.7.8.3 P5	27.48	0.0085
Clone R3.7.8.3 P6	3.38	<0.0001
Clone R3.7.8.3 P7	18.48	0.0112
Clone R3.7.8.3 P8	7.34	0.0033
Clone R3.7.8.3 P9	2.78	<0.0001
Clone R3.7.8.3 P10	8.05	0.0006

4.5 Neutralization of susceptible and resistant clones of R17532 in different HeLa cells

In previous studies, all hRSV isolates have been found to be susceptible to neutralization by PZ (Johnson *et al.*, 1997; DeVincenzo *et al.*, 2004). Resistant hRSV

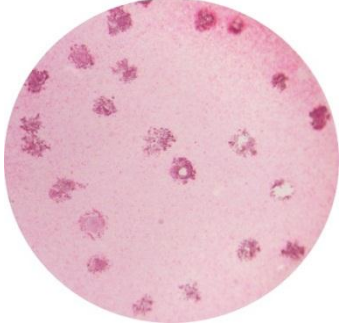
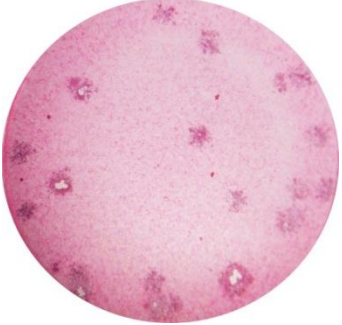






have only rarely been isolated from patients treated with PZ (Boivin *et al.*, 2008; Adams *et al.*, 2010; Zhu *et al.*, 2011). However, our laboratory was able to isolate neutralization resistant viruses to anti-F antibodies, including PZ from untreated patients. Thus, Welsh (2010) demonstrated that 74.2% of isolates made in Newcastle were resistant to neutralization by PZ. The HeLa NCL79 cell lines used for isolation in this study has been highly selected over twenty year for sensitivity to hRSV in the Newcastle diagnostic laboratories. We proposed the hypothesis that this HeLa NCL79 cell line may be exceptionally suitable for the replication of resistant strains of hRSV. To test this hypothesis, different HeLa cells with no history of selection for hRSV isolation (kindly provided from University of Leeds) were used to titrate both neutralization resistant parental clone R3.7.8 and susceptible clone R11.1.1 P11 and their neutralization by PZ was also compared.

The infectivity titres of the two clones in different HeLa cells are presented in Table 4.4. Titres of both clones using HeLa NCL79 were similar to those on HeLa CPV, whereas they were significantly higher on HeLa JSF and HeLa Lucy. However, plaque sizes of clone R11.1.1 P11 and parental clone R3.7.8 on HeLa NCL79 were larger than on other HeLa cells (Figure 4.10).

Table 4.4: Infectivity titres of R17532 clone R11.1.1 P11 and parental clone R3.7.8 in different HeLa cells and their p-values.

Virus	Cells	Infectivity titres (FFU/ml)	Student t-test P-value
			vs. HeLa NCL79
Parental clone R3.7.8	HeLa NCL79	$8.78 \times 10^5 \pm 2.75 \times 10^5$	
	HeLa JSF	$2.01 \times 10^6 \pm 4.79 \times 10^5$	0.0004
	HeLa Lucy	$1.38 \times 10^6 \pm 1.41 \times 10^5$	0.0065
	HeLa CPV	$1.14 \times 10^6 \pm 9.40 \times 10^4$	0.1043
R11.1.1 P11	HeLa NCL79	$5.09 \times 10^5 \pm 1.59 \times 10^5$	
	HeLa JSF	$1.38 \times 10^6 \pm 3.62 \times 10^5$	<0.0001
	HeLa Lucy	$1.16 \times 10^6 \pm 3.27 \times 10^5$	<0.0001
	HeLa CPV	$6.51 \times 10^5 \pm 7.68 \times 10^4$	0.1051

Figure 4.10: Immunoperoxidase foci of R17532 clones R11.1.1 P11 and parental clone R3.7.8 in different HeLa cells at 10x magnifications.

Virus	R11.1.1 P11	R3.7.8 P3
HeLa NCL79		
HeLa JSF		
HeLa CPV		
HeLa Lucy		

In neutralization assay, clone R11.1.1 P11 was shown to be susceptible to neutralization by PZ in all cells (Figure 4.11). In contrast, the resistant clone R3.7.8 in HeLa NCL79 was poorly neutralized by PZ as demonstrated previously. However, PZ EC₅₀ values in other HeLa lines, although always significantly higher than those for R11.1.1 were lower than in HeLa NCL79 (Table 4.5 and 4.6).

These results revealed a marked variation in the ability of PZ to neutralize infectivity of low passage R17532 in different lines of HeLa cells. It is possible that routine screening of cell lines for sensitivity in virus isolation operating in Newcastle in the 1970s selected for a HeLa cell line capable of supporting the replication of viruses in clinical specimens containing antiviral antibodies.

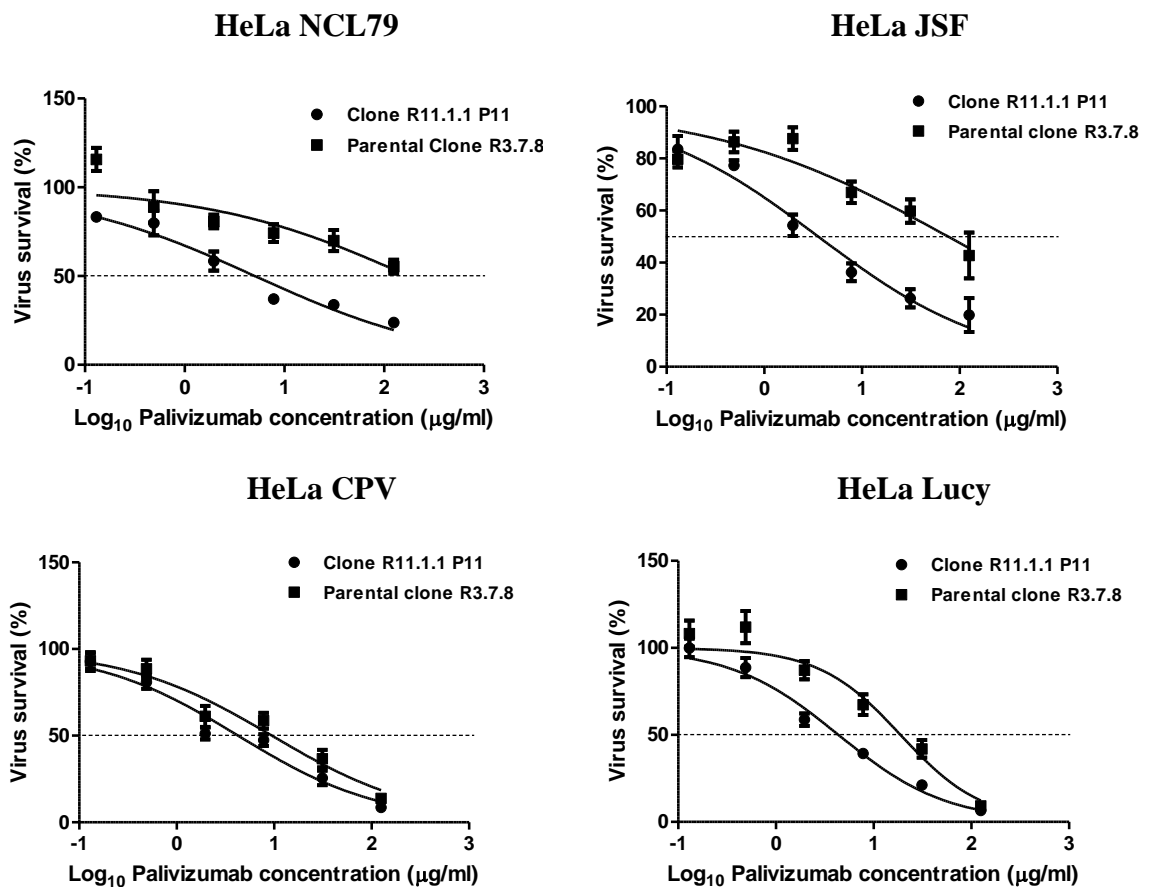


Figure 4.11: The percentage virus survival of R17532 clones R11.1.1 P11 and R3.7.8 after neutralization with PZ in HeLa NCL79, JSF, CPV and Lucy cells.

Plots were prepared from triplicate values and error bars show the standard error. The 50% reduction level is indicated by (...).

Table 4.5: The PZ EC₅₀ values of R17532 clones R11.1.1 P11 and R3.7.8 in different HeLa cells and their p-values compared between the two clones in the same cell lines.

Cells	EC ₅₀ (µg/ml)		Two way ANOVA P-value
	R11.1.1 P11	R3.7.8	R11.1.1 P11 vs. R3.7.8
HeLa NCL79	5.06	>125	<0.0001
HeLa JSF	3.57	76.06	<0.0001
HeLa Lucy	4.37	18.83	<0.0001
HeLa CPV	4.27	9.47	0.003

Table 4.6: The PZ EC₅₀ values of R17532 clones R11.1.1 P11 and R3.7.8 in different HeLa cells and their p-values compared each clone to EC₅₀ values from HeLa NCL79.

Virus	Cells	EC ₅₀ (µg/ml)	Two way ANOVA P-value
			vs. HeLa NCL79
Parental clone R3.7.8	HeLa NCL79	>125	
	HeLa JSF	76.06	<0.0001
	HeLa Lucy	18.83	<0.0001
	HeLa CPV	9.47	<0.0001
R11.1.1 P11	HeLa NCL79	5.06	
	HeLa JSF	3.57	0.22
	HeLa Lucy	4.27	0.89
	HeLa CPV	4.37	0.49

4.6 Neutralization of susceptible and resistant clones of R17532 in a human bronchial epithelial cell line.

The ability of hRSV isolates to evade neutralization by anti-F antibodies in some cell types may be relevant to the pathogenesis of virus infection *in vivo*. Epithelial cells of the respiratory tract may resemble HeLa NCL79 in being permissive of infection with anti-F antibody treated virus. To test the permissivity of human bronchial epithelial cells, PZ was titrated against the parental clone R3.7.8 and clone R11.1.1 in a focus reduction assay on 16HBE140, a line of human bronchial epithelial cells (Figure 4.12). Foci for both virus clones in 16HBE140 cells were small when compared to those in HeLa NCL79 (Figure 4.10 and 4.13). Although the PZ EC₅₀ for parental clone R3.7.8 was significantly higher than that for R11.1.1 P11 (P<0.0001), it was low compared to that obtained on HeLa NCL79 (P<0.0001).

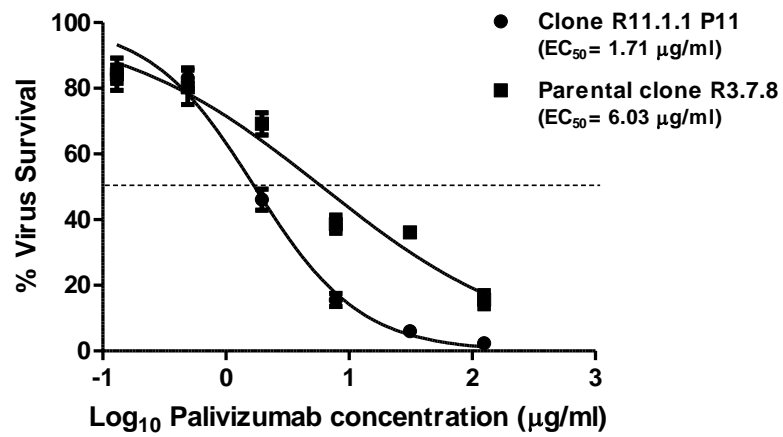


Figure 4.12: The percentage virus survival of R17532 clones R11.1.1 P11 and R3.7.8.3 P3 after neutralization with PZ using the immunoperoxidase focus reduction neutralization assay in 16HBE140 cells.

Plots were prepared from triplicate values and error bars show the standard error. The 50% reduction level is indicated by (...).

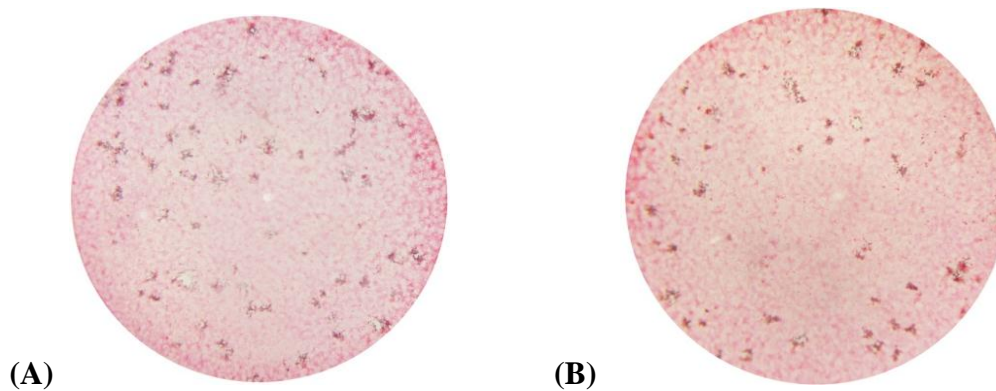


Figure 4.13: Immunoperoxidase foci of R17532 clone R11.1.1 P11 (A) and parental clone R3.7.8 (B) in 16HBE140 cells at 10x magnifications.

**Chapter 5: Investigation of the entry mechanism of palivizumab
neutralization susceptible and resistant clones of R17532**

5.1 Introduction

Previous studies have demonstrated that PZ binds equally well to both neutralization resistant and susceptible forms of R17532 (Marsh *et al.*, 2007; Welsh, 2010). The difference between the two viruses exhibited in HeLa NCL79 cells must therefore lie in the ability of bound anti-fusion glycoprotein antibody to block the infections process. This argues for a fundamental difference in the entry mechanism of the two viruses. Our present model of the entry mechanism of hRSV, based largely on studies of the sub-type A type strain A2 infection of HeLa and HEP2 cells, is incomplete. However, it is likely that the virus initially binds to glycosaminoglycans on the target cell membrane via the G and F glycoproteins (Feldman *et al.*, 2000). The virion is taken up into endocytic vacuoles via clathrin mediated endocytosis (Kolokoltsov *et al.*, 2007).

At some as yet undetermined point in this process the fusion glycoprotein is activated to its fusogenic form, by an, as yet, undefined trigger, and mediates fusion of the virus and vacuole membrane with release of the nucleocapsid into the cytoplasm (Melero, 2007). Previous studies have already demonstrated marked difference in the kinetics of attachment between resistant and susceptible clones of R17532 in HeLa NCL cells (Welsh, 2010). However, as PZ has been shown not to block virus binding, but to inhibit subsequent steps in the infections process, it is unclear how rapid binding per se would induce neutralization resistance.

Therefore, the first aim of this study was to evaluate whether resistant and susceptible clones of the virus also differ in their entry into target cells by clathrin-mediated endocytosis using two clathrin endocytosis inhibitors - monodansylcadaverine (MDC) and chlorpromazine (CP). The second aim was to compare the two clones with regard to factors involved in the activation of the fusion protein to the fusogenic form. These include the extent of post-translational processing, the amounts of the fusion proteins, and their response to compounds which inhibit the formation of six helix bundle in the F molecule - Heptad repeat 2 (HR2) peptide and small molecular weight inhibitors BTA9881 and BMS-433771. Resistant parental clone 3.7.8 with PZ EC_{50} in HeLa NCL79 $> 125 \mu\text{g/ml}$ and neutralization susceptible clone R11.1.1 P3 with PZ EC_{50} in HeLa NCL79 $= 2.38 \mu\text{g/ml}$ were used throughout these studies.

5.2 Viral entry of neutralization susceptible and resistant clones of R17532 in HeLa NCL79 cells

5.2.1 Toxicity studies of clathrin endocytosis inhibitors on HeLa NCL79 cells

Two clathrin endocytosis inhibitors, monodansylcadaverine (MDC) and chlorpromazine (CP), were diluted to different concentrations and tested on HeLa NCL79 cells to screen for their cytotoxicities using a trypan blue exclusion test (section 3.4.11). The 50% cytotoxic concentration (CC_{50}) of each inhibitor was evaluated to find the concentration that was non-toxic for the cells. The CC_{50} values of MDC and CP were 130.8 μ M and 49.20 μ g/ml, respectively (Figure 5.1).

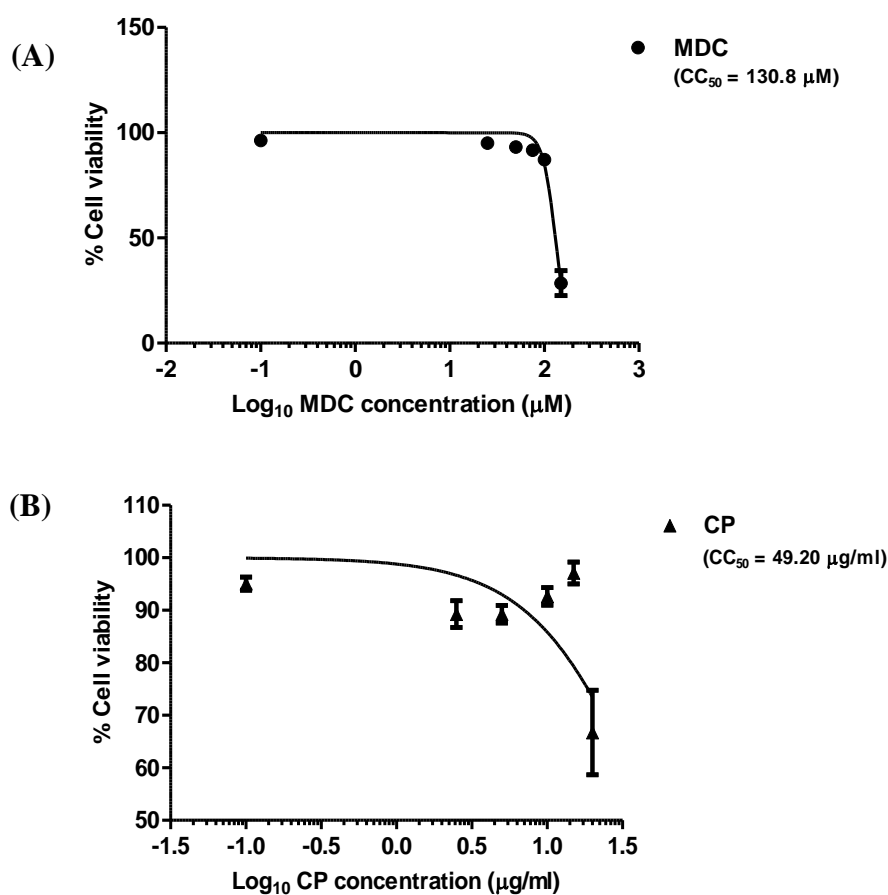


Figure 5.1: The percentage of cell viability and CC_{50} of MDC (A) and CP (B).

Plots were prepared from triplicate values and error bars show the standard error. The CC_{50} values of PZ are indicated in each graph.

5.2.2 Effect of clathrin endocytosis inhibitors on neutralization susceptible and resistant clones of R17532

Parental clone 3.7.8 and clone R11.1.1 P3 were treated with MDC at concentrations between 25 and 100 μM and with CP at concentrations between 2.5 and 20 $\mu\text{g/ml}$. The EC_{50} values of each inhibitor were evaluated in both viruses (section 3.4.11). The EC_{50} values of MDC in clone R11.1.1 P3 and parental clone R3.7.8 were 72.81 and 64.26 μM , respectively (Figure 5.2). For CP, clone R11.1.1 P3 and parental clone R3.7.8 had the EC_{50} values of 16.56 and 14.96 $\mu\text{g/ml}$, respectively (Figure 5.3). The EC_{50} values of MDC and CP were approximately 50 - 70% less than CC_{50} . The susceptibility of clones R11.1.1 P3 and parental clone R3.7.8 to MDC and CP were not significantly different ($P=0.09$ and $P=0.95$, respectively), indicating that both viruses required clathrin dependent endocytosis in their entry into the host cells.

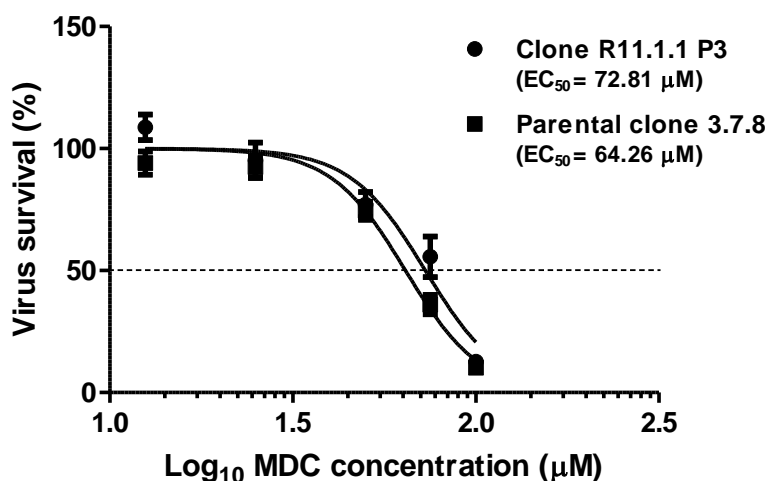


Figure 5.2: The percentage virus survival of clones R11.1.1 P3 and parental clone R3.7.8 after treatment with MDC.

Plots were prepared from triplicate values and error bars show the standard error. The 50% reduction level is indicated by (...).

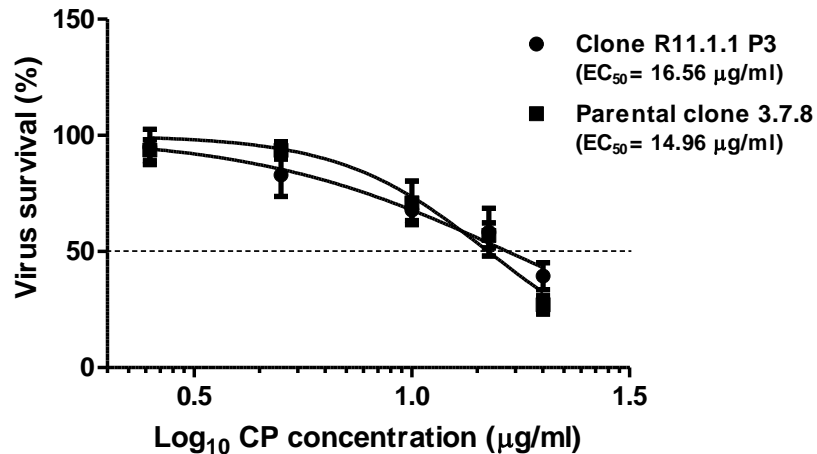


Figure 5.3: The percentage virus survival of clone R11.1.1 P3 and parental clone R3.7.8 after treatment with CP.

Plots were prepared from triplicate values and error bars show the standard error. The 50% reduction level is indicated by (...).

5.3 Analysis of F glycoprotein post-translational processing in neutralization susceptible and resistant clones of R17532

The F glycoprotein is post-translationally processed by proteolytic cleavage and glycosylation. To investigate whether F glycoprotein processing might underly the differences between susceptible and resistant clones. The viruses were analysed by SDS-PAGE to seek differences in migration of the F glycoprotein corresponding to differences in proteolytic cleavage or glycosylation.

Infected HeLa NCL79 cell lysates of susceptible clone R11.1.1 P3 and resistant parental clone R3.7.8 were run on SDS-PAGE and their proteins were transferred onto PVDF membrane. The F glycoproteins on the membrane were Western blotted with anti-F MAb 1E3 (section 3.6). The same pattern of two bands with the molecular weight of 52 and 20kDa occurred in both clones (Figure 5.4). The 20kDa band has previously been reported to be a protease resistant cleavage product of the F1 molecule (Lopez *et al.*, 1990). This band in parental clone R3.7.8 was of greater intensity than that in clone R11.1.1 P3 which may reflect the slower replication rate of the resistant clone which affords greater time for proteolytic degradation of virus proteins accumulating in the culture. The similar band pattern between the two clones indicates that there were no observable differences in post-translational processing.

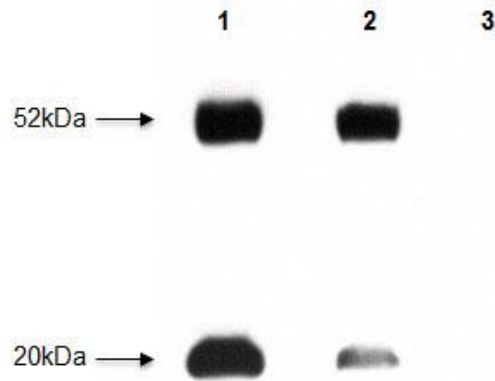


Figure 5.4: Western blot of the F glycoprotein in parental clone R3.7.8 P2 and clone R11.1.1 P3 infected cell lysates stained by the anti-F Mab 1E3.

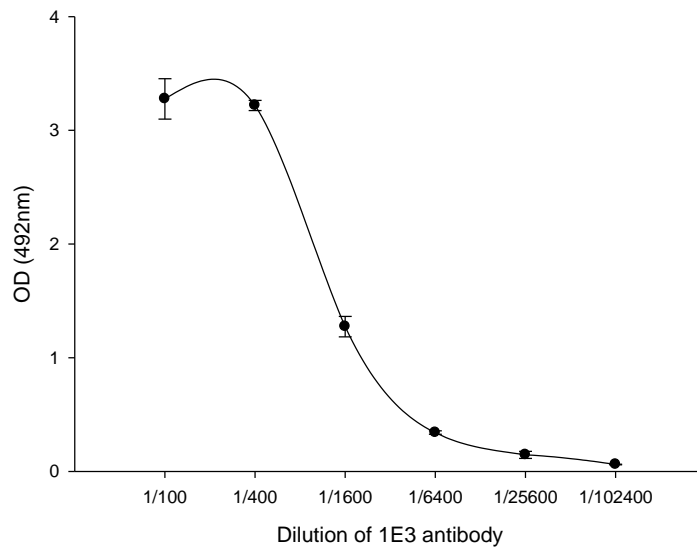
The lanes were loaded as follows; Lane 1: parental clone R3.7.8; Lane 2: R11.1.1 P3; Lane 3: HeLa cell (Negative control).

5.4 Comparison of the amounts of the fusion protein in neutralization susceptible and resistant clones of R17532

In previous studies, a high density of envelope glycoprotein expression was found on the virion surface of neutralization resistant primary HIV-1 isolates compared to laboratory adapted HIV-1 which was susceptible to neutralization by soluble CD4 (O'Brien *et al.*, 1994; Sullivan *et al.*, 1995). It is possible that high amount of the F glycoprotein on resistant hRSV virions is similarly responsible for resistance to neutralization by PZ. Gias (2006) have demonstrated that the level of F expression on purified R17532 resistant clone R3 virions was significantly higher than that on susceptible clone R11. However, in a resistant clone N1 of a separate isolate N5843, F glycoprotein expression was similar to that of susceptible clone N10a.

In an attempt to investigate this further by a different method, the F glycoprotein present on the surface of cells infected with the resistant parental clone R3.7.8 or susceptible clone R11.1.1 P3 were measured by anti-F MAb 1E3 using an ELISA whole cell method (section 3.4.7). The results are shown in Figure 5.5. 1E3 antibody equally bound to both parental clone R3.7.8 and clone R11.1.1 P3, the binding curves for both cell types being superimposable. This indicates that the same amounts of the F glycoprotein were present on both cell types.

Parental clone R3.7.8



Clone R11.1.1 P3

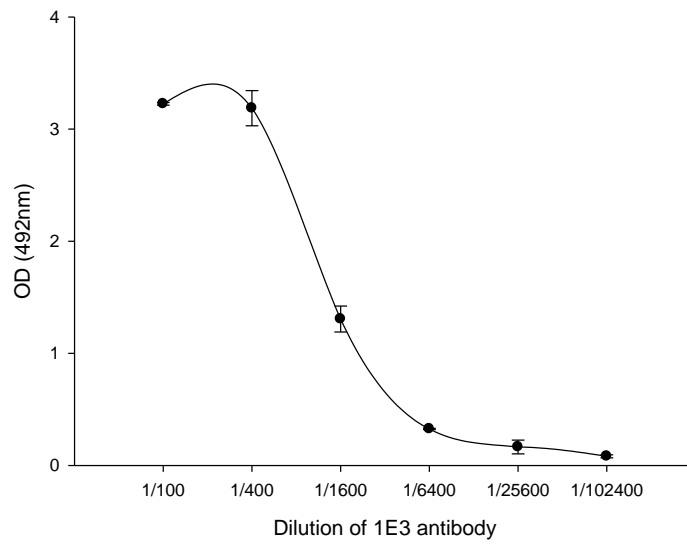


Figure 5.5: Amounts of the F glycoprotein on the surface of cells infected with parental clone R3.7.8 and clone R11.1.1 P3.
Plots were prepared from triplicate values and error bars show the standard deviation.

5.5 Effect of antiviral agents directed against the F glycoprotein on neutralization susceptible and resistant clones of R17532

The formation of the six helix bundle (6HB) in the F molecule occurs in the fusion process drawing the viral membrane and the host cell membrane into close apposition (Zhao *et al.*, 2000). Anti-F monoclonal antibodies appear to neutralize infectivity by blocking this process (Huang *et al.*, 2010). It was hypothesized that the 6HB formation in resistant virions may be different from that in susceptible virion.

To test this hypothesis, antiviral agents directed against the formation of 6HB in the F glycoproteins were tested in focus inhibition assays against both resistant and susceptible clones (section 3.4.12). These antiviral agents consisted of two small molecular weight inhibitors, BTA9881 and BMS-433771, and a peptide corresponding to heptad repeat 2 (HR2) of the R17532 F glycoprotein. This sequence is conserved in all PZ resistant and susceptible clones of virus sequence (see below chapter 6). The results are presented in Figure 5.6. No cellular toxicity was observed with any of these compounds (data not shown).

Clone R11.1.1 P3 was susceptible to R17532-HR2 peptide, BMS-433771 and BTA9881 with the EC₅₀ values of 13.04, 0.21 and 5.23 μ M, respectively. In contrast, none of these anti-fusion inhibitor compounds inhibited parental clone R3.7.8. These findings paralleled the neutralization of the two clones by PZ.

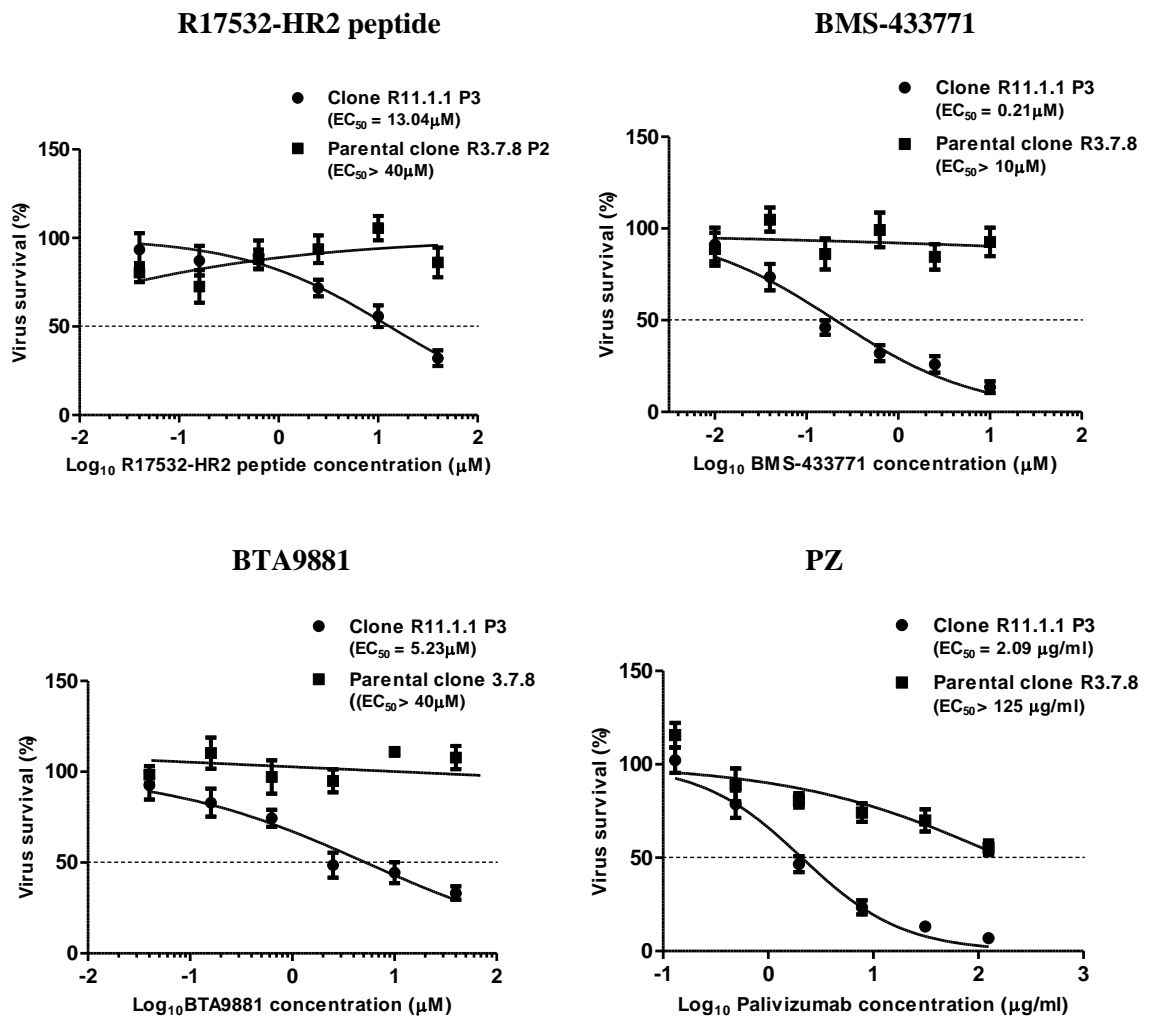


Figure 5.6: The percentage virus survival of clone R11.1.1 P3 and parental clone R3.7.8 after treatment with R17532-HR2 peptide, BMS-433771, BTA9881 and PZ.

Plots were prepared from triplicate values and error bars show the standard error. The 50% reduction level is indicated by (...).

**Chapter 6: Comparison of the membrane associated glycoprotein
genes of resistant and susceptible clones of R17532**

6.1 Introduction

Previous studies indicated that genetic changes in the membrane associated protein genes (M, SH, G, F, and their intergenic regions) were not associated with the conversion of slow growing - neutralization resistant variants to fast growing - neutralization susceptible variants (Gias, 2006; Marsh *et al.*, 2007). However, although sequences of the F, G and F-G intergenic regions were derived for uncloned virus stocks and confirmed on virus clones of established neutralization phenotype, the sequence analysis of the M, SH and the intergenic regions of both genes were determined only for uncloned virus stocks that probably contained a mixture of neutralization resistant and susceptible variants. Although the gene sequences obtained might represent those of the predominant variant, minor variants might be preferentially amplified resulting in a misleading interpretation. To further test the conclusions of Marsh *et al.* (2007), the M, SH genes and their intergenic regions for clone R11.1.1 P8 and R3.7.8.3 P3 were analysed in the first part of this study. The EC₅₀ of PZ against clone R3.7.8.3 P3 in the focus reduction assay was 48.46 µg/ml (Figure 4.6) and the 50% inhibitory dose in the tube neutralization assay was 9.52 µg/ml (Table 4.1). R11.1.1 P8 was titrated only in the tube neutralization assay where the 50% inhibitory dose was 0.39 µg/ml (Table 4.1).

6.2 Amplification of the M gene and associated intergenic regions of palivizumab resistant and susceptible clones of R17532

For this experiment, clone R11.1.1 P8 and R3.7.8.3 P3 were compared. In the hRSV strain A2 genome, the M gene stretches from nt 3,252 to nt 4,209 (GenBank accession number M74568). For each clone, total RNAs isolated as described in section 3.5.1 were reverse transcribed using the forward primer M1 and PCR reactions were performed using the M1: M2 primer pair (Table 3.5 and 3.6 for all primers). Negative controls using RNA extracted from uninfected HeLa NCL cells and DEPC treated water were included in the RT-PCR. The size of the target band was expected to be 1,184nt with autonomous sequence between nt 3,174 to nt 4,360. Strong bands of this size were observed in both clones as shown in Figure 6.1. No target band was detected in any negative control. Target bands were purified for direct sequencing as described in section 3.5.9.

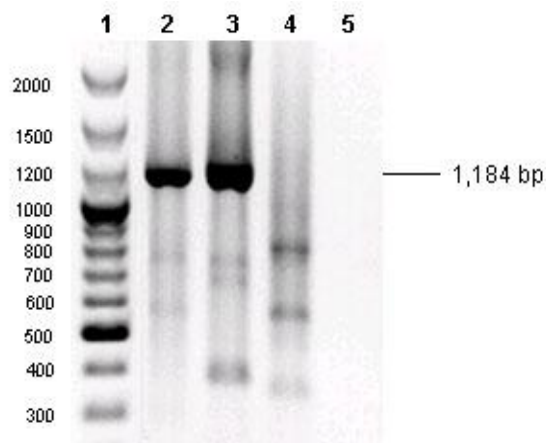


Figure 6.1: RT-PCR amplification of the M gene and P-M intergenic region of clones R11.1.1 P8 and R3.7.8.3 P3 using the M1: M2 primer pair.

The lanes were loaded as follows; Lane 1: 100bp DNA ladder; Lane 2: R11.1.1 P8; Lane 3: R3.7.8.3 P3; Lane 4: HeLa NCL cells (Negative control) and Lane 5: DEPC treated water (Negative control)

6.3 Amplification of the SH gene and associated intergenic regions of neutralization susceptible and resistant clones of R17532

For the hRSV strain A2 genome, the SH gene is encoded by nt 4,219 to nt 4,628 (GenBank accession number M74568). The M-SH intergenic region and the SH genes of clones R11.1.1 P8 and R3.7.8.3 P3 were reverse transcribed using the forward primer SH+ and amplified using the SH+: SH- primer pair (Table 3.5 and 3.6) to yield autonomous sequence between nt 3,994 to nt 4,842. Uninfected HeLa NCL cells and DEPC treated water were used as negative controls and amplified in parallel. The expected band of 849nt was found in both clones, but not in negative controls (Figure 6.2). This band was isolated and purified for direct sequencing as described in section 3.5.9.

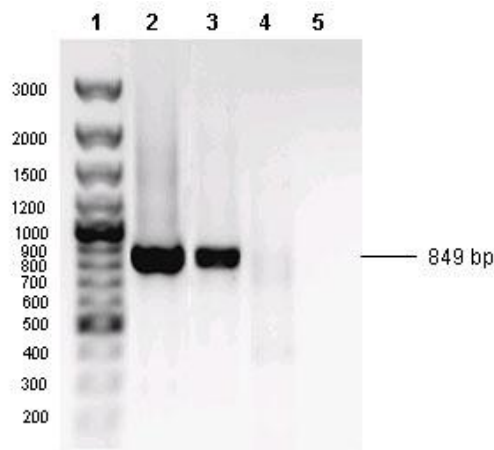


Figure 6.2: RT-PCR amplification of the SH gene and M-SH intergenic region of clones R11.1.1 P8 and R3.7.8.3 P3 using the SH+: SH- primer pair.

The lanes were loaded as follows; Lane 1: 100bp DNA ladder; Lane 2: R11.1.1 P8; Lane 3: R3.7.8.3 P3; Lane 4: HeLa NCL cells (Negative control) and Lane 5: DEPC treated water (Negative control)

6.4 Sequence comparison of the M and associated intergenic regions of neutralization susceptible and resistant clones of R17532 and A2 strain

The strategy for sequencing the M gene is depicted in Figure 6.3. The sequences of the P-M intergenic region (nt 3,243 to 3251), the 5'UTR (nt 3,252 to 3260) and the M coding region (nt 3,261 to 4,031) of clones R11.1.1 P8 and R3.7.8.3 P3 were analysed in the 5' to 3' direction (antigenome) using the forward primer M1 from the 1,184nt amplicand in section 6.2. The coding region and 3'UTR (nt 4,032 to 4,209) of the M gene was sequenced in the 3' to 5' direction using the reverse primer M2 from the 1,184nt amplicand in section 6.2 and in the 5' to 3' direction using the forward primer SH+ from the 849nt amplicand generated in section 6.3. The P-M intergenic region, 5'UTR and coding regions of the M gene were subsequently confirmed by sequencing in the 3' to 5' direction using the reverse primer P3459 from the 1,332nt amplicand generated for sequencing the P gene in section 7.8 below. All primers are presented in Figure 6.3, Table 3.5 and 3.6. This provided readable sequence from nt 3,140 to 4,695 based on the hRSV A2 genome (GenBank accession number M74568). Sequence from nt 3,763 to 4,014 was obtained from sequencing in only 3' to 5' direction using M2 primer; however, this sequence was in agreement with the study of Gias (2006).

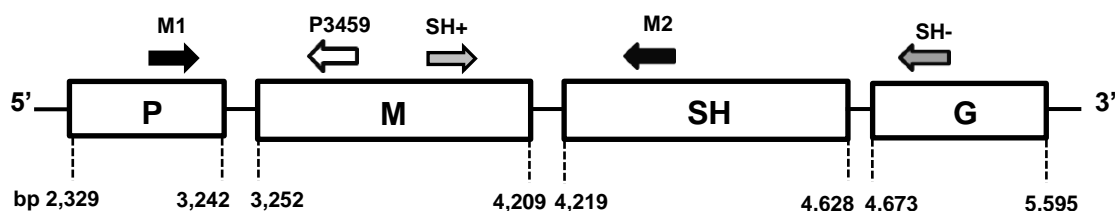


Figure 6.3: Schematic diagram of primers for amplification and sequencing of the M gene and associated intergenic regions on hRSV antigenome.

hRSV genes are depicted as rectangles (not to scale). Primers used in sections 6.2 and 6.4 are black arrows; sections 6.3 and 6.5 are grey arrows. Sequencing primer used in sections 7.8 is white arrow. Primers M1 (nt 3,174-3,197); P3459 (nt 3,459-3,437); SH+ (nt 3,994-4,017); M2 (nt 4,360-4,332); SH- (nt 4,842-4,825) [Nucleotide numbering is based on the A2 genome, GenBank accession number M74568].

Comparison of the M gene and associated intergenic region revealed no nucleotide or amino acid changes between clones R11.1.1 P8 and clone R3.7.8.3 P3 (Appendix Figure 10.1, 10.2 and 10.3). Thus, this gene was totally conserved in susceptible and resistant variants. However, several nucleotide differences between R17532 and the A2 strain were observed across these regions. In the P-M intergenic region, a deletion of six nucleotides and one nucleotide substitution were detected in the A2 strain compared to R17532 giving a low percentage of nucleotide identity of 22 (Table 6.1 and Appendix Figure 10.1). The nucleotide differences in the coding regions did not cause amino acid changes and the percentage of amino acid identity was 100 as shown in Table 6.1 and Appendix Figure 10.2.

Table 6.1: Percentage of nucleotide identity in the P-M intergenic region and the M gene of clone R17532 compared to the A2 strain.

Region	NT#	% NT ^a identity R17532 vs. A2	% AA ^b identity R17532 vs. A2
P-M IR ^c	1-3	22	N/A
M 5'UTR	4-13	100	N/A
M CDS ^d	1-771	97	100
M 3'UTR	1-176	90	N/A

^aNT: Nucleotide; ^bAA: Amino acid; ^cIR: Intergenic region; ^dCDS: Coding sequence.

6.5 Sequence comparison of the SH genes and associated intergenic regions of neutralization susceptible and resistant clones of R17532 and A2 strain

The sequences of the 849nt band for clone R11.1.1 P8 and R3.7.8.3 P3 were determined using the forward primer SH+ and the reverse primer SH- in the 5' to 3' and 3' to 5' directions (antigenome), respectively. Sequence readable in both direction was obtained from nt 4,093 to 4,695 based on the hRSV A2 genome (GenBank accession number M74568). No nucleotide changes in the M-SH intergenic region, 5'UTR and the coding sequence of the SH gene were observed between the two clones (Appendix Figure 10.4 and 10.5). In the 3'UTR region, a deletion of an A residue occurred at the SH gene end (GE) sequence of clone R11.1.1, which had 7As in the A-tract region (antigenome sense), compared to clone R3.7.8.3 P3 in which these were 8As (Appendix Figure 10.6). In this region, A2 had only 5As in the A-tract region. In addition, there were several nucleotide differences in the SH gene between A2 and R17532 strains and the percentage of nucleotide and amino acid identity in each region is shown in Table 6.2. In the coding region, two amino acid changes were observed between the two viruses giving the percentage of amino acid identity of 96 (Table 6.2 and Appendix Figure 10.5).

Table 6.2: Percentage of nucleotide identity in the M-SH intergenic region and the SH gene of clone R17532 compared to the A2 strain.

Region	NT#	% NT ^a identity R17532 vs. A2	% AA ^b identity R17532 vs. A2
M-SH IR ^c	1-9	77	N/A
SH 5'UTR	10-93	92	N/A
SH CDS ^d	1-195	97	96 ^e
SH 3'UTR	1-134	82	N/A

^aNT: Nucleotide; ^bAA: Amino acid; ^cIR: Intergenic region; ^dCDS: Coding sequence; ^eF29S and A62V.

6.6 Sequence comparison of the G gene, F gene and associated intergenic regions in neutralization resistant and susceptible clones of strain R17532

Although the sequences of the F and G genes have previously been determined from both virus stocks and clones, a limited number of virus clones were sequenced from two virus isolates, a resistant and a susceptible clone of isolate R17532 and two resistant and

one susceptible clones of isolate N5843 (Gias, 2006). Variability was observed in both the F and the G genes, but none of the mutations correlated with resistance when compared across all five clones. As multiple mutations might confer the same phenotypic change, it was of interest to further study both genes in additional susceptible and resistant clones from different passage levels.

Clone R3.7.8.3 was serially passaged from passage 3 until passage 10 and the neutralization phenotypes at each passage level determined as shown in section 4.4. Clone 3.7.8.3 at passage level 3 (PZ EC₅₀ in HeLa NCL79 = 48.46 µg/ml), 6 (PZ EC₅₀ in HeLa NCL79 = 3.38 µg/ml) and 9 (PZ EC₅₀ in HeLa NCL79 = 2.78 µg/ml) were selected to isolate total RNA for sequence analysis of the G and F genes as described in section 3.5.1.

6.6.1 Amplification of the G gene in neutralization resistant and susceptible clones of strain R17532

In the hRSV strain A2 genome, the G gene stretches from nt 4,673 to nt 5,595 (GenBank accession number M74568). Total RNA extracted from clones 3.7.8.3 P3, P6 and P9 were reverse transcribed using the forward primer SH292 (section 3.5.2) and amplified using the SH292: F164 primer pair (Figure 6.5, Table 3.5 and 3.6 for all primers) and the standard conditions (section 3.5.3) to yield autonomous sequence between nt 4,510 and nt 5,855. RNAs extracted from uninfected HeLa NCL cells and DEPC treated water were included in the RT-PCR as negative controls. The size of the expected band was 1,326nt. Target bands of this size were detected in all clones, but not in negative controls (Figure 6.4). PCR products were isolated and purified for direct sequencing as described in section 3.5.9.

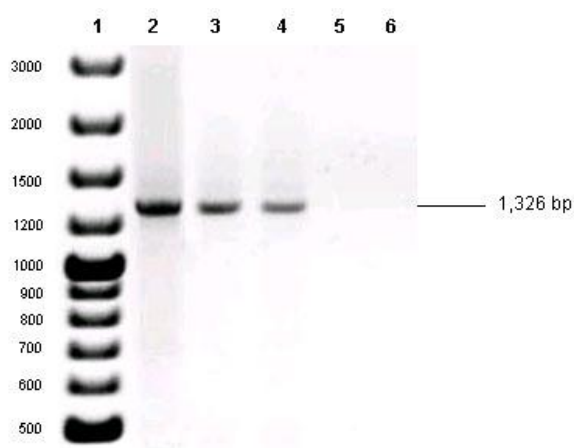


Figure 6.4: RT-PCR amplification of the G gene and associated intergenic regions in the susceptible and resistant clones of R17532 using the SH292: F164 primer pair.

The lanes were loaded as follows; Lane 1: 100bp DNA ladder; Lane 2: R3.7.8.3 P3; Lane 3: R3.7.8.3 P6; Lane 4: R3.7.8.3 P9; Lane 5: HeLa NCL cells (Negative control) and Lane 6: DEPC treated water (Negative control).

6.6.2 Amplification of the F gene in neutralization resistant and susceptible clones of strain R17532

For the hRSV strain A2 genome, the F gene is encoded by nucleotides nt 5,648 to nt 7,550 (GenBank accession number M74568). The F gene and associated intergenic regions were reverse transcribed from the RNA of clones 3.7.8.3 P3, P6 and P9 using the forward primer G886 and amplified in two overlapping fragments using the G886: F1000 and the A2R3: ALW2 primer pairs (Figure 6.5) and the standard conditions (section 3.5.3). The target band of the first fragment was 1,249nt with autonomous sequence between nt 5,558 and nt 6,806 and the second fragment was 869nt with autonomous sequence between nt 6,760 and nt 7,668 (Figure 6.7). Negative controls (HeLa NCL cell RNA and DEPC treated water) were amplified in parallel. Expected bands of 1,249nt and 869nt were observed in all clones of R17532 (Figure 6.6 and 6.7). They were isolated and purified for sequencing as previously described in section 3.5.9. No target bands or non-specific bands were present in negative controls.

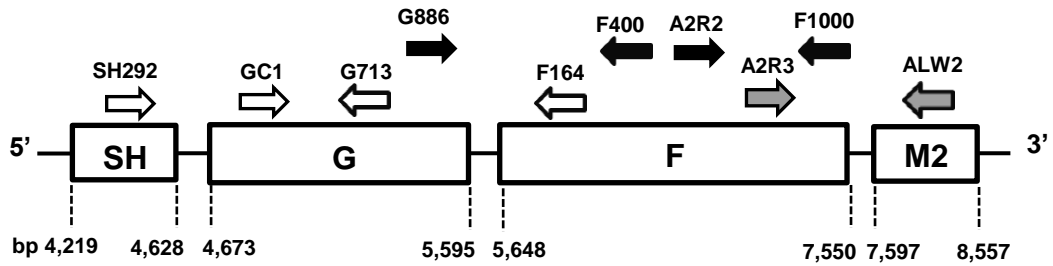


Figure 6.5: Schematic diagram of primers for amplification and sequencing of the F gene, G gene and associated intergenic regions on hRSV antigenome.

hRSV genes are depicted as rectangles (not to scale). Primers for the G gene are white arrows and primer for the first and second fragments of the F genes are black and grey arrows, respectively. Primers SH292 (nt 4,510-4,531); GC1 (nt 5,205-5,222); G713 (nt 5,408-5,385); G886 (nt 5,558-5,581); F164 (nt 5,855-5,833); F400 (nt 6,188-6,168); A2R2 (nt 6,125-6,234); A2R3 (nt 6,760-6,779); F1000 (nt 6,806-6,786); ALW2 (nt 7,668-7,628) [Nucleotide numbering is based on the A2 genome, GenBank accession number M74568].

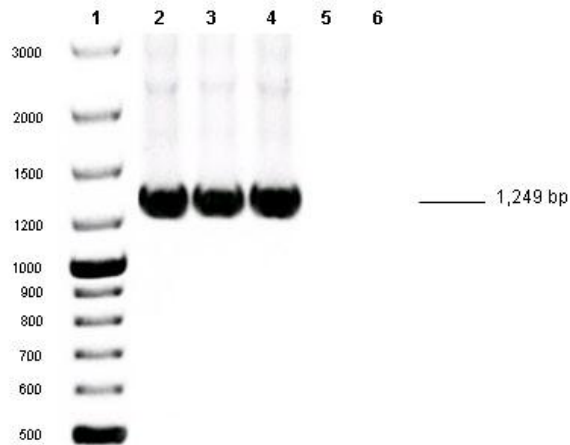


Figure 6.6: RT-PCR amplification of the first fragments of the F gene in the susceptible and resistant clones of R17532 using the G886: F1000 primer pairs.

The lanes were loaded as follows; Lane 1: 100bp DNA ladder; Lane 2: R3.7.8.3 P3; Lane 3: R3.7.8.3 P6; Lane 4: R3.7.8.3 P9; Lane 5: HeLa NCL cells (Negative control) and Lane 6: DEPC treated water (Negative control).

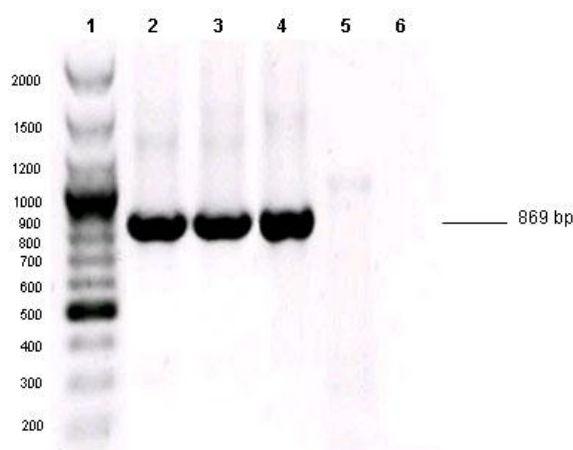


Figure 6.7: RT-PCR amplification of the second fragments of the F gene in the susceptible and resistant clones of R17532 using the A2R3: ALW2 primer pairs.

The lanes were loaded as follows; Lane 1: 100bp DNA ladder; Lane 2: R3.7.8.3 P3; Lane 3: R3.7.8.3 P6; Lane 4: R3.7.8.3 P9; Lane 5: HeLa NCL cells (Negative control) and Lane 6: DEPC treated water (Negative control).

6.6.3 Sequence comparison of the G gene, F gene and associated intergenic regions of neutralization resistant clones of R17532 and A2 strain

The sequence of the G gene was analysed using the forward primers SH292 and GC1 in the 5' to 3' direction and the reverse primers G713 and F164 in the 3' to 5' direction (antigenome). In the F gene, the first fragment was sequenced using the forward primers G886 and A2R2 in the 5' to 3' direction and the reverse primers F400 and F1000 in the 3' to 5' direction. The sequence of the second fragment for the F gene was determined both 5' to 3' and 3' to 5' directions using the forward primer A2R3 and the reverse primer ALW2, respectively. The comparison of the G, F genes and their intergenic regions revealed no nucleotide changes among the resistant (R3.7.8.3 P3) and susceptible clones (R3.7.8.3 P6 and P9).

6.7 Sequence comparison of the G gene, F gene and associated intergenic regions in different neutralization resistant and susceptible clones of R17532

In this study, several clones of R17532 from different passages were plaque purified and their neutralization phenotypes were determined. The sequence analysis of the G and F genes in both previously produced clones and newly generated clones were determined.

6.7.1 Neutralization of resistant and susceptible clones of R17532 at different passage levels

The lineage of all passage levels of R17532 is shown in Figure 6.8. Previously, anti-F monoclonal antibody neutralization resistant virus R17532 was isolated from the nasopharyngeal secretions of an infected infant on two separate occasions by Prof. G.L. Toms (P1-GLT) and Dr. A. Connor (P1-AC). The P1-GLT and P1-AC viruses were passaged in HeLa cells to level 10 in 1996 and in 1998, respectively. Their phenotypes remained resistant throughout, whereas, the P10-FF virus passaged from the P9-GLT virus in 2000 shifted to susceptible and retained its susceptible phenotype after passaged to level 11 (P11-RM). In addition, the P5-RM stock was passaged from the P2-GLT in 2001 and its phenotype also changed to susceptible during passage.

Several clones have been produced previously from different virus stocks at different passage levels. The clone R3.2-ELG and R3.7.8-ELG were resistant to neutralization by anti-F monoclonal antibody, whilst the clone R11.1.1-ELG and R11.2-ELG were susceptible. In this study, new clones were prepared as described in section 3.4.4 from the available virus stocks at different passage levels as detailed in Figure 6.8. New clones were designated with the suffix –WH. The PZ EC₅₀ values of clones in red colour in Figure 6.8 were determined as shown in Figure 6.9 and found to vary in susceptibility with PZ EC₅₀ values of 3 to 90 µg/ml. For each clone, total RNAs were reverse transcribed using the forward primer SH292 for the G gene and the forward primer G886 for the F gene (Figure 6.5, Table 3.5 and 3.6 for all primers). Amplification of the entire G gene was performed using the SH292: F164 primer pair, whereas two fragments of the F gene was amplified using the G886: F1000 and the A2R3: ALW2 primer pairs (data not shown).

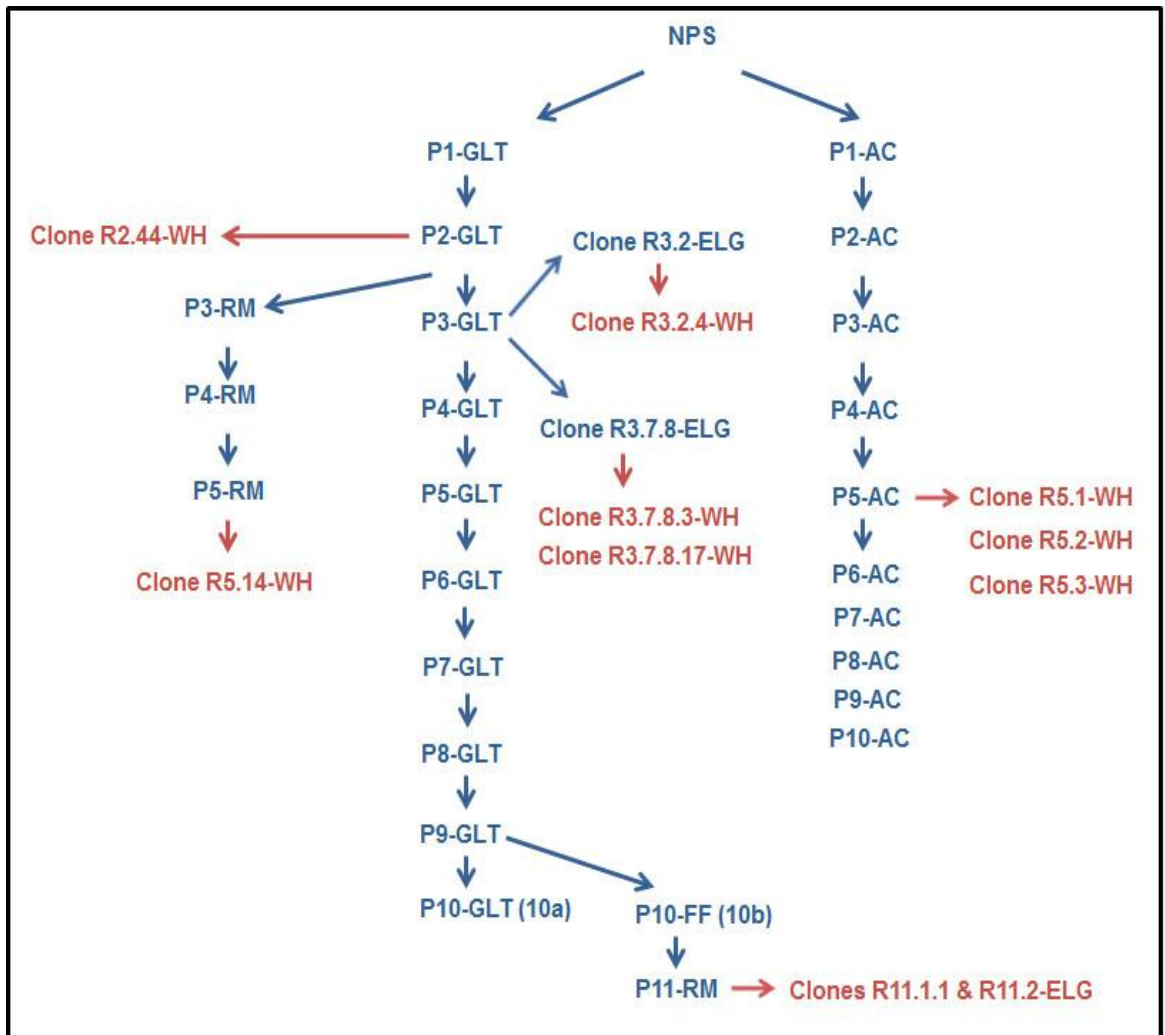


Figure 6.8: Lineage of different passage levels of hRSV strain R17532. Clones shown in red colour were used in this study.

GLT- grown by Prof.G.L.Toms; 1996. AC- grown by Dr. A. Connor; 1998 FF- grown by F. Fenwick; 2000. RM- grown by Dr. R. Marsh; 2001 ELG - cloned by Dr. E. Gias; 2006. WH- cloned by W. Hiriote; 2009

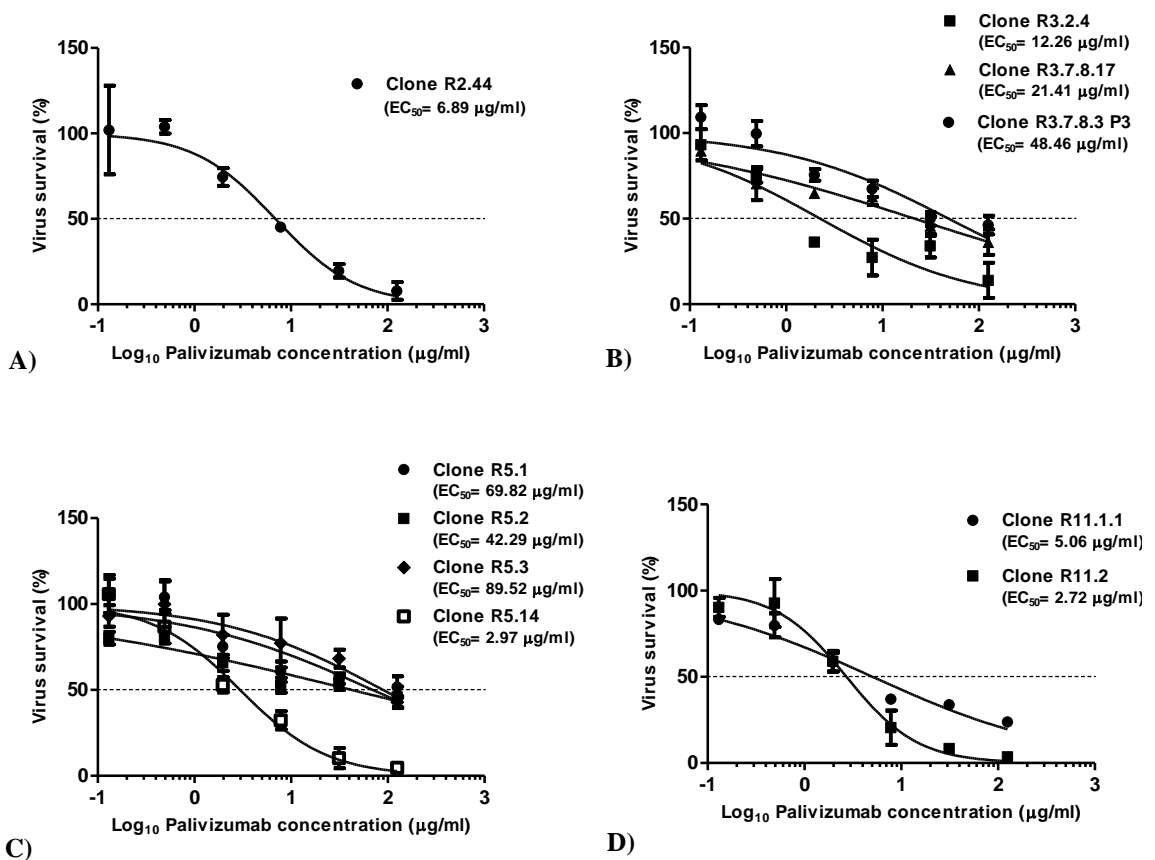


Figure 6.9: The percentage virus survival of R17532 (A) clone R2, (B) clone R3, (C) clone R5 and (D) clone R11 after neutralization with PZ in HeLa NCL79 cells.

Plots were prepared from triplicate values and error bars show the standard error. The 50% reduction level is indicated by (...).

6.7.2 Sequence comparison of the G gene and associated intergenic regions of resistant and susceptible clones of R17532 and A2 strain

The 1,326nt target band for both neutralization resistant and susceptible clones from R17532 clones with different passages histories (10 clones, Figure 6.8) were directly sequenced in both directions (section 3.5.9). The forward primers SH292 and GC1 were used for sequencing in the 5' to 3' direction (antigenome) and the reverse primers G713 and F164 in the 3' to 5' direction (Figure 6.5). The sequences of all clones were compared with the A2 strain (GenBank accession number M74568) and percentage comparisons are presented in Table 6.3.

The PZ EC₅₀ values for each clone and a summary of the variability in the SH gene end, G gene and G-F intergenic region are shown in Table 6.4 and 6.5. The sequences of the SH GE sequence and the SH-G intergenic region are presented in Appendix Figure 10.7. There was a deletion of an A residue from the SH GE sequence in four of five

susceptible clones (R2.44, R3.2.4, R11.1.1 and R11.2), resulting in only 7As in the A-tract as described in section 6.5 and Table 6.4. However, the susceptible clone R5.14 did not have this deletion and retained 8As. Four of the five resistant clones retained eight As, but one clone (R5.1) had only seven. Therefore, this mutation does not appear to be responsible for the phenotype switch, being both present and absent in different clones of both phenotypes. This apart, the percentage of nucleotide identity over the SH GE sequence and SH-G intergenic region was 100 between all clones. In this region, A2 lacked all three adenines having only 5As in the A-tract. Furthermore, there were four additional differences compared to the R17532 clones with 90% nucleotide identity (Table 6.3 and Appendix Figure 10.7). The sequence of the 5'untranslated region (5'UTR) of the G gene for all viruses is also presented in Appendix Figure 10.7. All R17532 clones and the A2 strain were identical in this region.

The full G coding region for all 10 clones and A2 are presented in Appendix Figure 10.8. In the G coding region, variation in the R17532 clones occurred at only one position, residue 884, (Table 6.4 and Appendix Figure 10.8) where a transition from T to C corresponded to an amino acid change at residue 295 (I → T) (Table 6.5). This mutation was in the region of the ectodomain in the mucin like variable region 2. T was present in four of the resistant, but also in two of the susceptible clones, R2.44 and R5.14. C was present in three of the susceptible clones and in the resistant clone R5.1. A similar switch at this position from T in the resistant stock to C in the susceptible stock of R17532 was reported by Marsh *et al.* (2007) who also found a mixture of both C and T in the chromatogram of a high passage resistant virus stock (P10 GLT). This mutation appeared to be present in both resistant and susceptible clones of virus and was therefore not correlated with neutralization phenotype.

The sequences of the 3'UTR of the G gene and the G-F intergenic region are presented in Appendix Figure 10.9. The 3'UTR regions were identical in all clones of R17532, although a nucleotide substitution and a deletion were observed in the G GE sequence of A2 giving only 84% nucleotide identity to R17532. In the G-F intergenic region, one clone, the resistant clone R5.1, differed from all the tests with a single T → C change at position 36. Again the A2 and R17532 strains showed considerably variation over this region with 84% nucleotide identity (Table 6.3).

Table 6.3: Percentage of nucleotide identity in the G gene of clone R17532 compared to the A2 strain.

Region	NT #	% NT ^a identity R17532 vs. A2	% AA ^b identity R17532 vs. A2
SH-G IR ^c	1-44	90	N/A
G 5'UTR	45-59	100	N/A
G CDS ^d	1-897	92	85
G 3'UTR	1-12	84	N/A
G-F IR	12-64	84	N/A

^aNT: Nucleotide; ^bAA: Amino acid; ^cIR: Intergenic region; ^dCDS: Coding sequence.

Table 6.4: Summary of nucleotides changes of R17532 in the G gene.

Gene	Nucleotide sequence										
	Nucleotide number	R5.3	R5.1	R3.7.8.3	R5.2	R3.7.8.17	R3.2.4	R2.44	R11.1.1	R5.14	R11.2
PZ EC ₅₀		90	70	48	42	21	12	7	5	3	2.7
SH GE ^a	-	8A	7A	8A	8A	8A	7A	7A	7A	8A	7A
G CDS ^b	884	T	C	T	T	T	C	T	C	T	C
G-F IR ^c	36	T	C	T	T	T	T	T	T	T	T

^aGE: Gene end sequence; ^bCDS: Coding sequence; ^cIR: Intergenic region

Table 6.5: Summary of amino acid changes of R17532 in the G glycoprotein.

Protein	Amino acid sequence										
	Amino acid number	R5.3	R5.1	R3.7.8.3	R5.2	R3.7.8.17	R3.2.4	R2.44	R11.1.1	R5.14	R11.2
PZ EC ₅₀		90	70	48	42	21	12	7	5	3	2.7
G CDS ^a	295	I	T	I	I	I	T	I	T	I	T

^aCDS: Coding sequence

6.7.3 Sequence comparison of the F genes and associated intergenic regions of resistant and susceptible clones of R17532 and A2 strain

The entire F genes of the 10 R17532 clones, amplified in two overlapping fragments, were sequenced in both directions as described in section 6.6.3. The 5'UTR, coding sequences and the 3'UTR of the F gene of all clones are compared with the A2 strain (GenBank accession number M74568) in Appendix Figure 10.10, 10.11 and 10.12, respectively and percentage comparisons are presented in Table 6.6.

A summary of the variability among the R17532 clones is presented in Table 6.7 and 6.8. There were no nucleotide differences among the clones of the R17532 in 5'UTR or 3'UTR of the F gene (Appendix Figure 10.10 and 10.12). However, several nucleotides in the A2 3'UTR were different from those in R17532 with percentage of nucleotide identity of 93 (Table 6.6). In the F coding region, one nucleotide change occurred from T in most of clones to G in susceptible clones R11.1.1 and R11.2 and resistant clone R5.1 in the position 456 (Table 6.7). This mutation caused an amino acid change in the residue 152 (I → M) located in the HR1 region of the F1 subunit (Table 6.8 and Appendix Figure 10.11). As clones with both resistant and susceptible phenotype occurred with both alternatives, this change does not appear to be directly related to the phenotype shift.

There were also two silent nucleotide changes in clone R3.2.4 at 946 (C → A) and 1082 (A → G) and a coding mutation observed in only resistant clone R3.7.8.17 at the residue 101. Most clones encoded proline (P), whereas clone R3.7.8.17 encoded serine (S), the change resulting from a nucleotide change from C to T at position 301 (Table 6.7 and 6.8). This mutation was also found in a previous study where a serine was found at this point in the F sequence of susceptible clone N10a of the isolate N5843 (Gias, 2006). Accordingly, this mutation is not apparently associated with the shift of resistance to susceptibility. The percentage of amino acid identity for the entire F gene of the R17532 and A2 was 96 as shown in Table 6.6.

Table 6.6: Percentage of nucleotide identity in the F gene of clone R17532 compared to the A2 strain.

Region	NT#	% NT ^a identity R17532 vs. A2	% AA ^b identity R17532 vs. A2
F 5'UTR	46-58	100	N/A
F CDS ^c	1-1725	96	96
F 3'UTR	1-171	93	N/A

^aNT: Nucleotide; ^bAA: Amino acid; ^cCDS: Coding sequence.

Table 6.7: Summary of nucleotides changes of R17532 in the F gene.

Gene	Nucleotide sequence										
	Nucleotide number	R5.3	R5.1	R3.7.8.3	R5.2	R3.7.8.17	R3.2.4	R2.44	R11.1.1	R5.14	R11.2
PZ EC ₅₀		90	70	48	42	21	12	7	5	3	2.7
F CDS ^a	301	C	C	C	C	T	C	C	C	C	C
	456	T	G	T	T	T	T	T	G	T	G
	946	C	C	C	C	C	A	C	C	C	C
	1082	A	A	A	A	A	G	A	A	A	A

^aCDS: Coding sequence

Table 6.8: Summary of amino acid changes of R17532 in the F glycoprotein.

Protein	Amino acid sequence										
	Amino acid number	R5.3	R5.1	R3.7.8.3	R5.2	R3.7.8.17	R3.2.4	R2.44	R11.1.1	R5.14	R11.2
PZ EC ₅₀		90	70	48	42	21	12	7	5	3	2.7
F CDS ^a	101	P	P	P	P	S	P	P	P	P	P
	152	I	M	I	I	I	I	I	M	I	M

^aCDS: Coding sequence

6.7.4 Summary of nucleotide changes of resistant and susceptible clones of R17532 in the membrane associated protein genes

Among the 10 virus clones analysed, variability between the SH GE sequence, the G and F genes occurred at seven sites (Table 6.9). The predominant resistant phenotype appears to be 8A/T/T/C/T/C/A with susceptible clones acquiring one or more mutations. However, clone R5.14 preserves this phenotype and is susceptible and clone R5.1 differs at 4 of the 7 variable regions yet preserves the resistant phenotypes. These results suggest that none of mutations in the membrane associated glycoprotein genes were correlated with the phenotypic shift. Changes elsewhere in the genome may be more important in determining the neutralization phenotype.

Table 6.9: Summary of nucleotide changes of R17532 in the SH GE sequence, G and F genes.

Gene	Nucleotide sequence										
	Nucleotide number	R5.3	R5.1	R3.7.8.3	R5.2	R3.7.8.17	R3.2.4	R2.44	R11.1.1	R5.14	R11.2
PZ EC ₅₀		90	70	48	42	21	12	7	5	3	2.7
SH GE ^a	1-3	8A	7A	8A	8A	8A	7A	7A	7A	8A	7A
G CDS ^b	884	T	C	T	T	T	C	T	C	T	C
G-F IR ^c	36	T	C	T	T	T	T	T	T	T	T
F CDS	301	C	C	C	C	T	C	C	C	C	C
	456	T	G	T	T	T	T	T	G	T	G
	946	C	C	C	C	C	A	C	C	C	C
	1082	A	A	A	A	A	G	A	A	A	A

^aGE: Gene end sequence, ^bCDS: Coding sequence; ^cIR: Intergenic region

In this section the sequences of the region of the hRSV R17532 genome encoding the membrane associated genes of the virus from M to F have been compared for resistant and susceptible clones R3.7.8.3 and R11.1.1. Changes were found in the R11.1.1 genome at 3 loci, in the SH GE sequence, in the G and F coding regions. Further analysis of multiple clones of differing susceptibility derived from two independent isolations of the virus from the original clinical sample revealed no clear cut correlation of any mutation with acquisition of resistance and in one clone (clone R5.41) acquisition of susceptibility was associated with no mutations in SH gene end the G or

the F genes. It can be concluded therefore that phenotype switching must be associated at least for this clone, with changes in other genes. The sequences of the rest of the genome of resistant and susceptible clones were analysed and the results are reported in the next chapter.

**Chapter 7: Comparison of the non-membrane protein genes of
resistant and susceptible clones of R17532**

7.1 Introduction

The results from chapter 6 confirmed the conclusion of Gias (2006) and Marsh *et al.* (2007) that mutations in the membrane associated protein genes (M, SH, G, F, and their intergenic regions) do not explain the neutralization phenotype shift. To investigate whether changes in the rest of the genome correlated with phenotypic change, nucleotide and deduced amino acid sequences of six non-membrane protein genes located both upstream (NS1, NS2, N and P) and downstream (M2 and L) of the membrane proteins including their intergenic regions were analysed and compared between neutralization R17532 susceptible clone R11.1.1 P8 and resistant clone R3.7.8.3 P3. To complete the full sequence of each clone, the 3'leader and 5'trailer sequences from both were also determined using genomic RNA circularization, 5'rapid amplification of cDNA ends (5'RACE) and 3'rapid amplification of cDNA ends (3'RACE) techniques.

7.2 Preparation of total RNA from infected cell lysates.

Total RNAs of clone R11.1.1 P8 (PZ 50% inhibitory dose = 0.39 µg/ml; see section 6.1) and clone R3.7.8.3 P3 (PZ EC₅₀ = 48.46 µg/ml) infected cell lysates were isolated (section 3.5.1) and this material was used as a template for the RT-PCR amplification of all the non-membrane protein genes of the two clones unless stated otherwise. All primers used in amplification and sequence analysis of these genes are presented in Table 3.5, 3.6 and 3.7.

7.3 Amplification of the NS1, NS2, N genes and associated intergenic regions of resistant and susceptible clones of R17532

In the hRSV strain A2 genome, the NS1, NS2 and N genes are encoded by nucleotides 45 to 576, nucleotides 596 to 1,098 and nucleotides 1,125 to 2,327, respectively (GenBank accession number M74568). The three genes and associated intergenic regions were amplified in two overlapping fragments. For the first fragment, total RNA templates were reverse transcribed using the forward NS1 primer (section 3.5.2) and amplified using the NS1: NS2-468 primer pair (Figure 7.1) to yield autonomous sequence between nt 2 to nt 1,090 and the standard condition described in section 3.5.3. Negative controls using RNA extracted from uninfected HeLa NCL cells and DEPC treated water were included in the RT-PCR.

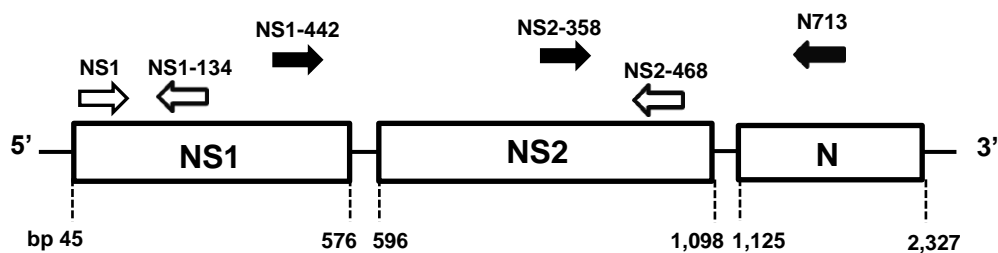


Figure 7.1: Schematic diagram of primers for amplification and sequencing of the NS1, NS2, N genes and associated intergenic regions on hRSV antigenome.

hRSV genes are depicted as rectangles (not to scale). Primers for the first and second fragments are white and black arrows, respectively. Primers NS1 (nt 2-20); NS1-134 (nt 201-178); NS1-442 (nt 486-511); NS2-358 (nt 953-976); NS2-468 (nt 1,090-1,063); N713 (nt 1,860-1,837) [Nucleotide numbering is based on the A2 genome, GenBank accession number M74568].

The expected size of the first fragment PCR product was 1,089nt. Both clones R11.1.1 P8 and R3.7.8.3 P3 showed two heavy bands and one weak band with the larger heavy band being approximately 1,089nt (Figure 7.2). No bands were present in DEPC negative controls. However, a number of bands of less than 1,000nt were present in the HeLa control. PCR products of the expected size for each primer pair were isolated and purified from agarose gels for direct nucleotide sequencing as described in section 3.5.9.

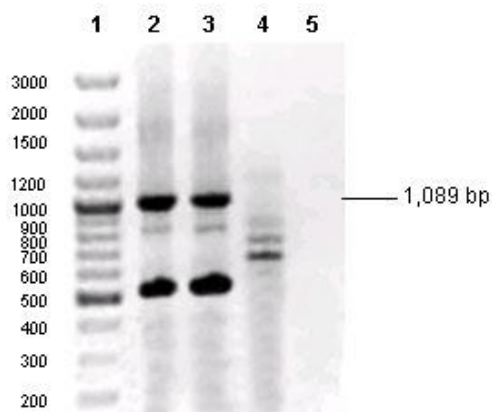


Figure 7.2: RT-PCR amplification of the first fragment of the NS1, NS2 genes and associated intergenic regions of clones R11.1.1 P8 and R3.7.8.3 P3 using the NS1: NS2-468 primer pair.

The lanes were loaded as follows; Lane 1: 100bp DNA ladder; Lane 2: R11.1.1 P8; Lane 3: R3.7.8.3 P3; Lane 4: HeLa NCL cells (Negative control) and Lane 5: DEPC treated water (Negative control)

For the second fragment, the forward NS1_442 primer was used in the reverse transcription reaction of a fragment of 1,375nt comprising the NS1-NS2 intergenic region, the NS2 gene, the NS2-N intergenic region and some part of the N gene. Attempts to amplify this fragment using the NS1_442: N713 primer pair to yield autonomous sequence between nt 486 to nt 1,860 were initially unsuccessful using

standard conditions (section 3.5.3). The PCR reaction was therefore optimized for magnesium concentration and annealing temperature on the cDNA of clone R11.1.1 P8 (Figure 7.3 and 7.4).

Figure 7.3 shows the optimization of magnesium concentration at annealing temperature 55°C. The expected band of 1,375nt with the least numbers of non-specific bands was detected in reaction performed with 7.5 mM MgCl₂. However, when the annealing temperature was increased to 60°C, the numbers of non-specific bands in the PCR reaction containing 3.75 mM MgCl₂ were less than the reaction performed with 7.5 mM MgCl₂ (Figure 7.4). Therefore, PCR reaction for both clone R11.1.1 P8 and R3.7.8.3 P3 were carried out with 3.75 mM MgCl₂ and an annealing temperature of 60°C and included HeLa NCL and DEPC negative controls. No band was detected in either negative control (Figure 7.5). The target bands of 1,375nt for both clones were isolated and purified from agarose gels for direct nucleotide sequencing (section 3.5.9)

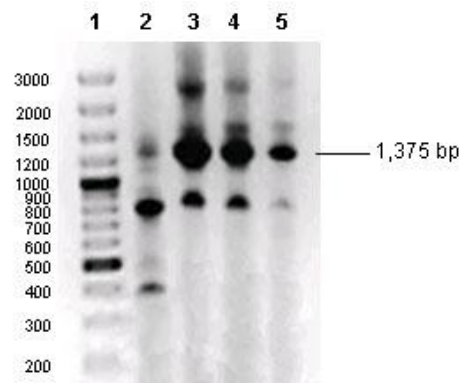


Figure 7.3: Optimization of magnesium concentration for the amplification of the second fragment included the NS1 gene, NS2 gene, N gene and associated intergenic regions of R11.1.1 P8 using the NS1_442: N713 primer pair at annealing temperature 55°C.

The lanes were loaded as follows; Lane 1: 100bp DNA ladder; Lane 2, 3, 4 and 5: PCR reaction performed with 2.5 mM, 3.75 mM, 5 mM, and 7.5 mM MgCl₂, respectively.

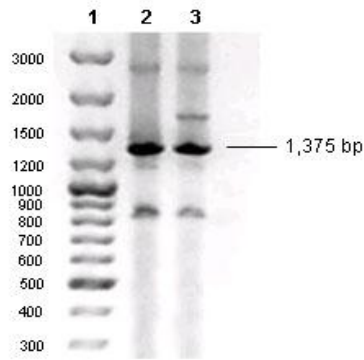


Figure 7.4: Optimization of magnesium concentration for the amplification of the second fragment included the NS1 gene, NS2 gene, N gene and associated intergenic regions of R11.1.1 P8 using the NS1_442: N713 primer pair at annealing temperature 60 °C.

The lanes were loaded as follows; Lane 1: 100bp DNA ladder; Lane 2 and 3: PCR reaction performed with 3.75 mM and 7.5 mM MgCl₂, respectively.

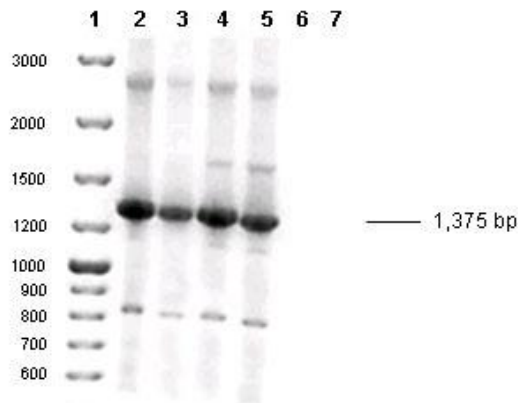


Figure 7.5: RT-PCR amplification of the second fragment included the NS1, NS2, N genes and associated intergenic regions of R11.1.1 P8 and R3.7.8.3 P3 using the NS1_442: N713 primer pair.

The lanes were loaded as follows; Lane 1: 100bp DNA ladder; Lane 2 and 3: R11.1.1 P8; Lane 4 and 5: R3.7.8.3 P3; Lane 6: HeLa NCL cells (Negative control) and Lane 7: DEPC treated water (Negative control)

7.4 Sequence comparison of the NS1, NS2, N genes and associated intergenic regions of resistant and susceptible clones of R17532 and A2 strain

The sequence analysis of the NS1 coding region, the NS1 3'UTR, the entire NS2 gene and associated intergenic regions were derived from the two fragments of clone R11.1.1 P11 and clone R3.7.8.3 P3 with the size of 1,089nt (nt 2-1090) and 1,375nt (nt 486-1860). The nucleotide numbering was based on the hRSV A2 genome (GenBank accession number M74568).

The first fragment was sequenced with the forward NS1 primer in the 5' to 3' direction (antigenome) and the reverse primers NS1-134 and NS2-468 in the 3' to 5' direction as described in section 3.5.9 and Figure 7.1. This provided readable sequence from nt 21

to 1,010. The second fragment was sequenced from forward primers NS1-442 and NS2-358 in the 5' to 3' direction and the reverse primers N713 in the 3' to 5' direction provided readable sequence from nt 535 to 1,788.

Comparison of the sequence data between the two clones revealed no nucleotide changes in the NS1 coding region (Appendix Figure 10.13), the NS1 3'UTR (Appendix Figure 10.14), the entire NS2 gene (Appendix Figure 10.15, 10.16 and 10.17) and associated intergenic regions (Appendix Figure 10.15 and 10.18). These regions were fully conserved in the neutralization resistant and susceptible clones of R17532.

There were several nucleotide differences between the R17532 strain and the A2 strain, leading to one amino acid change in the NS1 protein and three amino acid changes in the NS2 protein with the percentage of amino acid identity of 99 and 97, respectively (Table 7.1, Appendix Figure 10.13 and 10.16). The percentage of nucleotide identity in each region between the A2 and R17532 are shown in Table 7.1.

Table 7.1: Percentage of nucleotide identity in the NS1 gene, NS2 gene and associated intergenic regions of clone R17532 compared to the A2 strain.

Region	NT#	% NT ^a identity R17532 vs. A2	% AA ^b identity R17532 vs. A2
NS1 CDS ^c	1-420	95	99 ^d
NS1-3'UTR	1-57	96	N/A
NS1-NS2 IR	1-19	89	N/A
NS2 5'UTR	20-51	90	N/A
NS2 CDS	1-375	96	97 ^e
NS2 3'UTR	1-96	91	N/A

^aNT: Nucleotide; ^bAA: Amino acid; ^cCDS: Coding sequence; ^dI105L; ^eT8N, R38K and R55K.

7.5 Amplification of the N gene and associated intergenic regions of resistant and susceptible clones of R17532

cDNA comprising the N gene and N-P intergenic region of clone R11.1.1 P8 and clone R3.7.8.3 P3 was produced by reverse transcription using the forward NP1674 primer (section 3.5.2) and amplified using the NP1674: P162 primer pair (Figure 7.6) and the

standard conditions (section 3.5.3). Negative controls of HeLa NCL cells and DEPC treated water were included in the reaction. Intense bands of the expected size of 840nt with autonomous sequence between nt 1,674 to nt 2,513 were present for both clones, but not in either negative control (Figure 7.7). The target bands were isolated and purified for direct sequencing as described in section 3.5.9.

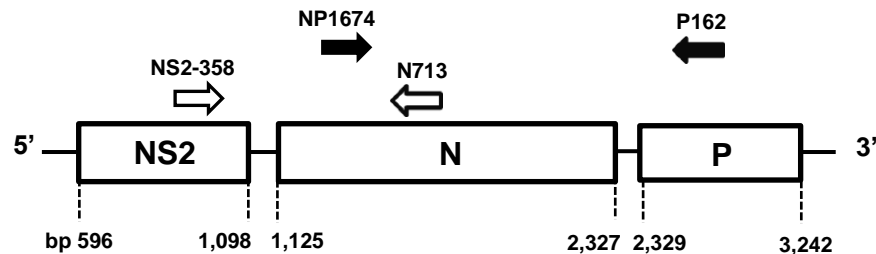


Figure 7.6: Schematic diagram of primers for amplification and sequencing of the NS2, N genes and associated intergenic regions on hRSV antigenome.

hRSV genes are depicted as rectangles (not to scale). Primers for the NS2, N genes and associated intergenic regions used in section 7.3 and 7.4 are white arrows and primers for the N gene and N-P intergenic region are black arrows. Primers NS2-358 (nt 953-976); NP1674 (nt 1,674-1,696); N713 (nt 1,860-1,837); P162 (nt 2,513-2,490) [Nucleotide numbering is based on the A2 genome, GenBank accession number M74568].

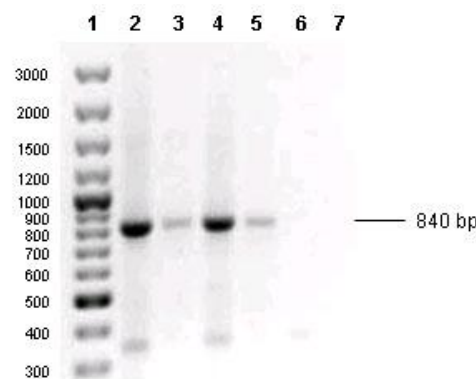


Figure 7.7: RT-PCR amplification of the N gene and associated intergenic regions of R11.1.1 P8 and R3.7.8.3 P3 using the NP1674: P162 primer pair.

The lanes were loaded as follows; Lane 1: 100bp DNA ladder; Lane 2 and 3: R11.1.1 P8; Lane 4 and 5: R3.7.8.3 P3; Lane 6: HeLa NCL cells (Negative control) and Lane 7: DEPC treated water (Negative control)

7.6 Sequence comparison of the N gene and associated intergenic regions of resistant and susceptible clones of R17532 and A2 strain

The NS2-N intergenic region and the N coding sequence for clones R11.1.1 P8 and R3.7.8.3 P3 were sequenced from the 1,375nt amplicand generated in section 7.3 in both directions using the forward primer NS2-358 in the 5' to 3' direction (antigenome)

and the reverse primer N713 in the 3' to 5' direction (Figure 7.6). This provided readable sequence from nt 535 to 1,788. The nucleotide numbering was based on the hRSV A2 genome (GenBank accession number M74568). The nucleotide sequence of the 840nt target band generated in section 7.5 was analysed using the forward primer NP1674 in the 5' to 3' direction and the reverse primer P162 in the 3' to 5' direction. This provided readable sequence from nt 1,725 to 2,457.

The nucleotide and amino acid sequence of the NS2-N intergenic region, the N gene and the N-P intergenic region in clone R11.1.1 P8 were the same as those in clone R3.7.8.3 P3, suggesting that the N gene was conserved during passage in HeLa cells (Appendix Figure 10.18, 10.19 and 10.20). There were, however, several nucleotide differences between the R17532 strain and the A2 strain. The NS2-N intergenic region, varied at 5 nucleotides giving a percentage of nucleotide identity of 80 (Table 7.2 and Appendix Figure 10.18). Three amino acid changes between the two viruses were observed and the percentage of amino acid identity was 99 (Table 7.2 and Appendix Figure 10.19). In the N-P intergenic region (2 nucleotides long), a deletion at the position 1 of the A2 was observed with only 50% nucleotide identity (Table 7.2 and Appendix Figure 10.20).

Table 7.2: Percentage of nucleotide identity in the N gene and associated intergenic regions of clone R17532 compared to the A2 strain.

Region	NT#	% NT ^a identity R17532 vs. A2	% AA ^b identity R17532 vs. A2
NS2-N IR	1-26	80	N/A
N 5'UTR	27-41	92	N/A
N CDS ^c	1-1176	97	99 ^d
N 3'UTR	1-13	100	N/A
N-P IR	14-15	50	N/A

^aNT: Nucleotide; ^bAA: Amino acid; ^cCDS: Coding sequence; ^dV64L, V160I and Y216H.

7.7 Amplification of the P gene and associated intergenic regions of resistant and susceptible clones of R17532

In the hRSV strain A2 genome, the P gene stretches from nt 2,329 to nt 3,242 (GenBank accession number M74568). The cDNA synthesis of a fragment consisting of the N-P

intergenic region, the P gene, and the P-M intergenic region was performed for both clone R11.1.1 P8 and clone R3.7.8.3 P3 using the forward P2128 primer and amplified in PCR reactions using the P2128: P3459 primer pair (Figure 7.8) to yield autonomous sequence between nt 2,128 to nt 3,459 and the standard conditions (section 3.5.3). Uninfected HeLa NCL cells and DEPC controls were included. An intense target band of expected size 1,332nt was detected in reactions for both viruses, whilst there were no bands in either negative control (Figure 7.9). These target bands were purified for direct sequencing as described in section 3.5.9.

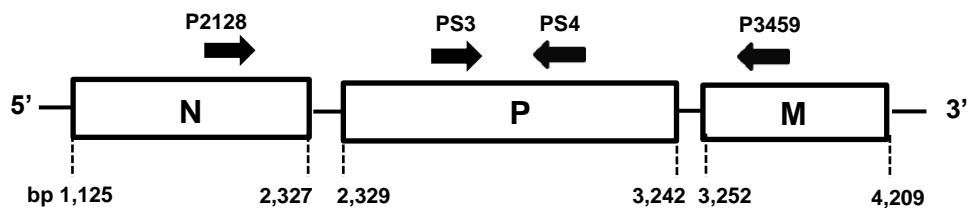


Figure 7.8: Schematic diagram of primers for amplification and sequencing of the P gene and associated intergenic regions on hRSV antigenome.

hRSV genes are depicted as rectangles (not to scale). Primers are black arrows. Primers P2128 (nt 2128-2149); PS3 (nt 2,720-2,748); PS4 (nt 2,971-2,944); P3459 (nt 3,459-3,437) [Nucleotide numbering is based on the A2 genome, GenBank accession number M74568].

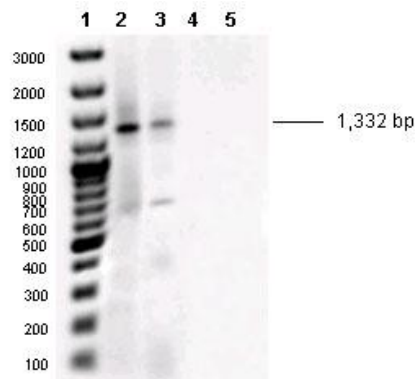


Figure 7.9: RT-PCR amplification of the P gene and associated intergenic regions of clones R11.1.1 P8 and R3.7.8.3 P3 using the P2128: P3459 primer pair.

The lanes were loaded as follows; Lane 1: 100bp DNA ladder; Lane 2: R11.1.1 P8; Lane 3: R3.7.8.3 P3; Lane 4: HeLa NCL cells (Negative control) and Lane 5: DEPC treated water (Negative control).

7.8 Sequence comparison of the P gene of resistant and susceptible clones of R17532 and A2 strain

The 1,332nt target for clones R11.1.1 P8 and R3.7.8.3 P3 was sequenced in the 5' to 3' direction (antigenome) using the forward primer P2128 and PS3. In the 3' to 5' direction, the reverse primers P3459 and PS4 were used in direct sequencing (Figure

7.8). Readable sequence both directions was obtained from nt 2,139 to 3,449 based on the hRSV A2 genome (GenBank accession number M74568). Sequence of the N-P and P-M intergenic regions between the R17532 and A2 were analysed above in section 7.6 and 6.4, respectively. The sequence of the P gene revealed no nucleotide changes between clones R11.1.1 P8 and R3.7.8.3 P3, suggesting this region was fully conserved (Appendix Figure 10.21, 10.22 and 10.23).

However, several nucleotide of A2 were different from those of the R17532. There were only two coding changes between the two viruses and the percentage of amino acid identity was 99 (Table 7.3 and Appendix Figure 10.22). In the P gene 3'UTR, a high level of sequence differences between the A2 and R17532 was observed with 87% identity percentage (Table 7.3 and Appendix Figure 10.23).

Table 7.3: Percentage of nucleotide identity in the N-P intergenic region and the P gene of clone R17532 compared to the A2 strain.

Region	NT#	% NT ^a identity R17532 vs. A2	% AA ^b identity R17532 vs. A2
P 5'UTR	4-17	100	N/A
P CDS ^c	1-726	97	99 ^d
P 3'UTR	1-171	87	N/A

^aNT: Nucleotide; ^bAA: Amino acid; ^cCDS: Coding sequence; ^dV73A and V171I.

7.9 Amplification of the M2 gene and associated intergenic regions of resistant and susceptible clones of R17532

For the hRSV strain A2 genome, the M2 gene is encoded by nucleotides nt 7,597 to nt 8,557 (GenBank accession number M74568). The F-M2 intergenic region and the M2 gene of clone R11.1.1 P8 and clone R3.7.8.3 P3 were reverse transcribed using the forward M2F primer and amplified using the M2F: M2R primer pair (Figure 7.10) and the standard conditions (section 3.5.3). Uninfected HeLa NCL cells and DEPC treated water were included as negative controls.

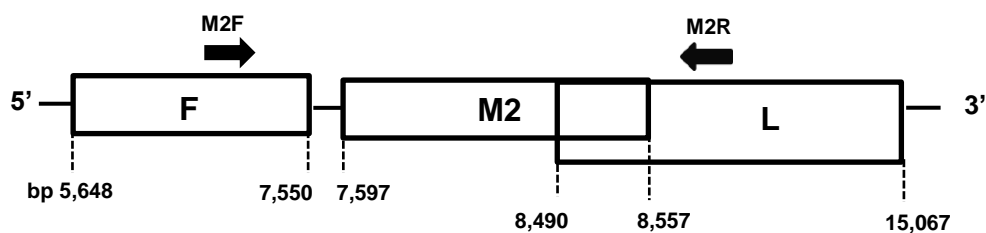


Figure 7.10: Schematic diagram of primers for amplification and sequencing of the F-M2 intergenic region and the M2 gene on hRSV antigenome.

hRSV genes are depicted as rectangles (not to scale). Primers are black arrows. Primers M2F (nt 7,411-7,434); M2R (nt 8,669-8,646) [Nucleotide numbering is based on the A2 genome, GenBank accession number M74568].

Heavy bands of the expected size of 1,259nt with autonomous sequence between nt 7,411 to nt 8,646 were produced in reactions for both virus clones. There was no target band in either negative control (Figure 7.11). The PCR products were extracted and purified for direct nucleotide sequencing as described in section 3.5.9.

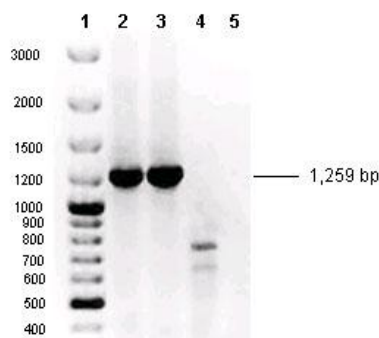


Figure 7.11: RT-PCR amplification of the F-M2 intergenic region and the M2 gene of clones R11.1.1 P8 and R3.7.8.3 P3 using the M2F: M2R primer pair.

The lanes were loaded as follows; Lane 1: 100bp DNA ladder; Lane 2: R11.1.1 P8; Lane 3: R3.7.8.3 P3; Lane 4: HeLa NCL cells (Negative control) and Lane 5: DEPC treated water (Negative control).

7.10 Sequence comparison of the F-M2 intergenic region and the M2 gene of resistant and susceptible clones of R17532 and A2 strain

The sequence of the 1,259nt band for clone R11.1.1 P8 and R3.7.8.3 P3 was analysed using the forward primer M2F and the reverse primer M2R in the 5' to 3' and 3' to 5' directions (antigenome), respectively. Sequence readable in both direction was obtained from nt 7,457 to 8,616 based on the hRSV A2 genome (GenBank accession number M74568). No nucleotide changes in this region were observed between both clones (Appendix Figure 10.24, 10.25 and 10.26).

The M2 sequence of the A2 (GenBank accession number M74568) differed from that of the R17532 at several positions. The percentages of nucleotide identity in each region are presented in Table 7.4. Two coding changes in the residue 120 and 182 were detected in the A2 compared to the R17532 and the percentage of amino acid identity was 98 (Table 7.4 and Figure 10.25).

Table 7.4: Percentage of nucleotide identity in the F-M2 intergenic region and the M2 gene of clone R17532 compared to the A2 strain.

Region	NT#	% NT ^a identity R17532 vs. A2	% AA ^b identity R17532 vs. A2
F-M2 IR	1-46	76	N/A
M2 5'UTR	47-55	100	N/A
M2 CDS ^c	1-585	97	98 ^d
M2 3'UTR	1-367	92	N/A

^aNT: Nucleotide; ^bAA: Amino acid; ^cCDS: Coding sequence; ^dP120L and N182S.

7.11 Amplification of the L gene of resistant and susceptible clones of R17532

In the hRSV strain A2 genome, the L gene stretches from nt 8,490 to nt 15,067, an approximate size of 7 kilo nucleotides (GenBank accession number M74568). Thus, it was amplified in 6 fragments which were LF1 (nt 8,444 to nt 9,815), LF2 (nt 9,605 to nt 10,845), LF3 (nt 10,598 to nt 12,007), LF4 (nt 11,830 to nt 13,059), LF5.1 (nt 12,891 to nt 14,319) and LF5.2 (nt 14,161 to nt 15,153). The reverse transcriptions of the LF1, LF2 and LF3 fragments were performed using the forward M2-848 primer (Figure 7.12).

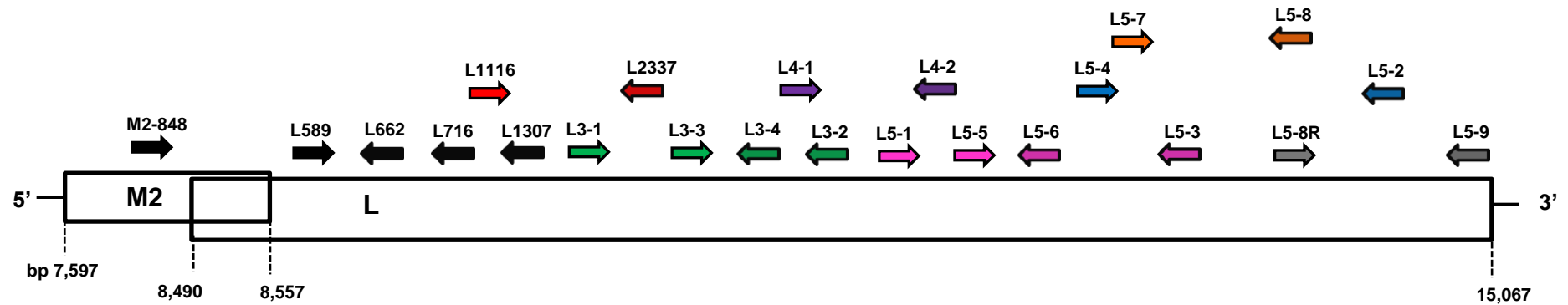


Figure 7.12: Schematic diagram of primers for amplification and sequencing of the M2 and L genes on hRSV antigenome.

hRSV genes are depicted as rectangles (not to scale). Primers for the fragments LF1, LF2, LF3, LF4, LF5.1 and LF5.2 are black, red, green, violet, pink and blue arrows, respectively. Primers for the second round amplification of the fragment LF5.2 are orange arrows. Primers for amplification of the base between 15,109 and 15,175 of clone R3.7.8.3 P3 are grey arrows. Primers M2-848 (nt 8,444-8,462); L589 (nt 9,078-9,097); L662 (nt 9,173-9,151); L716 (nt 9,226-9,205); L1116 (nt 9,605-9,629); L1307 (nt 9,815-9,796); L3-1 (nt 10,598-10,618); L2337 (nt 10,845-10,826); L3-3 (nt 11,250-11,275); L3-4 (nt 11,467-11,448); L4-1 (nt 11,830-11,856); L3-2 (nt 12,007-11,987); L5-1 (nt 12,891-12,914); L4-2 (nt 13,059-13,040); L5-5 (nt 13,426-13,449); L5-6 (nt 13,588-13,562); L5-4 (nt 14,161-14,184); L5-7 (nt 14,215-14,234); L5-3 (nt 14,319-14,300); L5-8R (nt 15,017-15,041); L5-8 (nt 15,041-15,017); L5-2 (nt 15,153-15,130); L5-9 (nt 15,222-15,199) [Nucleotide numbering is based on the A2 genome, GenBank accession number M74568].

The PCR reaction of the LF1 fragment was carried out using the M2-848: L1307 primer pair and uninfected HeLa NCL cells and DEPC controls were included. The expected size of this PCR product was 1,372nt. A band of this size was detected in both clone R11.1.1 P8 (faint band) and clone R3.7.8.3 P3 (strong band). Although no target band was observed in either negative control, there were some mis-priming products and non-specific bands in the reactions for both viruses (Figure 7.13). Nevertheless, the target bands were isolated and purified for direct nucleotide sequencing as described in section 3.5.9.

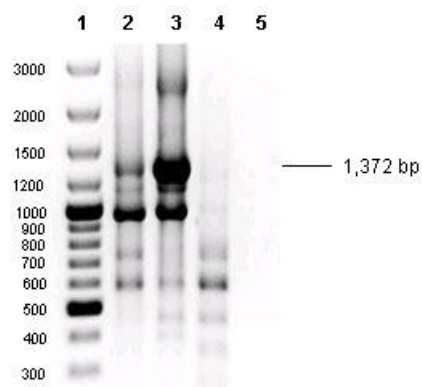


Figure 7.13: RT-PCR amplification of the LF1 fragments of clones R11.1.1 P8 and R3.7.8.3 P3 using the M2_848: L1307 primer pair.

The lanes were loaded as follows; Lane 1: 100bp DNA ladder; Lane 2: R11.1.1 P8; Lane 3: R3.7.8.3 P3; Lane 4: HeLa NCL cells (Negative control) and Lane 5: DEPC treated water (Negative control).

For the LF2 and LF3 fragments, the PCR reactions for clones R11.1.1 P8, R3.7.8.3 P3 and negative controls (uninfected HeLa NCL cells and DEPC treated water) were performed using the L1116: L2337 and L3-1: L3-2 primer pairs, respectively. The expected sizes of amplicons were 1,241nt for the LF2 fragment (Figure 7.14) and 1,410nt for the LF3 fragment (Figure 7.15). Bands of the correct size were obtained from the two clones, but not from the negative controls. Both target bands were isolated and purified for direct nucleotide sequenced as described in section 3.5.9.

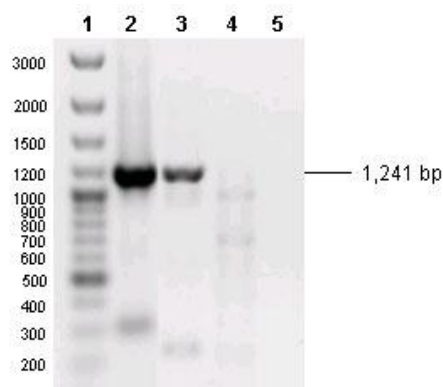


Figure 7.14: RT-PCR amplification of the LF2 fragments of clones R11.1.1 P8 and R3.7.8.3 P3 using the L1116: L2337 primer pair.

The lanes were loaded as follows; Lane 1: 100bp DNA ladder; Lane 2: R11.1.1 P8; Lane 3: R3.7.8.3 P3; Lane 4: HeLa NCL cells (Negative control) and Lane 5: DEPC treated water (Negative control).

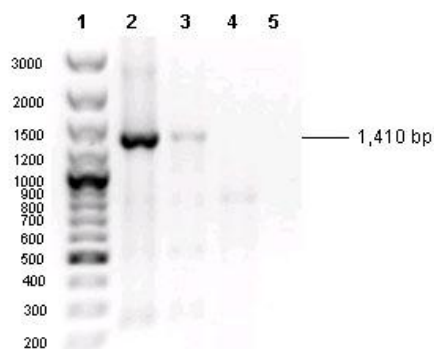


Figure 7.15: RT-PCR amplification of the LF3 fragments of clones R11.1.1 P8 and R3.7.8.3 P3 using the L3-1: L3-2 primer pair.

The lanes were loaded as follows; Lane 1: 100bp DNA ladder; Lane 2: R11.1.1 P8; Lane 3: R3.7.8.3 P3; Lane 4: HeLa NCL cells (Negative control) and Lane 5: DEPC treated water (Negative control).

The forward L4-1 primer was used in reverse transcription of the LF4 fragment in clone R11.1.1 P8, clone R3.7.8.3 P3, uninfected HeLa NCL cells and a DEPC treated water negative control. Amplicons of the expected size (1,230nt) for this fragment were produced from both clones using the L4-1: L4-2 primer pair. There was no amplicon of this size in either negative control (Figure 7.16). These target bands were isolated and purified for direct nucleotide sequencing as described in section 3.5.9.

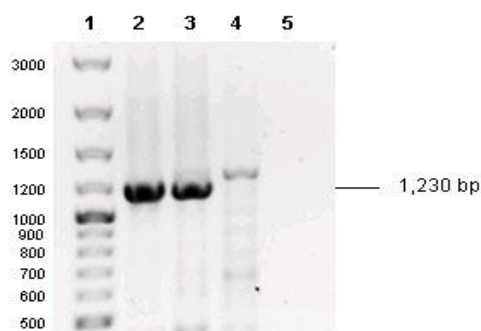


Figure 7.16: RT-PCR amplification of the LF4 fragments of clones R11.1.1 P8 and R3.7.8.3 P3 using the L4-1: L4-2 primer pair.

The lanes were loaded as follows; Lane 1: 100bp DNA ladder; Lane 2: R11.1.1 P8; Lane 3: R3.7.8.3 P3; Lane 4: HeLa NCL cells (Negative control) and Lane 5: DEPC treated water (Negative control).

Figure 7.17 and 7.18 show the amplification of the L5.1 and L5.2 fragments, respectively. Both fragments of clones R11.1.1 P8 and R3.7.8.3 P3 were reverse transcribed using the forward L5-1 primer and amplified using the L5-1: L5-3 primer pair for the L5.1 fragment and the L5-4: L5-2 primer pair for the L5.2 fragment. Negative controls of uninfected HeLa NCL cells and DEPC treated water were included. The target bands of the expected size, 1,429nt for the L5.1 and 993nt for the L5.2, were detected in both clones R11.1.1 P8 and R3.7.8.3 P3, but not in the negative controls. Direct nucleotide sequencing of the target bands was performed after isolation and purification as described in section 3.5.9.

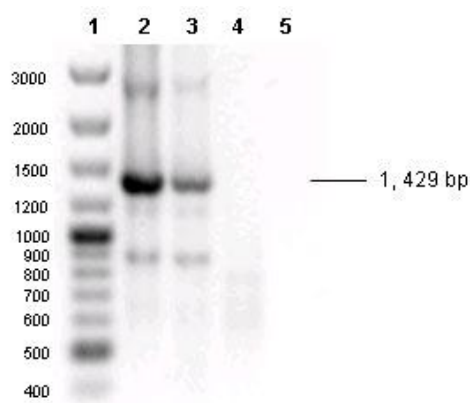


Figure 7.17: RT-PCR amplification of the LF5.1 fragments of clones R11.1.1 P8 and R3.7.8.3 P3 using the L5-1: L5-3 primer pair.

The lanes were loaded as follows; Lane 1: 100bp DNA ladder; Lane 2: R11.1.1 P8; Lane 3: R3.7.8.3 P3; Lane 4: HeLa NCL cells (Negative control) and Lane 5: DEPC treated water (Negative control).

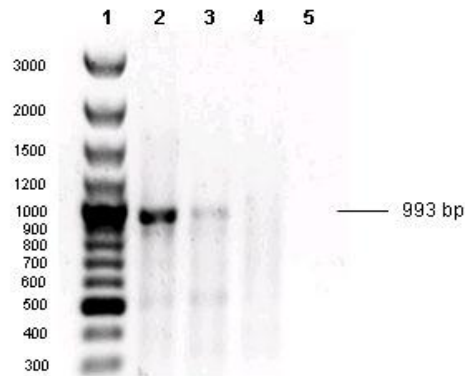


Figure 7.18: RT-PCR amplification of the LF5.2 fragments of clones R11.1.1 P8 and R3.7.8.3 P3 using the L5-2: L5-4 primer pair.

The lanes were loaded as follows; Lane 1: 100bp DNA ladder; Lane 2: R11.1.1 P8; Lane 3: R3.7.8.3 P3; Lane 4: HeLa NCL cells (Negative control) and Lane 5: DEPC treated water (Negative control).

7.12 Sequence comparison of the L gene of resistant and susceptible clones of R17532 and A2 strain

The entire L gene of clone R11.1.1 P8 and R3.7.8.3 P3 was amplified in six overlapping fragments and sequenced in the 5' to 3' direction (antigenome) using the forward primers M2-848, L589, L1116, L3-1, L3-3, L4-1, L5-1, L5-4 and L5-5. In the 3' to 5' direction, the same PCR products were sequenced using the reverse primers L1307, L662, L716, L2337, L3-2, L3-4, L4-2, L5-2, L5-3 and L5-6. These reactions yielded readable sequence in both directions between nt 8,528 and nt 15,108.

In the L coding region, two nucleotide changes were detected between clone R11 and R3 as shown in Appendix Figure 10.27. The first nucleotide change occurred at the nucleotide position 916 that was A in clone R3.7.8.3 P3 and G in clone R11.1.1 P8, leading to an amino acid change from asparagine to aspartic acid at residue 306. The second nucleotide change, T in clone R3.7.8.3 P3 changed to G in clone R11.1.1 P8 occurred at position 6162, resulting in an amino acid change from phenylalanine to leucine at residue 2054. The percentage of amino acid identity between clone R11 and R3 was 99.

A2 has an asparagine at residue 306 and a leucine at residue 2054 and the percentage of amino acid identity between R17532 and A2 was 98 (Table 7.5). There were 28 additional amino acid differences between A2 and R17532. In 3'UTR of the L gene,

there were no nucleotide changes between clone R11.1.1 P8 and R3.7.8.3 P3; but the percentage of nucleotide identity between A2 and R17532 was 91.

Table 7.5: Percentage of nucleotide identity in the L coding sequence and 3'UTR of the L gene of clone R17532 compared to the A2 strain.

Region	NT#	% NT ^a identity R17532 vs. A2	% AA ^b identity R17532 vs. A2
L 5'UTR	1-8	100	N/A
L CDS ^c	1-6,498	97	98
L 3'UTR	1-72	91	N/A

^aNT: Nucleotide; ^bAA: Amino acid; ^cCDS: Coding sequence

7.13 Amplification of the 3' leader, the 5'UTR of the NS1 gene and 5' trailer regions of resistant and susceptible clones of R17532

7.13.1 Genomic RNA circularization

Amplification of the 3' leader, the 5'UTR of the NS1 gene and 5' trailer regions from crude virus lysate

Total RNAs of infected cell lysates of clone R11.1.1 P8 (section 7.2) were circularized using T4 RNA ligase and the junction region including sequences of both the 3' and 5'ends were amplified by RT-PCR as described in section 3.5.4 and Figure 3.1. Negative controls (uninfected HeLa NCL cells and DEPC treated water) were included. The forward Lend primer was used for reverse transcription and the Lend: NS1end primer pair for 1st round PCR (Figure 7.19). The expected size of this PCR product was 642nt, but no band of this size appeared in any sample. Non-specific bands were present possibly resulting from mis-priming of RNA of host cells because they were also detected in uninfected HeLa NCL cell controls (Figure 7.20).

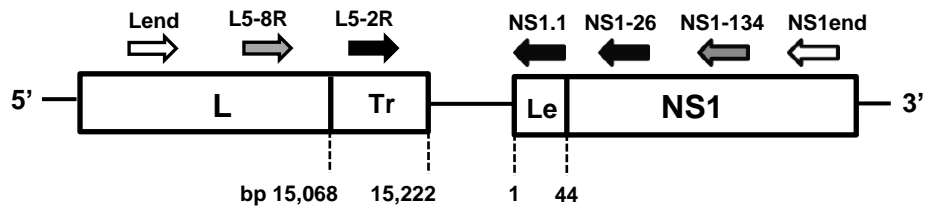


Figure 7.19: Schematic diagram of primers for amplification and sequencing of the genomic RNA ligation.

hRSV genes on the antigenome are depicted as rectangles (not to scale). Primers for the first round PCR amplification are white arrows and for the second round PCR are grey and black arrows. Lend (nt 14812-14825); L5-8R (nt 15017-15041); L5-2R (nt 15130-15153); NS1.1 (nt 44-21); NS1-26 (nt 92-70); NS1-134 (nt 201-178); NS1end (231-212) [Nucleotide numbering is based on the A2 genome, GenBank accession number M74568]. Tr: 5'trailer region; Le: 3'leader region.

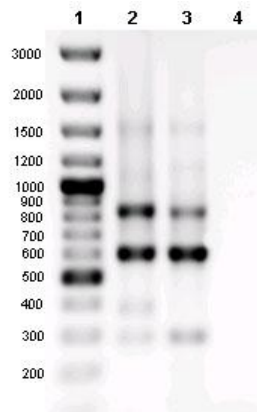


Figure 7.20: First round PCR amplification of the genomic RNA ligation of clones R11.1.1 P8 using the Lend: NS1end primer pair.

The lanes were loaded as follows; Lane 1: 100bp DNA ladder; Lane 2: R11.1.1 P8; Lane 3: HeLa NCL cells (Negative control) and Lane 4: DEPC treated water (Negative control).

The PCR products from the first round PCR were diluted and used as a template for the second round PCR using the L5-8R: NS1-134 primer pair. The expected size of amplicon was 383nt. However, the size of the visible band in clone R11.1.1 P8 (approximately 290nt) was less than size of the expected amplicon (Figure 7.21). The sequence of the 290nt band was analysed using the forward primer L5-8R and the reverse primer NS1-134 in the 5' to 3' and the 3' to 5' directions (antigenome), respectively. Sequence analysis of this band revealed it to be a ligation product between the 5'trailer region from base 15,068 to 15,209 (GenBank accession number M74568) not reaching to the end of genome and the NS1 gene from base 154 to 201, not the 3'leader region (data not shown). These finding suggested that circularization of broken genomes had occurred.

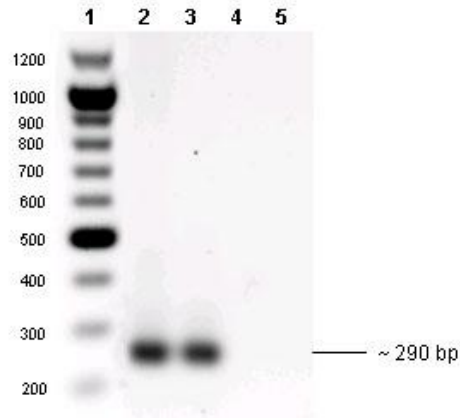


Figure 7.21: Second round PCR amplification of the genomic RNA ligation of clones R11.1.1 P8 using the L5-8R: NS1-134 primer pair.

The lanes were loaded as follows; Lane 1: 100bp DNA ladder; Lane 2: R11.1.1 P8 at dilution 10^{-1} , Lane 3: R11.1.1 P8 at dilution 10^{-2} , Lane 4: HeLa NCL cells (Negative control) and Lane 5: DEPC treated water (Negative control)

An alternative primer pair for the second round PCR L5-2R: NS1-26 was designed in the region close to both 5' and 3' ends to generate an amplicon with the expected size of 185nt. Figure 7.22 shows visible bands were slightly larger than the expected amplicon approximately 200nt in all dilutions of PCR products. The sequence of the 200nt band for clone R11.1.1 P8 was analysed using the forward primer L5-2R in the 5' to 3' direction and the reverse primer NS1-26 in the 3' to 5' direction (antigenome). Sequence analysis of this product revealed mixed sequences of the 5' termini connected with the 3' termini which were uninterpretable (Figure 7.23).

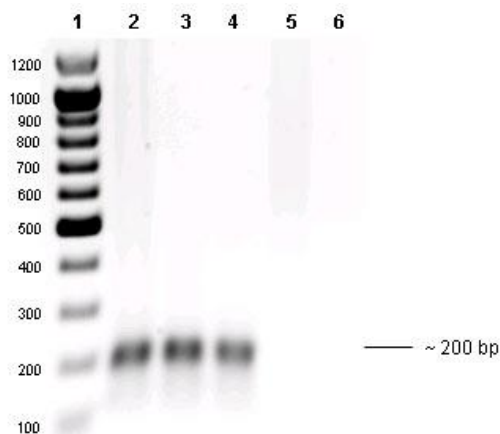


Figure 7.22: Second round PCR amplification of the genomic RNA ligation of clones R11.1.1 P8 using L5-2R: NS1-26 primer pair.

The lanes were loaded as follows; Lane 1: 100bp DNA ladder; Lane 2: R11.1.1 P8 at dilution 10^{-1} , Lane 3: R11.1.1 P8 at dilution 10^{-2} , Lane 4: R11.1.1 P8 at dilution 10^{-3} , Lane 5: HeLa NCL cells (Negative control) and Lane 6: DEPC treated water (Negative control)

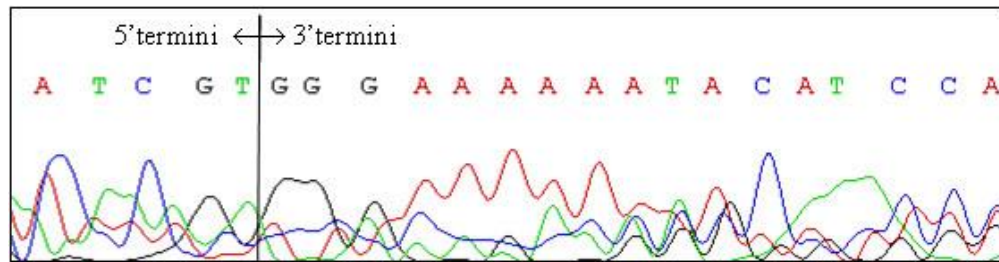


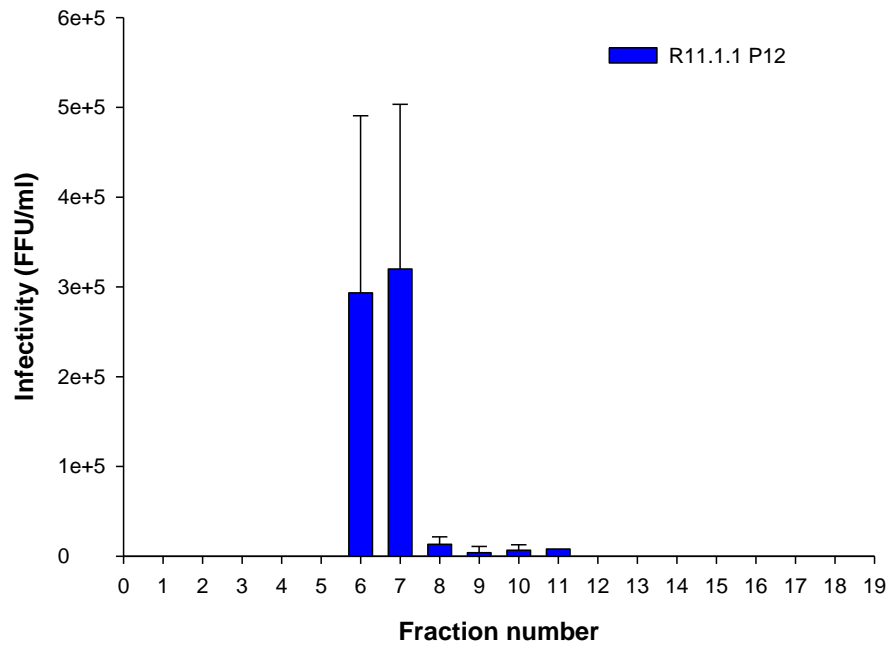
Figure 7.23: Sequence data of 5' and 3' termini of the R11.1.1 P8 genome.

Amplification of the 3' leader, the 5'UTR of the NS1 gene and 5' trailer regions from purified viruses

The above results failed to resolve the sequences of the 3' leader, the 5'UTR of the NS1 gene and 5' trailer regions. Consequently, an attempt was made to improve the quality of the sequences by using purified virus as a source for RNA. Clone R11.1.1 P12 and clone R3.7.8.3 P3 virions were purified by PEG precipitation followed by ultracentrifugation on discontinuous then continuous iodixanol density gradients as described in section 3.4.13. Two continuous gradients were prepared for each clone, fractionated and each fraction assayed for virus infectivity by infection focus assay (section 3.4.6).

In both clones, the density of 1.17 g/ml was the peak of infectivity. However, the infectivity of clone R11.1.1 P12 in gradient 1 and gradient 2 was distributed across fraction 6 – 11 with a density range of 1.14 – 1.23 g/ml and fraction 5 – 7 with a density range of 1.11 – 1.17 g/ml, respectively (Figure 7.24 and Table 7.6). Fraction 6 and 7 of gradient 1 and fraction 6 and 7 of gradient 2 were pooled and the infectivity titre of the pool was 3.4×10^6 . In clone R3.7.8.3 P3, the infectivity was distributed across fraction 6 – 9 in both gradient 1 and gradient 2 with a density range between 1.13 – 1.18 for gradient 1 and 1.14 – 1.18 for gradient 2 (Figure 7.25 and Table 7.6). Fraction 7 and 8 of gradient 1 and fraction 7 of gradient 2 were pooled to give a pool of infectivity 3.0×10^6 .

R11P12 Gradient 1



R11P12 Gradient 2

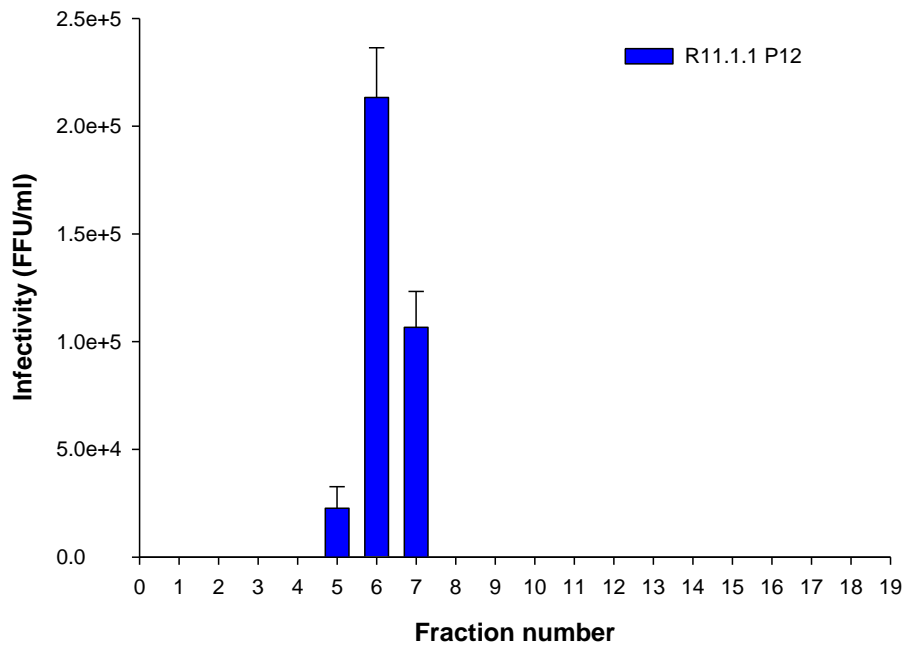
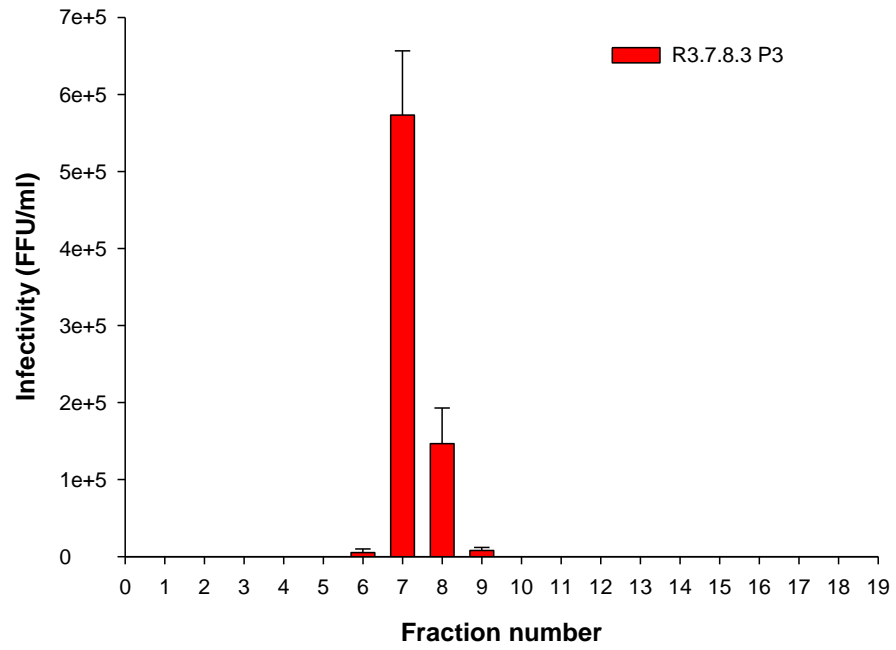


Figure 7.24: The recovery rate and distribution of clone R11.1.1 P12 infectivity across continuous iodixanol density gradient 1 and 2.

Bars were prepared from triplicate values and error bars represent the standard deviation.

R3.7.8.3 P3 Gradient 1



R3.7.8.3 P3 Gradient 2

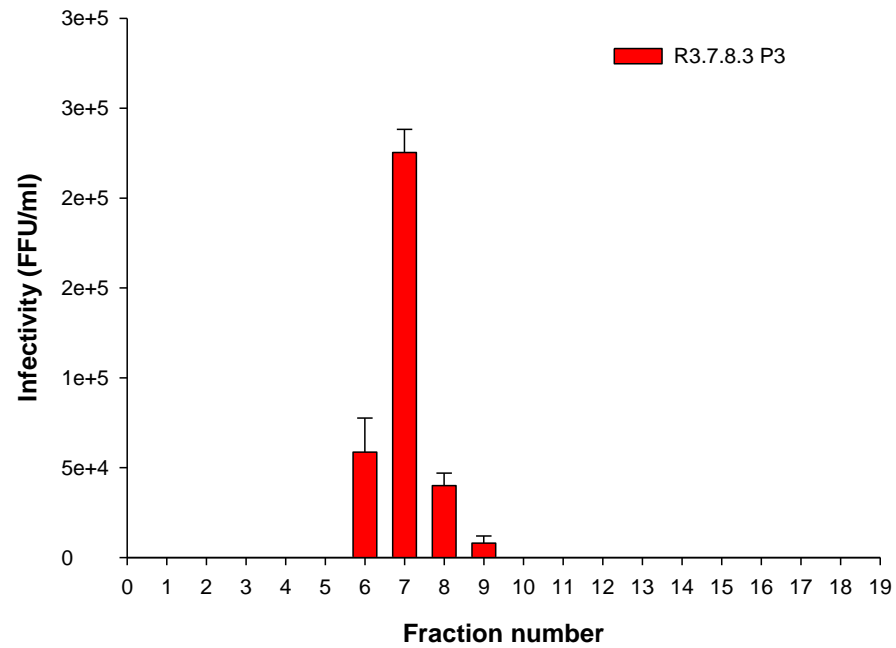


Figure 7.25: The recovery rate and distribution of clone R3.7.8.3 P3 infectivity across continuous iodixanol density gradient 1 and 2.

Bars were prepared from triplicate values and error bars represent the standard deviation.

Table 7.6: Summary of densities and viral titres of purified clones R11.1.1 P12 and R3.7.8.3 P3 in continuous iodixanol gradient 1 and 2.

Virus	Fraction	Gradient 1			Gradient 2		
		Density (g/ml)	Titre (FFU/ml)	Standard deviation	Density (g/ml)	Titre (FFU/ml)	Standard deviation
R11.1.1 P12	5	N/A	-	-	1.11	2.27×10^4	1.07×10^4
	6	1.14	2.93×10^5	1.97×10^5	1.15	2.13×10^5	2.31×10^4
	7	1.17	3.20×10^5	1.83×10^5	1.17	1.07×10^5	1.67×10^4
	8	1.18	1.33×10^4	8.33×10^3	N/A	-	-
	9	1.20	4.00×10^3	6.93×10^3	N/A	-	-
	10	1.20	6.67×10^3	6.11×10^3	N/A	-	-
	11	1.23	8.00×10^3	0	N/A	-	-
R3.7.8.3 P3	6	1.13	5.33×10^3	4.62×10^3	1.14	5.87×10^4	1.89×10^4
	7	1.17	5.73×10^5	8.34×10^4	1.17	2.25×10^5	1.29×10^4
	8	1.17	1.47×10^5	4.62×10^4	1.18	4.00×10^4	6.93×10^3
	9	1.18	8.00×10^3	4.00×10^3	1.18	8.00×10^3	4.00×10^3

The neutralization phenotype of each pool was determined by immunoperoxidase focus reduction neutralization assay against PZ. The purified clone R11.1.1 P12 was found susceptible to neutralization by PZ with an EC_{50} of 10.23. Purified clone R3.7.8.3 P3 was relatively resistant with an $EC_{50} > 125 \mu\text{g/ml}$ (Figure 7.26). Two-way ANOVA analysis showed the two clones to be significantly different ($P < 0.0001$).

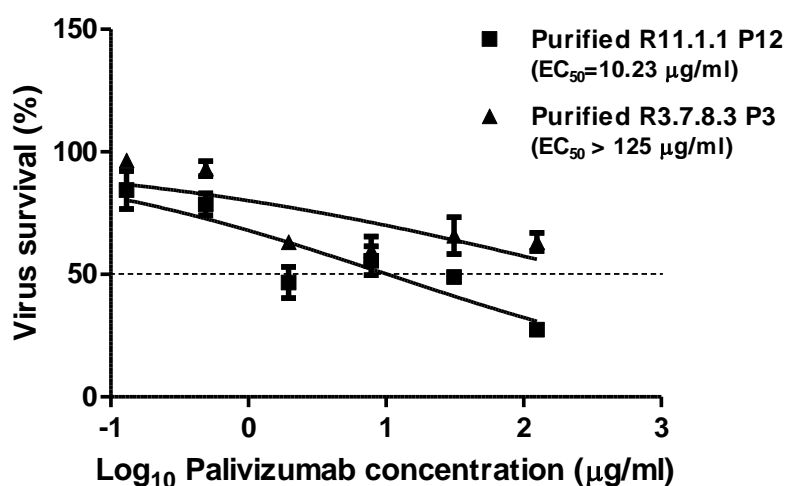


Figure 7.26: The percentage virus survival of purified R11.1.1 P12 and R3.7.8.3 P3 after neutralization with PZ.

Plots were prepared from triplicate values and error bars show the standard error. The 50% reduction level is indicated by (...).

RNA was extracted from purified clones R11.1.1 P12 and R3.7.8.3 P3 as described in section 3.5.1. The RNA genomes of both clones were circularized by T4 RNA ligase (section 3.5.4). First and second round PCR were carried out using the Lend: NS1end and L5-2R: NS1-26 primer pairs (Figure 7.19), respectively. The expected size of the product from the first round was 642nt. Non-specific bands were detected in the first round PCR of both purified clones R11.1.1 P12 and R3.7.8.3 P3 (Figure 7.27 and 7.28, respectively). In the second round, there were no non-specific bands, but the size of the visible bands for the two clones (approximately 210nt) was somewhat larger than the 185nt band expected (Figure 7.29 and 7.30).

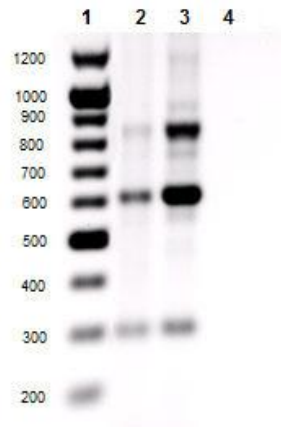


Figure 7.27: First round PCR amplification of the genomic RNA ligation of purified R11.1.1 P12 using the Lend: NS1end primer pair.

The lanes were loaded as follows; Lane 1: 100bp DNA ladder; Lane 2: purified R11.1.1 P12; Lane 3: HeLa NCL cells (Negative control) and Lane 4: DEPC treated water (Negative control).

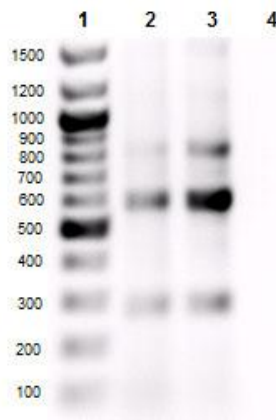


Figure 7.28: First round PCR amplification of the genomic RNA ligation of purified R3.7.8.3 P3 using the Lend: NS1end primer pair.

The lanes were loaded as follows; Lane 1: 100bp DNA ladder; Lane 2: purified R3.7.8.3 P3; Lane 3: HeLa NCL cells (Negative control) and Lane 4: DEPC treated water (Negative control)



Figure 7.29: Second round PCR amplification of the genomic RNA ligation of purified R11.1.1 P12 using the L5-2R: NS1-26 primer pair.

The lanes were loaded as follows; Lane 1: 100bp DNA ladder; Lane 2, 3 and 4: purified R11.1.1 P12 at dilution 10^{-1} , 10^{-3} and 10^{-5} . Lane 5: HeLa NCL cells (Negative control) and Lane 6: DEPC treated water (Negative control).

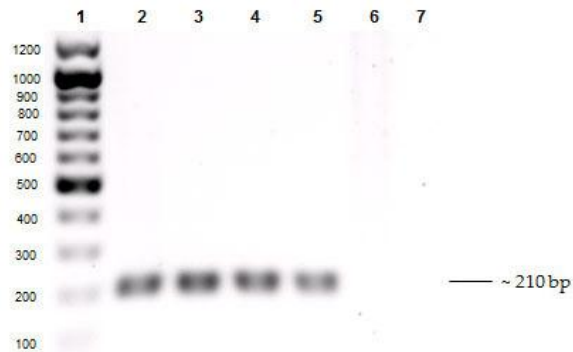


Figure 7.30: Second round PCR amplification of the genomic RNA ligation of purified R3.7.8.3 P3 using the L5-2R: NS1-26 primer pair.

The lanes were loaded as follows; Lane 1: 100bp DNA ladder; Lane 2, 3, 4 and 5: purified R3.7.8.3 P3 at neat, dilution 10^{-1} , 10^{-2} and 10^{-3} . Lane 6: HeLa NCL cells (Negative control) and Lane 7: DEPC treated water (Negative control)

The 210nt target for purified clone R11.1.1 P12 was sequenced in the 5' to 3' direction (antigenome) using the forward primer L5-2R and in the 3' to 5' direction using the reverse primer NS1-26. The sequence analysis for this region yielded clear sequences of the 5' and 3' ends, from nt 15,171 to nt 15,222 and from nt 1 to nt 92 respectively, when compared to the published genome end sequence for the A2 strain (GenBank accession number M74568); however, two base insertions of thymine were present at the junction of the two ends (Figure 7.31A). To confirm these insertions, the genomic RNA circularization and RT-PCR were repeated using the same RNA of purified R11.1.1 P12 and the same primer pairs. No insertions were detected in the sequence

analysis of the repeated PCR product, but the first position of 3' end showed multiple peaks of A, C and G bases, with G the largest chromatogram (Figure 7.31B).

Alternative reverse primer (NS1.1 primer) was chosen to replace the NS1-26 primer in the second round PCR. The expected size of amplicon of this reaction was 137nt. Dilution of the first round product from above (Figure 7.27) was reamplified with these primers and a band of this size was observed in undiluted PCR products (Figure 7.32). The 137nt band of purified clone R11.1.1 P12 was sequenced using the forward primer L5-2R and the reverse primer NS1.1 in the 5' to 3' and 3' to 5' directions, respectively. The sequence analysis of this band still gave multiple peaks at the beginning of 3' end (Figure 7.33)

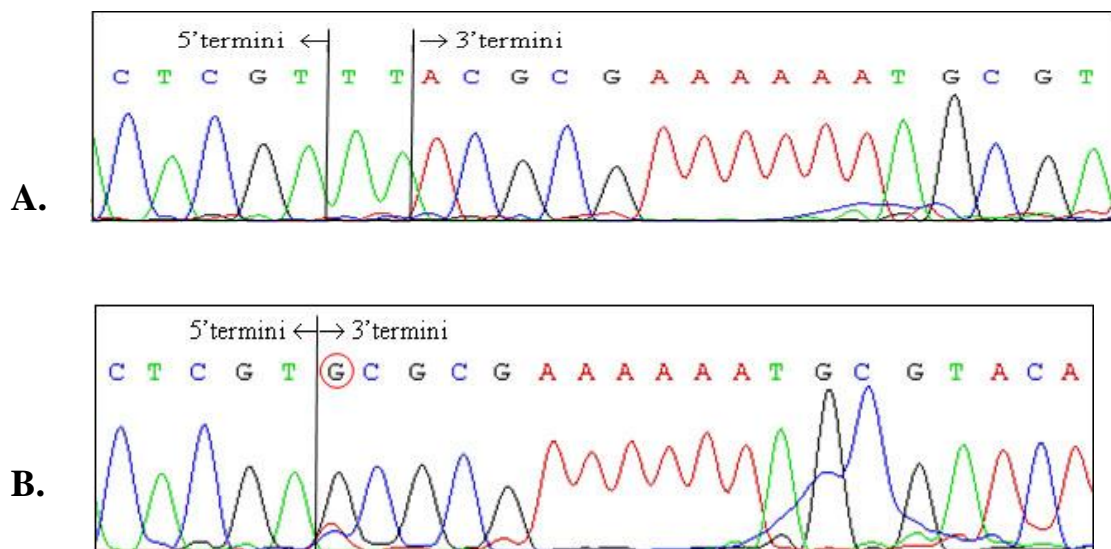


Figure 7.31: Sequence data of 5' and 3' termini of purified R11.1.1 P12 genome.

Panel A: chromatogram showing two nucleotides insertion between 5' and 3' end of genome. Panel B: chromatogram of repeated sequencing showing multiple peaks (red circle) in the beginning of 3' end genome and no insertion.

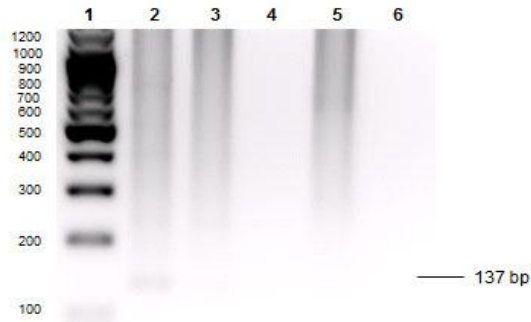


Figure 7.32: Second round PCR amplification of the genomic RNA ligation of purified R11.1.1 P12 using the L5-2R: NS1.1 primer pair.

The lanes were loaded as follows; Lane 1: 100bp DNA ladder; Lane 2, 3 and 4: purified R11.1.1 P12 at neat, dilution 10^{-1} and dilution 10^{-2} . Lane 5: HeLa NCL cells (Negative control) and Lane 6: DEPC treated water (Negative control)

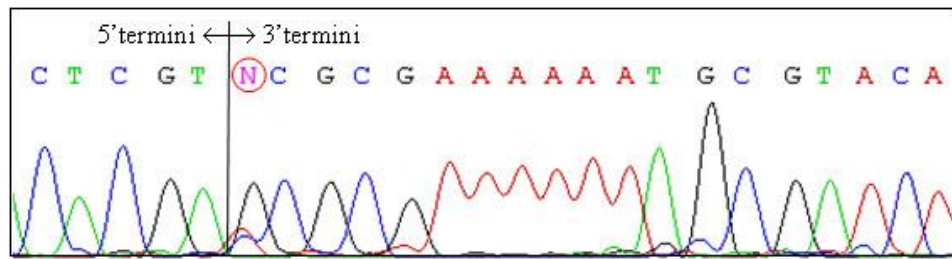


Figure 7.33: Sequence data of 5' and 3' termini of purified R11.1.1 P12 genome using the L5-2R: NS1.1 primer pair. The red circle shows multiple peaks at the beginning of 3' end genome.

For purified clone R3.7.8.3 P3, the sequence analysis of the 210nt product from Figure 7.30 using the forward primer L5-2R in the 5' to 3' direction and the reverse primer NS1-26 in the 3' to 5' direction revealed the L gene sequence directly connected to the N gene, not to the NS1 gene (data not shown). The sequence of the L gene also did not reach to the expected end of 5' trailer region. This suggests that RNA generated from purified clone R3.7.8.3 P3 may have insufficient or poor quality. It was concluded that circularization of genomic RNA was unlikely to yield interpretable sequences for the ends of the genomic.

7.13.2 Rapid amplification of cDNA ends (RACE)

5'RACE

A circularization of the genome proved unsuccessful, the sequence of the 5' end of susceptible and resistant clones was sought using 5'RACE as described in section 3.5.5 and Figure 3.2. RNA isolated from purified clone R11.1.1 P12 (PZ EC₅₀ = 10.23 µg/ml) was used to optimize the technique. After reverse transcription using the L5-8R primer, cDNA was ligated with the adaptor DT88 and amplified using the L5-8R: DT89 primer pair for a first round PCR and the L5-2R: DT89 primer pair for a hemi-nested second round PCR. Adaptor-ligated uninfected HeLa NCL cells cDNA, unligated purified clone R11.1.1 P12 cDNA, unligated HeLa NCL cells cDNA and DEPC treated water were amplified with the same primers as negative controls. The expected sizes of amplicons for the first and second round PCR were 233nt and 120nt, respectively.

Target bands were not visible in any sample after the first round PCR Figure 7.34. Hemi-nested second round PCR was carried out with several dilutions of PCR products from the first round. In the adaptor-ligated clone R11.1.1 P12 reactions only, there were visible bands with the expected size of 120nt. No band of this size was detected in negative control lanes, although multiple bands of non-specific products were observed in all samples (Figure 7.35).

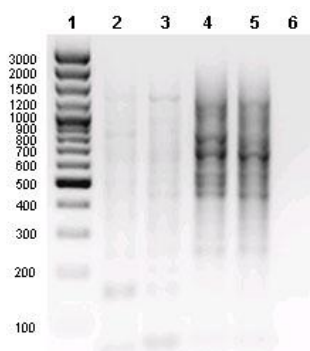


Figure 7.34: First round PCR amplification of adaptor-ligated cDNA of purified R11.1.1 P12 using the L5-8R: DT89 primer pair.

The lanes were loaded as follows; Lane 1: 100bp DNA ladder; Lane 2: adaptor-ligated and purified R11.1.1 P12; Lane 3: adaptor-ligated HeLa NCL cells (Negative control), Lane 4: unligated and purified R11.1.1 P12 (Negative control for ligation), Lane 5: unligated HeLa NCL cells (Negative control for ligation), Lane 6: DEPC treated water (Negative control for PCR)

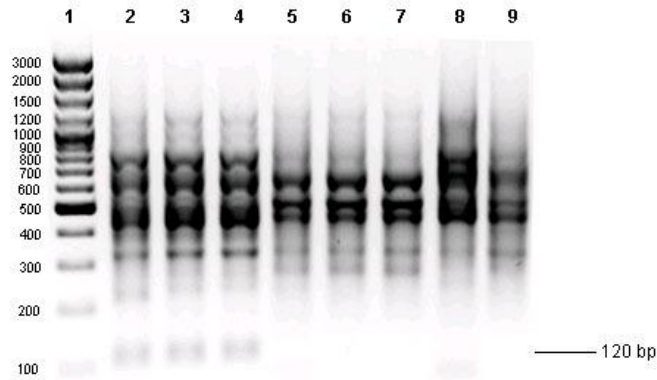


Figure 7.35: Hemi-nested second round PCR amplification of purified R11.1.1 P12 using the L5-2R: DT89 primer pair.

The lanes were loaded as follows; Lane 1: 100bp DNA ladder; Lane 2, 3 and 4: adaptor-ligated and purified R11.1.1 P12 at neat, dilution 10^{-1} and dilution 10^{-2} , respectively. Lane 5, 6 and 7: adaptor-ligated HeLa NCL cells (Negative control) at neat, dilution 10^{-1} and dilution 10^{-2} , respectively. Lane 8: unligated purified R11.1.1 P12 (Negative control for ligation), Lane 9: unligated HeLa NCL cells (Negative control for ligation).

The magnesium concentration in the second round was optimized and 7.5 mM $MgCl_2$ resulted in the most intense band of 120nt (Figure 7.36); however, the target band produced was inadequate for sequencing following purification. Therefore, the hemi-nested second round PCR product isolated from an agarose gel was reamplified with the same primers producing sufficient cDNA for direct sequencing (Figure 7.37).

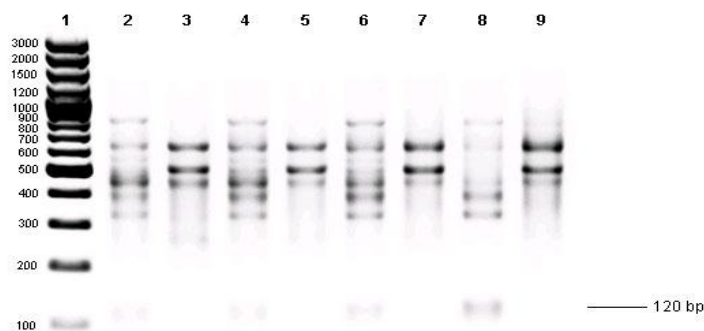


Figure 7.36: Optimization of magnesium concentration for the hemi-nested second round PCR amplification of purified R11.1.1 P12 using the L5-2R: DT89 primer pair.

The lanes were loaded as follows; Lane 1: 100bp DNA ladder; Lane 2, 4, 6 and 8: adaptor-ligated and purified R11.1.1 P12 in PCR reaction with 2.5, 3.5, 5.0 and 7.5 mM $MgCl_2$, respectively. Lane 3, 5, 7 and 9: adaptor-ligated HeLa in PCR reaction with 2.5, 3.5, 5.0 and 7.5 mM $MgCl_2$, respectively.

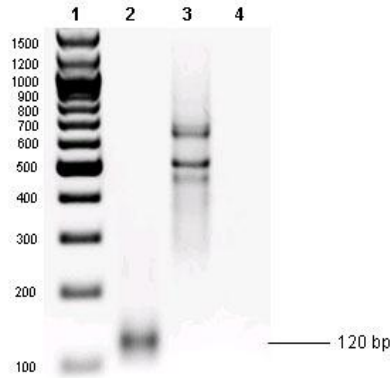


Figure 7.37: Re-amplification of the hemi-nested second round PCR products of purified R11.1.1 P12 using the L5-2R: DT89 primer pair.

The lanes were loaded as follows; Lane 1: 100bp DNA ladder; Lane 2: adaptor-ligated and purified R11.1.1 P12; Lane 3: unligated HeLa NCL cells (Negative control) and Lane 4: DEPC treated water (Negative control)

For the resistant clone 3.7.8.3 P3 (PZ $EC_{50} = 48.46 \mu\text{g/ml}$), 5'RACE was performed using the same condition as for purified R11.1.1 P12, but using RNA from unpurified virus infected cell lysate due to insufficient or poor quality of RNA from purified virus (section 7.13.1). Bands corresponding to the expected size of 233nt and 120nt were detected in the first round and second round PCR, respectively (Figure 7.38 and 7.39). Moreover, the PCR product of clone R3.7.8.3 P3 in the hemi-nested second round PCR was adequate for direct sequencing, thus the re-amplification of this product was not required.

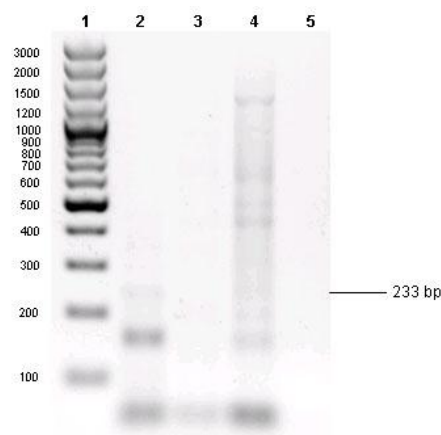


Figure 7.38: First round PCR amplification of adaptor-ligated cDNA of clone R3.7.8.3 P3 using the L5-8R: DT89 primer pair.

The lanes were loaded as follows; Lane 1: 100bp DNA ladder; Lane 2: adaptor-ligated R3.7.8.3 P3; Lane 3: unligated R3.7.8.3 P3 (Negative control for ligation), Lane 4: unligated HeLa NCL cells (Negative control), Lane 5: DEPC treated water (Negative control).

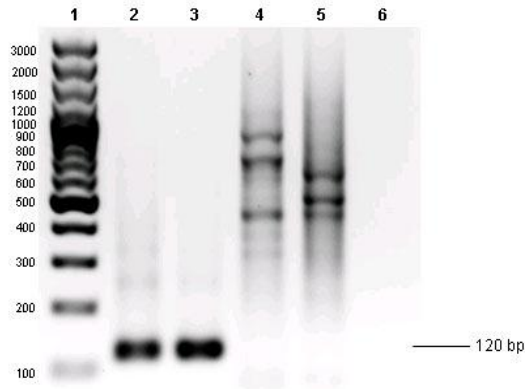


Figure 7.39: Hemi-nested second round PCR amplification of clone R3.7.8.3 P3 using the L5-2R: DT89 primer pair.

The lanes were loaded as follows; Lane 1: 100bp DNA ladder; Lane 2 and 3: adaptor-ligated R3.7.8.3 P3 at dilution 10^{-1} and dilution 10^{-2} , respectively. Lane 4: unligated R3.7.8.3 P3 (Negative control for ligation), Lane 5: unligated HeLa NCL cells (Negative control), Lane 6: DEPC treated water (Negative control).

The 120nt target band for purified clone R11.1.1 P12 and clone R3.7.8.3 P3 was sequenced using the forward primer L5-2R in the 5' to 3' direction (antigenome). The sequence analysis of the two clones showed the clear sequence of 5' termini from nt 15,176 to nt 15,222 linked with the adaptor DT88 sequence. The sequence chromatogram for clone R3.7.8.3 P3 is only present on Figure 7.40.

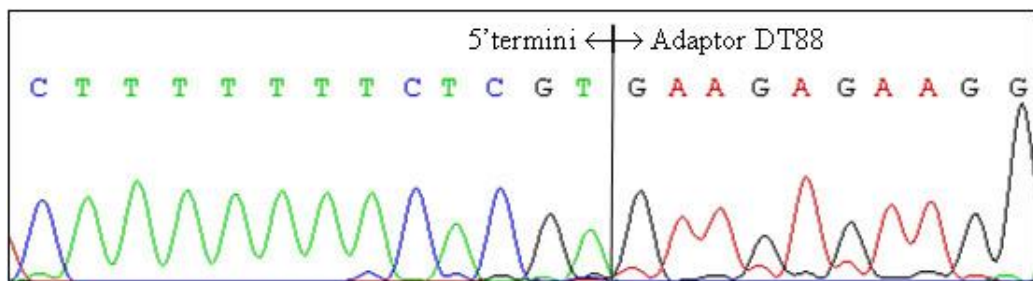


Figure 7.40: Sequence data of 5' trailer region of clone R3.7.8.3 P3 genome ligated with the adaptor DT88.

For clone R11.1.1 P8, the sequence of the L gene to base 15,108 was determined in section 7.12 and from base 15,109 to 15,209 in section 7.13.1 (genome circularization of unpurified virus using the sequencing primers L5-8R and NS1-134). The remaining sequence to base 15,222 was obtained from purified clone R11.1.1 P12 using genome circularization (section 7.13.1), albeit with an apparent insertion of two bases between the 5' and 3' ends of the genome. Following the current experiment, sequence for bases 15,176 and 15,222 has been determined confirming the terminal sequence obtained by

genome circularization, but demonstrating the absence of additional thymine residues on the 5' end. For clone R3.7.8.3 P3 only the sequence to base 15,108 had previously been determined (section 7.12). The current experiment provides sequence from base 15,176 to the end of the genome. Thus, the bases between 15,109 and 15,175 remain unknown. In order to sequence this region, RNA from unpurified virus infected cell lysate of clone R3.7.8.3 P3 was reverse transcribed using the L5-1 primer and PCR reactions were performed using the L5-8R: L5-9 primer pair (Figure 7.12). The expected size of 206nt was detected in clone R3.7.8.3 P3 (Figure 7.41). It was isolated, purified as described in section 3.5.9 and sequenced using the forward primer L5-8R and the reverse primer L5-9 in the 5' to 3' and 3' to 5' directions, respectively. Sequence readable in both directions was obtained from nt 15,018 to 15,221.

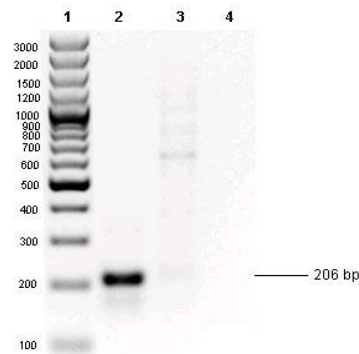


Figure 7.41: RT-PCR amplification of the L gene of R3.7.8.3 P3 using the L5-8R: L5-9 primer pair. The lanes were loaded as follows; Lane 1: 100bp DNA ladder; Lane 2: R3.7.8.3P3; Lane 3: HeLa NCL cells (Negative control) and Lane 4: DEPC treated water (Negative control).

Comparison of the sequence between clones R11.1.1 and R3.7.8.3 revealed no nucleotide change in the 5' trailer region (Appendix Figure 10.29). However, the nucleotide sequence of the A2 for this region differed from those of the R17532 and the percentage of nucleotide identity in each region are presented in Table 7.7. The length of the 5' trailer region in the A2 was shorter than in the R17532 by five bases.

3'RACE from the hRSV anti-genome

The sequence of 3' leader region (nt 1 to nt 44) and the 5'UTR of the NS1 gene (nt 45 to nt 98) in susceptible and resistant clones was determined using 3'RACE from the hRSV anti-genome (section 3.5.6 and Figure 3.3). The anti-genomic RNA from lysates of cells infected with parental clone R3.7.8 (PZ EC₅₀ > 125µg/ml) and clone R11.1.1 P11

(PZ EC₅₀ = 7.45µg/ml) was reverse transcribed using the NS206 primer, ligated with the adaptor DT88 by T4 RNA ligase and amplified using the NS1-206: modified DT89 primer pair for a first round PCR and the NS1-103: modified DT89 primer pair for a hemi-nested second round PCR. The expected sizes of target bands for the first and second round PCR were 297nt and 197nt, respectively. Adaptor-ligated uninfected HeLa NCL cells cDNA, unligated parental clone R3.7.8 cDNA, unligated clone R11.1.1 P11 cDNA, unligated HeLa NCL cells cDNA and DEPC treated water were amplified as negative controls.

In the first round PCR, bands of the expected size were not observed in any sample (Figure 7.42). Visible bands of approximately 150nt were detected in adaptor-ligated parental clone R3.7.8 and clone R11.1.1 P11 PCR products from the hemi-nested second round reaction (Figure 7.43), whereas the expected size for this reaction was 197nt. The sequence of the 150nt band for the two clones was analysed using the reverse primer NS1-103 in the 3'to 5'direction (antigenome). Sequence analysis of this band revealed a sequence from the NS1 gene start signal linked directly with the adaptor DT88 sequences in which 44nt of the 3'leader region was missing and a single A residue was inserted between the adaptor DT88 and the NS1 gene (Figure 7.44).

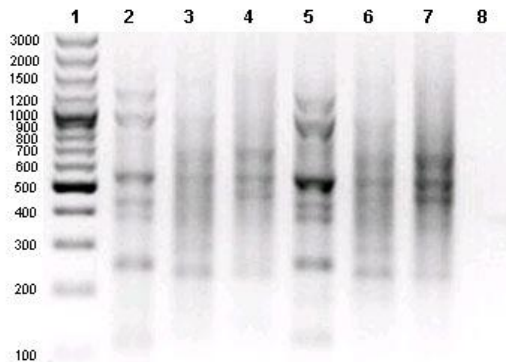


Figure 7.42: First round PCR amplification of adaptor-ligated cDNA of parental clone R3.7.8 and clone R11.1.1 P11 using the NS1-206: modified DT89 primer pair.

The lanes were loaded as follows; Lane 1: 100bp DNA ladder; Lane 2, 3 and 4: adaptor-ligated R3.7.8, R11.1.1 P11 and HeLa NCL cells, respectively. Lane 5, 6 and 7: unligated R3.7.8, R11.1.1 P11 and HeLa NCL cells (Negative control for ligation), respectively. Lane 8: DEPC treated water (Negative control).

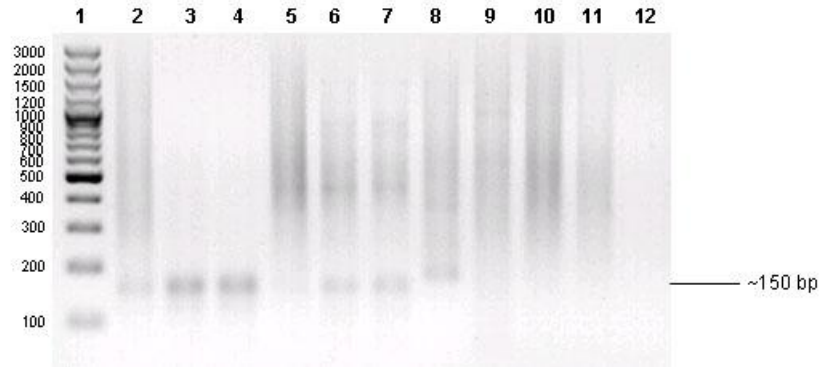


Figure 7.43: Hemi-nested second round PCR amplification of parental clone R3.7.8 and clone R11.1.1 P11 using the NS1-103: modified DT89 primer pair.

The lanes were loaded as follows; Lane 1: 100bp DNA ladder; Lane 2, 3 and 4: adaptor-ligated R3.7.8 at neat, dilution 10^{-1} and 10^{-2} , respectively. Lane 5, 6 and 7: adaptor-ligated R11.1.1 P11 at neat, dilution 10^{-1} and 10^{-2} , respectively. Lane 8: adaptor-ligated HeLa NCL cells (Negative control for ligation). Lane 9, 10 and 11: unligated R3.7.8, R11.1.1 P11 and HeLa NCL cells (Negative control for ligation), respectively. Lane 12: DEPC treated water (Negative control).

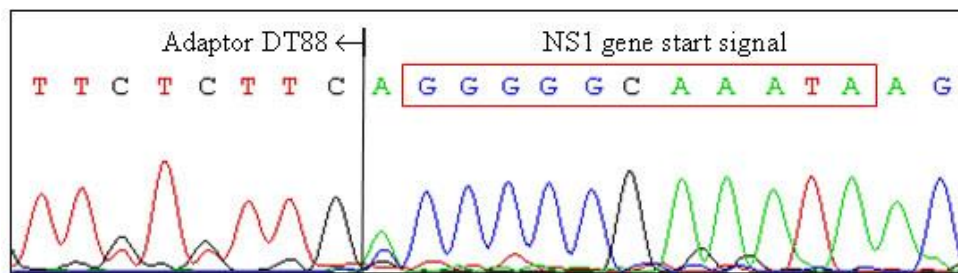


Figure 7.44: Sequence data of the NS1 gene start of clone R11.1.1 P11 ligated with the adaptor DT88.

3'RACE from the hRSV genome

In the previous experiment, sequencing in the 3' leader region and the 5'UTR of the NS1 gene from cDNA generated from the antigenome was unsuccessful. An alternative was to apply the 3'RACE method directly to the RNA genome (section 3.5.7 and Figure 3.4). Adaptor DT88 was ligated to the 3' end of RNA extracted from parental clone R3.7.8 (PZ $EC_{50} > 125\mu\text{g/ml}$) and clone R11.1.1 P11 (PZ $EC_{50} = 7.45\mu\text{g/ml}$). After cDNA synthesis using the DT89 primer, first round and hemi-nested second round PCR were performed using the modified DT89: NS1-206 and the modified DT89: NS1-103 primer pairs, respectively. The target band of the first round PCR had the expected size of 297nt, whilst the expected size of the target band of the hemi-nested second round PCR was 197nt. Adaptor-ligated uninfected HeLa NCL cells RNA, unligated clone R11.1.1 P11 RNA, unligated HeLa NCL cells RNA and DEPC treated water were used as negative controls.

The product of the first round PCR product of the adaptor-ligated R11.1.1 P11 was approximately 240nt which was smaller than expected (Figure 7.45). Nevertheless, target bands of 197nt were observed as expected in the second round PCR of this sample. No bands of this size were present any of the negative controls (Figure 7.46). Re-amplification of the hemi-nested second round PCR was required to increase the intensity of the target band (197nt band) for direct nucleotide sequencing (Figure 7.47).

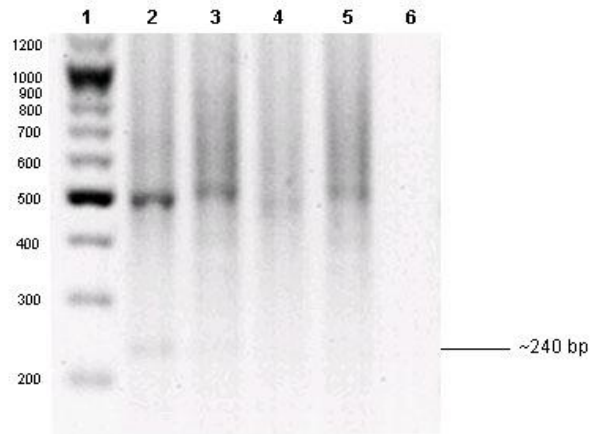


Figure 7.45: First round PCR amplification of adaptor-ligated genomic RNA of clone R11.1.1 P11 using the modified DT89: NS1-206 primer pair.

The lanes were loaded as follows; Lane 1: 100bp DNA ladder; Lane 2: adaptor-ligated R11.1.1 P11; Lane 3: HeLa NCL cells (Negative control); Lane 4 and 5: unligated R11.1.1 P11 and HeLa NCL cells (Negative control for ligation); Lane 6: DEPC treated water (Negative control).

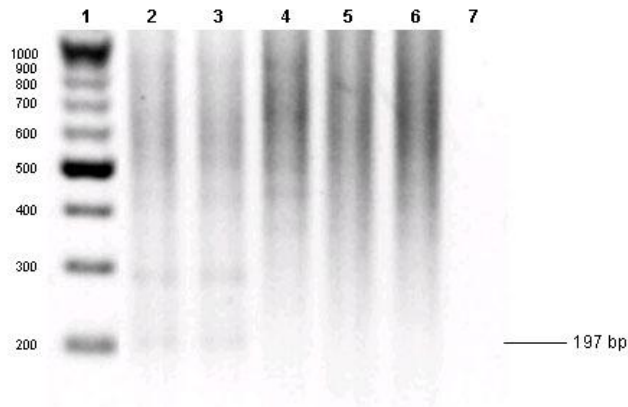


Figure 7.46: Hemi-nested second round PCR amplification of clone R11.1.1 P11 using the modified DT89: NS1-103 primer pair.

The lanes were loaded as follows; Lane 1: 100bp DNA ladder; Lane 2 and 3: adaptor-ligated R11.1.1 P11 at dilution 10^{-1} and 10^{-2} , respectively. Lane 4: HeLa NCL cells (Negative control); Lane 5 and 6: unligated R11.1.1 P11 and HeLa NCL cells (Negative control for ligation), respectively. Lane 7: DEPC treated water (Negative control).

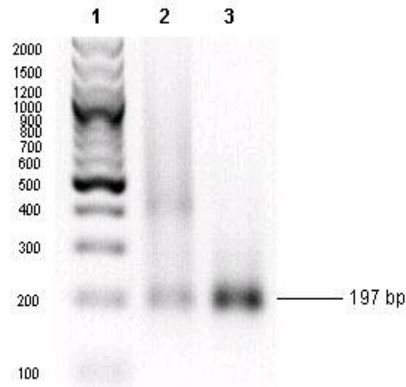


Figure 7.47: Re-amplification of the hemi-nested second round PCR of clone R11.1.1 P11 using the modified DT89: NS1-103 primer pair.

The lanes were loaded as follows; Lane 1: 100nt DNA ladder; Lane 2 and 3: adaptor-ligated R11.1.1 P11 at neat and dilution 10^{-2} , respectively.

The 3' end genome of parental clone R3.7.8 was amplified by the same method and the expected sizes of 297nt and 197nt were detected in the first and second round PCR, respectively (Figure 7.48 and 7.49). The second round PCR products of both clone R11.1.1 P11 and parental clone R3.7.8 were isolated, purified as described in section 3.5.9 and sequenced using the reverse primer NS103 in the 3' to 5' direction (antigenome). For both clones of sequence analysis, these target bands showed the 3' end sequence directly connected with the adaptor DT88. The sequence chromatogram for parental clone R3.7.8 is only present in Figure 7.50. Readable sequence was obtained from nt 1 to 113 which was numbered according to the hRSV A2 genome (GenBank accession number M74568). There were no thymidine additions to the 3' end of the either genome suggesting that the presence of two additional thymidines present in the circularization R11.1.1 P12 amplicand were artefactual.

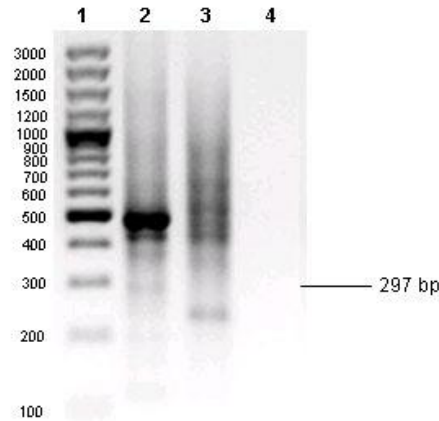


Figure 7.48: First round PCR amplification of adaptor-ligated genomic RNA of parental clone R3.7.8 using the modified DT89: NS1-206 primer pair.

The lanes were loaded as follows; Lane 1: 100bp DNA ladder; Lane 2: adaptor-ligated R3.7.8; Lane 3: unligated HeLa NCL cells (Negative control); Lane 4: DEPC treated water (Negative control).

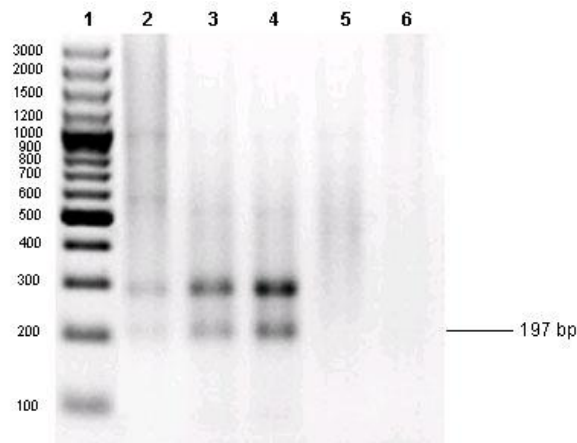


Figure 7.49: Reamplification by hemi-nested second round PCR of parental clone R3.7.8 using the modified DT89: NS1-103 primer pair.

The lanes were loaded as follows; Lane 1: 100bp DNA ladder; Lane 2, 3 and 4: adaptor-ligated R3.7.8 at neat, dilution 10^{-1} and 10^{-2} , respectively. Lane 5: unligated HeLa NCL cells (Negative control); Lane 12: DEPC treated water (Negative control).

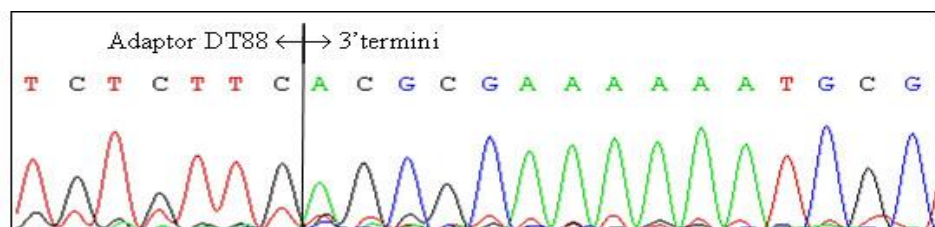


Figure 7.50: Sequence data of 3' leader region of parental clone R3.7.8 genome ligated with the adaptor DT88.

Comparison of the 3' leader region and the 5'UTR of the NS1 gene between the two clones, R11.1.1 P11 and parental clone R3.7.8, revealed no nucleotide differences. The R17532 genome differed somewhat from the A2 in their region (Table 7.7).

Table 7.7: Percentage of nucleotide identity in the 3' leader region, 5'UTR of the NS1 gene and 5' trailer region of clone R17532 compared to the A2 strain.

Region	NT#	% NT ^a identity R17532 vs. A2
3' leader region	1-44	97
NS1 5'UTR	45-98	96
5' trailer region	1-160	88

^aNT: Nucleotide

The whole genome of R3.7.8.3 P3 (PZ EC₅₀ = 48.46 µg/ml) has been sequenced in both direction apart from the ends, bases 1 to 44 at the 3' end obtained from parental clone R3.7.8 (PZ EC₅₀ > 125 µg/ml) and bases 15,068 to 15,222 at the 5' end from clone R3.7.8.3 P3 for which only one direction was achieved. For clone R11 base 1 to 113 has been sequenced from clone R11.1.1 P11 (PZ EC₅₀ = 7.45 µg/ml), base 114 - 4,695 from R11.1.1 P8 (PZ EC₅₀ = 0.39 µg/ml), base 4,696 - 15,175 from R11.1.1 P8 and base 15,176 - 15,222 from purified clone R11.1.1 P12 (PZ EC₅₀ = 10.23 µg/ml). Again only the ends (nt 1 – 113 of 3' end and 15,176 – 15,222 of 5' end) have not been sequenced in both directions. In the regions of the genome encoding non-membrane protein genes – from the 3' end to the SH GS sequence and from the F GE sequence to the 5' end – only two differences between R3 and R11 were apparent at positions 916 and 6162 in the L gene.

7.14 Identification of the L gene mutation on the resistant and susceptible clones of different high- and low-passage of R17532 clones

Comparison of the non-membrane protein genes between neutralization resistant and susceptible clone of R17532 revealed two mutations at position 916 and 6162 in the L gene. To confirm whether those mutations were correlated with the conversion of neutralization resistant phenotype to susceptible phenotypes, ten clones of R17532

previously determined the neutralization phenotype as described in section 6.7.1 analysed for these changes in the L gene.

7.14.1 Sequence analysis of the L gene at position 916 in clone R11.2

In susceptible clone R11.1.1 P8, the base G was observed at position 916 in the L gene, whereas it was A in resistant clone R3.7.8.3 P3 (Appendix Figure 10.27). However, the base A was also found in the A2 which is susceptible to neutralization by PZ. To investigate whether the base G was characteristic of susceptible strains of R17532, the L gene of another susceptible clone (R11.2) generated from the same stock as clone R11.1.1 was amplified and sequenced at position 916 located in the LF1 fragment.

The PCR reaction of this fragment was performed using the M2-848: L1307 primer pair and a band of the expected PCR product, 1,372nt, was detected (Figure 7.51). The target band was isolated, purified and direct sequenced as described in section 3.5.9. The sequence of the L gene at position 916 in clone R11.2 was the same as the sequence of R3.7.8.3 and A2 strain. Hence, the nucleotide change at this position was not associated with the shift from susceptible to resistant phenotype.

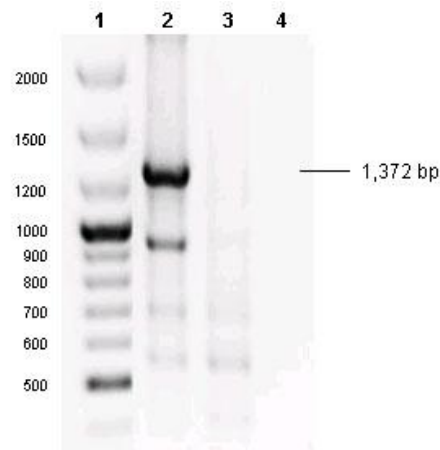


Figure 7.51: RT-PCR amplification of the L gene of clones R11.2 using the M2_848: L1307 primer pair.

The lanes were loaded as follows; Lane 1: 100bp DNA ladder; Lane 2: R11.2; Lane 3: HeLa NCL cells (Negative control) and Lane 4: DEPC treated water (Negative control).

7.14.2 Sequence analysis of the L gene at position 6162 in different clones of R17532

Sequence of L gene position 6162 in neutralization resistant clones of strain R17532 serially passaged until susceptible to neutralization

After passaging from level 3 until level 10, neutralization phenotypes of clone R3.7.8.3 at different passages were determined as shown in section 4.4. Clone R3.7.8.3 at passage level 3 (resistant clone), 6 (susceptible clone) and 9 (susceptible clone) were selected for total RNA isolation.

The L gene at position 6162 was located in the fragment 5.1; therefore, the cDNAs of all clones were synthesized using the forward primer L5-1. Amplification of this fragment was carried out using the L5-4: L5-2 primer pair and the expected bands with the size of 993nt were detected in all three clones as shown in Figure 7.52. RNA extracted from uninfected HeLa NCL cells and DEPC treated water were also tested as negative controls. The target bands were isolated and purified for direct sequencing (section 3.5.9) using the forward primer L5-4 and the reverse primer L5-2 in the 5' to 3' direction and in the 3' to 5' direction (antigenome), respectively. The sequence analysis revealed no variation at position 6162 in the L gene among the passage levels 3, 6 and 9. In all a T at position 6162 corresponded to a phenylalanine at position 2054 in the amino acid sequence.

Passage of clone R3.7.8.3 although producing a phenotypic change did not result in a change on any of variable sites in G, F or L genes identified in this study. It is surmised that the phenotypic change on passage occurred elsewhere in the genome.

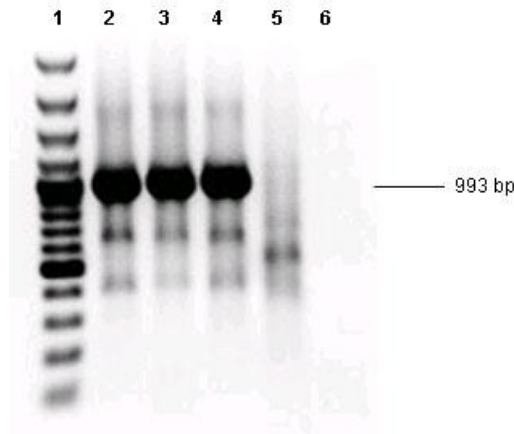


Figure 7.52: RT-PCR amplification of the L gene in the susceptible and resistant clones of R17532 using the L5-4: L5-2 primer pair.

The lanes were loaded as follows; Lane 1: 100bp DNA ladder; Lane 2: R3.7.8.3 P3; Lane 3: R3.7.8.3 P6; Lane 4: R3.7.8.3 P9; Lane 5: HeLa NCL cells (Negative control) and Lane 6: DEPC treated water (Negative control).

Sequence of L gene position 6162 in neutralization resistant and susceptible clones of strain R17532

The L gene at position 6162 of ten clones of R17532 described in Figure 6.8 was reverse transcribed using the forward primer L5-1 and amplified using the L5-4: L5-2 primer pair. The expected size of the target band was 993nt. The target bands were directly sequenced using the forward primer L5-4 in the 5' to 3' direction and the reverse primer L5-2 in the 3' to 5' direction (antigenome). Negative controls were performed in parallel, including uninfected HeLa NCL cells and DEPC treated water.

Figure 7.53 shows the target bands of 993nt in clone R2.44, R3.7.8.17, R3.2.4, R5.1, R5.2 and R11.2. No expected band was observed in clone R5.3, R5.14 and negative controls. Therefore, an alternative primer pair for the second round PCR, the L5-7: L5-8 primer pair (Figure 7.12), was used to re-amplify this region for those two clones. The expected size of 827nt was detected in all dilutions of PCR products from the first round PCR of both clone R5.3 and R5.14 (Figure 7.54).

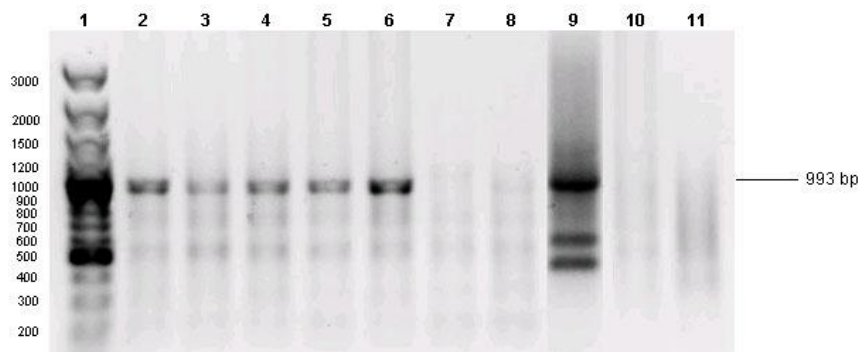


Figure 7.53: RT-PCR amplification of the L gene in the susceptible and resistant clones of R17532 using the L5-4: L5-2 primer pair.

The lanes were loaded as follows; Lane 1: 100bp DNA ladder; Lane 2: R2.44; Lane 3: R3.7.8.17; Lane 4: R3.2.4; Lane 5: R5.1; Lane 6: R5.2; Lane 7: R5.3; Lane 8: R5.14; Lane 9: R11.2, Lane 10: HeLa NCL cells (Negative control) and Lane 11: DEPC treated water (Negative control)

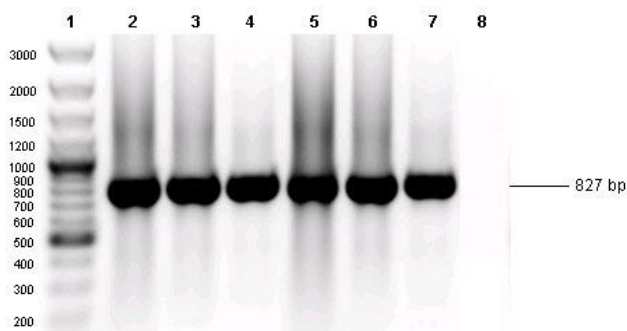


Figure 7.54: Reamplification by nested PCR of R5.3 and R5.14 using the L5-7: L5-8 primer pair.

The lanes were loaded as follows; Lane 1: 100bp DNA ladder; Lane 2, 3 and 4: R5.3 at dilution 10^{-1} , 10^{-2} and 10^{-3} , respectively. Lane 5, 6 and 7: R5.14 at dilution 10^{-1} , 10^{-2} and 10^{-3} , respectively. Lane 8: DEPC treated water (Negative control).

The nucleotides at position 6162 for all ten clones are shown in Table 7.8, together with the corresponding amino acid sequence at residue 2054. The clones were divisible into 2 groups following the lineage diagram in Figure 6.8. Clones in group 1 including clone R2.44, R3.2.4, R3.7.8.3, R3.7.8.17, R5.14, R11.1.1 and R11.2 were all produced from the P1-GLT virus stock. Those in group 2, comprising clone R5.1, R5.2 and R5.3, were generated from the P1-AC virus stock.

In group 1, there was a T at position 6162 in the two clones with an $EC_{50} > 20$ (R3.7.8.3 and R3.7.8.17), whilst the remaining clones with an $EC_{50} < 20$ derived from virus at passage level 2, 3, 5 and 11 had a G (R2.44, R3.2.4, R5.14, R11.1.1 and R11.2). This single nucleotide change corresponded to an amino acid change at residue 2054 from

phenylalanine in resistant clones to leucine in susceptible clones and is the only amino acid change correlated with the switch from resistance to susceptibility of R17532 in group 1. In group 2 of the clones had $EC_{50} > 20$, but had a G at position 6162 or leucine at position 2054. It is suggested that there may be another mutation holding these viruses in the resistant phenotype for this group.

Table 7.8: Summary of nucleotide and amino acid changes in the L gene at position 6162 of different clones of R17532 in the GLT lineage (A) and the AC lineage (B).

(A)

Type	EC_{50} ($\mu\text{g/ml}$)	L6162	L2054
		Nucleotide	Amino acid
R3.7.8.3	48.46	T	F
R3.7.8.17	21.41	T	F
R3.2.4	12.26	G	L
R2.44	6.89	G	L
R11.1.1	5.06	G	L
R5.14	2.97	G	L
R11.2	2.72	G	L

(B)

Type	EC_{50} ($\mu\text{g/ml}$)	L6162	L2054
		Nucleotide	Amino acid
R5.3	89.52	G	L
R5.1	69.82	G	L
R5.2	42.29	G	L

7.15 Summary of nucleotide changes of resistant and susceptible clones of R17532 in the non-membrane gene regions of the genome

In this section the non-membrane associated protein genes and the 3' and 5' ends of the genome were amplified and sequenced for resistant and susceptible virus clones. Variability was observed at two residues only, both in the L gene. Changes at residue 916 were found only between two equally susceptible clones of the susceptible R11 virus stock and were derived irrelevant to phenotype shift. Resistant R3.7.8.3 and both clones of susceptible R11.1.1 however differed at residue 6162. Further analysis of

variability at this locus in additional clones with differing susceptibility revealed a correlation of increased susceptibility with switch from T to G (amino acid F to L) at this site in the GLT lineage. In the second lineage of virus all three clones analysed carried a G at position L6162 despite releasing a high level of resistance. This suggests the existence of another mutation, already present in the resistant clones of the GLT lineage but absent from the AC lineage which is necessary for the switch to susceptibility.

Variable sites

		1	2
		(?)*	(L6162)
GLT lineage	Resistant	“s”	r (T)
	Susceptible	“s”	s (G)
AC lineage	Resistant	“r”	s (G)
	Susceptible	“s”	s (G)

*Hypothetical second site of variability contributing to increased susceptibility

r = base contributing to resistance

s = base contributing to susceptibility

Mutation at both sites is necessary for the acquisition of full susceptibility.

7.16 Overall conclusion from sequencing data

There were only four genomic changes identified between resistant R17532 clone R3.7.8.3 and susceptible clone R11.1.1, are in each of the SH, G, F and L genes. It must be concluded that these encode the observed phenotypic differences. For the clones derived from the GLT isolate, only the mutation at 6162 in the L gene correlates with increasing susceptibility to neutralization (Table 7.9) and may account for the difference in replication rate between the slow – growing resistant clone R3 and fast - growing susceptible clone R11 reported by Gias (2006). The three other sequence changes between R11.1.1 and R3.7.8.3 (section 6.7.4) may also contribute, however, it appears that none of the identified mutations alone is sufficient to confer susceptibility and they are all present in clone R5.1 derived from the AC isolate which remains resistant (Table 7.10). This argues for the presence of at least one other mutation necessary for the

acquisition of susceptibility, already present in R3.7.8.3 but not in the AC isolate derived clones. Sequencing of the whole genome of clones originated from the AC lineage should be determined in the future work. The role of individual mutations identified both clones and in concert, might be further investigated in a reverse genetics system.

Table 7.9: Summary of nucleotide and amino acid changes in the G, F and L genes of R17532 clones considering only the GLT passage arm of Figure 6.8

Gene	Nucleotide sequence							
	NT ^a #	R3.7.8.3	R3.7.8.17	R3.2.4	R2.44	R11.1.1	R5.14	R11.2
PZ EC ₅₀		48	21	12	7	5	3	2.7
SH GE	1-3	8A	8A	7A	7A	7A	8A	7A
G CDS ^b	884	T	T	C	T	C	T	C
G-F IR ^c	36	T	T	T	T	T	T	T
F CDS	301	C	T	C	C	C	C	C
	456	T	T	T	T	G	T	G
	946	C	C	A	C	C	C	C
	1082	A	A	G	A	A	A	A
L	6162	T	T	G	G	G	G	G

^aNT: nucleotide; ^bCDS: Coding sequence; ^cIR: Intergenic region

Table 7.10: Summary of nucleotide and amino acid changes in the G, F and L genes of R17532 clones considering only the AC passage arm of Figure 6.8

Gene	Nucleotide sequence			
	NT ^a #	R5.3	R5.1	R5.2
PZ EC ₅₀		90	70	42
SH GE	1-3	8A	7A	8A
G CDS ^b	884	T	C	T
G-F IR ^c	36	T	C	T
F CDS	301	C	C	C
	456	T	G	T
	946	C	C	C
	1082	A	A	A
L	6162	G	G	G

^aNT: nucleotide; ^bCDS: Coding sequence; ^cIR: Intergenic region

Chapter 8: Discussion

8.1 Neutralization of low passage resistant and high passage susceptible viruses in different cell lines

The first aim of this study was to produce stable stocks of both low passage resistant clones derived from hRSV R17532 clone R3.7.8.3 (clone R3) and high passage susceptible clone derived from R11.1.1 (clone R11). Virus infectivity and antibody neutralization may be assayed by either quantal or quantitative means. Here the neutralization phenotypes for each clone were evaluated by both a quantal method – the tube dilution endpoint assay (Reed and Muench, 1938) – and a quantitative assay, the focus reduction neutralization assay (modified from Dulbecco and Vogt (1954) and Welsh (2010)). For the latter, the effect of both cell types and focus visualization technique, immunofluorescence or immunoperoxidase staining, was also assessed. The immunoperoxidase focus reduction assay in HeLa NCL79 cells was selected to use throughout this project as in these cells both clones R3 and R11 produced well-defined foci which were easy to read with a low-power microscope. Foci in Vero cells were smaller less well defined and difficult to count (Figure 4.7). McKimm-Breschkin (2004) has also found hRSV pinpoint plaques were formed in Vero cells, whereas large plaques were detected in HEp-2 cells. hRSV plaques stained with neutral red in HEp-2 cells were clearly visible at 7 days postinfection, whilst in Vero cells at 9 days.

Neither the infectivity titre nor the neutralization results for clones R11 were significantly different between the immunofluorescent and immunoperoxidase methods (Figure 4.4). Similarly, immunoperoxidase and immunofluorescence assays, when used previously for the detection of hRSV in nasopharyngeal secretions, detected an identical number of positive specimens (Cevenini *et al.*, 1983).

Neutralization results determined by the three methods tested here showed that the low passage clone R3 was resistant and the high passage clone R11 was susceptible to neutralization by palivizumab (PZ), confirming the difference in susceptibility of these viruses reported by Gias (2006) and Marsh *et al.* (2007). Clone R3 appeared to be more sensitive to antibody in the dilution endpoint neutralization (Table 4.1) than in the focus reduction assay (Figure 4.3, 4.5 and 4.6), perhaps because in the former virus and antibody remain in contact with the cells for a longer period.

To test the hypothesis that HeLa NCL79 cells may be exceptionally suitable for the growth of resistant virus, different HeLa cells were used for titration and neutralization tests for both clones R3 and R11. hRSV foci for both clones in HeLa NCL79 cells were clearer than those in other HeLa cells, although infectivity titres of the two clones in HeLa JSF and Lucy were significantly higher than those in HeLa NCL79 (Table 4.4 and Figure 4.10). This suggests that whilst a lower number of virions in these virus populations may be capable of infecting HeLa NCL79, those that do infect produce larger foci, i.e. are capable of propagating more efficiently.

The PZ EC₅₀ values for the high passage clone R11 were not significantly different among all the different cell types studied. However, the EC₅₀ values for the low passage clone R3 using HeLa NCL79 cells was higher than those in other cells and in one HeLa line, HeLa CPV, PZ titres were similar for both R3 and R11 (Figure 4.11, Table 4.5 and 4.6).

Similar differences of neutralization results using various cell lines has been also shown in dengue virus (DENV). The plaque reduction neutralization test (PRNT) titres of different DENV strains against anti-DENV neutralizing antibody were different among three cell lines. The PRNT titres of DENV-1, -2 and -4 in BHK-21 cells were significantly less than those in Vero cells. In LLC-MK2 cells, titres of DENV-3 were increased, whereas those of DENV-4 were reduced (Thomas *et al.*, 2009). The mechanism caused the differences of PRNT titres in different cell lines is unresolved.

The particular resistance of the early passage R3 R17532 clone in HeLa NCL79 may explain the failure of other laboratories, using other cell lines, to report resistance of hRSV isolates to PZ. The origins of HeLa NCL79 cells are obscure. The line was selected for routine isolation of hRSV in the Newcastle virus diagnostic laboratory during the 1970s. Cell lines capable of isolating hRSV from clinical specimens were shared among the European virus diagnostic community and in Newcastle the available lines were selected for their susceptibility to hRSV in clinical material and subjected to regular screening to maintain sensitivity (R McGuckin personal communication).

Continuous selection of available cell lines for sensitivity to isolation of hRSV from cell culture might be expected to favour retention of any cells with increased capacity to replicate virus in the presence of neutralizing antibody which can be found in the secretions of infected infants from day 1 (Scott and Gardner, 1974).

In contrast, the other HeLa and Vero cells tested here are of unknown history, but are not known to have been selected for susceptibility to hRSV. Heterogeneity among different HeLa cell line is well established. Herrnsstadt *et al.* (2002) has reported that mitochondrial DNA (mtDNA) polymorphisms differ among various HeLa cell sublines. Three HeLa sublines (CCL2, 229 and S3-ATCC) obtained from the American Type Culture Collection (ATCC), one subline from the Los Alamos National Laboratory (S3-Los Alamos CalTech) and a Newcastle subline from this laboratory frozen in 1985 were analysed. HeLa CCL2 and HeLa 229 had no any mtDNA differences compared to the revised Cambridge reference sequence (CRS) for human mtDNA, whilst the other three HeLa sublines including the Newcastle line had a high rate of mtDNA polymorphism. These findings demonstrate that HeLa from different sublines may have distinct characteristics.

Whether the resistance of low passage virus isolation in HeLa NCL79 cells has any relevance to the pathogenesis of human hRSV infection is uncertain. The resistance of parental clone R3 on a more relevant cell line, 16HBE140, was significantly greater than that of R11 in the same cell line, but was low compared to that obtained on HeLa NCL79 cells (Figure 4.12). However, it remains uncertain to what extent 16HBE140 cells retain the authentic properties of human epithelial cells *in vivo*. It is noteworthy that 16HBE160 appeared less susceptible than HeLa NCL79 when plaque sizes were compared (Figure 4.10 and 4.13). Even if differences in sensitivity to neutralization are artefactual, the failure of PZ to neutralize low passage R17532 in HeLa NCL79 remains of interest as it indicates that the mechanism of hRSV neutralization is incompletely understood.

8.2 Neutralization susceptibility of low passage viruses after serial passage in cell cultures

From the lineage of R17532 in Figure 6.8, viruses passaged by Prof. G.L. Toms in 1996 (GLT) and Dr A. Connor in 1998 (AC) retained the resistant phenotype until passage level 10. In contrast, clone R3 in this study shifted from resistant to susceptible at passage level 4 similar results to those of Marsh (2002) and Gias (2006) who reported phenotype conversion at passage level 5 (Figure 4.9 and Table 4.3). Why the resistant phenotype has proved less stable in recent studies remains unknown.

Gias (2006) demonstrated that susceptible viruses were present even in apparently resistant virus stocks and that their proportion increased on passage. The number of susceptible clones of R17532 retrieved by plaque purification increased from 5% at passage level 3 to 44.4% at passage level 5. Welsh (2010) also reported the percentage of susceptible clones picked from R17532 passage 3 as 41.7% compared to 58.3% resistant clones. These results indicate that the predominant quasispecies in the virus population changes on passage.

A change in susceptibility to neutralization on serial passaged in cell culture has also been shown for other viruses. Two resistant variants of foot-and-mouth disease virus (FMDV), 1-OG2 and 1-HA6, became neutralization susceptible after repeated passage to level 20 and 30, respectively. The sequence of resistant variants 1-OG2 and 1-HA6 differed from the susceptible parental virus in the capsid proteins VP2 and VP1 at residue 72 (D72N) and residue 198 (D198G), respectively. However, in high passage susceptible viruses sequences reversed to those of the parental virus (D at both residue 72 and 198) (Gonzalez *et al.*, 1991). Anti-gp120 resistant variants of HIV-1 have also been found to be susceptible to neutralization by anti-gp 120 MAbs on further passage. Three amino acid changes in gp120 were detected in susceptible variants compared to those in resistant variants. One of them (G318R) was located in the V3 region which was a major target for neutralizing MAbs. The effects of the other two changes in the V2 (I166R) and C2 (I282N) regions remain unexplained (Wrin *et al.*, 1995). Thus, whilst here are precedents for increasing susceptibility to neutralization on adaptation to cell culture, hitherto these changes have been explicable by demonstration of mutations in the surface proteins of the virus. The phenotypic changes reported here and by Marsh

et al. (2007) have not been correlated with obvious changes to the viral surface glycoproteins.

8.3 Mechanism of resistance

8.3.1 Binding of neutralizing antibody to resistant and susceptible clones

In HIV-1, anti-gp 120 MAbs have been reported to bind equally to gp120 proteins expressed on the surface of either neutralization resistant or susceptible variants (Wrin *et al.*, 1995). In hRSV, Marsh (2002) also demonstrated no differences between binding of anti-F MAbs to isolated F glycoproteins of neutralization resistant and susceptible viruses. These findings are in agreement with Welsh (2010) who found that PZ bound equally to the F glycoprotein of either purified resistant or susceptible hRSV clones. These results suggest that the levels of F glycoprotein expression on the surface of cells infected with resistant virus are similar to those for susceptible clones. It has similarly been found that neutralization resistance of HIV-1 is not dependent on high amounts of envelope glycoprotein expression (Karlsson *et al.*, 1996).

However, in separate studies, neutralization resistant primary HIV-1 isolates have been reported to express higher levels of gp120 envelope glycoprotein compared to a neutralization susceptible laboratory - adapted strain (O'Brien *et al.*, 1994; Sullivan *et al.*, 1995). These findings suggest that resistance may arise as a result of quantitative increase of the envelope glycoprotein on the virus surface, increasing the amount of antibody necessary to block activation of the critical number of molecules.

Hence, it was interesting to study whether the amount of the F glycoprotein expressed was different between resistant and susceptible clones. Marsh (2002) could find no differences in the level of F glycoprotein expression between resistant and susceptible stocks of hRSV R17532 determined by Western blotting. However, Gias (2006) demonstrated that both crude virus infected cell lysates and purified virions of neutralization resistant clones of R17532 and a second strain N5843 had higher amounts of the F glycoprotein per unit infectivity than resistant clones as measured by F-capture ELISA assay. However, the F glycoprotein per genome copy measured by real-time PCR, whilst higher for the resistant clone of R17532, was the same for both clones of

N5843. The relevance of elevated F glycoprotein expression in resistance thus remains equivocal.

R17532 clone R3 is resistant to PZ not only in the neutralization assay but also in the fusion inhibition assay (Gias, 2006). If higher levels of F expression are the cause of this resistance the concentration of the F glycoprotein on the surface of infected cells would be expected to be higher for resistant clones and this can be measured by cell surface ELISA. This was carried out on cell cultures infected with equivalent titres of the two clones of virus using MAb 1E3 as the detection antibody. 1E3 was chosen as it has previously been shown (GL Toms personal communication) that the affinity of binding of 1E3 is the same for the F glycoprotein from both clones R3 and R11 of R17532 as determined by the half-saturation ELISA method (West *et al.*, 1994). Amounts of the F glycoprotein measured by the ELISA whole cell method with anti-F MAb 1E3 determination were identical for resistant clone R3 and susceptible clone R11 (Figure 5.5). These results agree with the semi-quantitative Western blot results of Marsh (2002) and indicate that higher F glycoprotein expression levels on the cell surface are not necessary for resistance of R17532 at least to fusion inhibition. In relating F glycoprotein expression to infectivity or genome number Gias (2006) introduced further undefined variables into the determination, those affecting the fragility of the virions. The differences she detected could represent differences in the survival of infectivity and integrity of the genome equally as well as those of F glycoprotein concentration.

8.3.2 Post-attachment stages of neutralization resistant and susceptible viruses

Huang *et al.* (2010) have reported that the pre-treatment of hRSV with PZ did not block viral attachment, whereas this step was inhibited by heparin, an attachment inhibitor. This suggests that neutralization by PZ occurs after the attachment step. In line with this Welsh (2010) demonstrated that PZ failed to block viral attachment of either neutralization resistant or susceptible R17532 virus clones, but there did appear to be differences in the attachment of resistant and susceptible viruses with the resistant attaching much more quickly. Binding of the resistant clone could not be blocked with heparinase or free heparin both of which inhibited binding of the susceptible clone suggesting that receptor usage differed between the two viruses. As PZ appears to act

post-attachment it is not clear how these differences relate to differences in susceptibility to PZ neutralization.

Clathrin-mediated endocytosis of neutralization resistant and susceptible viruses

Previous studies have shown that clathrin-mediated endocytosis is involved in the entry of cell culture adapted hRSV into target cells. Inhibition of clathrin coat construction in endocytosis by blocking the expression of clathrin associated protein or treatment with clathrin inhibitors resulted in inhibition of hRSV infection (Kolokoltsov *et al.*, 2007; Gutierrez-Ortega *et al.*, 2008). It was hypothesised that the requirement for clathrin-mediated endocytosis might differ between resistant and susceptible clones.

To test this hypothesis, PZ neutralization resistant and susceptible clones were treated with two clathrin inhibitors, monodansylcadaverine (MDC) and chlorpromazine (CP), and their susceptibility to these inhibitors were determined. Both clones were equally inhibited by MDC and CP suggesting that clathrin-mediated endocytosis is equally necessary for entry of both viruses into target cells (Figure 5.3). These results suggest that differences downstream of pinocytosis are involved in determining the susceptibility to neutralization by PZ.

Activation of the F glycoprotein in neutralization resistant and susceptible viruses

Activation of the fusion protein depends upon prior post-translational modification of the fusion protein precursor F0 and is fundamental to the post-pinocytotic stages of the infectious process, allowing fusion of virion and host cell membrane and penetration of the virus core. Factors involved in this process were therefore compared between the two variants including F glycoprotein post-translational processing and activation.

In order to evaluate post-translational processing involving proteolytic cleavage and glycosylation, the migration of the F glycoprotein in lysates of cells infected with low passage clone R3 and high passage clone R11 were analysed by SDS-PAGE and Western blotting using anti-F MAb 1E3. Two protein bands of the F1 subunit, 52 and 20kDa, were detected in both viruses (Figure 5.4). These results although differing in detail point to the same conclusion as those of Welsh (2010) who demonstrated three additional minor bands of 70, 48 and 44kDa in crude virus lysate of clones R3 and one

more band (70kDa) in clone R11. The 70kDa band corresponds in size to the uncleaved F0 precursor and its absence in the present study suggests that all the F glycoprotein has undergone cleavage at least one of the two potential cleavage sites (see section 1.4.10). Cleavage at the second site should release a 27 amino acid peptide (Gonzalez-Reyes *et al.*, 2001). Differences in the extent of second site cleavage between the two viruses should, therefore, be visible as differences in the size of the major F1 band. No such differences were apparent in either study. The minor 48 and 44kDa bands observed by Welsh (2010) in R17532 clone R3 were not present in crude lysates of another resistant clone N1 or in purified virions of either clones R3 or N1 and may be proteolytic breakdown products of the 52kDa F1 generated during the prolonged replication of this slow growing virus. However, Western blot analysis is a relatively insensitive means of investigating modification. Unfortunately more sensitive techniques, such as mass spectrometry, require purification of the F glycoprotein in quantities as yet unachievable with unstable antibody resistant virus clones studied here.

During the transition of the F glycoprotein from the pre-fusion to the post-fusion form in the fusion process, a 6HB is formed drawing viral and host cell membranes into close apposition. This complex occurs from interaction of the HR1 and HR2 domains of the F1 subunit (Zhao *et al.*, 2000). McLellan *et al.* (2011) have shown that motavizumab (MZ), a potent derivative of PZ, can tightly bind to the post-fusion conformation of the F glycoprotein. However, its epitope has been found on a domain which is not involved in the conformation changes. MZ may be capable of binding to multiple conformations of the F glycoprotein and may neutralize virus by interfering with the activation of the F molecule. Neither MZ nor PZ have been found to block the transition from a pre-fusion to a pre-hairpin conformation (Huang *et al.*, 2010). In the lipid-mixing assay, treatment with MZ and PZ was not able to inhibit the transfer of lipids from hRSV to target cells, but virus transcription and cell-to-cell fusion were inhibited by these antibodies. This suggests that PZ and MZ block the transition from either a pre-hairpin to a hairpin conformation or a hairpin to post-fusion conformation (Figure 8.1).

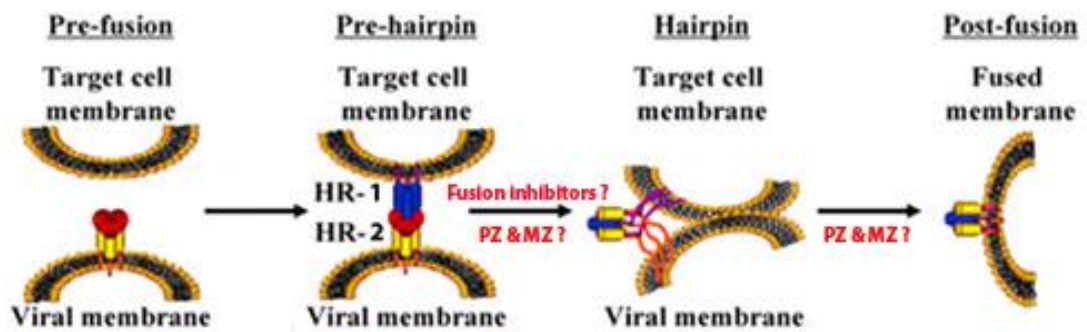


Figure 8.1: Model of the proposed actions of fusion inhibitors and anti-F MAbs in the process of rearrangement in the F glycoprotein.

[Modified from original by Huang *et al.* (2010)]

HR1: Hepatad repeat 1; HR2: Heptad repeat 2; PZ: palivizumab; MZ: motavizumaab.

To investigate the fusion activation, susceptibility of both resistant and susceptible clones to inhibition by anti-fusion inhibitor compounds directed against 6HB formation, two small molecular inhibitors (BTA9881 and BMS-433771) and an HR2 peptide (residues 488 – 522), were analysed. BMS-43771 has been reported to interact with HR1 in a hydrophobic cavity at pre-hairpin intermediate stage of the F glycoprotein, interfering with the formation of 6HB as shown in Figure 8.1 (Cianci *et al.*, 2005). Similarly, HR2 peptide is thought to bind to the HR1 peptide coiled coil interrupting the conformational change (Zhao *et al.*, 2000; Russell *et al.*, 2001). The mechanism of inhibition by BTA9881 is still unknown, but it is known that it inhibits F glycoprotein-mediated membrane fusion (Luttick *et al.*, 2007).

In focus inhibition assays, all compounds failed to inhibit resistant parental clone R3, but efficiently blocked infection by clone R11 (Figure 5.6). The EC₅₀ values of R17532-HR2 peptide, BMS-433771 and BTA9881 for clone R11 were 13.04, 0.21 and 5.23 µM. Lambert *et al.* (1996) reported that T-118 peptide, similar to R17532-HR2 peptide, inhibited infection with hRSV Long strain at EC₅₀ values of 0.05 µM which was 260 times lower than those in inhibition of susceptible clone R11 in this study. However, the two studies are not directly comparable in the absence of accurate information on the purity of the two peptide preparations.

Cianci *et al.* (2004c) found that the EC₅₀ value of BMS-433771 for a variety of hRSV strains and isolates varied between 0.012 and 0.05 µM some 4-fold or higher than that

for clone R11 determined here. However, in the study of Cianci *et al.* (2004c) EC₅₀ values were determined in assays measuring either cell protection or inhibition of virus specific proteins, whereas here the percentage of virus survival was measured. Hence, these values cannot be compared directly. For BTA9881, there are no previous reports of EC₅₀ value.

Resistance of HIV-1 to fusion inhibitors has been reported to be associated with an increase in either gp120/ coreceptor affinity or coreceptor density on the surface of target cells, leading to an increase rate of membrane fusion (Reeves *et al.*, 2002). A similar mechanism may also render early passage hRSV resistant to anti-fusion agents. Welsh (2010) found that for PZ resistant clones attachment was independent on cell surface heparan sulphate (HS) binding, whereas susceptible clones required HS. It is suggested that the neutralization susceptibility to PZ of low and high passage viruses may be affected by differences in receptor usage for cell binding, possibly resulting in differences in the kinetics of the F glycoprotein mediated fusion.

8.4 Comparison of nucleotide and deduced amino acid sequences of M and SH genes between neutralization resistant and susceptible virus clones

As previously demonstrated, genetic changes in the antibody binding sites of the F glycoprotein have been shown to be associated with resistance to neutralization in cell cultures and animal models among both laboratory virus strains and clinical isolates (Zhao *et al.*, 2004a; Boivin *et al.*, 2008; Adams *et al.*, 2010; Zhu *et al.*, 2011). The F glycoprotein associates with other membrane proteins including the G, SH and M proteins (Feldman *et al.*, 2001; Collins and Crowe, 2007). Therefore, it is postulated that genetic changes in their genes might also indirectly affect the interaction of the F glycoprotein with antibody leading to resistance to neutralization.

Marsh (2002) and Gias (2006) have reported that none of the mutations detected in either the F glycoprotein genes or other membrane associated protein gene of variants of R17532 and N5843 isolates were correlated with susceptibility to neutralization by anti-F MAbs. However, the sequence analysis of the M and SH genes were derived not from well characterized virus clones but from virus stocks subsequently shown to be a mixture of neutralization resistant and susceptible viruses. To confirm these results, the

sequences of both of these genes for resistant clone R3 and susceptible clone R11 were analysed.

The results showed no nucleotide changes in the coding region of the M gene between the two clones of R17532 (Appendix Figure 10.1, 10.2 and 10.3), suggesting that this gene was completely conserved and was not involved in neutralization phenotype shift confirming the conclusion of Gias (2006). The nucleotide sequence of R17532 was slightly different from A2 and the percentage of identity was 97. However, no amino acid changes were found between R17532 and A2, suggesting that the M protein was fully conserved among hRSV strains. These findings were in agreement with the report of Kumaria *et al.* (2011) who found no amino acid variability in the M gene among 14 hRSV strains which were isolated from nasopharyngeal washings of infected infants in Colorado, USA. Whole genomes of all these isolates were directly sequenced from patient specimens without passage in tissue culture (Kumaria *et al.*, 2011). The presence of highly conserved sequence in the M gene may be because the M protein is important in regulating viral transcription and viral assembly (Kaptur *et al.*, 1991; Lenard, 1996; Coronel *et al.*, 2001).

Analysis of the coding sequence in the SH gene showed no variations occurring between resistant clone R3 and susceptible clone R11. However, there were five nucleotide changes in this region of R17532 compared to A2 giving a percentage of nucleotide conservation of 97%. Two of five mutations caused amino acid changes at residue 29 and 62 resulting in 96% amino acid identity (Appendix Figure 10.5 and Table 6.2). This low level of nucleotide variability is consistent with the study of Cane and Pringle (1991) who reported nucleotide identity of the SH gene within the subgroups to be in the range 93% to 99%. A similar level of amino acid variation was observed by Lima *et al.* (2012) who analysed the SH gene from 424 isolates collected from 965 patients in Brazil and found very low variability of this gene. 93.5% of strains exhibited no amino acid substitution, but 6.5% had one or two altered amino acids.

The identity of the SH gene in resistant and susceptible R17532 clones indicates that the origin of the phenotypic differences between the clones does not lie here.

8.5 Comparison of nucleotide and deduced amino acid sequences of G and F genes between neutralization resistant and susceptible virus clones

In previous studies, the sequences of F and G genes were analysed from both virus stocks and clones. Whilst a number of genetic changes were identified, none were unambiguously associated with the shift from a slow growing-neutralization resistant to a fast growing-neutralization susceptible phenotype (Gias, 2006; Marsh *et al.*, 2007). However, these studies were carried out on a limited number of virus clones. Hence, to test this conclusion further, both G and F genes were sequenced from additional susceptible and resistant clones at different passage levels and degrees of resistance to neutralization.

Initially, resistant clone R3 was passaged from level 3 to 10 during the course of which susceptibility to neutralization increased by approximately ten fold (Figure 4.9), and the sequences of the G gene, F gene and associated intergenic regions at passage 3, 6 and 9 were analysed. There were no nucleotide changes observed among them, despite the increase in susceptibility to neutralization. Furthermore, comparison of the sequence from the end of the SH gene to the end of the F gene of 10 R17532 clones comprising resistant and susceptible clones derived from two separate isolations of the virus at different passage levels, although identifying variations at 7 sites found no clear cut correlation with phenotype (Table 6.9). This confirms the observation of Marsh *et al.* (2007) who reported that in one instance passage of a resistant stock of virus resulted in acquisition of susceptibility to neutralization without sequence change in the F or G genes.

8.5.1 Variability of the G gene in different clones

Among 10 clones of R17532 analysed, only one variable residue was found in the G coding sequence at nucleotide position 884 which varies between T and C (Table 6.4). This change caused an amino acid change from isoleucine to threonine at residue 295 (Appendix Figure 10.8). Both forms were found in susceptible and resistant clones. Marsh *et al.* (2007) have previously reported T or a mixture of T and C at this position in resistant R17532 stocks and C in a susceptible stock. However, the result presented

here indicates that this mutation is not involved in neutralization phenotype shift being present in both resistant and susceptible variants.

This change is located in the carboxy-terminal third of the G protein which is highly variable (Melero, 2007). Frameshift mutations have been found in this region in escape mutant viruses resistant to neutralization by anti-G MAbs. Frameshifts were caused by single adenosine insertions and/or deletions and resulted in truncated G proteins (Garcia-Barreno *et al.*, 1990; Rueda *et al.*, 1991). Variation in this part of the G protein did not affect to hRSV infectivity. Heterogeneity at position 884 has been reported previously. Sequence analysis of 14 isolates collected from patients in Colorado revealed nucleotide variation of T and C at position 884 (Kumaria *et al.*, 2011). Nine isolates had T, whilst five isolates had C at this position. In contrast in a Milwaukee population (Rebuffo-Scheer *et al.*, 2011), the predominant quasispecies variants were C at this position which were detected in 21 specimens, whilst T was present only in 3 specimens. These findings demonstrate that heterogeneity at this residue is widespread in clinical isolates, but its significance, if any, remains unclear.

8.5.2 Variability of the F gene in different clones

Sequence comparison of the F coding gene among 10 clones of R17532 with various neutralization phenotypes revealed four variable nucleotides, two of which resulted in amino acid changes (Table 6.7 and 6.8). In addition, one variable site occurred in the G-F intergenic region. Variability in residue 152, lying in the region encoding the HR1, was previously identified as variable in R17532 by Marsh *et al.* (2007) and Gias (2006). Whilst most clones carried a T at this site, a G was present in susceptible clones R11.1.1 and R11.2 and in resistant clone R5.1 corresponding to an amino acid change from isoleucine to methionine at residue 152 (Appendix Figure 10.11). Similarly, this variation was found in both resistant (P10-GLT) and susceptible (P10-FF) virus stocks (Marsh *et al.*, 2007). At this residue, a valine was present in A2, whereas 37 of 39 hRSV sequences published in GenBank have an isoleucine similar to the majority of R17532 clones and the other two have a valine like A2 (Kumaria *et al.*, 2011; Rebuffo-Scheer *et al.*, 2011).

The second coding mutation was found only in resistant clone R3.7.8.17 encoding serine at residue 101 dictated by a T at nucleotide 301, whilst most clones had a C encoding proline at this point. This variation was also reported by Gias (2006) who found a serine at this residue in susceptible clone N10a of isolate N5843.

In addition to the coding mutations, two silent mutations were observed in clone 3.2.4 at position 946 (C → A) and 1082 (A → G). These changes were not found in previous studies from either virus stocks or clones of R17532 (Gias, 2006; Marsh *et al.*, 2007). However, one isolate from a Milwaukee population had an A at position 946, whilst the majority of isolates carried a C at this point (Rebuffo-Scheer *et al.*, 2011).

One coding mutation of leucine in clone R3 to isoleucine in clone R11 at residue 386 reported in a previous study (Gias, 2006) was not found in R3 clone, R3.7.8.3, tested here which had an isoleucine at this point, although both R3 clones were derived from the same parent stock.

It is noteworthy that none of the coding mutations detected in previous studies or in this study were located within the known binding sites of PZ (around residue 272 – 275) or the two anti-F MAbs used in the study of Gias (2006) and Marsh *et al.* (2007), MAb19 (residues 422 – 438) and RS348 (residues 200 – 225 and 253 - 289).

8.6 Comparison of nucleotide sequences of all intergenic regions between neutralization resistant and susceptible virus clones

The intergenic regions of hRSV gene have been revealed to vary in length from 1 to 58 nucleotides among hRSV strains reported to date. They are not conserved in either nucleotide sequences or obvious features of secondary structures, except there is an A residue (genome sense) at the end of all genes (Collins *et al.*, 1986; Collins and Crowe, 2007). These regions have not been found in monocistronic mRNAs, indicating that the polymerase does not transcribe them, but moves across this region to reinitiate transcription at the downstream gene start region (Collins *et al.*, 1986; Rassa *et al.*, 2000).

In the present study, sequences of all intergenic regions were compared between resistant and susceptible variants of R17532 and also between R17532 and A2. The results showed no nucleotide changes between the two fully sequenced R17532 clones in any of the intergenic regions, suggesting that these regions are conserved and not involved in differences in neutralization phenotype. However, among the sequences of R17532 10 clones varying in neutralization susceptibility and passage levels a single nucleotide change (T → C) was observed in one clone, R5.1, at position 36 in the G-F intergenic region (Appendix Figure 10.9). These results are broadly in agreement with those of Marsh *et al.* (2007) who demonstrated identical sequences of the M-SH, SH-G and G-F intergenic regions in resistant and susceptible virus stocks and also with Gias (2006) who showed that the sequences of the G-F intergenic regions in resistant clones of isolates R17532 and N5843 did not differ from those of the susceptible clones. However, several variations were observed between R17532 and A2 as shown in Table 8.1. The percentage of nucleotide identity ranged from 22 to 100. The sequences of R17532 in all these regions were between 3 and 53 nucleotides in length and contained A at the end of each sequence confirming to the observations of Collins *et al.* (1986) and Collins and Crowe (2007).

In the N-P intergenic region, the percentage of nucleotide identity between R17532 and A2 was only 50% (Table 8.1). This was because this region in A2 contained a single nucleotide (3'...A...5', genome sense), whereas an insertion of C was observed in R17532 (3'...CA...5') (Appendix Figure 10.20). This variation was also found in 4 of 14 isolates in a Colorado population and 14 of 25 isolates in Milwaukee (Kumaria *et al.*, 2011; Rebuffo-Scheer *et al.*, 2011). Another study has also reported this change from 4 of 14 strains obtained from infected patients in USA (Alabama) and UK (Birmingham, Glasgow and Newcastle) and described the effect of this variation on transcription at the N/P gene junction (Moudy *et al.*, 2004). Replicons containing CA in the N-P intergenic region had a 2.5-fold increase in the synthesis of readthrough RNAs compared to replicons comprising A as in the A2 sequence, suggesting that this variation reduces the efficiency of termination of the upstream gene. However, the change did not affect the initiation of downstream gene transcription as demonstrated by identical initiation levels for the P gene of both CA and A variants. Hence, it can be inferred that termination at N/P gene junction in R17532 is likely to be less efficient than that in A2.

Table 8.1: Summary of percent nucleotide identity in all intergenic regions of R17532 and A2 strains.

Intergenic Region	Length (nt)	% NT ^a identity R17532 vs. A2
NS1-NS2	19	89
NS2-N	26	80
N-P	2	50
P-M	3	22
M-SH	9	77
SH-G	44	90
G-F	53	84
F-M2	46	76
M2-L	45	100

^aNT: Nucleotide.

The sequence of the P-M intergenic region in R17532 (5'...GAT...3') was also substantially different from A2 (5'...GGAAAGGGT...3') giving a very low percentage of identity of 22 (Table 8.1). A deletion of six nucleotides (5'...GGAAAG...3') and one nucleotide change (G → A) at position 8 in A2 were observed in R17532 (Appendix Figure 10.1). This variation has also been reported previously, being present in 6 of 14, hRSV strains isolated from infected infants in Colorado, USA (Kumaria *et al.*, 2011). Moreover, 14 of 25 hRSV specimens collected from patients in Milwaukee (Rebuffo-Scheer *et al.*, 2011) and 8 of 14 hRSV strains isolated from USA and UK (Moudy *et al.*, 2004) also had this change. Moudy *et al.* (2004) have shown that alteration of the sequence and the length in the P-M intergenic region did not affect either efficient termination of the upstream gene or initiation of the downstream gene. Therefore, the different sequence and nucleotide length of the P-M intergenic region between R17532 and A2 would not be expected to affect either termination of the P gene or initiation of the M gene transcription.

8.7 Comparison of nucleotide sequences of the 5' untranslated regions (UTR) of all genes between neutralization resistant and susceptible virus clones

The 5'UTR of all genes was analysed in resistant and susceptible clones of R17532 and A2. The results showed identical sequences in these regions between the two R17532 clones, suggesting that they were fully conserved as previously reported by Marsh (2002) and Gias (2006) for the 5'UTR of the M, SH, G and F genes. The sequences of R17532 slightly differed from those of A2 in the range 92% to 100% as shown in Table 8.2. For six genes the homology between the two viruses in this region was 100%. This may be because these are the shorter intergenic regions and contain a gene start (GS) sequence which is highly conserved. The 5'UTR of the M, M2 and L genes consists only of the GS. The GS consensus sequence for hRSV is 3'-CCCCGUUUA-5', except in the L gene (3'-CCCUGUUU-5'). The GS sequence is important in regulating the initiation of mRNA synthesis (Collins and Crowe, 2007). Kuo *et al.* (1997) has reported that most of the positions in the GS sequence appear to affect its activity. Substitution with any nucleotide at position 1, 3, 6, 7 and 9 has shown to decrease transcription levels.

Table 8.2: Summary of percent nucleotide identity in the 5' untranslated regions (UTR) of all genes of R17532 and A2 strains.

5'UTR	Length (nt)	% NT ^a identity R17532 vs. A2
NS1	54	96
NS2	32	90
N	15	92
P	17	100
M	9	100
SH	84	92
G	15	100
F	13	100
M2	9	100
L	8	100

^aNT: Nucleotide.

8.8 Comparison of nucleotide sequences of the 3' untranslated regions (UTR) of all genes between neutralization resistant and susceptible virus clones

The 3'UTR containing the gene end (GE) sequence is present in all hRSV genes and is an important region involved in viral transcription. The GE sequence is semiconserved and consists of three regions (presented in genome sense): an upstream conserved pentanucleotide region (3'-UCAAU-5'), a non-conserved central region (N₁₋₄) and a downstream conserved U-tract (U₄₋₇). It directs polyadenylation of mRNA by slippage on the U-tract template and termination of transcription by mRNA release (Barr and Wertz, 2001; Harmon *et al.*, 2001). Efficient termination depends on the specific sequence of the GE sequence. Positions 2 to 6 are necessary for termination and highly sensitive to base changes and position 8 is allowed to be only A or U due to the requirement for weak nucleotide pairing between the template and mRNA during reiterative transcription or termination (Harmon *et al.*, 2001).

The position of the U-tract is also important in transcriptional termination and its proper location has been shown to be at position 8 to 13. In addition, the length of the U-tract is critical and the minimum number of the U residue allowing efficient activity is 5 residues (Harmon *et al.*, 2001). A U₄-tract combined with an intergenic region containing A at the beginning has been reported to reduce transcriptional termination at the M-SH and F-M2 intergenic region (Sutherland *et al.*, 2001; Harmon and Wertz, 2002). Increasing the length of the U-tract in the F GE sequence from 5 to 8 U residues has also been shown to decrease efficient termination (Sutherland *et al.*, 2001).

The sequence analysis of the 3'UTR in the SH gene between resistant clone R3 and susceptible clone R11 revealed one nucleotide difference occurring in the U-tract of the GE sequence or the A-tract in the antigenome sense as presented here (Appendix Figure 10.6). There were 8 adenosines in the A-tract (8As) in clone R3, but only 7 in clone R11. This contrasts to results of Marsh (2002) who found 7As in both resistant and susceptible virus stocks of R17532. This region was also sequenced in additional susceptible and resistant clones. 7As was detected in four of five susceptible clones (R3.2.4, R2.44, R11.1.1 and R11.2) and one of the resistant clone (R5.1), whereas 8As was found in four of five resistant clones (R5.3, R3.7.8.3, R5.2 and R3.7.8.17), and one of the susceptible clone (R5.14) (Appendix Figure 10.7). This suggested that this

mutation may play some role in the neutralization phenotype conversion. From 39 sequences of hRSV isolates published in GenBank (accession number JF920046 – JF920070 and GU591758 – GU591771) only 5As (the same as A2) and 6As were reported in the SH GE sequence. That the A-tract of R17532 is longer than that of A2 suggests that termination in R17532 may be less efficient than in A2 (Sutherland *et al.*, 2001).

Apart from the SH gene, there were no nucleotide changes observed in the 3'UTRs in the rest of the genome between clones R3 and R11. However, several changes were found between R17532 and A2 as shown in Table 8.3. In the 3'UTR of the M gene, there were 5As in the GE sequence in R17532 which is shorter than that in A2 which contains 6As (Appendix Figure 10.3). This suggests that the M GE sequence of R17532 terminates more efficiently than A2.

Table 8.3: Summary of percent nucleotide identity in the 3' untranslated regions (UTR) of all genes of R17532 and A2 strains.

3'UTR	Length (nt)	% NT ^a identity R17532 vs. A2
NS1	57	96
NS2	96	91
N	13	100
P	171	87
M	176	90
SH	134	83
G	12	84
F	165	93
M2	99	92
L	72	91

^aNT: Nucleotide.

In the 3'UTR of the G gene (Appendix Figure 10.9), there was a Nucleotide substitution at position 4 from C in R17532 to T in A2 (A4G) and a deletion of C at position 6 (-6G) giving percent nucleotide identity of 84 (Table 8.3). These variations were also found

in the virus stock of R17532 reported by Marsh (2002) and in 33 of 39 hRSV specimens published in GenBank (Kumaria *et al.*, 2011; Rebuffo-Scheer *et al.*, 2011).

Moudy *et al.* (2003) have shown that replicons containing either the A4G variation alone or the combination between A4G and -6G variations in the G GE sequence reduced the termination efficiency and the initiation of the upstream gene. The A4G variation alone produced a readthrough 10-fold higher than A2, whilst only a 4-fold higher readthrough occurred with the combination of A4G and -6G compared to A2. In contrast, the -6G variation alone only slightly affected termination, suggesting that a partial compensation for A4G may occur in the presence of the two variations. From these findings, it appears likely that the termination efficiency at the G-F junction in R17532 may be less than that in A2, resulting in a reduction in F gene expression.

8.9 Comparison of nucleotide sequences of the 3' leader and 5' trailer regions between neutralization resistant and susceptible virus clones

The 3' leader and 5' trailer regions contain promoters which are necessary for the synthesis of mRNA and the antigenome, respectively (Collins and Crowe, 2007). It has been reported that the first 11-nt of the genome are required for both transcription and replication (Fearn's *et al.*, 2002). To investigate whether these regions were related to a difference in susceptibility to neutralization by PZ. Sequences of these regions were compared between resistant and susceptible clones.

The genomic RNA circularization method was initially adopted to sequence both the 3' leader and 5' trailer regions. This method has previously been used for determination of complete consensus sequences of two hMPV isolates, CAN97-83 and CAN98-75 (Biacchesi *et al.*, 2003). However, in this study, incomplete sequence of 5' trailer region for clone R11 and none of sequence for clone R3 were obtained using this method. The RNA templates used were extracted from gradient purified viruses to avoid interference from mRNA. One possibility for failure was that the templates were insufficient or of poor quality, especially for clone R3, where virus titres in cultures prior to purification were lower.

5'rapid amplification of cDNA ends (5'RACE) and 3'RACE were subsequently developed. In these assays, RNA for clone R3 was isolated from cell lysates which was higher quality than that from purified samples. The 5'end and 3'end of the genome for both resistant clone R3 and susceptible clone R11 was successfully sequenced by 5'RACE from the antigenome and 3'RACE from the genome (Figure 7.40 and 7.50), respectively. The method of 3'RACE from the antigenome failed to sequence the 3'end possibly due to interference from mRNA. Whilst all sequences for clone R3 were derived from a parental clone R3.7.8 and a single passage 3 preparation of clone R3.7.8.3, for clone R11 three preparations were used. The 5'end sequence was derived from R11.1.1 passage 8 and 12 and the 3'end sequence from R11.1.1 passage 11 and 12. All preparations of this clone preserved the susceptible phenotype .

Analysis of the 3'leader (44 nucleotides) and 5'trailer (160 nucleotides) regions revealed no nucleotide changes between resistant and susceptible clones (Appendix Figure 10.29 and 10.30), suggesting that these regions were completely conserved. However, R17532 sequences in these regions were slightly different from A2 with 97% and 91% nucleotide identity in 3' and 5'end of the genome, respectively. The length of the 5'trailer region of R17532 was longer than that of A2 by five bases. However, the 26 nucleotides at the terminal of the 3'leader in R17532 and the complementary sequence in the terminal of the 5'trailer region thought to be important element in the promoter of genome and antigenome respectively (Mink *et al.*, 1991), were fully conserved.

8.10 Comparison of nucleotide and deduced amino acid sequences of non-membrane protein genes between neutralization resistant and susceptible virus clones

As sequence comparison of membrane protein genes, the genome ends or intergenic regions of neutralization resistant and susceptible clones revealed no mutations which unequivocally correlated with the neutralization phenotype alteration attention turned to the non-membrane protein genes. Sequences of the NS1, NS2, N, P, M2 and L coding regions were compared between clones R3 and R11. The results showed that nucleotide sequences for the two clones were identical in the NS1, NS2, N, P and M2 genes.

The sequences of the coding region of these genes in R17532 differed a little from A2 in a range from 95 – 97% for nucleotide identity and 97 – 99% for amino acid level (Table 8.4). All of these proteins are necessary for hRSV infection and have previously been found to be highly conserved (Kumaria *et al.*, 2011; Rebuffo-Scheer *et al.*, 2011). The NS1 protein had only one amino acid substitution (Table 7.1), two substitutions occurred in the P and M2 genes (Table 7.3 and 7.4) and three substitutions in the NS2 and N protein (Table 7.1 and 7.2). One and two amino acid changes respectively observed in the NS1 and NS2 protein were also reported in two isolates by Kumaria *et al.* (2011).

The L gene was less well conserved. There were 28 nucleotide changes between R17532 and A2 (Appendix Figure 10.27), giving a percentage of nucleotide identity of 97% (Table 8.4) and two changes between the two clones of R17532 at positions 912 and 6162.

Table 8.4: Summary of percent nucleotide identity in the coding region of the NS1, NS2, N, P, M2 and L gene of R17532 and A2 strains.

Coding region	% NT ^a identity R17532 vs. A2	% AA ^b identity R17532 vs. A2
NS1	95	99
NS2	96	97
N	97	99
P	97	99
M2	97	98
L	97	98

^aNT: Nucleotide; ^bAA: Amino acid.

In the first variation of the L gene between the R17532 clones, an A in resistant clone R3.7.8.3 was changed to a G in susceptible clone R11.1.1 at position 916 resulting in a shift of amino acid from asparagine to aspartic acid at residue 306 (Appendix Figure 10.27). However, another susceptible clone R11.2 had an A at this position, the same as R3 and A2. This change is not correlated with phenotype shift. The second variation occurred at position 6162 (T → G) causing an amino acid change from phenylalanine in

clone R3 to leucine in clone R11 at residue 2054. The prevalence of this change in the virus clones derived from various passage levels of R17532 isolated from a clinical specimen in 1996 (the GLT lineage) was investigated (Table 7.8). This isolate lost resistance on passage at passage 5 on one occasion and at passage 10 on another and both resistant and susceptible clones were derived from it. Whilst both resistant clones, derived from passage 3 of this isolate, had a T at this position, all of the susceptible clones carried a G. Thus, for this lineage of the virus change at L6162 correlates with phenotype shift. However, a separate isolation of virus from the same stored specimen was made two years later. This isolate preserved the resistant phenotype to passage 10 and only resistant clones were recovered from it (the AC lineage). All three of these carried a G at L6162 demonstrating that this mutation alone is insufficient to confer susceptibility. It is necessary to postulate that at least one additional mutation is necessary and that this has already occurred by passage 2 in the GLT lineage.

The L protein is a major component of the viral RNA dependent RNA polymerase complex which also includes P, N and M2 proteins. It plays a major role in all enzymatic activities during viral replication and transcription, including capping, methylation and polyadenylation (Collins and Crowe, 2007). It has been shown that omission of this protein abrogates RNA synthesis (Yu *et al.*, 1995). Therefore, the mutation occurring in this gene at L6162 may influence hRSV infection and underly differences in replication ability between the slow-growing resistant clone R3 and fast-growing susceptible clone R11 reported by Gias (2006) as both of these clones originated from the P1-GLT virus stock.

This study has confirmed the relative resistance of low passage isolates of hRSV to neutralization by PZ and their F glycoprotein inhibitors. In culture, this resistance is transient. The switch to antibody susceptibility was not associated with changes in PZ epitopes on the F glycoprotein but may be associated with mutations in the L gene and increased rates of virus replication. Whether the resistance to neutralization of clinical isolates is an artefact of replication in cell culture or a property of the virus experienced in the infant respiratory tract remains uncertain. The results of the IMPACT study (The IMPact-RSV Study Group, 1998) indicate that prophylactic PZ ameliorates the clinical effects of hRSV infection. Antibody epitope escape mutants have been recovered from

treated patients suggesting that PZ is effective in limiting virus infection *in vivo*. However, this cannot be construed as evidence that virus *in vivo* is sensitive to neutralization as the mode of action of PZ is not known and mechanisms other than neutralization may limit virus infection. Thus, non-neutralizing anti-hRSV G glycoprotein antibodies provide *in vivo* protection, in mice acting at least partially via complement mediated pathways (Mekseepralard *et al.*, 2006). Further studies of early passage isolates possibly in authentic primary human bronchiolar cell cultures, may serve to resolve this issue.

Chapter 9: Conclusion and future work

The aim of this study was to investigate the mechanism of neutralization phenotype change by a comparison of resistant and susceptible clones of the R17532 virus isolate. This and previous studies have shown anti-F antibodies bind equally to both resistant and susceptible virus clones, but that there are striking differences in the interaction of the two viruses with the host cell. Resistant viruses bind more rapidly to HeLa cells, are less GAG dependent and are resistant, not only, to anti-F antibody but also to compounds which block activation of the fusion protein. This suggests that there are major differences in the mechanism of entry of the two clones into the cells. This however is cell-line dependent with cell lines varying in their permissiveness to antibody treated virus.

In future work it will be of interest to compare fusion kinetics between resistant and susceptible clones which may give rise to differences in susceptibility to anti-fusion inhibitors. The surface proteins of host cells involved in entry of resistant virus should also be investigated among different cell lines. It will be important also to seek confirmation of the conclusions, concerning post-translational modification of F in clones of both phenotypes by a more defined technique e.g. mass spectrometry.

The genetic basis for differences between resistant and susceptible phenotypes has proved complex. Although, on passage of the virus, genetic changes are most prevalent in the surface protein genes, none correlates simply with the phenotypic change. Sequencing of the whole genome of a susceptible and a resistant clone revealed only 4 changes, one or all of which must be responsible for the phenotypic differences. However, none of these changes correlate individually with susceptibility in other clones.

The best correlation exists between the L6162 mutation and the acquisition of susceptibility in the GLT lineage of R17532. How a change in the L gene may result in alterations in susceptibility to antibody neutralization is obscure. Mutations in the L gene have previously been associated with changes in transcription and replication rates and it is conceivable that L6162 may account for the change in replication rate in HeLa cells and that increased transcription and replication rates may affect changes in the interaction between the infected cell and virus with consequent changes in the

composition of the virion membrane. Confirmation of this interpretation could be sought by appropriate reverse genetics techniques in future work.

Although in the GLT lineage, a G at L6162 was associated with susceptibility, clones in the AC lineage with a G at position 6162 retained resistance, suggesting that additional mutations already present at passage 2 in the GLT lineage may be necessary for the acquisition of susceptibility. To test this hypothesis future work should analyse the whole genome of clones originated from the AC lineage.

Chapter 10: Appendix

	P-M	M GS sequence	
	→ IR	→ 5' UTR	
R3.7.8.3	-----GAT	<u>GGGGCAAAT</u>	12
R11.1.1		
A2	GGAAAG.G.....		

Figure 10.1: Nucleotide sequence comparison of the P-M intergenic region (P-M IR) and 5'UTR of the neutralization resistant and susceptible clones of R17532 and A2 strain.

Dots indicate identical nucleotides compared to clone R.3.7.8.3, dashes indicate alignment gaps and underlined bases indicate different nucleotides of clone R3.7.8.3 compared to another strain.

	→ M Gene Start codon	
R3.7.8.3	<u>ATG</u> GAAACATACGTGAACAAA <u>CTT</u> CACGAAGGCTCCACATACACAGCTGCTGTT	54
	M E T Y V N K L H E G S T Y T A A V	18
R11.1.1	
A2G.....	
R3.7.8.3	CAATACAATGTC <u>C</u> TAGAAAAAGACGATGACCCTGCATCACTTACAATATGGGTG	108
	Q Y N V L E K D D D P A S L T I W V	36
R11.1.1	
A2T.....	
R3.7.8.3	CCCATGTTCCAATCATCC <u>C</u> ATGCCAGCAGATTTACTTATAAAAGAACTAGCTAAT	162
	P M F Q S S M P A D L L I K E L A N	54
R11.1.1	
A2T.....	
R3.7.8.3	GTCAACATACTAGTGAAACAAATATCCACACCCAAAGGACCTTCATTAAGAGTA	216
	V N I L V K Q I S T P K G P S L R V	72
R11.1.1	
A2G.....C.....C	
R3.7.8.3	ATGATAAACTCAAGAAGTGCAGTGCTAGCACAAATGCCAGCAAATTC <u>ACTATA</u>	270
	M I N S R S A V L A Q M P S K F T I	90
R11.1.1	
A2T..C...	
R3.7.8.3	TGCGCCAATGTGTCTTGGATGAAAGAAGCAAGCTGGCATATGATGTAACCACA	324
	C A N V S L D E R S K L A Y D V T T	108
R11.1.1	
A2T.....A..A.....	
R3.7.8.3	CCCTGCGAAATCAAGGCATGTAGTCTAACATGCCTAAAAATCAAAAAATATGTTA	378
	P C E I K A C S L T C L K S K N M L	126
R11.1.1	
A2T.....G	

```

R3.7.8.3 ACTACAGTTAAAGATCTCACTATGAAAACACTCAACCCAACACATGACATCATT 432
          T T V K D L T M K T L N P T H D I I 144

R11.1.1 .....

A2 .....G.....T.....T..T...

R3.7.8.3 GCTTTATGTGAATTTGAAAATATAGTAACATCAAAAAAGTCATAATACCAACA 486
          A L C E F E N I V T S K K V I I P T 162

R11.1.1 .....

A2 .....C.....

R3.7.8.3 TACCTAAGATCCATCAGTGTCAGAAATAAAGATCTGAACACACTTGAAAATATA 540
          Y L R S I S V R N K D L N T L E N I 180

R11.1.1 .....

A2 .....

R3.7.8.3 ACAACCACCGAATTCAAAAATGCCATCACAAAATGCAAAAAATCATCCCTTACTCA 594
          T T T E F K N A I T N A K I I P Y S 198

R11.1.1 .....

A2 .....T.....T.....

R3.7.8.3 GGATTACTGTTAGTCATCACAGTGACTGACAACAAAGGAGCATTCAAATACATA 648
          G L L L V I T V T D N K G A F K Y I 216

R11.1.1 .....

A2 .....A.....

R3.7.8.3 AAGCCACAAAGTCAATTCATAGTAGATCTTGGAGCTTACCTAGAAAAAGAAAGT 702
          K P Q S Q F I V D L G A Y L E K E S 234

R11.1.1 .....

A2 .....

R3.7.8.3 ATATATTATGTTACAACAAATGGAAGCACACAGCTACACGATTTGCAATCAAA 756
          I Y Y V T T N W K H T A T R F A I K 252

R11.1.1 .....

A2 .....C.....

          Stop codon
R3.7.8.3 CCCATGGAAGATTAA 771
          P M E D XXX 256

R11.1.1 .....

A2 .....

```

Figure 10.2: Comparison of nucleotide and deduced amino acid sequences of the M gene coding region of the neutralization resistant and susceptible clones of R17532 and A2 strain.

Dots indicate identical nucleotides compared to clone R3.7.8.3 and underlined bases indicate different nucleotides of clone R3.7.8.3 compared to another strain. Deduced amino acid sequences are under the nucleotide sequence.

|→ M gene 3' UTR

R3.7.8.3 CCTTTT-CCTCTACATCAGCTAGTTGATTCATACACACTTTCTACCTACATTCT 53
R11.1.1
A2T.....TGT...A.....A.....

R3.7.8.3 TCACTTCACAAACATAATCACCAACCCTCTGTGGTTTAACCAATCAAACAAAAC 107
R11.1.1
A2C.T..C.....A..A.....C.....

R3.7.8.3 TTATCTGGAGTCTCAGATCATCCCAAGTCATTATTCATCAGATCTAGTACTCAA 161
R11.1.1
A2A....C.....G..T.....

M GE sequence

R3.7.8.3 ATAAAGTTAATAAAAA- 176
R11.1.1
A2A

Figure 10.3: Nucleotide sequence comparison of the 3'UTR of the M gene of neutralization resistant and susceptible clones of R17532 and A2 strain.

Dots indicate identical nucleotides compared to clone R.3.7.8.3, dashes indicate alignment gaps and underlined bases indicate different nucleotides of clone R3.7.8.3 compared to another strain.

SH GS sequence

|→ M-SH |→ 5' UTR
IR

R3.7.8.3 TACCCACATGGGGCAAATAAATCATCGGAGGAAATCCAACTAATCACAATATCTG 54
R11.1.1
A2 ..TA.....T.....

R3.7.8.3 TCAACATAGACAAGTCAACACGCCAAACAAAATCAACCA 93
R11.1.1
A2 .T.....C....A...T...G.....

Figure 10.4: Nucleotide sequence comparison of the M-SH intergenic region (M-SH IR) and 5'UTR of the neutralization resistant and susceptible clones of R17532 and A2 strain.

Dots indicate identical nucleotides compared to clone R3.7.8.3 and underlined bases indicate different nucleotides of clone R3.7.8.3 compared to another strain.

		PZ		
		EC ₅₀	SH GE sequence	→ SH-G IR
R5.3	89		<u>AGTTAATTAAAAAAA</u> TAGTCATAACAATGAACTA <u>AGATATTAAGACT</u>	32
R5.1	70	-.....	
R3.7.8.3	48		
R5.2	42		
R3.7.8.17	21		
R3.2.4	12	-.....	
R2.44	7	-.....	
R11.1.1	5	-.....	
R5.14	3		
R11.2	2.7	-.....	
A2		-...G....C.....	
G GS sequence				
→ 5' UTR				
R5.3	89		AACAACAACGTT <u>GGGGCAAAT</u> GCAAAC	59
R5.1	70		
R3.7.8.3	48		
R5.2	42		
R3.7.8.17	21		
R3.2.4	12		
R2.44	7		
R11.1.1	5		
R5.14	3		
R11.2	2.7		
A2		T...A.....	

Figure 10.7: Nucleotide sequence comparison of the SH GE sequence, the SH-G intergenic region and 5'UTR of the neutralization resistant and susceptible clones of R17532 and A2 strain. Dots indicate identical nucleotides compared to clone R5.3, dashes indicate alignment gaps and underlined bases indicate different nucleotides of clone R5.3 compared to another strain.

PZ Cytoplasmic tail →
 EC₅₀ | → G Gene Start codon

R5.3	89	<u>ATG</u> TCCAAAACCAAGGACCAACGCACCGCCAAGACACTAGAAAAGACC	48
		M S K T K D Q R T A K T L E K T	16
R5.1	70	
R3.7.8.3	48	
R5.2	42	
R3.7.8.17	21	
R3.2.4	12	
R2.44	7	
R11.1.1	5	
R5.14	3	
R11.2	2.7	
A2	A.....T.....T.....G..... N R	

R5.3	89	TGGGACTCTCAATCATCTATTATTTCATATCATCGTGCTTATACAAG	96
		W D T L N H L L F I S S C L Y K	32
R5.1	70	
R3.7.8.3	48	
R5.2	42	
R3.7.8.17	21	
R3.2.4	12	
R2.44	7	
R11.1.1	5	
R5.14	3	
R11.2	2.7	
A2	T.....T.....	

←|→

R5.3	89	TTAAATCTTAAATCTATAGCACAAATCACATTATCCATTCTGGCAATG	144
		L N L K S I A Q I T L S I L A M	48
R5.1	70	
R3.7.8.3	48	
R5.2	42	
R3.7.8.17	21	
R3.2.4	12	
R2.44	7	
R11.1.1	5	
R5.14	3	
R11.2	2.7	
A2	G..... V	

PZ
EC₅₀ Hydrophobic transmembrane domain ←|

R5.3	89	ATAATCTCAACTTCACTTATAATTGTAGCCATCATATTCATAGCCTCA	192
		I I S T S L I I <u>V</u> A I I F I A S	64
R5.1	70	
R3.7.8.3	48	
R5.2	42	
R3.7.8.17	21	
R3.2.4	12	
R2.44	7	
R11.1.1	5	
R5.14	3	
R11.2	2.7	
A2	C.....G	
		A	

⇒ Ectodomain |→ Mucin-like VR1

R5.3	89	GCAAACAACAAAGTCACACTAACAACCTGCAATCATACAAGATGCAACA	240
		A N <u>N</u> K V T <u>L</u> T T A I I Q D A T	80
R5.1	70	
R3.7.8.3	48	
R5.2	42	
R3.7.8.17	21	
R3.2.4	12	
R2.44	7	
R11.1.1	5	
R5.14	3	
R11.2	2.7	
A2	C.....C.....	
		H P	

R5.3	89	AGCCAGATCAAGAACACAACCCCAACATACCTGACCCAGAATCCCCAG	288
		S Q I K N T T P T Y <u>L</u> T Q N P Q	96
R5.1	70	
R3.7.8.3	48	
R5.2	42	
R3.7.8.17	21	
R3.2.4	12	
R2.44	7	
R11.1.1	5	
R5.14	3	
R11.2	2.7	
A2	C.....T.....	

PZ
EC₅₀

R5.3 89 CTTGGAATCAGCTTCTTTAATCTGTCTGGAACTACATCACAAACCACC 336
L G I S F F N L S G T T S Q T T 112

R5.1 70

R3.7.8.3 48

R5.2 42

R3.7.8.17 21

R3.2.4 12

R2.44 7

R11.1.1 5

R5.14 3

R11.2 2.7

A2TCC..C.....C.....A..T.....T.....
P S P E I I

R5.3 89 GCCACACTAGCTTTAAACAACACCAAGTGTGCGAGTCAATCCTGCAATCT 384
A T L A L T T P S V E S I L Q S 128

R5.1 70

R3.7.8.3 48

R5.2 42

R3.7.8.17 21

R3.2.4 12

R2.44 7

R11.1.1 5

R5.14 3

R11.2 2.7

A2 A...T.....C.....G.A...A.....C.....C
T I S G K T

R5.3 89 ACAACAGTCAAGACCAAAAAACAACAACAACC^UCAAATACAACCCAGC 432
T T V K T K N T T T T Q I Q P S 144

R5.1 70

R3.7.8.3 48

R5.2 42

R3.7.8.17 21

R3.2.4 12

R2.44 7

R11.1.1 5

R5.14 3

R11.2 2.7

A2T...C.....
T

PZ
EC₅₀ ← |

R5.3	89	AAGCCCACCACAAAAACAACGCCAAAAACAACCGCCAAACAAACCCAAT	480
		K P T T K Q R Q N K P P N K P N	160
R5.1	70	
R3.7.8.3	48	
R5.2	42	
R3.7.8.17	21	
R3.2.4	12	
R2.44	7	
R11.1.1	5	
R5.14	3	
R11.2	2.7	
A2	A.....G..... S	

| → Central region segment

R5.3	89	AATGATTTTCACTTTGAAGTGTTCAACTTTGTACCCTGCAGCATATGC	528
		N D F H F E V F N F V P C S I C	176
R5.1	70	
R3.7.8.3	48	
R5.2	42	
R3.7.8.17	21	
R3.2.4	12	
R2.44	7	
R11.1.1	5	
R5.14	3	
R11.2	2.7	
A2		

← |

R5.3	89	AGCAACAATCCAACCTTGCTGGGCCATCTGCAAAAAGAATACCAAGCAA	576
		S N N P T C W A I C K R I P S K	192
R5.1	70	
R3.7.8.3	48	
R5.2	42	
R3.7.8.17	21	
R3.2.4	12	
R2.44	7	
R11.1.1	5	
R5.14	3	
R11.2	2.7	
A2	C.....T.....A..... N	

PZ
 EC₅₀ | → Mucin-like VR2

R5.3 89 AAACCTGGAAAGAAAACCACCACCAAGCCCACAAAAAACCAACCATC 624
 K P G K K T T T K P T K K P T I 208

R5.1 70
 R3.7.8.3 48
 R5.2 42
 R3.7.8.17 21
 R3.2.4 12
 R2.44 7
 R11.1.1 5
 R5.14 3
 R11.2 2.7
 A2A.....T.....C..
 L

R5.3 89 AAGACAACCAAAAAAGATCTCAAACCTCAAACCACAAAACCAAAGGAA 672
 K T T K K D L K P Q T T K P K E 224

R5.1 70
 R3.7.8.3 48
 R5.2 42
 R3.7.8.17 21
 R3.2.4 12
 R2.44 7
 R11.1.1 5
 R5.14 3
 R11.2 2.7
 A2C.....T..T.....
 P S

R5.3 89 GCACCTACCACCAAGCCCACAGAAAAGCCAACCATCAACATCACCAAA 720
 A P T T K P T E K P T I N I T K 240

R5.1 70
 R3.7.8.3 48
 R5.2 42
 R3.7.8.17 21
 R3.2.4 12
 R2.44 7
 R11.1.1 5
 R5.14 3
 R11.2 2.7
 A2 .T...C.....G.....C.....
 V E T

PZ
EC₅₀

R5.3	89	<u>C</u> CAAACATCAGAACTACACTGCTCACCAACAGTACCACAGGAAATCTA 768 P N I R T T L L T N S T T G N L 256
R5.1	70
R3.7.8.3	48
R5.2	42
R3.7.8.17	21
R3.2.4	12
R2.44	7
R11.1.1	5
R5.14	3
R11.2	2.7
A2		A.....T.....A.....TC..AC.....C. T I S N P
R5.3	89	GAACACACAAGTCAAGAGGAAAACCTCCATTCAACCTCCTCCGAAGGC 816 E H T S Q E E T L H S T S S E G 272
R5.1	70
R3.7.8.3	48
R5.2	42
R3.7.8.17	21
R3.2.4	12
R2.44	7
R11.1.1	5
R5.14	3
R11.2	2.7
A2		...T.....AT.....T....C....T..... L M F
R5.3	89	AATACAAGCCCTTCACAAGTCTATACAACATCCGAGTACCTATCACAA 864 N T S P S Q V Y T T S E Y L S Q 288
R5.1	70
R3.7.8.3	48
R5.2	42
R3.7.8.17	21
R3.2.4	12
R2.44	7
R11.1.1	5
R5.14	3
R11.2	2.7
A2		...C.....T.....C.....C..... P S P

	PZ		Stop codon
	EC ₅₀		
R5.3	89	CCT <u>CC</u> ATCTCCAT <u>CC</u> AAACATAA <u>CAA</u> ACCTG <u>TAG</u> 897	
		P P S P S N I T N L XXX 298	
R5.1	70C.....	
		T	
R3.7.8.3	48	
R5.2	42	
R3.7.8.17	21	
R3.2.4	12C.....	
		T	
R2.44	7	
R11.1.1	5C.....	
		T	
R5.14	3	
R11.2	2.7C.....	
		T	
A2		...T.....C.....C.C..CG..A....	
		S P T P R Q	

Figure 10.8: Comparison of nucleotide and deduced amino acid sequences of the G gene coding region of the neutralization resistant and susceptible clones of R17532 and A2 strain.

Dots indicate identical nucleotides compared to clone R5.3 and underlined bases indicate different nucleotides of clone R5.3 compared to another strain. Deduced amino acid sequences are under the nucleotide sequence.

	PZ	→ 3' UTR	→ G-F IR
	EC ₅₀	G GE sequence	
R5.3	89	<u>TAGTCA</u> -TTAAAAA <u>GCGTATTATTGCAAAAAACCATGACTAAATCAAAC</u> 46	
		XXX	
R5.1	70C.....	
R3.7.8.3	48	
R5.2	42	
R3.7.8.17	21	
R3.2.4	12	
R2.44	7	
R11.1.1	5	
R5.14	3	
R11.2	2.7	
A2		...T.C.....-A.....CA.....G.....C.C.T....	

R5.3	89	AGAATCAA <u>AAATAAG</u> CTCT 64
R5.1	70
R3.7.8.3	48
R5.2	42
R3.7.8.17	21
R3.2.4	12
R2.44	7
R11.1.1	5
R5.14	3
R11.2	2.7
A2	A.....

Figure 10.9: Nucleotide sequence comparison of the 3'UTR of the G gene and G-F intergenic region of the neutralization resistant and susceptible clones of R17532 and A2 strain.

Dots indicate identical nucleotides compared to clone R5.3 and underlined bases indicate different nucleotides of clone R5.3 compared to another strain.

	PZ	F GS - signal
	EC ₅₀	→ 5'UTR
R5.3	89	<u>GGGGCAAAT</u> AACA 13
R5.1	70
R3.7.8.3	48
R5.2	42
R3.7.8.17	21
R3.2.4	12
R2.44	7
R11.1.1	5
R5.14	3
R11.2	2.7
A2	

Figure 10.10: Nucleotide sequence comparison of the SH-G intergenic region and 5'UTR of the neutralization resistant and susceptible clones of R17532 and A2 strain.

Dots indicate identical nucleotides compared to clone R5.3 and underlined bases indicate different nucleotides of clone R5.3 compared to another strain.

NH₂-terminal signal peptide

PZ
EC₅₀ | → F Gene Start codon

R5.3	89	<u>A</u> TG <u>G</u> AGTTG <u>C</u> CAATCCTCAAAA <u>C</u> AAATGCAATTACCACAATCCT <u>T</u> GCT 48	
		M E L P I L K T N A I T T I L A	16
R5.1	70	
R3.7.8.3	48	
R5.2	42	
R3.7.8.17	21	
R3.2.4	12	
R2.44	7	
R11.1.1	5	
R5.14	3	
R11.2	2.7	
A2	T.....T.....G.....CA..	
		L A T	
		←	
R5.3	89	GCAGTCACACTCTGTTTCGCTTCCAGTCAAAACATCACTGAAGAATTT 96	
		A V T L C F A S S Q N I T E E F	32
R5.1	70	
R3.7.8.3	48	
R5.2	42	
R3.7.8.17	21	
R3.2.4	12	
R2.44	7	
R11.1.1	5	
R5.14	3	
R11.2	2.7	
A2	T.T.....T.....TG.....	
		F G	
R5.3	89	TATCAATCAACATGCAGTGCAGTTAGCAAAGGCTATCTTAGTGCTTTA 144	
		Y Q S T C S A V S K G Y L S A L	48
R5.1	70	
R3.7.8.3	48	
R5.2	42	
R3.7.8.17	21	
R3.2.4	12	
R2.44	7	
R11.1.1	5	
R5.14	3	
R11.2	2.7	
A2	C.G	

	PZ		
	EC ₅₀	→ Heptad repeat 3	
R5.3	89	AGAACTGGTTGGTATACTAGTGTATAACTATAGAATTAAGTAATATC	192
		R T G W Y T S V I T I E L S N I	64
R5.1	70	
R3.7.8.3	48	
R5.2	42	
R3.7.8.17	21	
R3.2.4	12	
R2.44	7	
R11.1.1	5	
R5.14	3	
R11.2	2.7	
A2	C.....	
R5.3	89	AAGGAAAATAAGTGTAATGGAACAGACGCTAAGGTAATAATGATAAAA	240
		K E N K C N G T D A K V K L I K	80
R5.1	70	
R3.7.8.3	48	
R5.2	42	
R3.7.8.17	21	
R3.2.4	12	
R2.44	7	
R11.1.1	5	
R5.14	3	
R11.2	2.7	
A2	T.....	
R5.3	89	CAAGAATTAGATAAAATATAAAAAATGCTGTAACAGAAATTGCAGTTGCTC	288
		Q E L D K Y K N A V T E L Q L L	96
R5.1	70	
R3.7.8.3	48	
R5.2	42	
R3.7.8.17	21	
R3.2.4	12	
R2.44	7	
R11.1.1	5	
R5.14	3	
R11.2	2.7	
A2	T.....	

	PZ	Heptad	Cleavage site I	
	EC ₅₀	repeat 3 ←	←→	
R5.3	89	ATGCAAAGCACACCAGCAGCCAACAATCGAGCCAGAAGAGAACTACCA		336
		M Q S T P A A N N R A R R E L P		112
R5.1	70		
R3.7.8.3	48		
R5.2	42		
R3.7.8.17	21T.....		
		S		
R3.2.4	12		
R2.44	7		
R11.1.1	5		
R5.14	3		
R11.2	2.7		
A2	C..A.A.....		
		P T		

R5.3	89	AAGTTTATGAATTATACACTCAACAACACCAAAAAATACCAATGTAACA		384
		K F M N Y T L N N T K N T N V T		128
R5.1	70		
R3.7.8.3	48		
R5.2	42		
R3.7.8.17	21		
R3.2.4	12		
R2.44	7		
R11.1.1	5		
R5.14	3		
R11.2	2.7		
A2		.G.....TG.....A.....		
		R A K		

F2 Subunit ←|→ F1 Subunit

| Cleavage site II|→ Fusion peptide

R5.3	89	TTAAGCAAGAAAAGGAAAAGAAGATTTCTTGGCTTTTGTAGGTGTT		432
		L S K K R K R R F L G F L L G V		144
R5.1	70		
R3.7.8.3	48		
R5.2	42		
R3.7.8.17	21		
R3.2.4	12		
R2.44	7		
R11.1.1	5		
R5.14	3		
R11.2	2.7		
A2	TT.....		
		V		

PZ Fusion
EC₅₀ peptide ←|→ Heptad repeat 1

R5.3 89 GGATCTGCAATCGCCAGTGGCATTGCTGTATCTAAAGTCCTGCACCTA 480
G S A I A S G I A V S K V L H L 160

R5.1 70G.....
M

R3.7.8.3 48

R5.2 42

R3.7.8.17 21

R3.2.4 12

R2.44 7

R11.1.1 5G.....
M

R5.14 3

R11.2 2.7G.....
M

A2G.G.....G.....
V

R5.3 89 GAAGGGGAAGTGAACAAAAATCAAAAGTGCTCTACTATCCACAAACAAG 528
E G E V N K I K S A L L S T N K 176

R5.1 70

R3.7.8.3 48

R5.2 42

R3.7.8.17 21

R3.2.4 12

R2.44 7

R11.1.1 5

R5.14 3

R11.2 2.7

A2G.....

R5.3 89 GCTGTAGTCAGCTTATCAAATGGAGTTAGTGTCTTAACCAGCAAAGTG 576
A V V S L S N G V S V L T S K V 192

R5.1 70

R3.7.8.3 48

R5.2 42

R3.7.8.17 21

R3.2.4 12

R2.44 7

R11.1.1 5

R5.14 3

R11.2 2.7

A2 ...C.....
L

	PZ		
	EC ₅₀		Heptad repeat 1 ←
R5.3	89	TTAGACCTCAAAAACTATATAGATAAACAGTTGTTACCTATTGTGAAC	624
		L D L K N Y I D K Q L L P I V N	208
R5.1	70	
R3.7.8.3	48	
R5.2	42	
R3.7.8.17	21	
R3.2.4	12	
R2.44	7	
R11.1.1	5	
R5.14	3	
R11.2	2.7	
A2	A.....	
R5.3	89	AAGCAAAGCTGCAGCATATCAAACATTGAAACTGTGATAGAATTCCAA	672
		K Q S C S I S N I E T V I E F Q	224
R5.1	70	
R3.7.8.3	48	
R5.2	42	
R3.7.8.17	21	
R3.2.4	12	
R2.44	7	
R11.1.1	5	
R5.14	3	
R11.2	2.7	
A2	T.A.....G.....	
R5.3	89	CAAAAGAACAACAGACTACTAGAGATTACCAGGGAATTTAGTGTTAAT	720
		Q K N N R L L E I T R E F S V N	240
R5.1	70	
R3.7.8.3	48	
R5.2	42	
R3.7.8.17	21	
R3.2.4	12	
R2.44	7	
R11.1.1	5	
R5.14	3	
R11.2	2.7	
A2		

PZ
EC₅₀

R5.3	89	GCAGGTGTA ^A ACTACACCTGTAAGCACTTATATGTTAACAAATAGTGAA 768 A G V T T P V S T Y M L T N S E 256
R5.1	70
R3.7.8.3	48
R5.2	42
R3.7.8.17	21
R3.2.4	12
R2.44	7
R11.1.1	5
R5.14	3
R11.2	2.7
A2	C.....T.....

|→

R5.3	89	TTATTATCATTAATCAATGATATGCCTATAACAAATGATCAGAAAAAG 816 L L S L I N D M P I T N D Q K K 272
R5.1	70
R3.7.8.3	48
R5.2	42
R3.7.8.17	21
R3.2.4	12
R2.44	7
R11.1.1	5
R5.14	3
R11.2	2.7
A2	G.....

binding site
Palivizumab ←|

R5.3	89	TTAATGTCCAACAATGTTCAAATAGTTAGACAGCAAAGTTACTCTATC 864 L M S N N V Q I V R Q Q S Y S I 288
R5.1	70
R3.7.8.3	48
R5.2	42
R3.7.8.17	21
R3.2.4	12
R2.44	7
R11.1.1	5
R5.14	3
R11.2	2.7
A2	G.....

PZ
EC₅₀

R5.3	89	ATGTCCATAATAAAGGAGGAAGTCTTAGCATATGTAGTACAATTACCA 912
		M S I I K E E V L A Y V V Q L P 304
R5.1	70
R3.7.8.3	48
R5.2	42
R3.7.8.17	21
R3.2.4	12
R2.44	7
R11.1.1	5
R5.14	3
R11.2	2.7
A2	G.....

|→ Cysteine-rich domain

R5.3	89	CTATATGGTGTAATAGATACACCTTGTGGAAACTACACACATCCCCT 960
		L Y G V I D T P C W K L H T S P 320
R5.1	70
R3.7.8.3	48
R5.2	42
R3.7.8.17	21
R3.2.4	12A.....
R2.44	7
R11.1.1	5
R5.14	3
R11.2	2.7
A2	T.....C.....

R5.3	89	CTATGTACAACCAACACAAAGGAAGGGTCCAACATCTGTTTAAACAAGA 1008
		L C T T N T K E G S N I C L T R 336
R5.1	70
R3.7.8.3	48
R5.2	42
R3.7.8.17	21
R3.2.4	12
R2.44	7
R11.1.1	5
R5.14	3
R11.2	2.7
A2	A.....

PZ
EC₅₀

R5.3	89	ACCGACAGAGGATGGTACTGTGACAATGCAGGATCAGT <u>G</u> TCTTTCTTC	1056
		T D R G W Y C D N A G S V S F F	352
R5.1	70	
R3.7.8.3	48	
R5.2	42	
R3.7.8.17	21	
R3.2.4	12	
R2.44	7	
R11.1.1	5	
R5.14	3	
R11.2	2.7	
A2		..T.....A.....	
R5.3	89	CCACAAGCTGAAACATGTAAAGTTCAATCGAATCGAGTATTTTGTGAC	1104
		P Q A E T C K V <u>Q</u> S N R V F C D	352
R5.1	70	
R3.7.8.3	48	
R5.2	42	
R3.7.8.17	21	
R3.2.4	12G.....	
R2.44	7	
R11.1.1	5	
R5.14	3	
R11.2	2.7	
A2	A.....	
R5.3	89	ACAATGAACAGTTTAAACATTACCAAGTGAAGTAAATCTCTGCAACATT	1152
		T M N S L T L P S E V N L C N I	384
R5.1	70	
R3.7.8.3	48	
R5.2	42	
R3.7.8.17	21	
R3.2.4	12	
R2.44	7	
R11.1.1	5	
R5.14	3	
R11.2	2.7	
A2	A.....TG..	
		I V	

	PZ			
	EC ₅₀			
R5.3	89	GACATATTCAACCCCAAATATGATTG <u>C</u> AAAAATTATGACTTCAAAAACA	1200	
		D I F N P K Y D C K I M T S K T	400	
R5.1	70		
R3.7.8.3	48		
R5.2	42		
R3.7.8.17	21		
R3.2.4	12		
R2.44	7		
R11.1.1	5		
R5.14	3		
R11.2	2.7		
A2	T.....		
R5.3	89	GATGTAAGCAGCTCTGTTATCACATCTCTAGGAGCCATTGTGTCATGC	1248	
		D V S S S V I T S L G A I V S C	416	
R5.1	70		
R3.7.8.3	48		
R5.2	42		
R3.7.8.17	21		
R3.2.4	12		
R2.44	7		
R11.1.1	5		
R5.14	3		
R11.2	2.7		
A2	C.....		
R5.3	89	TATGGCAAAACTAAATGTACAGCATCCAATAAAAAATCGTGGAAATCATA	1296	
		Y G K T K C T A S N K N R G I I	432	
R5.1	70		
R3.7.8.3	48		
R5.2	42		
R3.7.8.17	21		
R3.2.4	12		
R2.44	7		
R11.1.1	5		
R5.14	3		
R11.2	2.7		
A2	C.....		

	PZ		
	EC ₅₀	Cysteine-rich Domain ←	
R5.3	89	AAGACATTTTCTAACGGGTG <u>T</u> GATTATGTATCAAATAAGGGGGTGGAC	1344
		K T F S N G C D Y V S N K G V D	448
R5.1	70	
R3.7.8.3	48	
R5.2	42	
R3.7.8.17	21	
R3.2.4	12	
R2.44	7	
R11.1.1	5	
R5.14	3	
R11.2	2.7	
A2	C.....A...A.....	M
R5.3	89	ACTGTATCTGTAGGTAATACATTATATTTATGTAAATAAGCAAGAAGGA	1392
		T V S V G N T L Y Y V N K Q E G	464
R5.1	70	
R3.7.8.3	48	
R5.2	42	
R3.7.8.17	21	
R3.2.4	12	
R2.44	7	
R11.1.1	5	
R5.14	3	
R11.2	2.7	
A2	G.....C.....T	
		→ Heptad repeat 2	
R5.3	89	AAAAGTCTCTATGTAAAAGGTGAACCAATAATAAATTTCTATGACCCA	1440
		K S L Y V K G E P I I N F Y D P	480
R5.1	70	
R3.7.8.3	48	
R5.2	42	
R3.7.8.17	21	
R3.2.4	12	
R2.44	7	
R11.1.1	5	
R5.14	3	
R11.2	2.7	
A2		

PZ
EC₅₀

R5.3	89	TTAGT <u>G</u> TTCCCTTCTGATGAATTTGATGCATCAATATCTCAAGTCAAT	1488
		L V F P S D E F D A S I S Q V N	496
R5.1	70	
R3.7.8.3	48	
R5.2	42	
R3.7.8.17	21	
R3.2.4	12	
R2.44	7	
R11.1.1	5	
R5.14	3	
R11.2	2.7	
A2	A.....C.....	

R5.3	89	GAGAAGATTAACCAGAGCCTAGCATTATTTCGTAAATCTGATGAATTA	1536
		E K I N Q S L A F I R K S D E L	512
R5.1	70	
R3.7.8.3	48	
R5.2	42	
R3.7.8.17	21	
R3.2.4	12	
R2.44	7	
R11.1.1	5	
R5.14	3	
R11.2	2.7	
A2	C.....	

Domain

Heptad repeat 2 ←|→ Transmembrane

R5.3	89	TTACATAATGTAAATGTTGGTAAATCCACCACAAATATCATGATAACT	1584
		L H N V N V G K S T T N I M I T	528
R5.1	70	
R3.7.8.3	48	
R5.2	42	
R3.7.8.17	21	
R3.2.4	12	
R2.44	7	
R11.1.1	5	
R5.14	3	
R11.2	2.7	
A2	C.....	

PZ
EC₅₀

R5.3	89	ACTATAATTATAGTGATTATAGTAATATTGTTATTATTAATTGCAGTT	1632
		T I I I V I I V I L L L I A V	544
R5.1	70	
R3.7.8.3	48	
R5.2	42	
R3.7.8.17	21	
R3.2.4	12	
R2.44	7	
R11.1.1	5	
R5.14	3	
R11.2	2.7	
A2	C..... S	

		Transmembrane domain ← → Cytoplasmic tail	
R5.3	89	GGACTGTTCCCTATACTGCAAGGCCAGAAGCACACCAGTCACACTAAGC	1680
		G L F L Y C K A R S T P V T L S	560
R5.1	70	
R3.7.8.3	48	
R5.2	42	
R3.7.8.17	21	
R3.2.4	12	
R2.44	7	
R11.1.1	5	
R5.14	3	
R11.2	2.7	
A2	C..T.....T..... L	

			← Stop codon
R5.3	89	AAGGATCAACTGAGTGGTATAAAATAATATTGCATTTAGTAACTGA	1725
		K D Q L S G I N N I A F S N XXX	574
R5.1	70	
R3.7.8.3	48	
R5.2	42	
R3.7.8.17	21	
R3.2.4	12	
R2.44	7	
R11.1.1	5	
R5.14	3	
R11.2	2.7	
A2		..A.....A.	

Figure 10.11: Comparison of nucleotide and deduced amino acid sequences of the F gene coding region of the neutralization resistant and susceptible clones of R17532 and A2 strain.

Dots indicate identical nucleotides compared to clone R5.3 and underlined bases indicate different nucleotides of clone R5.3 compared to another strain. Deduced amino acid sequences are under the nucleotide sequence.

	PZ		
	EC ₅₀	→ F Gene 3' UTR	
R5.3	89	ATAAAAATAG <u>T</u> ACCTAATCATGTTCTTACAATGGTT <u>C</u> ACTATCC <u>G</u> ATC	48
R5.1	70	
R3.7.8.3	48	
R5.2	42	
R3.7.8.17	21	
R3.2.4	12	
R2.44	7	
R11.1.1	5	
R5.14	3	
R11.2	2.7	
A2	C.....T.....T.C..	
R5.3	89	ATAGACAACCCATCTATCATTGGATTTTCTTAAAG <u>T</u> CTGAACTTCAT <u>T</u>	96
R5.1	70	
R3.7.8.3	48	
R5.2	42	
R3.7.8.17	21	
R3.2.4	12	
R2.44	7	
R11.1.1	5	
R5.14	3	
R11.2	2.7	
A2	G.....A.....C	

	PZ		
	EC ₅₀		
R5.3	89	<u>G</u> CAACTCTCATCTATAAAACCATCTCACTTACACTATTTAAGTAGATTC	144
R5.1	70	
R3.7.8.3	48	
R5.2	42	
R3.7.8.17	21	
R3.2.4	12	
R2.44	7	
R11.1.1	5	
R5.14	3	
R11.2	2.7	
A2		.A.....	

		F GE sequence	
R5.3	89	CTATTTTAT <u>AGTTATATAAAA</u>	165
R5.1	70	
R3.7.8.3	48	
R5.2	42	
R3.7.8.17	21	
R3.2.4	12	
R2.44	7	
R11.1.1	5	
R5.14	3	
R11.2	2.7	
A2		

Figure 10.12: Nucleotide sequence comparison of the 3'UTR of the F gene of the neutralization resistant and susceptible clones of R17532 and A2 strain.

Dots indicate identical nucleotides compared to clone R5.3 and underlined bases indicate different nucleotides of clone R5.3 compared to another strain.

	→ NS1 Gene Start codon		
R3.7.8.3	<u>ATG</u> GGCAGCAATTCATTGAGTATGATAAAAGTTAGATTACAAAATTTATTTGAC	54	
	M G S N S L S M I K V R L Q N L F D	18	
R11.1.1		
A2G.....		
R3.7.8.3	AATGATGAAGTAGCATTGTTAAAAATAAC <u>CT</u> GCTATACTGACAAAT <u>TG</u> AATACAT	108	
	N D E V A L L K I T C Y T D K L I H	36	
R11.1.1		
A2A.....T.....A.....		

```

R3.7.8.3  TTAACTTAATGCTTTGGCTAAGGCAGTGATACATAACAATCAAATTGAATGGCATT 162
          L T N A L A K A V I H T I K L N G I 54

R11.1.1  .....

A2       .....C.....

R3.7.8.3  GTATTTGTGCATGTTATTACAAGTAGTGATATTTGCCCTAATAATAATATTGTA 216
          V F V H V I T S S D I C P N N N I V 72

R11.1.1  .....

A2       .....

R3.7.8.3  GTGAAATCCAACTTCACAACAATGCCAGTGTTACAAAATGGAGGTTATATATGG 270
          V K S N F T T M P V L Q N G G Y I W 90

R11.1.1  .....

A2       ..A.....T.....AC.....

R3.7.8.3  GAAATGATGGAATTAACACACTGCTCTCAACCCAATGGCCTAATAGATGACAAT 324
          E M M E L T H C S Q P N G L I D D N 108

R11.1.1  .....

A2       .....T.....T.....T...C.....
                                     L

R3.7.8.3  TGTGAAATCAAATTCTCCAAAAAAACTAAGCGATTCAACAATGACCAACTATATG 378
          C E I K F S K K L S D S T M T N Y M 126

R11.1.1  .....

A2       .....T.....T.....T.....

                                     Stop codon
R3.7.8.3  AATCAATTATCTGAATTACTTGGATTTGATCTTAATCCATAA 420
          N Q L S E L L G F D L N P XXX 140

R11.1.1  .....

A2       .....

```

Figure 10.13: Comparison of nucleotide and deduced amino acid sequences of the NS1 gene coding region of the neutralization resistant and susceptible clones of R17532 and A2 strain.

Dots indicate identical nucleotides compared to clone R3.7.8.3 and underlined bases indicate different nucleotides of clone R3.7.8.3 compared to another strain. Deduced amino acid sequences are under the nucleotide sequence

```

      |→ NS1 Gene 3'UTR                                NS1 GE sequence
R11  ATTATAATAAAATATCAACTAGAAATCAGTGTCACTAACACCATTAGTTAATATAAAA 57
R3   .....
A2   .....T.....A.....

```

Figure 10.14: Nucleotide sequence comparison of the 3'UTR of the NS1 gene of neutralization resistant and susceptible clones of R17532 and A2 strain.

Dots indicate identical nucleotides compared to clone R.3.7.8.3 and underlined bases indicate different nucleotides of clone R3.7.8.3 compared to another strain.

|→ N Gene Start codon

R3.7.8.3 ATGGCTCTTAGCAAAGTCAAGTTGAACGATACACTCAACAAAGATCAACTTCTG 54
M A L S K V K L N D T L N K D Q L L 18

R11.1.1

A2T.....

R3.7.8.3 TCATCCAGCAAATACACCATCCAACGGAGCACAGGAGATAGTATTGATACTCCT 108
S S S K Y T I Q R S T G D S I D T P 36

R11.1.1

A2

R3.7.8.3 AATTATGATGTACAGAAACACATCAACAAGTTATGTGGCATGTTATTAATCACA 162
N Y D V Q K H I N K L C G M L L I T 54

R11.1.1

A2G.....T.....

R3.7.8.3 GAAGATGCTAATCATAAATTCAGTGGGGTAATAGGTATGTTATATGCTATGTCT 216
E D A N H K F T G V I G M L Y A M S 72

R11.1.1

A2T.....G.....
L

R3.7.8.3 AGATTAGGAAGAGAAGACACCATAAAAATACTCAGAGATGCGGGATATCATGTA 270
R L G R E D T I K I L R D A G Y H V 90

R11.1.1

A2 ..G.....

R3.7.8.3 AAAGCAAATGGAGTGGATGTAACAACACATCGTCAAGACATTAATGGGAAAGAA 324
K A N G V D V T T H R Q D I N G K E 108

R11.1.1

A2A.....A.....

R3.7.8.3 ATGAAATTTGAAGTGTTAACATTGGCAAGCTTAACAACACTGAAATTCAAATCAAC 378
M K F E V L T L A S L T T E I Q I N 126

R11.1.1

A2

R3.7.8.3 ATTGAGATAGAATCTAGAAAATCCTACAAAAAATGCTAAAAGAAATGGGAGAG 432
I E I E S R K S Y K K M L K E M G E 144

R11.1.1

A2

R3.7.8.3 GTAGCTCCAGAATACAGGCATGACTCTCCTGATTGTGGGATGATAGTATTATGT 486
V A P E Y R H D S P D C G M I V L C 162

R11.1.1

A2A.....
I

R3.7.8.3 ATAGCAGCATTAGTAATAACCAAATTAGCAGCAGGGGATAGATCTGGTCTCACA 540
I A A L V I T K L A A G D R S G L T 180

R11.1.1

A2T.....C.....T....

R3.7.8.3 GCTGTAATTAGGAGAGCTAATAATGTTCTAAAAAATGAAATGAAACGTTATAAA 594
A V I R R A N N V L K N E M K R Y K 198

R11.1.1

A2 ..C..G.....C.....C...

R3.7.8.3 GGCTTACTACCAAAGGATATAGCCAACAGCTTCTATGAAAGTGTGAAAAATAT 648
G L L P K D I A N S F Y E V F E K Y 216

R11.1.1

A2C.....C.....C.
H

R3.7.8.3 CCTCACTTTATAGATGTTTTTGTTCATTTTGGTATAGCACAAATCTTCTACCAGA 702
P H F I D V F V H F G I A Q S S T R 234

R11.1.1

A2 ..C.....

R3.7.8.3 GGTGGCAGTAGAGTTGAAGGGATTTTTGCAGGATTGTTTATGAATGCCTATGGT 756
G G S R V E G I F A G L F M N A Y G 252

R11.1.1

A2

R3.7.8.3 GCAGGGCAAGTGATGTTACGGTGGGGGTCTTAGCAAAATCAGTTAAAAATATT 810
A G Q V M L R W G V L A K S V K N I 270

R11.1.1

A2A.....

R3.7.8.3 ATGCTAGGACACGCTAGTGTGCAAGCAGAAATGGAACAAGTTGTGGAGGTTTAT 864
M L G H A S V Q A E M E Q V V E V Y 288

R11.1.1

A2 ...T.....T.....T.....

R3.7.8.3 GAATATGCCCAAAAATTGGGTGGAGAAGCAGGATTCTACCATATATTGAACAAC 918
E Y A Q K L G G E A G F Y H I L N N 306

R11.1.1

A2T.....

R3.7.8.3 CCAAAAGCATCATTATTATCTTTGACTCAATTCCCCACTTTTCCAGTGTAGTA 972
P K A S L L S L T Q F P H F S S V V 324

R11.1.1

A2T..T.....C.....

```

R3.7.8.3 TTAGGCAATGCTGCTGGCCTAGGCATAATGGGAGAATACAGAGGTACACCAAGG 1026
          L G N A A G L G I M G E Y R G T P R 342
R11.1.1 .....
A2 .....G.....G...

R3.7.8.3 AATCAAGATCTATATGATGCTGCAAAGGCATATGCTGAACAACCTCAAAGAAAAT 1080
          N Q D L Y D A A K A Y A E Q L K E N 360
R11.1.1 .....
A2 .....A.....

R3.7.8.3 GGTGTGATTAACCTACAGTGTATTAGACTTGACAGCAGAAGAAGACTAGAGGCTATC 1134
          G V I N Y S V L D L T A E E L E A I 378
R11.1.1 .....
A2 .....C.....

                                     Stop codon
R3.7.8.3 AAACATCAGCTTAATCCAAAAGATAATGATGTAGAGCTTTGA 1176
          K H Q L N P K D N D V E L XXX 391
R11.1.1 .....
A2 .....

```

Figure 10.19: Comparison of nucleotide and deduced amino acid sequences of the N gene coding region of the neutralization resistant and susceptible clones of R17532 and A2 strain.

Dots indicate identical nucleotides compared to clone R3.7.8.3 and underlined bases indicate different nucleotides of clone R3.7.8.3 compared to another strain. Deduced amino acid sequences are under the nucleotide sequence.

```

          N GE
          sequence   N-P
          |→ 3' UTR | IR |
R3.7.8.3 TGAGTTAATAAAAAAGT 15
          XXX
R11.1.1 .....
A2 .....- .

```

Figure 10.20: Nucleotide sequence comparison of the 3'UTR of the N gene and the N-P intergenic region (N-P IR) of neutralization resistant and susceptible clones of R17532 and A2 strain.

Dots indicate identical nucleotides compared to clone R3.7.8.3, dashes indicate alignment gaps and underlined bases indicate different nucleotides of clone R3.7.8.3 compared to another strain.

P GS sequence
 |→ 5' UTR

R3.7.8.3 GGGGCAAATAAATCATC 17
 R11.1.1
 A2

Figure 10.21: Nucleotide sequence comparison of 5'UTR of the neutralization resistant and susceptible clones of R17532 and A2 strain.

Dots indicate identical nucleotides compared to clone R.3.7.8.3 and underlined bases indicate different nucleotides of clone R3.7.8.3 compared to another strain.

|→ P Gene Start codon

R3.7.8.3 ATGGAAAAGTTTGCTCCTGAATTCCATGGAGAAGACCGCAAACAACAGAGCTACT 54
 M E K F A P E F H G E D A N N R A T 18
 R11.1.1
 A2T.....G.....

R3.7.8.3 AAATTCCTAGAATCAATAAAAGGGCAAATTCACATCACCTAAAGATCCCAAGAAA 108
 K F L E S I K G K F T S P K D P K K 36
 R11.1.1
 A2C.....

R3.7.8.3 AAAGATAGTATCATATCTGTCAACTCAATAGATATAGAAGTAACCAAGAAAGC 162
 K D S I I S V N S I D I E V T K E S 54
 R11.1.1
 A2

R3.7.8.3 CCTATAACATCAAATTC AACCATTTATAAACCCCTACAAATGAGACAGATGATACT 216
 P I T S N S T I I N P T N E T D D T 72
 R11.1.1
 A2T.....C.....A.....

R3.7.8.3 GTAGGGAACAAGCCCAATTATCAAAGGAAACCTCTAGTAAGTTTCAAAGAAGAC 270
 V G N K P N Y Q R K P L V S F K E D 90
 R11.1.1
 A2 .C.....A.....
 A

R3.7.8.3 CCTACACCAAGTGATAATCCCTTTTCAA^{AA}ACTATACAAAAGAAACCATAGAAACA 324
 P T P S D N P F S K L Y K E T I E T 108
 R11.1.1
 A2T.....


```

R3.7.8.3 TTTGATAACAATGAAGAAGAATCTAGCTATTCATATGAAGAAATAAATGATCAG 378
          F D N N E E E S S Y S Y E E I N D Q 126
R11.1.1 .....
A2 .....C.....C.....

R3.7.8.3 ACAAACGATAATATAACAGCAAGATTAGATAGGATTGATGAAAAATTAAGTGAA 432
          T N D N I T A R L D R I D E K L S E 144
R11.1.1 .....
A2 .....

R3.7.8.3 ATACTAGGAATGCTTCACACACTAGTAGTAGCGGAGTGCGGGACCTACATCTGCT 486
          I L G M L H T L V V A S A G P T S A 162
R11.1.1 .....
A2 .....T.....G..A....A.....

R3.7.8.3 CGGGATGGTATAAGAGATGCCATGGTTGGTTTAAAGAGAAGAAATGATAGAAAAA 540
          R D G I R D A M V G L R E E M I E K 180
R11.1.1 .....
A2 .....A.....
          I

R3.7.8.3 ATCAGAAGCTGAAGCATTAAATGACCAATGATAGATTAGAAGCTATGGCAAGACTC 594
          I R T E A L M T N D R L E A M A R L 198
R11.1.1 .....
A2 .....C.....

R3.7.8.3 AGGAATGAGGAAAGTGAAAAGATGGCAAAAGATACATCAGATGAAGTGTCTCTC 648
          R N E E S E K M A K D T S D E V S L 216
R11.1.1 .....
A2 .....C.....

R3.7.8.3 AATCCAACATCAGAAAAATTGAACAACCTGTTGGAAGGGGAATGATAGTGACAAT 702
          N P T S E K L N N L L E G N D S D N 234
R11.1.1 .....
A2 .....G.....A.....

          Stop codon
R3.7.8.3 GATCTATCACTTGAAGATTTCTGA 726
          D L S L E D F XXX 241
R11.1.1 .....
A2 .....

```

Figure 10.22: Comparison of nucleotide and deduced amino acid sequences of the P gene coding region of the neutralization resistant and susceptible clones of R17532 and A2 strain. Dots indicate identical nucleotides compared to clone R3.7.8.3 and underlined bases indicate different nucleotides of clone R3.7.8.3 compared to another strain. Deduced amino acid sequences are under the nucleotide sequence.

|→ P Gene 3' UTR

R3.7.8.3 TCAGTTACCAATCTGCACATCAACACACAACACCAACAGAGACCGACAAACA 54
R11.1.1
A2 .T.....C...T.....T.....A.....T.

R3.7.8.3 AACAACCTCACCTATCCAACCAAACATCTATCTGCCAATCATCCAACCAGCCAAA 108
R11.1.1
A2 .C....C..ATC.....T.....C...C.....G...A.....C

P GE

R3.7.8.3 AAAACACCCAGCCAATCCAAAACACTAGTCACCCGGAAAAAATCGATACTATAGTT 162
R11.1.1
A2A.....AC.....T...A.....

sequence

R3.7.8.3 ACAAAAAA 171
R11.1.1
A2

Figure 10.23: Nucleotide sequence comparison of the 3'UTR of the P gene of neutralization resistant and susceptible clones of R17532 and A2 strain.
Dots indicate identical nucleotides compared to clone R.3.7.8.3 and underlined bases indicate different nucleotides of clone R3.7.8.3 compared to another strain.

|→ F-M2 IR M2 GS - signal
|→ 5' UTR

R3.7.8.3 AACTACTGAGTACCAGATTAACTCACTATTTGTAAAAATTAGAAATGGGGCAAAT 55
R11.1.1
A2 C..A.T...A.G.....T..C..C.....G.A..C.....

Figure 10.24: Nucleotide sequence comparison of the F-M2 intergenic region (F-M2 IR) and 5'UTR of the neutralization resistant and susceptible clones of R17532 and A2 strain.
Dots indicate identical nucleotides compared to clone R.3.7.8.3 and underlined bases indicate different nucleotides of clone R3.7.8.3 compared to another strain.

```

|→ M2 Gene Start codon
R3.7.8.3 ATGTCACGAAGGAATCCTTGCAAATTTGAAATTCGAGGTCATTGCTTGAATGGT 54
          M S R R N P C K F E I R G H C L N G 18
R11.1.1 .....
A2 .....A.....

R3.7.8.3 AAGAGGTGTCATTTTAGTCATAATTATTTTGAATGGCCACCCCATGCACTGCTT 108
          K R C H F S H N Y F E W P P H A L L 36
R11.1.1 .....
A2 .....

R3.7.8.3 GTAAGACAAAACCTTTATGTTAAACAGAATACTTAAGTCTATGGATAAAAAGCATA 162
          V R Q N F M L N R I L K S M D K S I 54
R11.1.1 .....
A2 .....T...

R3.7.8.3 GATACTTTATCAGAAATAAGTGGAGCTGCAGAGTTGGACAGAACTGAAGAGTAT 216
          D T L S E I S G A A E L D R T E E Y 72
R11.1.1 .....
A2 .....C.....A.....

R3.7.8.3 GCCCTCGGTGTAGTTGGAGTGCTAGAGAGTTATATAGGATCAATAAAATAATATA 270
          A L G V V G V L E S Y I G S I N N I 90
R11.1.1 .....
A2 ..T..T.....C.....

R3.7.8.3 ACTAAACAATCAGCATGTGTTGCCATGAGCAAACCTCCTCACTGAACTCAACAGT 324
          T K Q S A C V A M S K L L T E L N S 108
R11.1.1 .....
A2 .....T.....

R3.7.8.3 GATGACATCAAAAAACTAAGGGACAATGAAGAGCCAAATTCACCCAAGATAAGA 378
          D D I K K L R D N E E P N S P K I R 126
R11.1.1 .....
A2 .....T.....
          L

R3.7.8.3 GTGTACAATACTGTCATATCATATATTGAAAGCAACAGGAAAAACAATAACAA 432
          V Y N T V I S Y I E S N R K N N K Q 144
R11.1.1 .....
A2 .....

R3.7.8.3 ACTATCCATCTGTTAAAAAGATTGCCAGCAGACGTATTGAAGAAAACCATCAAA 486
          T I H L L K R L P A D V L K K T I K 162
R11.1.1 .....
A2 .....

```

R3.7.8.3 AACACATTGGATATCCCAAGAGCATAACCATCAATAACCCAAAAGAATCAACT 540
 N T L D I H K S I T I N N P K E S T 180

R11.1.1

A2T.....C.....

Stop codon

R3.7.8.3 GTTAATGATACAAACGACCATGCCAAAAATAATGATACTACCTGA 585
 V N D T N D H A K N N D T T XXX 194

R11.1.1

A2G.....T.....
 S

Figure 10.25: Comparison of nucleotide and deduced amino acid sequences of the M2 gene coding region of the neutralization resistant and susceptible clones of R17532 and A2 strain.

Dots indicate identical nucleotides compared to clone R3.7.8.3 and underlined bases indicate different nucleotides of clone R3.7.8.3 compared to another strain. Deduced amino acid sequences are under the nucleotide sequence.

|→ M2 Gene 3' UTR

R3.7.8.3 CAAATATCCTTGTAGTATAAAATTCCATACTAATAACAAGTAGTTGTAGAGTTAC 54

R11.1.1

A2C.....A.....

R3.7.8.3 TATGTATAATCAAAAGAACACACTATATTTCAATCAAAACAACCAAAATAACCA 108

R11.1.1

A2C.....

R3.7.8.3 TATATACTCACCAAATCAACCATTCAATGAAATCCATTGGACCTCTCAAGACTT 162

R11.1.1

A2 ...G.....G.....A.....A..

R3.7.8.3 GATTGATGCAATTCAAAATTTTCTACAACATCTAGGTGTTACTGATGATATATA 216

R11.1.1

A2CA.....T.....A...T...G.....

R3.7.8.3 CACAATATATATATTAGTGTGCATAACACTCAATACCAATACTTACCACATCATC 270

R11.1.1

A2 T.....T.T..C...C.....G.T

5' UTR |→ L Gene Start codon
 L GS - sequence

R3.7.8.3 AAACTTATTAACTCAAACAATTCAAACCATGGGACAAAATGATCCCATTTATTAAT 325
 M D P I I N 6

R11.1.1

A2 .C.T.....T.....GTTG.....

M2 GE sequence

R3.7.8.3 GGAAATTCTGCTAATGTTTATCTAACCGATAGTTATTTAAAA 367
 G N S A N V Y L T D S Y L K 20

R11.1.1

A2

Figure 10.26: Nucleotide sequence comparison of the 3'UTR of the M2 gene and 5'UTR of the L gene of neutralization resistant and susceptible clones of R17532 and A2 strain.
 Dots indicate identical nucleotides compared to clone R.3.7.8.3 and underlined bases indicate different nucleotides of clone R3.7.8.3 compared to another strain.

| → L Gene Start codon M2 GE

R3.7.8.3 ATGGATCCCATTATTAATGGAAATTCTGCTAATGTTTATCTAACCGATAGTTAT 54
 M D P I I N G N S A N V Y L T D S Y 18

R11.1.1

A2

sequence

R3.7.8.3 TTAAAGGTGTATTTTCTTTCTCAGAATGTAATGCTTTAGGAAGTTACATATTC 108
 L K G V I S F S E C N A L G S Y I F 36

R11.1.1

A2C.....G.....

R3.7.8.3 AATGGTCCTTATCTCAAAAATGATTACCAACTTAATTAGTAGACAAAATCCA 162
 N G P Y L K N D Y T N L I S R Q N P 54

R11.1.1

A2T.....

R3.7.8.3 TTAATAGAACACATAAAATCTAAAGAAATTAAATATAACACAGTCCTTAATATCT 216
 L I E H I N L K K L N I T Q S L I S 72

R11.1.1

A2G.....C.....
 M

R3.7.8.3 AAGTATCATAAAGGTGAAATAAAAATAGAAGAACCTACTTATTTTCAGTCATTA 270
 K Y H K G E I K I E E P T Y F Q S L 90

R11.1.1

A2T.....
 L

R3.7.8.3 CTTATGACATACAAGAGTATGACCTCGTCAGAACAGATTACTACCACTAATTTA 324
 L M T Y K S M T S S E Q I T T T N L 108

R11.1.1

A2G.....
 A

R3.7.8.3 CTTAAAAGATAATAAGAAGAGCTATAGAAATTAGTGATGTCAAAGTCTATGCT 378
 L K K I I R R A I E I S D V K V Y A 126

R11.1.1

A2A.....

R3.7.8.3 ATATTGAATAAACTGGGGCTTAAAGAAAAAGACAAGATTAAATCCAACAATGGA 432
I L N K L G L K E K D K I K S N N G 144

R11.1.1

A2A.....G.....

R3.7.8.3 CAAGATGAAGACAACCTCAGTTATTACAACCATAATCAAAGATGATATACTTTTA 486
Q D E D N S V I T T I I K D D I L L 162

R11.1.1

A2G.....C.
S

R3.7.8.3 GCTGTTAAGGATAATCAATCTCATCTTAAAGCAGGCAAAAATCACTCTACAAA 540
A V K D N Q S H L K A G K N H S T K 180

R11.1.1

A2A.....A.....
D

R3.7.8.3 CAAAAAGATACTATCAAAAACAACACTCTTGAAAAAATTAATGTGTTCGATGCAA 594
Q K D T I K T T L L K K L M C S M Q 198

R11.1.1

A2C..A.....G....G.....A.....

R3.7.8.3 CATCCTCCATCATGGTTAATACATTGGTTTAAATTTATACACAAAATTAACAAC 648
H P P S W L I H W F N L Y T K L N N 216

R11.1.1

A2C.....

R3.7.8.3 ATATTAACACAGTATCGATCAAATGAGGTAAAAAACCATGGTTTATATTGATA 702
I L T Q Y R S N E V K N H G F I L I 234

R11.1.1

A2G....C.....
T

R3.7.8.3 GATAATCATACTCTCAATGGATTCCAATTTATTTTGAATCAATATGGTTGTATA 756
D N H T L N G F Q F I L N Q Y G C I 252

R11.1.1

A2A.....T.G.....T.....C.....
Q S

R3.7.8.3 GTTTATCATAAGGAACTCAAAAGAATTACTGTGACAACCTATAATCAATTCTTG 810
V Y H K E L K R I T V T T Y N Q F L 270

R11.1.1

A2

R3.7.8.3 ACATGGAAAGATATTAGCCTTAGTAGATTAAATGTTTGTTTAATTACATGGATT 864
T W K D I S L S R L N V C L I T W I 288

R11.1.1

A2

R3.7.8.3 AGTAACTGTTTGAACACATTAAACA^{AAA}AGCTTAGGCTTAAGATGTGGATTCAAT 918
S N C L N T L N K S L G L R C G F N 306
R11.1.1G..
D
A2C.....T.....C.....

R3.7.8.3 AATGTTATCTTGACACA^{ACT}ATTCC^{TTT}TATGGAGATTGTATAT^{TAAA}ACTATTC 972
N V I L T Q L F L Y G D C I L K L F 324
R11.1.1
A2C....G.....T

R3.7.8.3 CACAATGAAGGGTTCTACATAATA^{AAA}AGAGGTAGAGGGATTTATTATGTCTCTA 1026
H N E G F Y I I K E V E G F I M S L 342
R11.1.1
A2G.....

R3.7.8.3 ATTTTAAATATAACAGAAGAAGATCAATTCAGAAAACGGTTTATAATAGTATG 1080
I L N I T E E D Q F R K R F Y N S M 360
R11.1.1
A2A.....

R3.7.8.3 CTCAACAACATCACAGATGCTGCTAATA^{AA}AGCTCAGAAAAATCTGCTATCAAGA 1134
L N N I T D A A N K A Q K N L L S R 378
R11.1.1
A2

R3.7.8.3 GTATGTCATACATTATTAGATAAGACAGTATCCGATAATATAATAAATGGCAGA 1188
V C H T L L D K T V S D N I I N G R 396
R11.1.1
A2G.....

R3.7.8.3 TGGATAATTCTATTAAGTAAGTTCCTTAAATTAATTAAGCTTGCAGGTGACAAT 1242
W I I L L S K F L K L I K L A G D N 414
R11.1.1
A2

R3.7.8.3 AACCTTAACAATCTGAGTGAATTATATTTTTTATTCAGAAATATTTGGACACCCA 1296
N L N N L S E L Y F L F R I F G H P 432
R11.1.1
A2C.....G.....

R3.7.8.3 ATGGTAGATGAAAGACAAGCCATGGATGCTGTTAAAGTTAATTGCAACGAGACC 1350
M V D E R Q A M D A V K V N C N E T 450
R11.1.1
A2A.....T.....
I

R3.7.8.3 AAATTTTACTTGTTAAGCAGTTTGAGTATGTTAAGAGGTGCCTTTATATATAGA 1404
K F Y L L S S L S M L R G A F I Y R 468

R11.1.1
A2C.....

R3.7.8.3 ATTATAAAAGGGTTTGTAAATAATTACAACAGATGGCCTACTTTAAGGAATGCT 1458
I I K G F V N N Y N R W P T L R N A 486

R11.1.1
A2A.....

R3.7.8.3 ATTGTTTTACCCTTAAGATGGTTAACTTACTATAAACTAAACACTTATCCTTCC 1512
I V L P L R W L T Y Y K L N T Y P S 504

R11.1.1
A2T

R3.7.8.3 TTGTTGGAACCTTACAGAAAGAGATTTGATTGTTTTATCAGGACTACGTTTCTAT 1566
L L E L T E R D L I V L S G L R F Y 522

R11.1.1
A2G.....

R3.7.8.3 CGTGAGTTTCGGTTGCCTAAAAAAGTGGATCTTGAAATGATCATAAATGATAAG 1620
R E F R L P K K V D L E M I I N D K 540

R11.1.1
A2T.....A

R3.7.8.3 GCTATATCACCTCCTAAAAATTTGATATGGACTAGTTTCCCTAGAAATTATATG 1674
A I S P P K N L I W T S F P R N Y M 558

R11.1.1
A2C...

R3.7.8.3 CCGTCACACATACAAAATTATATAGAACATGAAAAATTAAAATTTTCCGAGAGT 1728
P S H I Q N Y I E H E K L K F S E S 576

R11.1.1
A2 ..A.....C.....

R3.7.8.3 GATAAATCAAGAAGAGTATTAGAGTACTATTTAAGAGATAACAAATTCAATGAA 1782
D K S R R V L E Y Y L R D N K F N E 594

R11.1.1
A2T.....

R3.7.8.3 TGTGATTTATATAACTGTGTAGTTAATCAAAGCTACCTTAACAACCCTAATCAT 1836
C D L Y N C V V N Q S Y L N N P N H 612

R11.1.1
A2C.....T..T..C.....

R3.7.8.3 GTGGTATCATTGACTGGCAAAGAAAGAGAACTCAGTGTAGGTAGAATGTTTGCA 1890
V V S L T G K E R E L S V G R M F A 630

R11.1.1

A2A.....

R3.7.8.3 ATGCAACCAGGAATGTTTCAGACAAGTTCAAATATTAGCAGAGAAAATGATAGCT 1944
M Q P G M F R Q V Q I L A E K M I A 648

R11.1.1

A2G.....G.....G.....

R3.7.8.3 GAAACATTTTACAATTCTTTCTGAAAGTCTTACAAGATATGGTGATCTAGAA 1998
E N I L Q F F P E S L T R Y G D L E 666

R11.1.1

A2

R3.7.8.3 TTACAGAAAATATTAGAATTGAAAGCGGGAATAAGTAACAAATCAAATCGTTAC 2052
L Q K I L E L K A G I S N K S N R Y 684

R11.1.1

A2 C...A.....A.....C...

R3.7.8.3 AATGACAGTTACAACAATTACATCAGTAAGTGCTCTATCATCACAGATCTCAGC 2106
N D S Y N N Y I S K C S I I T D L S 702

R11.1.1

A2T.A.....T.....
N

R3.7.8.3 AAATTCAATCAAGCATTTCGGTATGAAACATCATGTATTTGTAGTGATGTTCTG 2160
K F N Q A F R Y E T S C I C S D V L 720

R11.1.1

A2A.....G.....G...

R3.7.8.3 GATGAACTGCATGGAGTACAATCTCTATTTTCTGGTTACATTTAACTATTCCT 2214
D E L H G V Q S L F S W L H L T I P 738

R11.1.1

A2T.....

R3.7.8.3 CATGTCACAATAATATGCACATATAGGCATGCACCCCCCTATATAAGAGATCAC 2268
H V T I I C T Y R H A P P Y I R D H 756

R11.1.1

A2G.....T
G

R3.7.8.3 ATTGTGGATCTTAAACAATGTAGATGAACAAAGTGGATTATATAGATATCATATG 2322
I V D L N N V D E Q S G L Y R Y H M 774

R11.1.1

A2A.....C...

R3.7.8.3 GGTGGTATCGAAGGGTGGTGTCAAAAACTATGGACCATAGAAGCTATATCACTA 2376
 G G I E G W C Q K L W T I E A I S L 792

R11.1.1
 A2C.....G.....

R3.7.8.3 TTGGATCTAATATCTCTCAAAGGGAAATTCTCAATTACTGCCTTAATTAATGGT 2430
 L D L I S L K G K F S I T A L I N G 810

R11.1.1
 A2T.....

R3.7.8.3 GACAATCAATCAATAGATATAAGCAAACCAGTCAGACTCATGGAAGGTCAAACT 2484
 D N Q S I D I S K P V R L M E G Q T 828

R11.1.1
 A2A.....
 I

R3.7.8.3 CATGCTCAAGCAGATTATTTGCTAGCATTAAATAGTCTTAAATGCTGTATAAA 2538
 H A Q A D Y L L A L N S L K L L Y K 846

R11.1.1
 A2C.....A.....

R3.7.8.3 GAGTATGCAGGCATAGGCCACAAATTAAAAAGGAACTGGAGACTTATATATCAAGA 2592
 E Y A G I G H K L K G T E T Y I S R 864

R11.1.1
 A2C..

R3.7.8.3 GATATGCAATTTATGAGTAAACAATTCAACATAACGGTGTATATTACCCAGCT 2646
 D M Q F M S K T I Q H N G V Y Y P A 882

R11.1.1
 A2

R3.7.8.3 AGTATAAAGAAAGTCCTAAGAGTGGGACCGTGGATAAACACTATACTTGATGAT 2700
 S I K K V L R V G P W I N T I L D D 900

R11.1.1
 A2

R3.7.8.3 TTCAAAGTGAGTCTAGAATCTATAGGTAGTTTGACACAAGAAATTAGAATATAGA 2754
 F K V S L E S I G S L T Q E L E Y R 918

R11.1.1
 A2

R3.7.8.3 GGTGAAAGTCTATTATGCAGTTTAAATATTTAGAAATGTGTGGTTATATAATCAA 2808
 G E S L L C S L I F R N V W L Y N Q 936

R11.1.1
 A2A.....G

R3.7.8.3 ATTGCTTTACAACTAAAAAATCATGCATTATGTAACAATAAAATTTATATTTGGAC 2862
I A L Q L K N H A L C N N K L Y L D 954
R11.1.1
A2C.....T.....C.....

R3.7.8.3 ATATTAAGGTTCTGAAACACTTAAAAACCTTTTTTAATCTTGATAATATTGAT 2916
I L K V L K H L K T F F N L D N I D 972
R11.1.1
A2

R3.7.8.3 ACAGCATTAAACATTGTATATGAATTTGCCTATGTTATTTGGTGGTGGTGATCCC 2970
T A L T L Y M N L P M L F G G G D P 990
R11.1.1
A2A..C.....

R3.7.8.3 AACCTGTTATATCGAAGTTTCTATAGAAGAACTCCTGATTTCTCACAGAGGCT 3024
N L L Y R S F Y R R T P D F L T E A 1008
R11.1.1
A2 ...T.....C.....

R3.7.8.3 ATAGTTCACTCTGTGTTTACTTAGTTATTATACAAACCATGATTTAAAAGAT 3078
I V H S V F I L S Y Y T N H D L K D 1026
R11.1.1
A2C.....

R3.7.8.3 AAACCTCAAGATCTGTCAGACGATAGATTGAATAAGTTCTTAACATGCATAATC 3132
K L Q D L S D D R L N K F L T C I I 1044
R11.1.1
A2T.....

R3.7.8.3 ACGTTTGACAAAAACCTAATGCTGAATTCGTAACATTGATGAGAGATCCTCAA 3186
T F D K N P N A E F V T L M R D P Q 1062
R11.1.1
A2

R3.7.8.3 GCCTTAGGGTCTGAGAGGCAAGCTAAAAATTACTAGCGAAATCAATAGACTGGCA 3240
A L G S E R Q A K I T S E I N R L A 1080
R11.1.1
A2 ..T.....A.....

R3.7.8.3 GTTACTGAGGTTTTGAGCACAGCTCCAAACAAAATATTTCTCCAAAAGTGCACAA 3294
V T E V L S T A P N K I F S K S A Q 1098
R11.1.1
A2A.....T.....

R3.7.8.3 CACTATACCACTACAGAGATAGATCTAAATGATATTATGCAAAATATAGAACCT 3348
H Y T T T E I D L N D I M Q N I E P 1116
R11.1.1
A2 ..T.....T.....

R3.7.8.3 ACATATCCTCATGGGCTAAGAGTTGTTTATGAAAGTTTACCCTTTTACAAAGCA 3402
T Y P H G L R V V Y E S L P F Y K A 1134
R11.1.1
A2T.....

R3.7.8.3 GAGAAAATAGTAAATCTTATATCCGGTACAAAATCTATAACTAACATACTGGAA 3456
E K I V N L I S G T K S I T N I L E 1152
R11.1.1
A2A.....

R3.7.8.3 AAGACTTCTGCCATAGACTTAAACAGATATTGATAGAGCCACTGAGATGATGAGG 3510
K T S A I D L T D I D R A T E M M R 1170
R11.1.1
A2 ..A.....

R3.7.8.3 AAAAACATAACTTTGCTTATAAGGATATTTCCATTAGATTGTAACAGAGATAAA 3564
K N I T L L I R I F P L D C N R D K 1188
R11.1.1
A2C.....
L

R3.7.8.3 AGAGAAATATTGAGTATGGAAAACCTAAGTATTACTGAATTAAGCAAATATGTT 3618
R E I L S M E N L S I T E L S K Y V 1206
R11.1.1
A2G.....

R3.7.8.3 AGAGAAAGATCTTGGTCTTTATCCAATATAGTTGGTGTACATCACCCAGTATC 3672
R E R S W S L S N I V G V T S P S I 1224
R11.1.1
A2 ..G.....

R3.7.8.3 ATGTATACAATGGACATCAAATATACAACAAGCACTATAGCTAGTGGCATAATC 3726
M Y T M D I K Y T T S T I A S G I I 1242
R11.1.1
A2T.....T.....
S

R3.7.8.3 ATAGAGAAATATAATGTCAACAGTTTAAACACGTGGTGAGAGAGGCCCACTAAA 3780
I E K Y N V N S L T R G E R G P T K 1260
R11.1.1
A2T.....

R3.7.8.3 CCATGGGTTGGTTCATCTACACAAGAGAAAAACAATGCCAGTTTATAATAGA 3834
P W V G S S T Q E K K T M P V Y N R 1278

R11.1.1
A2

R3.7.8.3 CAAGTTTAAACCAAAAAACAGAGAGATCAAATGATCTATTAGCAAAATTGGAT 3888
Q V L T K K Q R D Q I D L L A K L D 1296

R11.1.1
A2C.....A.....

R3.7.8.3 TGGGTGTATGCATCTATAGATAACAAGGATGAATTCATGGAAGAACTTAGCATA 3942
W V Y A S I D N K D E F M E E L S I 1314

R11.1.1
A2C.....

R3.7.8.3 GGAACCTTTGGGTTAACATATGAGAAAGCCAAAAAATTATTTCCACAATATTTA 3996
G T L G L T Y E K A K K L F P Q Y L 1332

R11.1.1
A2A..G....G.....

R3.7.8.3 AGTGTTAACTATTTGCATCGCCTTACAGTCAGTAGTAGACCATGTGAATTCCT 4050
S V N Y L H R L T V S S R P C E F P 1350

R11.1.1
A2C..T.....

R3.7.8.3 GCATCAATACCAGCTTATAGAACTACAAATTATCACTTTGATACTAGCCCTATT 4104
A S I P A Y R T T N Y H F D T S P I 1368

R11.1.1
A2A.....C.....

R3.7.8.3 AATCGCATATTAACAGAAAAGTATGGTGATGAAGATATTGATATAGTATTCCAA 4158
N R I L T E K Y G D E D I D I V F Q 1386

R11.1.1
A2C.....

R3.7.8.3 AACTGTATAAGCTTTGGCCTTAGCTTAATGTCAGTAGTAGAGCAATTTACCAAT 4212
N C I S F G L S L M S V V E Q F T N 1404

R11.1.1
A2T.....A.....T...

R3.7.8.3 GTATGTCCTAATAGAATTATTCTCATACCCAAGCTTAACGAGATACACTTGATG 4266
V C P N R I I L I P K L N E I H L M 1422

R11.1.1
A2C.....T.....T.....T.....

R3.7.8.3 AAACCTCCCATATTCACAGGTGATGTTGATATTCACAAGTTAAAACAAGTGATC 4320
K P P I F T G D V D I H K L K Q V I 1440

R11.1.1
A2A

R3.7.8.3 CAAAAACAGCATATGTTTTTACCAGACAAAATAAGTTTGACTCAATATGTGGAA 4374
Q K Q H M F L P D K I S L T Q Y V E 1458

R11.1.1
A2

R3.7.8.3 TTATTCTTAAGTAATAAAAACACTCAAATCTGGATCTCATGTTAATTCTAATTTA 4428
L F L S N K T L K S G S H V N S N L 1476

R11.1.1
A2

R3.7.8.3 ATATTGGCACATAAGATATCTGACTATTTTCATAATACTTACATTTTAAGTACT 4482
I L A H K I S D Y F H N T Y I L S T 1494

R11.1.1
A2A.....

R3.7.8.3 AATTTAGCTGGACATTGGATTCTGATTATACAACCTTATGAAAGATTCTAAAGGT 4536
N L A G H W I L I I Q L M K D S K G 1512

R11.1.1
A2

R3.7.8.3 ATTTTTGAAAAAGATTGGGGAGAGGGATATATAACTGATCATATGTTTCATTAAT 4590
I F E K D W G E G Y I T D H M F I N 1530

R11.1.1
A2T.....

R3.7.8.3 TTGAAAGTTTTCTTCAATGCTTATAAGACCTATCTCTTGTGTTTTTCATAAAGGT 4644
L K V F F N A Y K T Y L L C F H K G 1548

R11.1.1
A2

R3.7.8.3 TACGGCAGAGCAAAGCTGGAGTGTGATATGAATACTTCAGATCTCCTATGTGTA 4698
Y G R A K L E C D M N T S D L L C V 1566

R11.1.1
A2 ..T...A.....
K

R3.7.8.3 TTGGAATTAATAGACAGTAGTTATTGGAAGTCTATGTCTAAGGTATTTTTAGAA 4752
L E L I D S S Y W K S M S K V F L E 1584

R11.1.1
A2

R3.7.8.3 CAAAAAGTTATCAAATACATTCTCAGCCAGGATGCAAGTTTACATAGAGTAAA 4806
Q K V I K Y I L S Q D A S L H R V K 1602
R11.1.1
A2T.....A.....

R3.7.8.3 GGATGTCATAGCTTCAAACTATGGTTTCTTAAACGCTTAATGTAGCAGAATTC 4860
G C H S F K L W F L K R L N V A E F 1620
R11.1.1
A2T.....

R3.7.8.3 ACAGTTTGCCCTTGGGTTGTTAACATAGATTATCATCCAACACATATGAAAGCA 4914
T V C P W V V N I D Y H P T H M K A 1638
R11.1.1
A2

R3.7.8.3 ATATTAACTTATATAGATCTTGTTAGAATGGGATTGATAAAATATAGATAGAATA 4968
I L T Y I D L V R M G L I N I D R I 1656
R11.1.1
A2

R3.7.8.3 TACATTAAAAATAAACACAAATTCAATGATGAATTTTATACTTCTAATCTCTTT 5022
Y I K N K H K F N D E F Y T S N L F 1674
R11.1.1
A2 C.....
H

R3.7.8.3 TACATTAATTATAACTTCTCAGATAATACTCATCTATTAACTAAACATATAAGG 5076
Y I N Y N F S D N T H L L T K H I R 1692
R11.1.1
A2

R3.7.8.3 ATTGCTAATTCTGAATTAGAAAATAATTACAACAAATTATATCATCCTACACCT 5130
I A N S E L E N N Y N K L Y H P T P 1710
R11.1.1
A2A

R3.7.8.3 GAAACTCTAGAAAATATACTAACCAATCCGGTTAAATGCGATGACAAAAAGATA 5184
E T L E N I L T N P V K C D D K K I 1728
R11.1.1
A2C.....G.....G.....A.....A.TA.....C.
A I S N T

R3.7.8.3 CTGAATGACTATTGTATAGGTAAAAATGTTGACTCAATAATGTTACCATTGTTA 5238
L N D Y C I G K N V D S I M L P L L 1746
R11.1.1
A2

R3.7.8.3 TCTAATAAGAAGCTTATTAAATCGTCTACAATGATTAGAACCAATTACAGCAA 5292
S N K K L I K S S T M I R T N Y S K 1764
R11.1.1
A2G.....
A

R3.7.8.3 CAAGATTTGTATAATTTATTTCCCTACGGTTGTGATTGATAAAATTATAGATCAT 5346
Q D L Y N L F P T V V I D K I I D H 1782
R11.1.1
A2T.....G.....
M R

R3.7.8.3 TCAGGTAATACAGCCAAATCTAACCAACTTTACTACTACTTCTCATCAAATA 5400
S G N T A K S N Q L Y T T T S H Q I 1800
R11.1.1
A2C.....C.....C..C.....

R3.7.8.3 TCTTTAGTACACAATAGCACATCACTTTATTGCATGCTTCCTTGGCATCATATT 5454
S L V H N S T S L Y C M L P W H H I 1818
R11.1.1
A2G.....C.....

R3.7.8.3 AATAGATTCAATTTTGTGTTTAGTTCTACAGGTTGTAAAATTAGTATAGAGTAT 5508
N R F N F V F S S T G C K I S I E Y 1836
R11.1.1
A2A.....

R3.7.8.3 ATTTTAAAAGACCTTAAAATTAAAGATCCCTAATTGTATAGCATTTCATAGGTGAA 5562
I L K D L K I K D P N C I A F I G E 1854
R11.1.1
A2T.....C.....

R3.7.8.3 GGAGCAGGGAATTTATTGTTGCGTACAGTAGTGGAACCTTCATCCTGATATAAGA 5616
G A G N L L L R T V V E L H P D I R 1872
R11.1.1
A2A.....C.....

R3.7.8.3 TATATTTACAGAAGTCTGAAAAGATTGCAATGATCATAGTTTACCTATTGAGTTT 5670
Y I Y R S L K D C N D H S L P I E F 1890
R11.1.1
A2

R3.7.8.3 TTAAGGCTGTACAATGGACATATCAACATTGATTATGGTGAAAATTTGACCATT 5724
L R L Y N G H I N I D Y G E N L T I 1908
R11.1.1
A2

R3.7.8.3 CCGCTACAGATGCAACCAACAACATTCATTGGTCTTATTTGCATATAAAGTTT 5778
P A T D A T N N I H W S Y L H I K F 1926
R11.1.1
A2 ..T.....A.....

R3.7.8.3 GCTGAACCTATCAGTCTTTTTGTTTGTGATGCTGAATTGCCTGTAACAGTCAAC 5832
A E P I S L F V C D A E L P V T V N 1944
R11.1.1
A2C.....C.....T.....
S

R3.7.8.3 TGGAGTAAAATCATAATAGAGTGGAGCAAGCATGTAAGAAAATGCAAGTACTGT 5886
W S K I I I E W S K H V R K C K Y C 1962
R11.1.1
A2T.....A.....G.....

R3.7.8.3 TCCTCAGTTAATAAATGTACGTTAATAGTAAAATATCATGCTCAAGATGATATC 5940
S S V N K C T L I V K Y H A Q D D I 1980
R11.1.1
A2T.....T
M

R3.7.8.3 GATTTCAAATTAGACAACAATAACTATATTA AAAACTTATGTATGCTTAGGCAGT 5994
D F K L D N I T I L K T Y V C L G S 1998
R11.1.1
A2T.....

R3.7.8.3 AAGTTAAAGGGTCTGAAGTTTACTTAGTCCTTACAATAGGCCCTGCAAATGTG 6048
K L K G S E V Y L V L T I G P A N V 2016
R11.1.1
A2A..G..G.....T.....G...A.A
I

R3.7.8.3 TTCCCAGTATTTAATGTAGTACAAAATGCTAAATGATACTATCAAGAACCAAA 6102
F P V F N V V Q N A K L I L S R T K 2034
R11.1.1
A2

R3.7.8.3 AATTTTCATCATGCCTAAGAAGGCTGATAAAGAGTCTATTGATGCAAATATTTAA 6156
N F I M P K K A D K E S I D A N I K 2052
R11.1.1
A2A.....

R3.7.8.3 AGTTTTATACCCTTTCTTTGTTACCCTATAACAAAAAAGGAATTAATACTGCA 6210
S F I P F L C Y P I T K K G I N T A 2070
R11.1.1G.....
L
A2G.....
L

```

R3.7.8.3  TTGTCAAAAACTAAAGAGTGTTTTAGTGGAGATATACTATCATATTCTATAGCT 6264
          L S K L K S V V S G D I L S Y S I A 2088

R11.1.1  .....

A2       .....

R3.7.8.3  GGACGTAATGAAGTTTTTCAGCAATAAACTTATAAATCATAAGCATATGAACATC 6318
          G R N E V F S N K L I N H K H M N I 2106

R11.1.1  .....

A2       .....

R3.7.8.3  TTAAAGTGGTTCAATCATGTTTTAAATTTTCAGATCAACAGAACTCAACTATAAT 6372
          L K W F N H V L N F R S T E L N Y N 2124

R11.1.1  .....

A2       .....A.....A.....C

R3.7.8.3  CATTTATATATGGTAGAATCTACATATCCTTATCTAAGTGAATTGTTAAACAGC 6426
          H L Y M V E S T Y P Y L S E L L N S 2142

R11.1.1  .....

A2       .....C.....

R3.7.8.3  TTGACAACTAATGAACTTAAAAAACTGATTAAAATCACAGGTAGTTTGTTTATAC 6480
          L T T N E L K K L I K I T G S L L Y 2160

R11.1.1  .....

A2       .....C.....C.....

                Stop codon
R3.7.8.3  AACTTTCATAATGAATAA 6498
          N F H N E XXX 2165

R11.1.1  .....

A2       .....

```

Figure 10.27: Comparison of nucleotide and deduced amino acid sequences of the L gene coding region of the neutralization resistant and susceptible clones of R17532 and A2 strain.

Dots indicate identical nucleotides compared to clone R3.7.8.3 and underlined bases indicate different nucleotides of clone R3.7.8.3 compared to another strain. Deduced amino acid sequences are under the nucleotide sequence.

|→ L Gene 3' UTR

```

R3.7.8.3  TGAATAAAAATCTTATATTTAAAAATTCCCACATCTACACACTAACACTGTATTC 54
R11.1.1  .....
A2       .....G.....A.....T.G...T.....

```

L GE sequence

```

R3.7.8.3  AATTATAGTTATTTAAAA 72
R11.1.1  .....
A2       .....A.....

```

Figure 10.28: Nucleotide sequence comparison of the 3'UTR of the L gene of neutralization resistant and susceptible clones of R17532 and A2 strain.
Dots indicate identical nucleotides compared to clone R.3.7.8.3 and underlined bases indicate different nucleotides of clone R3.7.8.3 compared to another strain.

|→ 5' trailer region

```

R3.7.8.3  TTAAAAATTATAAATTATATAATTTTT--AATAACTTTTAGTGGACTAATCCTA 52
R11.1.1  .....
A2       .....C-----.....TA.....A.....

R3.7.8.3  AAATTATCATTTTGATCTAGGAGGTATAAATTTAAATCCAAATCTAATTGGTTT 106
R11.1.1  .....
A2       ..G.....A...T...A.....C..T.....

R3.7.8.3  ATATGTATATTAACTAAACTACGAGATATTAGTTTTTGACACTTTTTTTCTCGT 160
R11.1.1  .....
A2       .....G.....T.....

```

Figure 10.29: Nucleotide sequence comparison of the 5'trailer region of neutralization resistant and susceptible clones of R17532 and A2 strain.
Dots indicate identical nucleotides compared to clone R.3.7.8.3, dashes indicate alignment gaps and underlined bases indicate different nucleotides of clone R3.7.8.3 compared to another strain.

	→ 3' Leader region	→ 5' UTR	NS1 GS sequence
R3.7.8.3	ACGCGAAAAAATGCGTACAACAAACTT <u>GCG</u> TAAACCAAAAAAAT <u>GGGGCAAAT</u> A		54
R11.1.1		
A2 <u>A</u>		
R3.7.8.3	AGAATTTGATAAGTACCACTTAAATT <u>CAACTCCT</u> TTGGTTAGAG		98
R11.1.1		
A2 <u>T</u> <u>C</u>		

Figure 10.30: Nucleotide sequence comparison of the 3' leader region and 3'UTR of the NS1 gene of neutralization resistant and susceptible clones of R17532 and A2 strain.

Dots indicate identical nucleotides compared to clone R.3.7.8.3 and underlined bases indicate different nucleotides of clone R3.7.8.3 compared to another strain.

Chapter 11: References

Aberle, J.H., Aberle, S.W., Dworzak, M.N., Mandl, C.W., Rebhandl, W., Vollnhofer, G., Kundi, M. and Popow-Kraupp, T. (1999) 'Reduced interferon-gamma expression in peripheral blood mononuclear cells of infants with severe respiratory syncytial virus disease', *Am J Respir Crit Care Med*, 160(4), pp. 1263-8.

Adams, O., Bonzel, L., Kovacevic, A., Mayatepek, E., Hoehn, T. and Vogel, M. (2010) 'Palivizumab-resistant human respiratory syncytial virus infection in infancy', *Clin Infect Dis*, 51(2), pp. 185-8.

Aherne, W., Bird, T., Court, S.D., Gardner, P.S. and McQuillin, J. (1970) 'Pathological changes in virus infections of the lower respiratory tract in children', *J Clin Pathol*, 23(1), pp. 7-18.

Ahmadian, G., Randhawa, J.S. and Easton, A.J. (2000) 'Expression of the ORF-2 protein of the human respiratory syncytial virus M2 gene is initiated by a ribosomal termination-dependent reinitiation mechanism', *Embo J*, 19(11), pp. 2681-9.

Alexopoulou, L., Holt, A.C., Medzhitov, R. and Flavell, R.A. (2001) 'Recognition of double-stranded RNA and activation of NF-kappaB by Toll-like receptor 3', *Nature*, 413(6857), pp. 732-8.

Alwan, W.H., Kozłowska, W.J. and Openshaw, P.J. (1994) 'Distinct types of lung disease caused by functional subsets of antiviral T cells', *J Exp Med*, 179(1), pp. 81-9.

Alwan, W.H., Record, F.M. and Openshaw, P.J. (1992) 'CD4+ T cells clear virus but augment disease in mice infected with respiratory syncytial virus. Comparison with the effects of CD8+ T cells', *Clin Exp Immunol*, 88(3), pp. 527-36.

Anderson, K., Stott, E.J. and Wertz, G.W. (1992) 'Intracellular processing of the human respiratory syncytial virus fusion glycoprotein: amino acid substitutions affecting folding, transport and cleavage', *J Gen Virol*, 73 (Pt 5), pp. 1177-88.

Anderson, L.J., Hierholzer, J.C., Tsou, C., Hendry, R.M., Fernie, B.F., Stone, Y. and McIntosh, K. (1985) 'Antigenic characterization of respiratory syncytial virus strains with monoclonal antibodies', *J Infect Dis*, 151(4), pp. 626-33.

Andries, K., Moeremans, M., Gevers, T., Willebrords, R., Sommen, C., Lacrampe, J., Janssens, F. and Wyde, P. (2003) 'Substituted benzimidazoles with nanomolar activity against respiratory syncytial virus', *Antiviral Res*, 60, pp. 209-219.

Apostolopoulos, V. and McKenzie, I.F. (1994) 'Cellular mucins: targets for immunotherapy', *Crit Rev Immunol*, 14(3-4), pp. 293-309.

Arbiza, J., Taylor, G., Lopez, J.A., Furze, J., Wyld, S., Whyte, P., Stott, E.J., Wertz, G., Sullender, W., Trudel, M. and et al. (1992) 'Characterization of two antigenic sites

recognized by neutralizing monoclonal antibodies directed against the fusion glycoprotein of human respiratory syncytial virus', *J Gen Virol*, 73 (Pt 9), pp. 2225-34.

Armstrong, S.J. and Dimmock, N.J. (1992) 'Neutralization of influenza virus by low concentrations of hemagglutinin-specific polymeric immunoglobulin A inhibits viral fusion activity, but activation of the ribonucleoprotein is also inhibited', *J Virol*, 66(6), pp. 3823-32.

Armstrong, S.J., Outlaw, M.C. and Dimmock, N.J. (1990) 'Morphological studies of the neutralization of influenza virus by IgM', *J Gen Virol*, 71 (Pt 10), pp. 2313-9.

Arnold, R., Konig, B., Werchau, H. and Konig, W. (2004) 'Respiratory syncytial virus deficient in soluble G protein induced an increased proinflammatory response in human lung epithelial cells', *Virology*, 330(2), pp. 384-97.

Asenjo, A., Calvo, E. and Villanueva, N. (2006) 'Phosphorylation of human respiratory syncytial virus P protein at threonine 108 controls its interaction with the M2-1 protein in the viral RNA polymerase complex', *J Gen Virol*, 87(Pt 12), pp. 3637-42.

Asenjo, A. and Villanueva, N. (2000) 'Regulated but not constitutive human respiratory syncytial virus (HRSV) P protein phosphorylation is essential for oligomerization', *FEBS Lett*, 467(2-3), pp. 279-84.

Atkinson, H.A., Daniels, A. and Read, N.D. (2002) 'Live-cell imaging of endocytosis during conidial germination in the rice blast fungus, *Magnaporthe grisea*', *Fungal Genet Biol*, 37(3), pp. 233-44.

Atreya, P.L. and Kulkarni, S. (1999) 'Respiratory syncytial virus strain A2 is resistant to the antiviral effects of type I interferons and human MxA', *Virology*, 261(2), pp. 227-41.

Atreya, P.L., Peeples, M.E. and Collins, P.L. (1998) 'The NS1 protein of human respiratory syncytial virus is a potent inhibitor of minigenome transcription and RNA replication', *J Virol*, 72(2), pp. 1452-61.

Bachi, T. and Howe, C. (1973) 'Morphogenesis and ultrastructure of respiratory syncytial virus', *J Virol*, 12(5), pp. 1173-80.

Barik, S., McLean, T. and Dupuy, L.C. (1995) 'Phosphorylation of Ser232 directly regulates the transcriptional activity of the P protein of human respiratory syncytial virus: phosphorylation of Ser237 may play an accessory role', *Virology*, 213(2), pp. 405-12.

Barr, F.E., Pedigo, H., Johnson, T.R. and Shepherd, V.L. (2000) 'Surfactant protein-A enhances uptake of respiratory syncytial virus by monocytes and U937 macrophages', *Am J Respir Cell Mol Biol*, 23(5), pp. 586-92.

Barr, J.N. and Wertz, G.W. (2001) 'Polymerase slippage at vesicular stomatitis virus gene junctions to generate poly(A) is regulated by the upstream 3'-AUAC-5' tetranucleotide: implications for the mechanism of transcription termination', *J Virol*, 75(15), pp. 6901-13.

Batonick, M., Oomens, A.G. and Wertz, G.W. (2008) 'Human respiratory syncytial virus glycoproteins are not required for apical targeting and release from polarized epithelial cells', *J Virol*, 82(17), pp. 8664-72.

Batonick, M. and Wertz, G. (2011) 'Requirements for Human Respiratory Syncytial Virus Glycoproteins in Assembly and Egress from Infected Cells', *Advances in Virology*, 2011, pp. 1-11.

Becker, S., Quay, J. and Soukup, J. (1991) 'Cytokine (tumor necrosis factor, IL-6, and IL-8) production by respiratory syncytial virus-infected human alveolar macrophages', *J Immunol*, 147(12), pp. 4307-12.

Beeler, J.A. and van Wyke Coelingh, K. (1989) 'Neutralization epitopes of the F glycoprotein of respiratory syncytial virus: effect of mutation upon fusion function', *J Virol*, 63(7), pp. 2941-50.

Behera, A.K., Matsuse, H., Kumar, M., Kong, X., Lockey, R.F. and Mohapatra, S.S. (2001) 'Blocking intercellular adhesion molecule-1 on human epithelial cells decreases respiratory syncytial virus infection', *Biochem Biophys Res Commun*, 280(1), pp. 188-95.

Belshe, R.B., Anderson, E.L. and Walsh, E.E. (1993) 'Immunogenicity of purified F glycoprotein of respiratory syncytial virus: clinical and immune responses to subsequent natural infection in children', *J Infect Dis*, 168(4), pp. 1024-9.

Bembridge, G.P., Lopez, J.A., Bustos, R., Melero, J.A., Cook, R., Mason, H. and Taylor, G. (1999) 'Priming with a secreted form of the fusion protein of respiratory syncytial virus (RSV) promotes interleukin-4 (IL-4) and IL-5 production but not pulmonary eosinophilia following RSV challenge', *J Virol*, 73(12), pp. 10086-94.

Bermingham, A. and Collins, P.L. (1999) 'The M2-2 protein of human respiratory syncytial virus is a regulatory factor involved in the balance between RNA replication and transcription', *Proc Natl Acad Sci U S A*, 96(20), pp. 11259-64.

Biacchesi, S., Skiadopoulos, M.H., Boivin, G., Hanson, C.T., Murphy, B.R., Collins, P.L. and Buchholz, U.J. (2003) 'Genetic diversity between human metapneumovirus subgroups', *Virology*, 315(1), pp. 1-9.

Biota Holdings Limited (2009) *RSV program returned to Biota*. Melbourne. [Online]. Available at: http://www.biota.com.au/uploaded/154/1021541_94rsvprogramreturnedtobio.pdf.

Biota Scientific Management Pty Ltd (2007) *Safety study of oral BTA9881 to treat RSV infection*. Available at: <http://clinicaltrials.gov/ct2/show/NCT00504907> (Accessed: 18 February 2012).

Bishop, K.A., Hickey, A.C., Khetawat, D., Patch, J.R., Bossart, K.N., Zhu, Z., Wang, L.F., Dimitrov, D.S. and Broder, C.C. (2008) 'Residues in the stalk domain of the hendra virus g glycoprotein modulate conformational changes associated with receptor binding', *J Virol*, 82(22), pp. 11398-409.

Bitko, V., Oldenburg, A., Garmon, N.E. and Barik, S. (2003) 'Profilin is required for viral morphogenesis, syncytium formation, and cell-specific stress fiber induction by respiratory syncytial virus', *BMC Microbiol*, 3, p. 9.

Bitko, V., Shulyayeva, O., Mazumder, B., Musiyenko, A., Ramaswamy, M., Look, D.C. and Barik, S. (2007) 'Nonstructural proteins of respiratory syncytial virus suppress premature apoptosis by an NF-kappaB-dependent, interferon-independent mechanism and facilitate virus growth', *J Virol*, 81(4), pp. 1786-95.

Boivin, G., Caouette, G., Frenette, L., Carbonneau, J., Ouakki, M. and De Serres, G. (2008) 'Human respiratory syncytial virus and other viral infections in infants receiving palivizumab', *J Clin Virol*, 42(1), pp. 52-7.

Bolt, G., Pedersen, L.O. and Birkeslund, H.H. (2000) 'Cleavage of the respiratory syncytial virus fusion protein is required for its surface expression: role of furin', *Virus Res*, 68(1), pp. 25-33.

Bond, S., Draffan, A., Lambert, J., Lim, C., Lin, B., Luttick, A., Mitchell, J., Morton, C., Nearn, R., Sanford, V. and Tucker, S. (2007) 'Discovery of a new class of polycyclic RSV inhibitors', *Antiviral Res*, 74, pp. A1-A97.

Bonfanti, J.F., Meyer, C., Doublet, F., Fortin, J., Muller, P., Queguiner, L., Gevers, T., Janssens, P., Szel, H., Willebrords, R., Timmerman, P., Wuyts, K., van Remoortere, P., Janssens, F., Wigerinck, P. and Andries, K. (2008) 'Selection of a respiratory syncytial virus fusion inhibitor clinical candidate. 2. Discovery of a morpholinopropylaminobenzimidazole derivative (TMC353121)', *J Med Chem*, 51(4), pp. 875-96.

Bont, L., Heijnen, C.J., Kavelaars, A., van Aalderen, W.M., Brus, F., Draaisma, J.M., Pekelharing-Berghuis, M., van Diemen-Steenvoorde, R.A. and Kimpen, J.L. (2001) 'Local interferon-gamma levels during respiratory syncytial virus lower respiratory tract infection are associated with disease severity', *J Infect Dis*, 184(3), pp. 355-8.

Bourgeois, C., Bour, J.B., Lidholt, K., Gauthray, C. and Pothier, P. (1998) 'Heparin-like structures on respiratory syncytial virus are involved in its infectivity in vitro', *J Virol*, 72(9), pp. 7221-7.

Bourgeois, C., Corvaisier, C., Bour, J.B., Kohli, E. and Pothier, P. (1991) 'Use of synthetic peptides to locate neutralizing antigenic domains on the fusion protein of respiratory syncytial virus', *J Gen Virol*, 72 (Pt 5), pp. 1051-8.

Brandenburg, A.H., Kleinjan, A., van Het Land, B., Moll, H.A., Timmerman, H.H., de Swart, R.L., Neijens, H.J., Fokkens, W. and Osterhaus, A.D. (2000) 'Type 1-like immune response is found in children with respiratory syncytial virus infection regardless of clinical severity', *J Med Virol*, 62(2), pp. 267-77.

Brutkiewicz, R.R., Lin, Y., Cho, S., Hwang, Y.K., Sriram, V. and Roberts, T.J. (2003) 'CD1d-mediated antigen presentation to natural killer T (NKT) cells', *Crit Rev Immunol*, 23(5-6), pp. 403-19.

Buchholz, U.J., Granzow, H., Schuldt, K., Whitehead, S.S., Murphy, B.R. and Collins, P.L. (2000) 'Chimeric bovine respiratory syncytial virus with glycoprotein gene substitutions from human respiratory syncytial virus (HRSV): effects on host range and evaluation as a live-attenuated HRSV vaccine', *J Virol*, 74(3), pp. 1187-99.

Buckingham, S.C., Jafri, H.S., Bush, A.J., Carubelli, C.M., Sheeran, P., Hardy, R.D., Ottolini, M.G., Ramilo, O. and DeVincenzo, J.P. (2002) 'A randomized, double-blind, placebo-controlled trial of dexamethasone in severe respiratory syncytial virus (RSV) infection: effects on RSV quantity and clinical outcome', *J Infect Dis*, 185(9), pp. 1222-8.

Bui, R.H., Molinaro, G.A., Kettering, J.D., Heiner, D.C., Imagawa, D.T. and St Geme, J.W., Jr. (1987) 'Virus-specific IgE and IgG4 antibodies in serum of children infected with respiratory syncytial virus', *J Pediatr*, 110(1), pp. 87-90.

Bukreyev, A., Murphy, B.R. and Collins, P.L. (2000) 'Respiratory syncytial virus can tolerate an intergenic sequence of at least 160 nucleotides with little effect on transcription or replication in vitro and in vivo', *J Virol*, 74(23), pp. 11017-26.

Bukreyev, A., Whitehead, S.S., Murphy, B.R. and Collins, P.L. (1997) 'Recombinant respiratory syncytial virus from which the entire SH gene has been deleted grows efficiently in cell culture and exhibits site-specific attenuation in the respiratory tract of the mouse', *J Virol*, 71(12), pp. 8973-82.

Bukreyev, A., Yang, L., Fricke, J., Cheng, L., Ward, J.M., Murphy, B.R. and Collins, P.L. (2008) 'The secreted form of respiratory syncytial virus G glycoprotein helps the virus evade antibody-mediated restriction of replication by acting as an antigen decoy and through effects on Fc receptor-bearing leukocytes', *J Virol*, 82(24), pp. 12191-204.

Bullough, P.A., Hughson, F.M., Skehel, J.J. and Wiley, D.C. (1994) 'Structure of influenza haemagglutinin at the pH of membrane fusion', *Nature*, 371(6492), pp. 37-43.

Burke, E., Dupuy, L., Wall, C. and Barik, S. (1998) 'Role of cellular actin in the gene expression and morphogenesis of human respiratory syncytial virus', *Virology*, 252(1), pp. 137-48.

Burke, E., Mahoney, N.M., Almo, S.C. and Barik, S. (2000) 'Profilin is required for optimal actin-dependent transcription of respiratory syncytial virus genome RNA', *J Virol*, 74(2), pp. 669-75.

Burton, D.R., Saphire, E.O. and Parren, P.W.H.I. (2001) 'A model for neutralization of viruses based on antibody coating of the virion surface', *Curr Top Microbiol Immunol*, 260, pp. 109-143.

Burton, D.R., Williamson, R.A. and Parren, P.W. (2000) 'Antibody and virus: binding and neutralization', *Virology*, 270(1), pp. 1-3.

Byeon, J.H., Lee, J.C., Choi, I.S., Yoo, Y., Park, S.H. and Choung, J.T. (2009) 'Comparison of cytokine responses in nasopharyngeal aspirates from children with viral lower respiratory tract infections', *Acta Paediatr*, 98(4), pp. 725-30.

Calder, L.J., Gonzalez-Reyes, L., Garcia-Barreno, B., Wharton, S.A., Skehel, J.J., Wiley, D.C. and Melero, J.A. (2000) 'Electron microscopy of the human respiratory syncytial virus fusion protein and complexes that it forms with monoclonal antibodies', *Virology*, 271(1), pp. 122-31.

Campanini, G., Percivalle, E., Baldanti, F., Rovida, F., Bertaina, A., Marchi, A., Stronati, M. and Gerna, G. (2007) 'Human respiratory syncytial virus (hRSV) RNA quantification in nasopharyngeal secretions identifies the hRSV etiologic role in acute respiratory tract infections of hospitalized infants', *J Clin Virol*, 39(2), pp. 119-24.

Cane, P.A. (2001) 'Molecular epidemiology of respiratory syncytial virus', *Rev Med Virol*, 11(2), pp. 103-16.

Cane, P.A., Matthews, D.A. and Pringle, C.R. (1994) 'Analysis of respiratory syncytial virus strain variation in successive epidemics in one city', *J Clin Microbiol*, 32(1), pp. 1-4.

Cane, P.A. and Pringle, C.R. (1991) 'Respiratory syncytial virus heterogeneity during an epidemic: analysis by limited nucleotide sequencing (SH gene) and restriction mapping (N gene)', *J Gen Virol*, 72 (Pt 2), pp. 349-57.

Cannon, M.J., Openshaw, P.J. and Askonas, B.A. (1988) 'Cytotoxic T cells clear virus but augment lung pathology in mice infected with respiratory syncytial virus', *J Exp Med*, 168(3), pp. 1163-8.

Cannon, M.J., Stott, E.J., Taylor, G. and Askonas, B.A. (1987) 'Clearance of persistent respiratory syncytial virus infections in immunodeficient mice following transfer of primed T cells', *Immunology*, 62(1), pp. 133-8.

Carbonell-Estrany, X., Simoes, E.A., Dagan, R., Hall, C.B., Harris, B., Hultquist, M., Connor, E.M. and Losonsky, G.A. (2010) 'Motavizumab for prophylaxis of respiratory syncytial virus in high-risk children: a noninferiority trial', *Pediatrics*, 125(1), pp. e35-51.

Carr, C.M. and Kim, P.S. (1993) 'A spring-loaded mechanism for the conformational change of influenza hemagglutinin', *Cell*, 73(4), pp. 823-32.

Carroneu, C., Simabuco, F.M., Tamura, R.E., Farinha Arcieri, L.E. and Ventura, A.M. (2007) 'Intracellular localization of human respiratory syncytial virus L protein', *Arch Virol*, 152(12), pp. 2259-63.

Cartee, T.L., Megaw, A.G., Oomens, A.G. and Wertz, G.W. (2003) 'Identification of a single amino acid change in the human respiratory syncytial virus L protein that affects transcriptional termination', *J Virol*, 77(13), pp. 7352-60.

Cartee, T.L. and Wertz, G.W. (2001) 'Respiratory syncytial virus M2-1 protein requires phosphorylation for efficient function and binds viral RNA during infection', *J Virol*, 75(24), pp. 12188-97.

Castagne, N., Barbier, A., Bernard, J., Rezaei, H., Huet, J.C., Henry, C., Da Costa, B. and Eleouet, J.F. (2004) 'Biochemical characterization of the respiratory syncytial virus P-P and P-N protein complexes and localization of the P protein oligomerization domain', *J Gen Virol*, 85(Pt 6), pp. 1643-53.

Cevenini, R., Donati, M., Moroni, A., Franchi, L. and Rumpianesi, F. (1983) 'Rapid immunoperoxidase assay for detection of respiratory syncytial virus in nasopharyngeal secretions', *J Clin Microbiol*, 18(4), pp. 947-9.

Chambers, P., Pringle, C.R. and Easton, A.J. (1990) 'Heptad repeat sequences are located adjacent to hydrophobic regions in several types of virus fusion glycoproteins', *J Gen Virol*, 71 (Pt 12), pp. 3075-80.

Chan, D.C. and Kim, P.S. (1998) 'HIV entry and its inhibition', *Cell*, 93(5), pp. 681-4.

Chanock, R. and Finberg, L. (1957) 'Recovery from infants with respiratory illness of a virus related to chimpanzee coryza agent (CCA). II. Epidemiologic aspects of infection in infants and young children', *Am J Hyg*, 66(3), pp. 291-300.

Chanock, R., Roizman, B. and Myers, R. (1957) 'Recovery from infants with respiratory illness of a virus related to chimpanzee coryza agent (CCA). I. Isolation, properties and characterization', *Am J Hyg*, 66(3), pp. 281-90.

Chapman, J., Abbott, E., Alber, D.G., Baxter, R.C., Bithell, S.K., Henderson, E.A., Carter, M.C., Chambers, P., Chubb, A., Cockerill, G.S., Collins, P.L., Dowdell, V.C., Keegan, S.J., Kelsey, R.D., Lockyer, M.J., Luongo, C., Najarro, P., Pickles, R.J., Simmonds, M., Taylor, D., Tyms, S., Wilson, L.J. and Powell, K.L. (2007) 'RSV604, a novel inhibitor of respiratory syncytial virus replication', *Antimicrob Agents Chemother*, 51(9), pp. 3346-53.

Chen, J., Lee, K.H., Steinhauer, D.A., Stevens, D.J., Skehel, J.J. and Wiley, D.C. (1998) 'Structure of the hemagglutinin precursor cleavage site, a determinant of influenza pathogenicity and the origin of the labile conformation', *Cell*, 95(3), pp. 409-17.

Chen, L., Gorman, J.J., McKimm-Breschkin, J., Lawrence, L.J., Tulloch, P.A., Smith, B.J., Colman, P.M. and Lawrence, M.C. (2001) 'The structure of the fusion glycoprotein of Newcastle disease virus suggests a novel paradigm for the molecular mechanism of membrane fusion', *Structure*, 9(3), pp. 255-66.

Chen, M.D., Vazquez, M., Buonocore, L. and Kahn, J.S. (2000) 'Conservation of the respiratory syncytial virus SH gene', *J Infect Dis*, 182(4), pp. 1228-33.

Cheng, F.W., Lee, V., Shing, M.M. and Li, C.K. (2008) 'Prolonged shedding of respiratory syncytial virus in immunocompromised children: implication for hospital infection control', *J Hosp Infect*, 70(4), pp. 383-5.

Cheng, X., Park, H., Zhou, H. and Jin, H. (2005) 'Overexpression of the M2-2 protein of respiratory syncytial virus inhibits viral replication', *J Virol*, 79(22), pp. 13943-52.

Cherrie, A.H., Anderson, K., Wertz, G.W. and Openshaw, P.J. (1992) 'Human cytotoxic T cells stimulated by antigen on dendritic cells recognize the N, SH, F, M, 22K, and 1b proteins of respiratory syncytial virus', *J Virol*, 66(4), pp. 2102-10.

Chiba, Y., Higashidate, Y., Suga, K., Honjo, K., Tsutsumi, H. and Ogra, P.L. (1989) 'Development of cell-mediated cytotoxic immunity to respiratory syncytial virus in human infants following naturally acquired infection', *J Med Virol*, 28(3), pp. 133-9.

Chin, J., Magoffin, R.L., Shearer, L.A., Schieble, J.H. and Lennette, E.H. (1969) 'Field evaluation of a respiratory syncytial virus vaccine and a trivalent parainfluenza virus vaccine in a pediatric population', *Am J Epidemiol*, 89(4), pp. 449-63.

Chipps, B.E., Sullivan, W.F. and Portnoy, J.M. (1993) 'Alpha-2A-interferon for treatment of bronchiolitis caused by respiratory syncytial virus', *Pediatr Infect Dis J*, 12(8), pp. 653-8.

Cianci, C., Genovesi, E.V., Lamb, L., Medina, I., Yang, Z., Zadjura, L., Yang, H., D'Arienzo, C., Sin, N., Yu, K.L., Combrink, K., Li, Z., Colonno, R., Meanwell, N., Clark, J. and Krystal, M. (2004a) 'Oral efficacy of a respiratory syncytial virus inhibitor in rodent models of infection', *Antimicrob Agents Chemother*, 48(7), pp. 2448-54.

Cianci, C., Langley, D.R., Dischino, D.D., Sun, Y., Yu, K.L., Stanley, A., Roach, J., Li, Z., Dalterio, R., Colonna, R., Meanwell, N.A. and Krystal, M. (2004b) 'Targeting a binding pocket within the trimer-of-hairpins: small-molecule inhibition of viral fusion', *Proc Natl Acad Sci U S A*, 101(42), pp. 15046-51.

Cianci, C., Meanwell, N. and Krystal, M. (2005) 'Antiviral activity and molecular mechanism of an orally active respiratory syncytial virus fusion inhibitor', *J Antimicrob Chemother*, 55(3), pp. 289-92.

Cianci, C., Yu, K.L., Combrink, K., Sin, N., Pearce, B., Wang, A., Civiello, R., Voss, S., Luo, G., Kadow, K., Genovesi, E.V., Venables, B., Gulgeze, H., Trehan, A., James, J., Lamb, L., Medina, I., Roach, J., Yang, Z., Zadjura, L., Colonna, R., Clark, J., Meanwell, N. and Krystal, M. (2004c) 'Orally active fusion inhibitor of respiratory syncytial virus', *Antimicrob Agents Chemother*, 48(2), pp. 413-22.

Collins, B.M., McCoy, A.J., Kent, H.M., Evans, P.R. and Owen, D.J. (2002) 'Molecular architecture and functional model of the endocytic AP2 complex', *Cell*, 109(4), pp. 523-35.

Collins, P.L., Anderson, K., Langer, S.J. and Wertz, G.W. (1985) 'Correct sequence for the major nucleocapsid protein mRNA of respiratory syncytial virus', *Virology*, 146(1), pp. 69-77.

Collins, P.L. and Crowe, J.E., Jr (2007) 'Respiratory syncytial virus and metapneumovirus', in D.M., Knipe and P.M., Howely (eds.) *Fields Virology*. 5th edn. Philadelphia: Lippincott Williams & Wolters Kluwer Business, pp. 1601-1689.

Collins, P.L., Dickens, L.E., Buckler-White, A., Olmsted, R.A., Spriggs, M.K., Camargo, E. and Coelingh, K.V. (1986) 'Nucleotide sequences for the gene junctions of human respiratory syncytial virus reveal distinctive features of intergenic structure and gene order', *Proc Natl Acad Sci U S A*, 83(13), pp. 4594-8.

Collins, P.L., Hill, M.G., Camargo, E., Grosfeld, H., Chanock, R.M. and Murphy, B.R. (1995) 'Production of infectious human respiratory syncytial virus from cloned cDNA confirms an essential role for the transcription elongation factor from the 5' proximal open reading frame of the M2 mRNA in gene expression and provides a capability for vaccine development', *Proc Natl Acad Sci U S A*, 92(25), pp. 11563-7.

Collins, P.L., Hill, M.G., Cristina, J. and Grosfeld, H. (1996) 'Transcription elongation factor of respiratory syncytial virus, a nonsegmented negative-strand RNA virus', *Proc Natl Acad Sci U S A*, 93(1), pp. 81-5.

Collins, P.L., Hill, M.G. and Johnson, P.R. (1990) 'The two open reading frames of the 22K mRNA of human respiratory syncytial virus: sequence comparison of antigenic subgroups A and B and expression in vitro', *J Gen Virol*, 71 (Pt 12), pp. 3015-20.

Collins, P.L., Huang, Y.T. and Wertz, G.W. (1984) 'Nucleotide sequence of the gene encoding the fusion (F) glycoprotein of human respiratory syncytial virus', *Proc Natl Acad Sci U S A*, 81(24), pp. 7683-7.

Collins, P.L. and Melero, J.A. (2011) 'Progress in understanding and controlling respiratory syncytial virus: still crazy after all these years', *Virus Res*, 162(1-2), pp. 80-99.

Collins, P.L., Mink, M.A. and Stec, D.S. (1991) 'Rescue of synthetic analogs of respiratory syncytial virus genomic RNA and effect of truncations and mutations on the expression of a foreign reporter gene', *Proc Natl Acad Sci U S A*, 88(21), pp. 9663-7.

Collins, P.L. and Mottet, G. (1991) 'Post-translational processing and oligomerization of the fusion glycoprotein of human respiratory syncytial virus', *J Gen Virol*, 72 (Pt 12), pp. 3095-101.

Collins, P.L. and Mottet, G. (1992) 'Oligomerization and post-translational processing of glycoprotein G of human respiratory syncytial virus: altered O-glycosylation in the presence of brefeldin A', *J Gen Virol*, 73 (Pt 4), pp. 849-63.

Collins, P.L. and Mottet, G. (1993) 'Membrane orientation and oligomerization of the small hydrophobic protein of human respiratory syncytial virus', *J Gen Virol*, 74 (Pt 7), pp. 1445-50.

Collins, P.L. and Murphy, B.R. (2005) 'New generation live vaccines against human respiratory syncytial virus designed by reverse genetics', *Proc Am Thorac Soc*, 2(2), pp. 166-73.

Collins, P.L. and Wertz, G.W. (1983) 'cDNA cloning and transcriptional mapping of nine polyadenylated RNAs encoded by the genome of human respiratory syncytial virus', *Proc Natl Acad Sci U S A*, 80(11), pp. 3208-12.

Collins, P.L. and Wertz, G.W. (1985) 'Nucleotide sequences of the 1B and 1C nonstructural protein mRNAs of human respiratory syncytial virus', *Virology*, 143(2), pp. 442-51.

Colman, P.M. and Lawrence, M.C. (2003) 'The structural biology of type I viral membrane fusion', *Nat Rev Mol Cell Biol*, 4(4), pp. 309-19.

Committee on infectious disease (1996) 'Reassessment of the indications for ribavirin therapy in respiratory syncytial virus infections. American Academy of Pediatrics Committee on Infectious Diseases', *Pediatrics*, 97(1), pp. 137-40.

Committee on infectious disease (2009) 'From the American Academy of Pediatrics: Policy statements--Modified recommendations for use of palivizumab for prevention of respiratory syncytial virus infections', *Pediatrics*, 124(6), pp. 1694-701.

Connor, A. (1998) *Molecular analysis of antigenic variation in the fusion glycoprotein of respiratory syncytial virus*. PhD thesis. University of Newcastle upon Tyne.

Connors, M., Collins, P.L., Firestone, C.Y. and Murphy, B.R. (1991) 'Respiratory syncytial virus (RSV) F, G, M2 (22K), and N proteins each induce resistance to RSV challenge, but resistance induced by M2 and N proteins is relatively short-lived', *J Virol*, 65(3), pp. 1634-7.

Corey, E.A. and Iorio, R.M. (2009) 'Measles virus attachment proteins with impaired ability to bind CD46 interact more efficiently with the homologous fusion protein', *Virology*, 383(1), pp. 1-5.

Coronel, E.C., Takimoto, T., Murti, K.G., Varich, N. and Portner, A. (2001) 'Nucleocapsid incorporation into parainfluenza virus is regulated by specific interaction with matrix protein', *J Virol*, 75(3), pp. 1117-23.

Cowton, V.M., McGivern, D.R. and Fearn, R. (2006) 'Unravelling the complexities of respiratory syncytial virus RNA synthesis', *J Gen Virol*, 87(Pt 7), pp. 1805-21.

Cozens, A.L., Yezzi, M.J., Kunzelmann, K., Ohrui, T., Chin, L., Eng, K., Finkbeiner, W.E., Widdicombe, J.H. and Gruenert, D.C. (1994) 'CFTR expression and chloride secretion in polarized immortal human bronchial epithelial cells', *Am J Respir Cell Mol Biol*, 10(1), pp. 38-47.

Crowe, J.E., Jr. (1999) 'Host responses to respiratory virus infection and immunization', *Curr Top Microbiol Immunol*, 236, pp. 191-214.

Crowe, J.E., Jr., Bui, P.T., Davis, A.R., Chanock, R.M. and Murphy, B.R. (1994a) 'A further attenuated derivative of a cold-passaged temperature-sensitive mutant of human respiratory syncytial virus retains immunogenicity and protective efficacy against wild-type challenge in seronegative chimpanzees', *Vaccine*, 12(9), pp. 783-90.

Crowe, J.E., Jr., Bui, P.T., London, W.T., Davis, A.R., Hung, P.P., Chanock, R.M. and Murphy, B.R. (1994b) 'Satisfactorily attenuated and protective mutants derived from a partially attenuated cold-passaged respiratory syncytial virus mutant by introduction of additional attenuating mutations during chemical mutagenesis', *Vaccine*, 12(8), pp. 691-9.

Crowe, J.E., Jr., Bui, P.T., Siber, G.R., Elkins, W.R., Chanock, R.M. and Murphy, B.R. (1995) 'Cold-passaged, temperature-sensitive mutants of human respiratory syncytial virus (RSV) are highly attenuated, immunogenic, and protective in seronegative chimpanzees, even when RSV antibodies are infused shortly before immunization', *Vaccine*, 13(9), pp. 847-55.

Crowe, J.E., Jr., Firestone, C.Y. and Murphy, B.R. (2001) 'Passively acquired antibodies suppress humoral but not cell-mediated immunity in mice immunized with live attenuated respiratory syncytial virus vaccines', *J Immunol*, 167(7), pp. 3910-8.

Cuesta, I., Geng, X., Asenjo, A. and Villanueva, N. (2000) 'Structural phosphoprotein M2-1 of the human respiratory syncytial virus is an RNA binding protein', *J Virol*, 74(21), pp. 9858-67.

Curran, J., Marq, J.B. and Kolakofsky, D. (1995) 'An N-terminal domain of the Sendai paramyxovirus P protein acts as a chaperone for the NP protein during the nascent chain assembly step of genome replication', *J Virol*, 69(2), pp. 849-55.

Cusi, M.G., Martorelli, B., Di Genova, G., Terrosi, C., Campoccia, G. and Correale, P. (2010) 'Age related changes in T cell mediated immune response and effector memory to Respiratory Syncytial Virus (RSV) in healthy subjects', *Immun Ageing*, 7, p. 14.

Dall'Acqua, W.F., Kiener, P.A. and Wu, H. (2006) 'Properties of human IgG1s engineered for enhanced binding to the neonatal Fc receptor (FcRn)', *J Biol Chem*, 281(33), pp. 23514-24.

de Waal, L., Power, U.F., Yuksel, S., van Amerongen, G., Nguyen, T.N., Niesters, H.G., de Swart, R.L. and Osterhaus, A.D. (2004) 'Evaluation of BBG2Na in infant macaques: specific immune responses after vaccination and RSV challenge', *Vaccine*, 22(8), pp. 915-22.

Delwart, E.L., Mosialos, G. and Gilmore, T. (1990) 'Retroviral envelope glycoproteins contain a "leucine zipper"-like repeat', *AIDS Res Hum Retroviruses*, 6(6), pp. 703-6.

DeVincenzo, J.P., Hall, C.B., Kimberlin, D.W., Sanchez, P.J., Rodriguez, W.J., Jantusch, B.A., Corey, L., Kahn, J.S., Englund, J.A., Suzich, J.A., Palmer-Hill, F.J., Branco, L., Johnson, S., Patel, N.K. and Piazza, F.M. (2004) 'Surveillance of clinical isolates of respiratory syncytial virus for palivizumab (Synagis)-resistant mutants', *J Infect Dis*, 190(5), pp. 975-8.

Dickens, L.E., Collins, P.L. and Wertz, G.W. (1984) 'Transcriptional mapping of human respiratory syncytial virus', *J Virol*, 52(2), pp. 364-9.

Dieffenbach, C. and Dveksler, S. (2003) *PCR primer: a laboratory manual*. 2nd edn. NY: Cold Spring Harbor Laboratory Press.

Dimmock, N.J. (1993) 'Neutralization of animal viruses', *Curr Top Microbiol Immunol*, 183, pp. 1-149.

Dimmock, N.J., Easton, A.J. and Leppard, K.N. (2007) *Introduction to modern virology*. 6 edn. Malden, Massachusetts, USA: Blackwell.

Domurat, F., Roberts, N.J., Jr., Walsh, E.E. and Dagan, R. (1985) 'Respiratory syncytial virus infection of human mononuclear leukocytes in vitro and in vivo', *J Infect Dis*, 152(5), pp. 895-902.

Douglas, J.L., Panis, M.L., Ho, E., Lin, K.Y., Krawczyk, S.H., Grant, D.M., Cai, R., Swaminathan, S., Chen, X. and Cihlar, T. (2005) 'Small molecules VP-14637 and JNJ-2408068 inhibit respiratory syncytial virus fusion by similar mechanisms', *Antimicrob Agents Chemother*, 49(6), pp. 2460-6.

Downham, M.A., Scott, R., Sims, D.G., Webb, J.K. and Gardner, P.S. (1976) 'Breast-feeding protects against respiratory syncytial virus infections', *Br Med J*, 2(6030), pp. 274-6.

Dulbecco, R. and Vogt, M. (1954) 'Plaque formation and isolation of pure lines with poliomyelitis viruses', *J Exp Med*, 99(2), pp. 167-82.

Dupuy, L.C., Dobson, S., Bitko, V. and Barik, S. (1999) 'Casein kinase 2-mediated phosphorylation of respiratory syncytial virus phosphoprotein P is essential for the transcription elongation activity of the viral polymerase; phosphorylation by casein kinase 1 occurs mainly at Ser(215) and is without effect', *J Virol*, 73(10), pp. 8384-92.

Durrer, P., Galli, C., Hoenke, S., Corti, C., Gluck, R., Vorherr, T. and Brunner, J. (1996) 'H⁺-induced membrane insertion of influenza virus hemagglutinin involves the HA2 amino-terminal fusion peptide but not the coiled coil region', *J Biol Chem*, 271(23), pp. 13417-21.

Earp, L.J., Delos, S.E., Park, H.E. and White, J.M. (2005) 'The many mechanisms of viral membrane fusion proteins', *Curr Top Microbiol Immunol*, 285, pp. 25-66.

Elango, N., Prince, G.A., Murphy, B.R., Venkatesan, S., Chanock, R.M. and Moss, B. (1986) 'Resistance to human respiratory syncytial virus (RSV) infection induced by immunization of cotton rats with a recombinant vaccinia virus expressing the RSV G glycoprotein', *Proc Natl Acad Sci U S A*, 83(6), pp. 1906-10.

Elliott, J., Lynch, O.T., Suessmuth, Y., Qian, P., Boyd, C.R., Burrows, J.F., Buick, R., Stevenson, N.J., Touzelet, O., Gadina, M., Power, U.F. and Johnston, J.A. (2007) 'Respiratory syncytial virus NS1 protein degrades STAT2 by using the Elongin-Cullin E3 ligase', *J Virol*, 81(7), pp. 3428-36.

Englund, J.A., Sullivan, C.J., Jordan, M.C., Dehner, L.P., Vercellotti, G.M. and Balfour, H.H., Jr. (1988) 'Respiratory syncytial virus infection in immunocompromised adults', *Ann Intern Med*, 109(3), pp. 203-8.

Evans, J.E., Cane, P.A. and Pringle, C.R. (1996) 'Expression and characterisation of the NS1 and NS2 proteins of respiratory syncytial virus', *Virus Res*, 43(2), pp. 155-61.

- Everard, M.L., Swarbrick, A., Wraitham, M., McIntyre, J., Dunkley, C., James, P.D., Sewell, H.F. and Milner, A.D. (1994) 'Analysis of cells obtained by bronchial lavage of infants with respiratory syncytial virus infection', *Arch Dis Child*, 71(5), pp. 428-32.
- Falsey, A.R. and Walsh, E.E. (1996) 'Safety and immunogenicity of a respiratory syncytial virus subunit vaccine (PFP-2) in ambulatory adults over age 60', *Vaccine*, 14(13), pp. 1214-8.
- Fearn, R. and Collins, P.L. (1999a) 'Model for polymerase access to the overlapped L gene of respiratory syncytial virus', *J Virol*, 73(1), pp. 388-97.
- Fearn, R. and Collins, P.L. (1999b) 'Role of the M2-1 transcription antitermination protein of respiratory syncytial virus in sequential transcription', *J Virol*, 73(7), pp. 5852-64.
- Fearn, R., Collins, P.L. and Peeples, M.E. (2000) 'Functional analysis of the genomic and antigenomic promoters of human respiratory syncytial virus', *J Virol*, 74(13), pp. 6006-14.
- Fearn, R., Peeples, M.E. and Collins, P.L. (2002) 'Mapping the transcription and replication promoters of respiratory syncytial virus', *J Virol*, 76(4), pp. 1663-72.
- Feldman, S.A., Audet, S. and Beeler, J.A. (2000) 'The fusion glycoprotein of human respiratory syncytial virus facilitates virus attachment and infectivity via an interaction with cellular heparan sulfate', *J Virol*, 74(14), pp. 6442-7.
- Feldman, S.A., Crim, R.L., Audet, S.A. and Beeler, J.A. (2001) 'Human respiratory syncytial virus surface glycoproteins F, G and SH form an oligomeric complex', *Arch Virol*, 146(12), pp. 2369-83.
- Feldman, S.A., Hendry, R.M. and Beeler, J.A. (1999) 'Identification of a linear heparin binding domain for human respiratory syncytial virus attachment glycoprotein G', *J Virol*, 73(8), pp. 6610-7.
- Fenton, C., Scott, L.J. and Plosker, G.L. (2004) 'Palivizumab: a review of its use as prophylaxis for serious respiratory syncytial virus infection', *Paediatr Drugs*, 6(3), pp. 177-97.
- Fernie, B.F. and Gerin, J.L. (1980) 'The stabilization and purification of respiratory syncytial virus using MgSO₄', *Virology*, 106(1), pp. 141-4.
- Ferron, F., Longhi, S., Henrissat, B. and Canard, B. (2002) 'Viral RNA-polymerases -- a predicted 2'-O-ribose methyltransferase domain shared by all Mononegavirales', *Trends Biochem Sci*, 27(5), pp. 222-4.

Fix, J., Galloux, M., Blondot, M.L. and Eleouet, J.F. (2011) 'The insertion of fluorescent proteins in a variable region of respiratory syncytial virus L polymerase results in fluorescent and functional enzymes but with reduced activities', *Open Virol J*, 5, pp. 103-8.

Fleming, D.M. and Cross, K.W. (1993) 'Respiratory syncytial virus or influenza?', *Lancet*, 342(8886-8887), pp. 1507-10.

Frabasile, S., Delfraro, A., Facal, L., Videla, C., Galiano, M., de Sierra, M.J., Ruchansky, D., Vitoreira, N., Berois, M., Carballal, G., Russi, J. and Arbiza, J. (2003) 'Antigenic and genetic variability of human respiratory syncytial viruses (group A) isolated in Uruguay and Argentina: 1993-2001', *J Med Virol*, 71(2), pp. 305-12.

Friedewald, W.T., Forsyth, B.R., Smith, C.B., Gharpure, M.A. and Chanock, R.M. (1968) 'Low-temperature-grown RS virus in adult volunteers', *JAMA*, 204(8), pp. 690-4.

Friedrich, L., Pitrez, P.M., Stein, R.T., Goldani, M., Tepper, R. and Jones, M.H. (2007) 'Growth rate of lung function in healthy preterm infants', *Am J Respir Crit Care Med*, 176(12), pp. 1269-73.

Friedrich, L., Stein, R.T., Pitrez, P.M., Corso, A.L. and Jones, M.H. (2006) 'Reduced lung function in healthy preterm infants in the first months of life', *Am J Respir Crit Care Med*, 173(4), pp. 442-7.

Fuentes, S., Tran, K.C., Luthra, P., Teng, M.N. and He, B. (2007) 'Function of the respiratory syncytial virus small hydrophobic protein', *J Virol*, 81(15), pp. 8361-6.

Fulginiti, V.A., Eller, J.J., Sieber, O.F., Joyner, J.W., Minamitani, M. and Meiklejohn, G. (1969) 'Respiratory virus immunization. I. A field trial of two inactivated respiratory virus vaccines; an aqueous trivalent parainfluenza virus vaccine and an alum-precipitated respiratory syncytial virus vaccine', *Am J Epidemiol*, 89(4), pp. 435-48.

Fulton, R.B., Meyerholz, D.K. and Varga, S.M. (2010) 'Foxp3+ CD4 regulatory T cells limit pulmonary immunopathology by modulating the CD8 T cell response during respiratory syncytial virus infection', *J Immunol*, 185(4), pp. 2382-92.

Gallaher, W.R. (1987) 'Detection of a fusion peptide sequence in the transmembrane protein of human immunodeficiency virus', *Cell*, 50(3), pp. 327-8.

Gallaher, W.R., Ball, J.M., Garry, R.F., Griffin, M.C. and Montelaro, R.C. (1989) 'A general model for the transmembrane proteins of HIV and other retroviruses', *AIDS Res Hum Retroviruses*, 5(4), pp. 431-40.

Gan, S.W., Ng, L., Lin, X., Gong, X. and Torres, J. (2008) 'Structure and ion channel activity of the human respiratory syncytial virus (hRSV) small hydrophobic protein transmembrane domain', *Protein Sci*, 17(5), pp. 813-20.

Garcia-Barreno, B., Delgado, T. and Melero, J.A. (1996) 'Identification of protein regions involved in the interaction of human respiratory syncytial virus phosphoprotein and nucleoprotein: significance for nucleocapsid assembly and formation of cytoplasmic inclusions', *J Virol*, 70(2), pp. 801-8.

Garcia-Barreno, B., Palomo, C., Penas, C., Delgado, T., Perez-Brena, P. and Melero, J.A. (1989) 'Marked differences in the antigenic structure of human respiratory syncytial virus F and G glycoproteins', *J Virol*, 63(2), pp. 925-32.

Garcia-Barreno, B., Portela, A., Delgado, T., Lopez, J.A. and Melero, J.A. (1990) 'Frame shift mutations as a novel mechanism for the generation of neutralization resistant mutants of human respiratory syncytial virus', *Embo J*, 9(12), pp. 4181-7.

Garcia, J., Garcia-Barreno, B., Vivo, A. and Melero, J.A. (1993) 'Cytoplasmic inclusions of respiratory syncytial virus-infected cells: formation of inclusion bodies in transfected cells that coexpress the nucleoprotein, the phosphoprotein, and the 22K protein', *Virology*, 195(1), pp. 243-7.

Gasteiger, E., Gattiker, A., Hoogland, C., Ivanyi, I., Appel, R.D. and Bairoch, A. (2003) 'ExPASy: The proteomics server for in-depth protein knowledge and analysis', *Nucleic Acids Res*, 31(13), pp. 3784-8.

Gharpure, M.A., Wright, P.F. and Chanock, R.M. (1969) 'Temperature-sensitive mutants of respiratory syncytial virus', *J Virol*, 3(4), pp. 414-21.

Ghildyal, R., Baulch-Brown, C., Mills, J. and Meanger, J. (2003) 'The matrix protein of Human respiratory syncytial virus localises to the nucleus of infected cells and inhibits transcription', *Arch Virol*, 148(7), pp. 1419-29.

Ghildyal, R., Hartley, C., Varrasso, A., Meanger, J., Voelker, D.R., Anders, E.M. and Mills, J. (1999) 'Surfactant protein A binds to the fusion glycoprotein of respiratory syncytial virus and neutralizes virion infectivity', *J Infect Dis*, 180(6), pp. 2009-13.

Ghildyal, R., Ho, A. and Jans, D.A. (2006) 'Central role of the respiratory syncytial virus matrix protein in infection', *FEMS Microbiology Reviews*, 30(5), pp. 692-705.

Ghildyal, R., Li, D., Peroulis, I., Shields, B., Bardin, P.G., Teng, M.N., Collins, P.L., Meanger, J. and Mills, J. (2005) 'Interaction between the respiratory syncytial virus G glycoprotein cytoplasmic domain and the matrix protein', *Journal of General Virology*, 86(7), pp. 1879-1884.

Ghildyal, R., Mills, J., Murray, M., Vardaxis, N. and Meanger, J. (2002) 'Respiratory syncytial virus matrix protein associates with nucleocapsids in infected cells', *J Gen Virol*, 83(Pt 4), pp. 753-7.

Gias, E. (2006) *Mechanism of human respiratory syncytial virus (hRSV) resistance to neutralization by anti-fusion glycoprotein antibodies*. PhD thesis. University of Newcastle upon Tyne.

Gias, E., Nielsen, S.U., Morgan, L.A. and Toms, G.L. (2008) 'Purification of human respiratory syncytial virus by ultracentrifugation in iodixanol density gradient', *J Virol Methods*, 147(2), pp. 328-32.

Gimenez, H.B., Cash, P. and Melvin, W.T. (1984) 'Monoclonal antibodies to human respiratory syncytial virus and their use in comparison of different virus isolates', *J Gen Virol*, 65 (Pt 5), pp. 963-71.

Gimenez, H.B., Hardman, N., Keir, H.M. and Cash, P. (1986) 'Antigenic variation between human respiratory syncytial virus isolates', *J Gen Virol*, 67 (Pt 5), pp. 863-70.

Glezen, W.P., Paredes, A., Allison, J.E., Taber, L.H. and Frank, A.L. (1981) 'Risk of respiratory syncytial virus infection for infants from low-income families in relationship to age, sex, ethnic group, and maternal antibody level', *J Pediatr*, 98(5), pp. 708-15.

Gonzalez-Reyes, L., Ruiz-Arguello, M.B., Garcia-Barreno, B., Calder, L., Lopez, J.A., Albar, J.P., Skehel, J.J., Wiley, D.C. and Melero, J.A. (2001) 'Cleavage of the human respiratory syncytial virus fusion protein at two distinct sites is required for activation of membrane fusion', *Proc Natl Acad Sci U S A*, 98(17), pp. 9859-64.

Gonzalez, M.J., Saiz, J.C., Laor, O. and Moore, D.M. (1991) 'Antigenic stability of foot-and-mouth disease virus variants on serial passage in cell culture', *J Virol*, 65(7), pp. 3949-53.

Gorman, J.J., Ferguson, B.L., Speelman, D. and Mills, J. (1997) 'Determination of the disulfide bond arrangement of human respiratory syncytial virus attachment (G) protein by matrix-assisted laser desorption/ionization time-of-flight mass spectrometry', *Protein Sci*, 6(6), pp. 1308-15.

Gower, T.L., Peeples, M.E., Collins, P.L. and Graham, B.S. (2001) 'RhoA is activated during respiratory syncytial virus infection', *Virology*, 283(2), pp. 188-96.

Graham, B.S., Bunton, L.A., Wright, P.F. and Karzon, D.T. (1991) 'Role of T lymphocyte subsets in the pathogenesis of primary infection and rechallenge with respiratory syncytial virus in mice', *J Clin Invest*, 88(3), pp. 1026-33.

Graham, B.S., Henderson, G.S., Tang, Y.W., Lu, X., Neuzil, K.M. and Colley, D.G. (1993) 'Priming immunization determines T helper cytokine mRNA expression patterns in lungs of mice challenged with respiratory syncytial virus', *J Immunol*, 151(4), pp. 2032-40.

- Groothuis, J.R. (1994) 'The role of RSV neutralizing antibodies in the treatment and prevention of respiratory syncytial virus infection in high-risk children', *Antiviral Res*, 23(1), pp. 1-10.
- Groothuis, J.R., Gutierrez, K.M. and Lauer, B.A. (1988) 'Respiratory syncytial virus infection in children with bronchopulmonary dysplasia', *Pediatrics*, 82(2), pp. 199-203.
- Groothuis, J.R., King, S.J., Hogerman, D.A., Paradiso, P.R. and Simoes, E.A. (1998) 'Safety and immunogenicity of a purified F protein respiratory syncytial virus (PFP-2) vaccine in seropositive children with bronchopulmonary dysplasia', *J Infect Dis*, 177(2), pp. 467-9.
- Guerrero-Plata, A., Baron, S., Poast, J.S., Adegboyega, P.A., Casola, A. and Garofalo, R.P. (2005) 'Activity and regulation of alpha interferon in respiratory syncytial virus and human metapneumovirus experimental infections', *J Virol*, 79(16), pp. 10190-9.
- Gutierrez-Ortega, A., Sanchez-Hernandez, C. and Gomez-Garcia, B. (2008) 'Respiratory syncytial virus glycoproteins uptake occurs through clathrin-mediated endocytosis in a human epithelial cell line', *Virol J*, 5, p. 127.
- Haagsman, H.P. (1998) 'Interactions of surfactant protein A with pathogens', *Biochim Biophys Acta*, 1408(2-3), pp. 264-77.
- Hall, C.B. (1998) 'Respiratory syncytial virus', in R.D., Feigin and J.D., Cherry (eds.) *Textbook of Pediatric Infectious Diseases*. Philadelphia, PA: WB Saunders.
- Hall, C.B. (2001) 'Respiratory syncytial virus and parainfluenza virus', *N Engl J Med*, 344(25), pp. 1917-28.
- Hall, C.B. and Douglas, R.G., Jr. (1981) 'Modes of transmission of respiratory syncytial virus', *J Pediatr*, 99(1), pp. 100-3.
- Hall, C.B., Douglas, R.G., Jr. and Geiman, J.M. (1975) 'Quantitative shedding patterns of respiratory syncytial virus in infants', *J Infect Dis*, 132(2), pp. 151-6.
- Hall, C.B., Douglas, R.G., Jr., Simons, R.L. and Geiman, J.M. (1978) 'Interferon production in children with respiratory syncytial, influenza, and parainfluenza virus infections', *J Pediatr*, 93(1), pp. 28-32.
- Hall, C.B., Geiman, J.M., Biggar, R., Kotok, D.I., Hogan, P.M. and Douglas, G.R., Jr. (1976) 'Respiratory syncytial virus infections within families', *N Engl J Med*, 294(8), pp. 414-9.
- Hall, C.B., McBride, J.T., Walsh, E.E., Bell, D.M., Gala, C.L., Hildreth, S., Ten Eyck, L.G. and Hall, W.J. (1983) 'Aerosolized ribavirin treatment of infants with respiratory

syncytial viral infection. A randomized double-blind study', *N Engl J Med*, 308(24), pp. 1443-7.

Hall, C.B., Powell, K.R., MacDonald, N.E., Gala, C.L., Menegus, M.E., Suffin, S.C. and Cohen, H.J. (1986) 'Respiratory syncytial viral infection in children with compromised immune function', *N Engl J Med*, 315(2), pp. 77-81.

Hall, C.B., Walsh, E.E., Long, C.E. and Schnabel, K.C. (1991) 'Immunity to and frequency of reinfection with respiratory syncytial virus', *J Infect Dis*, 163(4), pp. 693-8.

Hallak, L.K., Collins, P.L., Knudson, W. and Peeples, M.E. (2000a) 'Iduronic acid-containing glycosaminoglycans on target cells are required for efficient respiratory syncytial virus infection', *Virology*, 271(2), pp. 264-75.

Hallak, L.K., Spillmann, D., Collins, P.L. and Peeples, M.E. (2000b) 'Glycosaminoglycan sulfation requirements for respiratory syncytial virus infection', *J Virol*, 74(22), pp. 10508-13.

Haller, A.A., Miller, T., Mitiku, M. and Coelingh, K. (2000) 'Expression of the surface glycoproteins of human parainfluenza virus type 3 by bovine parainfluenza virus type 3, a novel attenuated virus vaccine vector', *J Virol*, 74(24), pp. 11626-35.

Han, L.L., Alexander, J.P. and Anderson, L.J. (1999) 'Respiratory syncytial virus pneumonia among the elderly: an assessment of disease burden', *J Infect Dis*, 179(1), pp. 25-30.

Hancock, G.E., Speelman, D.J., Heers, K., Bortell, E., Smith, J. and Cosco, C. (1996) 'Generation of atypical pulmonary inflammatory responses in BALB/c mice after immunization with the native attachment (G) glycoprotein of respiratory syncytial virus', *J Virol*, 70(11), pp. 7783-91.

Hanley, L.L., McGivern, D.R., Teng, M.N., Djang, R., Collins, P.L. and Fearn, R. (2010) 'Roles of the respiratory syncytial virus trailer region: effects of mutations on genome production and stress granule formation', *Virology*, 406(2), pp. 241-52.

Harcourt, J., Alvarez, R., Jones, L.P., Henderson, C., Anderson, L.J. and Tripp, R.A. (2006) 'Respiratory syncytial virus G protein and G protein CX3C motif adversely affect CX3CR1+ T cell responses', *J Immunol*, 176(3), pp. 1600-8.

Hardy, R.W., Harmon, S.B. and Wertz, G.W. (1999) 'Diverse gene junctions of respiratory syncytial virus modulate the efficiency of transcription termination and respond differently to M2-mediated antitermination', *J Virol*, 73(1), pp. 170-6.

Hardy, R.W. and Wertz, G.W. (1998) 'The product of the respiratory syncytial virus M2 gene ORF1 enhances readthrough of intergenic junctions during viral transcription', *J Virol*, 72(1), pp. 520-6.

Hardy, R.W. and Wertz, G.W. (2000) 'The Cys(3)-His(1) motif of the respiratory syncytial virus M2-1 protein is essential for protein function', *J Virol*, 74(13), pp. 5880-5.

Harmon, S.B., Megaw, A.G. and Wertz, G.W. (2001) 'RNA sequences involved in transcriptional termination of respiratory syncytial virus', *J Virol*, 75(1), pp. 36-44.

Harmon, S.B. and Wertz, G.W. (2002) 'Transcriptional termination modulated by nucleotides outside the characterized gene end sequence of respiratory syncytial virus', *Virology*, 300(2), pp. 304-15.

Harpen, M., Barik, T., Musiyenko, A. and Barik, S. (2009) 'Mutational analysis reveals a noncontractile but interactive role of actin and profilin in viral RNA-dependent RNA synthesis', *J Virol*, 83(21), pp. 10869-76.

Harvey, F.L. (2007) *Molecular cell biology*. 6th edn. Basingstoke: Palgrave Macmillan.

Hassan, M.A., Eldin, A.M. and Ahmed, M.M. (2008) 'T - helper2 /T - helper1 imbalance in respiratory syncytial virus bronchiolitis in relation to disease severity and outcome', *Egypt J Immunol*, 15(2), pp. 153-60.

Heidema, J., Lukens, M.V., van Maren, W.W., van Dijk, M.E., Otten, H.G., van Vught, A.J., van der Werff, D.B., van Gestel, S.J., Semple, M.G., Smyth, R.L., Kimpen, J.L. and van Bleek, G.M. (2007) 'CD8+ T cell responses in bronchoalveolar lavage fluid and peripheral blood mononuclear cells of infants with severe primary respiratory syncytial virus infections', *J Immunol*, 179(12), pp. 8410-7.

Heminway, B.R., Yu, Y., Tanaka, Y., Perrine, K.G., Gustafson, E., Bernstein, J.M. and Galinski, M.S. (1994) 'Analysis of respiratory syncytial virus F, G, and SH proteins in cell fusion', *Virology*, 200(2), pp. 801-5.

Henderson, G., Murray, J. and Yeo, R.P. (2002) 'Sorting of the respiratory syncytial virus matrix protein into detergent-resistant structures is dependent on cell-surface expression of the glycoproteins', *Virology*, 300(2), pp. 244-254.

Hendricks, D.A., Baradaran, K., McIntosh, K. and Patterson, J.L. (1987) 'Appearance of a soluble form of the G protein of respiratory syncytial virus in fluids of infected cells', *J Gen Virol*, 68 (Pt 6), pp. 1705-14.

Hendricks, D.A., McIntosh, K. and Patterson, J.L. (1988) 'Further characterization of the soluble form of the G glycoprotein of respiratory syncytial virus', *J Virol*, 62(7), pp. 2228-33.

Henley, J.R., Cao, H. and McNiven, M.A. (1999) 'Participation of dynamin in the biogenesis of cytoplasmic vesicles', *FASEB J*, 13 Suppl 2, pp. S243-7.

Herlocher, M.L., Ewasyshyn, M., Sambhara, S., Gharaee-Kermani, M., Cho, D., Lai, J., Klein, M. and Maassab, H.F. (1999) 'Immunological properties of plaque purified strains of live attenuated respiratory syncytial virus (RSV) for human vaccine', *Vaccine*, 17(2), pp. 172-81.

Herrnstadt, C., Preston, G., Andrews, R., Chinnery, P., Lightowlers, R.N., Turnbull, D.M., Kubacka, I. and Howell, N. (2002) 'A high frequency of mtDNA polymorphisms in HeLa cell sublines', *Mutat Res*, 501(1-2), pp. 19-28.

Hickling, T.P., Bright, H., Wing, K., Gower, D., Martin, S.L., Sim, R.B. and Malhotra, R. (1999) 'A recombinant trimeric surfactant protein D carbohydrate recognition domain inhibits respiratory syncytial virus infection in vitro and in vivo', *Eur J Immunol*, 29(11), pp. 3478-84.

Hickling, T.P., Malhotra, R., Bright, H., McDowell, W., Blair, E.D. and Sim, R.B. (2000) 'Lung surfactant protein A provides a route of entry for respiratory syncytial virus into host cells', *Viral Immunol*, 13(1), pp. 125-35.

Hoffman, S.J., Laham, F.R. and Polack, F.P. (2004) 'Mechanisms of illness during respiratory syncytial virus infection: the lungs, the virus and the immune response', *Microbes Infect*, 6(8), pp. 767-72.

Holberg, C.J., Wright, A.L., Martinez, F.D., Ray, C.G., Taussig, L.M. and Lebowitz, M.D. (1991) 'Risk factors for respiratory syncytial virus-associated lower respiratory illnesses in the first year of life', *Am J Epidemiol*, 133(11), pp. 1135-51.

Hsieh, S.Y., Yang, P.Y., Chen, H.C. and Liaw, Y.F. (1997) 'Cloning and characterization of the extreme 5'-terminal sequences of the RNA genomes of GB virus C/hepatitis G virus', *Proc Natl Acad Sci U S A*, 94(7), pp. 3206-10.

Huang, K., Incognito, L., Cheng, X., Ulbrandt, N.D. and Wu, H. (2010) 'Respiratory syncytial virus-neutralizing monoclonal antibodies motavizumab and palivizumab inhibit fusion', *J Virol*, 84(16), pp. 8132-8140.

Huang, X. and Madan, A. (1999) 'CAP3: A DNA sequence assembly program', *Genome Res*, 9(9), pp. 868-77.

Hull, J., Thomson, A. and Kwiatkowski, D. (2000) 'Association of respiratory syncytial virus bronchiolitis with the interleukin 8 gene region in UK families', *Thorax*, 55(12), pp. 1023-7.

Huq, F., Rahman, M., Nahar, N., Alam, A., Haque, M., Sack, D.A., Butler, T. and Haider, R. (1990) 'Acute lower respiratory tract infection due to virus among hospitalized children in Dhaka, Bangladesh', *Rev Infect Dis*, 12 Suppl 8, pp. S982-7.

Hussell, T. and Openshaw, P.J. (1998) 'Intracellular IFN-gamma expression in natural killer cells precedes lung CD8+ T cell recruitment during respiratory syncytial virus infection', *J Gen Virol*, 79 (Pt 11), pp. 2593-601.

International Committee on Taxonomy of Viruses (2011) *Virus Taxonomy: 2011 Release*. Available at: <http://www.ictvonline.org/virusTaxonomy.asp?version=2011> (Accessed: 14 May 2012).

Jin, H., Cheng, X., Zhou, H.Z., Li, S. and Seddiqui, A. (2000a) 'Respiratory syncytial virus that lacks open reading frame 2 of the M2 gene (M2-2) has altered growth characteristics and is attenuated in rodents', *J Virol*, 74(1), pp. 74-82.

Jin, H. and Elliott, R.M. (1992) 'Mutagenesis of the L protein encoded by Bunyamwera virus and production of monospecific antibodies', *J Gen Virol*, 73 (Pt 9), pp. 2235-44.

Jin, H., Zhou, H., Cheng, X., Tang, R., Munoz, M. and Nguyen, N. (2000b) 'Recombinant respiratory syncytial viruses with deletions in the NS1, NS2, SH, and M2-2 genes are attenuated in vitro and in vivo', *Virology*, 273(1), pp. 210-8.

Johnson, J.E., Gonzales, R.A., Olson, S.J., Wright, P.F. and Graham, B.S. (2007) 'The histopathology of fatal untreated human respiratory syncytial virus infection', *Mod Pathol*, 20(1), pp. 108-19.

Johnson, P.R. and Collins, P.L. (1988) 'The fusion glycoproteins of human respiratory syncytial virus of subgroups A and B: sequence conservation provides a structural basis for antigenic relatedness', *J Gen Virol*, 69 (Pt 10), pp. 2623-8.

Johnson, P.R. and Collins, P.L. (1989) 'The 1B (NS2), 1C (NS1) and N proteins of human respiratory syncytial virus (RSV) of antigenic subgroups A and B: sequence conservation and divergence within RSV genomic RNA', *J Gen Virol*, 70 (Pt 6), pp. 1539-47.

Johnson, P.R., Spriggs, M.K., Olmsted, R.A. and Collins, P.L. (1987) 'The G glycoprotein of human respiratory syncytial viruses of subgroups A and B: extensive sequence divergence between antigenically related proteins', *Proc Natl Acad Sci U S A*, 84(16), pp. 5625-9.

Johnson, S., Oliver, C., Prince, G.A., Hemming, V.G., Pfarr, D.S., Wang, S.C., Dormitzer, M., O'Grady, J., Koenig, S., Tamura, J.K., Woods, R., Bansal, G., Couchenour, D., Tsao, E., Hall, W.C. and Young, J.F. (1997) 'Development of a humanized monoclonal antibody (MEDI-493) with potent in vitro and in vivo activity against respiratory syncytial virus', *J Infect Dis*, 176(5), pp. 1215-24.

Johnson, T.R. and Graham, B.S. (1999) 'Secreted respiratory syncytial virus G glycoprotein induces interleukin-5 (IL-5), IL-13, and eosinophilia by an IL-4-independent mechanism', *J Virol*, 73(10), pp. 8485-95.

Johnson, T.R., Hong, S., Van Kaer, L., Koezuka, Y. and Graham, B.S. (2002) 'NK T cells contribute to expansion of CD8(+) T cells and amplification of antiviral immune responses to respiratory syncytial virus', *J Virol*, 76(9), pp. 4294-303.

Junghans, R.P. (1997) 'Finally! The Brambell receptor (FcRB). Mediator of transmission of immunity and protection from catabolism for IgG', *Immunol Res*, 16(1), pp. 29-57.

Kahn, J.S., Schnell, M.J., Buonocore, L. and Rose, J.K. (1999) 'Recombinant vesicular stomatitis virus expressing respiratory syncytial virus (RSV) glycoproteins: RSV fusion protein can mediate infection and cell fusion', *Virology*, 254(1), pp. 81-91.

Kallewaard, N.L., Bowen, A.L. and Crowe, J.E., Jr. (2005) 'Cooperativity of actin and microtubule elements during replication of respiratory syncytial virus', *Virology*, 331(1), pp. 73-81.

Kapikian, A.Z., Mitchell, R.H., Chanock, R.M., Shvedoff, R.A. and Stewart, C.E. (1969) 'An epidemiologic study of altered clinical reactivity to respiratory syncytial (RS) virus infection in children previously vaccinated with an inactivated RS virus vaccine', *Am J Epidemiol*, 89(4), pp. 405-21.

Kaptur, P.E., Rhodes, R.B. and Lyles, D.S. (1991) 'Sequences of the vesicular stomatitis virus matrix protein involved in binding to nucleocapsids', *J Virol*, 65(3), pp. 1057-65.

Karger, A., Schmidt, U. and Buchholz, U.J. (2001) 'Recombinant bovine respiratory syncytial virus with deletions of the G or SH genes: G and F proteins bind heparin', *J Gen Virol*, 82(Pt 3), pp. 631-40.

Karlsson, G.B., Gao, F., Robinson, J., Hahn, B. and Sodroski, J. (1996) 'Increased envelope spike density and stability are not required for the neutralization resistance of primary human immunodeficiency viruses', *J Virol*, 70(9), pp. 6136-42.

Karron, R.A., Buonagurio, D.A., Georgiu, A.F., Whitehead, S.S., Adamus, J.E., Clements-Mann, M.L., Harris, D.O., Randolph, V.B., Udem, S.A., Murphy, B.R. and Sidhu, M.S. (1997) 'Respiratory syncytial virus (RSV) SH and G proteins are not essential for viral replication in vitro: clinical evaluation and molecular characterization of a cold-passaged, attenuated RSV subgroup B mutant', *Proc Natl Acad Sci U S A*, 94(25), pp. 13961-6.

Karron, R.A., Makhene, M., Gay, K., Wilson, M.H., Clements, M.L. and Murphy, B.R. (1996) 'Evaluation of a live attenuated bovine parainfluenza type 3 vaccine in two- to six-month-old infants', *Pediatr Infect Dis J*, 15(8), pp. 650-4.

Karron, R.A., Wright, P.F., Belshe, R.B., Thumar, B., Casey, R., Newman, F., Polack, F.P., Randolph, V.B., Deatly, A., Hackell, J., Gruber, W., Murphy, B.R. and Collins, P.L. (2005) 'Identification of a recombinant live attenuated respiratory syncytial virus

vaccine candidate that is highly attenuated in infants', *J Infect Dis*, 191(7), pp. 1093-104.

Kaul, T.N., Welliver, R.C., Wong, D.T., Udwardia, R.A., Riddlesberger, K. and Ogra, P.L. (1981) 'Secretory antibody response to respiratory syncytial virus infection', *Am J Dis Child*, 135(11), pp. 1013-6.

Kelly, B.T., McCoy, A.J., Spate, K., Miller, S.E., Evans, P.R., Honing, S. and Owen, D.J. (2008) 'A structural explanation for the binding of endocytic dileucine motifs by the AP2 complex', *Nature*, 456(7224), pp. 976-79.

Khattar, S.K., Yunus, A.S., Collins, P.L. and Samal, S.K. (2000) 'Mutational analysis of the bovine respiratory syncytial virus nucleocapsid protein using a minigenome system: mutations that affect encapsidation, RNA synthesis, and interaction with the phosphoprotein', *Virology*, 270(1), pp. 215-28.

Kielian, M. (2006) 'Class II virus membrane fusion proteins', *Virology*, 344(1), pp. 38-47.

Kielian, M. and Rey, F.A. (2006) 'Virus membrane-fusion proteins: more than one way to make a hairpin', *Nat Rev Microbiol*, 4(1), pp. 67-76.

Kim, H.W., Arrobio, J.O., Brandt, C.D., Jeffries, B.C., Pyles, G., Reid, J.L., Chanock, R.M. and Parrott, R.H. (1973) 'Epidemiology of respiratory syncytial virus infection in Washington, D.C. I. Importance of the virus in different respiratory tract disease syndromes and temporal distribution of infection', *Am J Epidemiol*, 98(3), pp. 216-25.

Kim, H.W., Arrobio, J.O., Pyles, G., Brandt, C.D., Camargo, E., Chanock, R.M. and Parrott, R.H. (1971) 'Clinical and immunological response of infants and children to administration of low-temperature adapted respiratory syncytial virus', *Pediatrics*, 48(5), pp. 745-55.

Kim, H.W., Canchola, J.G., Brandt, C.D., Pyles, G., Chanock, R.M., Jensen, K. and Parrott, R.H. (1969) 'Respiratory syncytial virus disease in infants despite prior administration of antigenic inactivated vaccine', *Am J Epidemiol*, 89(4), pp. 422-34.

Klasse, P.J. and Sattentau, Q.J. (2002) 'Occupancy and mechanism in antibody-mediated neutralization of animal viruses', *J Gen Virol*, 83(Pt 9), pp. 2091-108.

Klenk, H.D. and Garten, W. (1994) 'Host cell proteases controlling virus pathogenicity', *Trends Microbiol*, 2(2), pp. 39-43.

Knudson, C.B. and Knudson, W. (1993) 'Hyaluronan-binding proteins in development, tissue homeostasis, and disease', *FASEB J*, 7(13), pp. 1233-41.

Kohlmeier, J.E. and Woodland, D.L. (2009) 'Immunity to respiratory viruses', *Annu Rev Immunol*, 27, pp. 61-82.

Kolokoltsov, A.A., Deniger, D., Fleming, E.H., Roberts, N.J., Jr., Karpilow, J.M. and Davey, R.A. (2007) 'Small interfering RNA profiling reveals key role of clathrin-mediated endocytosis and early endosome formation for infection by respiratory syncytial virus', *J Virol*, 81(14), pp. 7786-800.

Krempl, C., Murphy, B.R. and Collins, P.L. (2002) 'Recombinant respiratory syncytial virus with the G and F genes shifted to the promoter-proximal positions', *J Virol*, 76(23), pp. 11931-42.

Krempl, C.D., Lamirande, E.W. and Collins, P.L. (2005) 'Complete sequence of the RNA genome of pneumonia virus of mice (PVM)', *Virus Genes*, 30(2), pp. 237-49.

Krilov, L.R., Hendry, R.M., Godfrey, E. and McIntosh, K. (1987) 'Respiratory virus infection of peripheral blood monocytes: correlation with ageing of cells and interferon production in vitro', *J Gen Virol*, 68 (Pt 6), pp. 1749-53.

Krishnamurthy, S. and Samal, S.K. (1998) 'Identification of regions of bovine respiratory syncytial virus N protein required for binding to P protein and self-assembly', *J Gen Virol*, 79 (Pt 6), pp. 1399-403.

Krusat, T. and Streckert, H.J. (1997) 'Heparin-dependent attachment of respiratory syncytial virus (RSV) to host cells', *Arch Virol*, 142(6), pp. 1247-54.

Kumaria, R., Iyer, L.R., Hibberd, M.L., Simoes, E.A. and Sugrue, R.J. (2011) 'Whole genome characterization of non-tissue culture adapted HRSV strains in severely infected children', *Virol J*, 8, p. 372.

Kuo, L., Fearn, R. and Collins, P.L. (1996a) 'The structurally diverse intergenic regions of respiratory syncytial virus do not modulate sequential transcription by a dicistronic minigenome', *J Virol*, 70(9), pp. 6143-50.

Kuo, L., Fearn, R. and Collins, P.L. (1997) 'Analysis of the gene start and gene end signals of human respiratory syncytial virus: quasi-templated initiation at position 1 of the encoded mRNA', *J Virol*, 71(7), pp. 4944-53.

Kuo, L., Grosfeld, H., Cristina, J., Hill, M.G. and Collins, P.L. (1996b) 'Effects of mutations in the gene-start and gene-end sequence motifs on transcription of monocistronic and dicistronic minigenomes of respiratory syncytial virus', *J Virol*, 70(10), pp. 6892-901.

Kurt-Jones, E.A., Popova, L., Kwinn, L., Haynes, L.M., Jones, L.P., Tripp, R.A., Walsh, E.E., Freeman, M.W., Golenbock, D.T., Anderson, L.J. and Finberg, R.W.

(2000) 'Pattern recognition receptors TLR4 and CD14 mediate response to respiratory syncytial virus', *Nat Immunol*, 1(5), pp. 398-401.

Kurts, C. (2008) 'Th17 cells: a third subset of CD4+ T effector cells involved in organ-specific autoimmunity', *Nephrol Dial Transplant*, 23(3), pp. 816-9.

Lahti, M., Lofgren, J., Marttila, R., Renko, M., Kilaavuniemi, T., Haataja, R., Ramet, M. and Hallman, M. (2002) 'Surfactant protein D gene polymorphism associated with severe respiratory syncytial virus infection', *Pediatr Res*, 51(6), pp. 696-9.

Lambert, D.M., Barney, S., Lambert, A.L., Guthrie, K., Medinas, R., Davis, D.E., Bucy, T., Erickson, J., Merutka, G. and Petteway Jr, S.R. (1996) 'Peptides from conserved regions of paramyxovirus fusion (F) proteins are potent inhibitors of viral fusion', *Proc Natl Acad Sci U S A*, 93(5), pp. 2186-2191.

Langedijk, J.P., de Groot, B.L., Berendsen, H.J. and van Oirschot, J.T. (1998) 'Structural homology of the central conserved region of the attachment protein G of respiratory syncytial virus with the fourth subdomain of 55-kDa tumor necrosis factor receptor', *Virology*, 243(2), pp. 293-302.

Langedijk, J.P., Meloen, R.H., Taylor, G., Furze, J.M. and van Oirschot, J.T. (1997) 'Antigenic structure of the central conserved region of protein G of bovine respiratory syncytial virus', *J Virol*, 71(5), pp. 4055-61.

Langedijk, J.P., Schaaper, W.M., Meloen, R.H. and van Oirschot, J.T. (1996) 'Proposed three-dimensional model for the attachment protein G of respiratory syncytial virus', *J Gen Virol*, 77 (Pt 6), pp. 1249-57.

Larkin, M.A., Blackshields, G., Brown, N.P., Chenna, R., McGettigan, P.A., McWilliam, H., Valentin, F., Wallace, I.M., Wilm, A., Lopez, R., Thompson, J.D., Gibson, T.J. and Higgins, D.G. (2007) 'Clustal W and Clustal X version 2.0', *Bioinformatics*, 23(21), pp. 2947-8.

Lawless-Delmedico, M.K., Sista, P., Sen, R., Moore, N.C., Antczak, J.B., White, J.M., Greene, R.J., Leanza, K.C., Matthews, T.J. and Lambert, D.M. (2000) 'Heptad-repeat regions of respiratory syncytial virus F1 protein form a six-membered coiled-coil complex', *Biochemistry*, 39(38), pp. 11684-95.

Lechmann, M., Murata, K., Satoi, J., Vergalla, J., Baumert, T.F. and Liang, T.J. (2001) 'Hepatitis C virus-like particles induce virus-specific humoral and cellular immune responses in mice', *Hepatology*, 34(2), pp. 417-23.

Leclair, J.M., Freeman, J., Sullivan, B.F., Crowley, C.M. and Goldmann, D.A. (1987) 'Prevention of nosocomial respiratory syncytial virus infections through compliance with glove and gown isolation precautions', *N Engl J Med*, 317(6), pp. 329-34.

Lee, D.C., Harker, J.A., Tregoning, J.S., Atabani, S.F., Johansson, C., Schwarze, J. and Openshaw, P.J. (2010) 'CD25+ natural regulatory T cells are critical in limiting innate and adaptive immunity and resolving disease following respiratory syncytial virus infection', *J Virol*, 84(17), pp. 8790-8.

Lee, M.S., Greenberg, D.P., Yeh, S.H., Yogev, R., Reisinger, K.S., Ward, J.I., Blatter, M.M., Cho, I., Holmes, S.J., Cordova, J.M., August, M.J., Chen, W., Mehta, H.B., Coelingh, K.L. and Mendelman, P.M. (2001) 'Antibody responses to bovine parainfluenza virus type 3 (PIV3) vaccination and human PIV3 infection in young infants', *J Infect Dis*, 184(7), pp. 909-13.

Legg, J.P., Hussain, I.R., Warner, J.A., Johnston, S.L. and Warner, J.O. (2003) 'Type 1 and type 2 cytokine imbalance in acute respiratory syncytial virus bronchiolitis', *Am J Respir Crit Care Med*, 168(6), pp. 633-9.

Lenard, J. (1996) 'Negative-strand virus M and retrovirus MA proteins: all in a family?', *Virology*, 216(2), pp. 289-98.

LeVine, A.M., Gwozdz, J., Stark, J., Bruno, M., Whitsett, J. and Korfhagen, T. (1999) 'Surfactant protein-A enhances respiratory syncytial virus clearance in vivo', *J Clin Invest*, 103(7), pp. 1015-21.

Levine, S., Klaiber-Franco, R. and Paradiso, P.R. (1987) 'Demonstration that glycoprotein G is the attachment protein of respiratory syncytial virus', *J Gen Virol*, 68 (Pt 9), pp. 2521-4.

Li, B., Wu, F.L., Feng, X.B., Sun, D.K., Cui, Q.Q. and Zhao, Z.X. (2012) '[Changes and the clinical significance of CD4 + CD25 + regulatory T cells and Th17 cells in peripheral blood of infants with respiratory syncytial virus bronchiolitis]', *Xi bao yu fen zi mian yi xue za zhi = Chinese journal of cellular and molecular immunology*, 28(4), pp. 426-428.

Li, D., Jans, D.A., Bardin, P.G., Meanger, J., Mills, J. and Ghildyal, R. (2008) 'Association of respiratory syncytial virus M protein with viral nucleocapsids is mediated by the M2-1 protein', *Journal of Virology*, 82(17), pp. 8863-8870.

Li, Z., Yu, M., Zhang, H., Wang, H.Y. and Wang, L.F. (2005) 'Improved rapid amplification of cDNA ends (RACE) for mapping both the 5' and 3' terminal sequences of paramyxovirus genomes', *J Virol Methods*, 130(1-2), pp. 154-6.

Lima, H.N., Botosso, V.F., Oliveira, D.B., Campos, A.C., Leal, A.L., Silva, T.S., Bosso, P.A., Moraes, C.T., Filho, C.G., Vieira, S.E., Gilio, A.E., Stewien, K.E. and Durigon, E.L. (2012) 'Molecular epidemiology of the SH (small hydrophobic) gene of human respiratory syncytial virus (HRSV), over 2 consecutive years', *Virus Res*, 163(1), pp. 82-6.

- Ling, Z., Tran, K.C. and Teng, M.N. (2009) 'Human respiratory syncytial virus nonstructural protein NS2 antagonizes the activation of beta interferon transcription by interacting with RIG-I', *J Virol*, 83(8), pp. 3734-42.
- Liu, X.S., Liu, W.J., Zhao, K.N., Liu, Y.H., Leggatt, G. and Frazer, I.H. (2002) 'Route of administration of chimeric BPV1 VLP determines the character of the induced immune responses', *Immunol Cell Biol*, 80(1), pp. 21-9.
- Liuzzi, M., Mason, S.W., Cartier, M., Lawetz, C., McCollum, R.S., Dansereau, N., Bolger, G., Lapeyre, N., Gaudette, Y., Lagace, L., Massariol, M.J., Do, F., Whitehead, P., Lamarre, L., Scouten, E., Bordeleau, J., Landry, S., Rancourt, J., Fazal, G. and Simoneau, B. (2005) 'Inhibitors of respiratory syncytial virus replication target cotranscriptional mRNA guanylation by viral RNA-dependent RNA polymerase', *J Virol*, 79(20), pp. 13105-15.
- Lo, M.S., Brazas, R.M. and Holtzman, M.J. (2005) 'Respiratory syncytial virus nonstructural proteins NS1 and NS2 mediate inhibition of Stat2 expression and alpha/beta interferon responsiveness', *J Virol*, 79(14), pp. 9315-9.
- Lofgren, J., Marttila, R., Renko, M., Ramet, M. and Hallman, M. (2010) 'Toll-like receptor 4 Asp299Gly polymorphism in respiratory syncytial virus epidemics', *Pediatr Pulmonol*, 45(7), pp. 687-92.
- Lofgren, J., Ramet, M., Renko, M., Marttila, R. and Hallman, M. (2002) 'Association between surfactant protein A gene locus and severe respiratory syncytial virus infection in infants', *J Infect Dis*, 185(3), pp. 283-9.
- Lopez, J.A., Andreu, D., Carreno, C., Whyte, P., Taylor, G. and Melero, J.A. (1993) 'Conformational constraints of conserved neutralizing epitopes from a major antigenic area of human respiratory syncytial virus fusion glycoprotein', *J Gen Virol*, 74 (Pt 12), pp. 2567-77.
- Lopez, J.A., Bustos, R., Orvell, C., Berois, M., Arbiza, J., Garcia-Barreno, B. and Melero, J.A. (1998) 'Antigenic structure of human respiratory syncytial virus fusion glycoprotein', *J Virol*, 72(8), pp. 6922-8.
- Lopez, J.A., Penas, C., Garcia-Barreno, B., Melero, J.A. and Portela, A. (1990) 'Location of a highly conserved neutralizing epitope in the F glycoprotein of human respiratory syncytial virus', *J Virol*, 64(2), pp. 927-30.
- Lu, B., Ma, C.H., Brazas, R. and Jin, H. (2002) 'The major phosphorylation sites of the respiratory syncytial virus phosphoprotein are dispensable for virus replication in vitro', *J Virol*, 76(21), pp. 10776-84.

Lund, J.M., Alexopoulou, L., Sato, A., Karow, M., Adams, N.C., Gale, N.W., Iwasaki, A. and Flavell, R.A. (2004) 'Recognition of single-stranded RNA viruses by Toll-like receptor 7', *Proc Natl Acad Sci U S A*, 101(15), pp. 5598-603.

Luttick, A., Lin, B., Morton, C., Tucker, S., Bond, S., Draffan, A., Lambert, J., Lim, C., Mitchell, J., Sanford, V., McCarthy, M., Suzich, J., Patel, N. and Richter, B. (2007) 'Characterization of a new class of polycyclic RSV inhibitors', *Antiviral Res*, 74, pp. A1-A97.

MacDonald, N.E., Hall, C.B., Suffin, S.C., Alexson, C., Harris, P.J. and Manning, J.A. (1982) 'Respiratory syncytial viral infection in infants with congenital heart disease', *N Engl J Med*, 307(7), pp. 397-400.

Magro, M., Andreu, D., Gomez-Puertas, P., Melero, J.A. and Palomo, C. (2010) 'Neutralization of human respiratory syncytial virus infectivity by antibodies and low-molecular-weight compounds targeted against the fusion glycoprotein', *J Virol*, 84(16), pp. 7970-82.

Magro, M., Mas, V., Chappell, K., Vazquez, M., Cano, O., Luque, D., Terron, M.C., Melero, J.A. and Palomo, C. (2012) 'Neutralizing antibodies against the preactive form of respiratory syncytial virus fusion protein offer unique possibilities for clinical intervention', *Proc Natl Acad Sci U S A*, 109(8), pp. 3089-94.

Makrides, S.C., Nygren, P.A., Andrews, B., Ford, P.J., Evans, K.S., Hayman, E.G., Adari, H., Uhlen, M. and Toth, C.A. (1996) 'Extended in vivo half-life of human soluble complement receptor type 1 fused to a serum albumin-binding receptor', *J Pharmacol Exp Ther*, 277(1), pp. 534-42.

Malley, R., Vernacchio, L., Devincenzo, J., Ramilo, O., Dennehy, P.H., Meissner, H.C., Gruber, W.C., Jafri, H.S., Sanchez, P.J., Macdonald, K., Montana, J.B., Thompson, C.M. and Ambrosino, D.M. (2000) 'Enzyme-linked immunosorbent assay to assess respiratory syncytial virus concentration and correlate results with inflammatory mediators in tracheal secretions', *Pediatr Infect Dis J*, 19(1), pp. 1-7.

Mallipeddi, S.K., Lupiani, B. and Samal, S.K. (1996) 'Mapping the domains on the phosphoprotein of bovine respiratory syncytial virus required for N-P interaction using a two-hybrid system', *J Gen Virol*, 77 (Pt 5), pp. 1019-23.

Mandelberg, A., Tal, G., Naugolny, L., Cesar, K., Oron, A., Houry, S., Gilad, E. and Somekh, E. (2006) 'Lipopolysaccharide hyporesponsiveness as a risk factor for intensive care unit hospitalization in infants with respiratory syncytial virus bronchiolitis', *Clin Exp Immunol*, 144(1), pp. 48-52.

Marsh, R. (2002) *Genotypic and phenotypic changes in human respiratory syncytial virus on passage in cell culture*. PhD thesis. University of Newcastle upon Tyne.

- Marsh, R., Connor, A., Gias, E. and Toms, G.L. (2007) 'Increased susceptibility of human respiratory syncytial virus to neutralization by anti-fusion protein antibodies on adaptation to replication in cell culture', *J Med Virol*, 79(6), pp. 829-37.
- Martin-Gallardo, A., Fien, K.A., Hu, B.T., Farley, J.F., Seid, R., Collins, P.L., Hildreth, S.W. and Paradiso, P.R. (1991) 'Expression of the F glycoprotein gene from human respiratory syncytial virus in Escherichia coli: mapping of a fusion inhibiting epitope', *Virology*, 184(1), pp. 428-32.
- Martinez, I., Dopazo, J. and Melero, J.A. (1997) 'Antigenic structure of the human respiratory syncytial virus G glycoprotein and relevance of hypermutation events for the generation of antigenic variants', *J Gen Virol*, 78 (Pt 10), pp. 2419-29.
- Martinez, I. and Melero, J.A. (1998) 'Enhanced neutralization of human respiratory syncytial virus by mixtures of monoclonal antibodies to the attachment (G) glycoprotein', *J Gen Virol*, 79 (Pt 9), pp. 2215-20.
- Martinez, I. and Melero, J.A. (2000) 'Binding of human respiratory syncytial virus to cells: implication of sulfated cell surface proteoglycans', *J Gen Virol*, 81(Pt 11), pp. 2715-22.
- Marty, A., Meanger, J., Mills, J., Shields, B. and Ghildyal, R. (2004) 'Association of matrix protein of respiratory syncytial virus with the host cell membrane of infected cells', *Archives of Virology*, 149(1), pp. 199-210.
- Mason, S.W., Aberg, E., Lawetz, C., DeLong, R., Whitehead, P. and Liuzzi, M. (2003) 'Interaction between human respiratory syncytial virus (RSV) M2-1 and P proteins is required for reconstitution of M2-1-dependent RSV minigenome activity', *J Virol*, 77(19), pp. 10670-6.
- Matthews, J.M., Young, T.F., Tucker, S.P. and Mackay, J.P. (2000) 'The core of the respiratory syncytial virus fusion protein is a trimeric coiled coil', *J Virol*, 74(13), pp. 5911-20.
- Mazumder, B. and Barik, S. (1994) 'Requirement of casein kinase II-mediated phosphorylation for the transcriptional activity of human respiratory syncytial viral phosphoprotein P: transdominant negative phenotype of phosphorylation-defective P mutants', *Virology*, 205(1), pp. 104-11.
- McGinnes, L.W., Gravel, K.A., Finberg, R.W., Kurt-Jones, E.A., Massare, M.J., Smith, G., Schmidt, M.R. and Morrison, T.G. (2011) 'Assembly and immunological properties of Newcastle disease virus-like particles containing the respiratory syncytial virus F and G proteins', *J Virol*, 85(1), pp. 366-77.

McGivern, D.R., Collins, P.L. and Fearn, R. (2005) 'Identification of internal sequences in the 3' leader region of human respiratory syncytial virus that enhance transcription and confer replication processivity', *J Virol*, 79(4), pp. 2449-60.

McIntosh, K., Masters, H.B., Orr, I., Chao, R.K. and Barkin, R.M. (1978) 'The immunologic response to infection with respiratory syncytial virus in infants', *J Infect Dis*, 138(1), pp. 24-32.

McKimm-Breschkin, J.L. (2004) 'A simplified plaque assay for respiratory syncytial virus--direct visualization of plaques without immunostaining', *J Virol Methods*, 120(1), pp. 113-7.

McLellan, J.S., Yang, Y., Graham, B.S. and Kwong, P.D. (2011) 'Structure of respiratory syncytial virus fusion glycoprotein in the postfusion conformation reveals preservation of neutralizing epitopes', *J Virol*, 85(15), pp. 7788-96.

McMahon, H.T. and Boucrot, E. (2011) 'Molecular mechanism and physiological functions of clathrin-mediated endocytosis', *Nat Rev Mol Cell Biol*, 12(8), pp. 517-33.

McNamara, P.S. and Smyth, R.L. (2002) 'The pathogenesis of respiratory syncytial virus disease in childhood', *Br Med Bull*, 61, pp. 13-28.

MedImmune (2010) *Medimmune discontinues development of motavizumab for rsv prophylaxis indication*. Available at: <http://pressroom.medimmune.com/press-releases/2010/12/21/medimmune-discontinues-development-of-motavizumab-for-rsv-prophylaxis-indication/> (Accessed: 17 February 2012).

MedImmune LLC (2008a) *A Randomized, Double-Blind, Placebo-Controlled Study to Evaluate Safety of MEDI-559 in Healthy 1 to <24 Month-Old Children*. Available at: <http://www.clinicaltrials.gov/ct2/show/nct00767416?term=medi-559&rank=1> (Accessed: 7 May 2012).

MedImmune LLC (2008b) *A Study to Evaluate the Safety, Tolerability, Immunogenicity and Vaccine-like Viral Shedding of MEDI-534, Against Respiratory Syncytial Virus (RSV) and Parainfluenza Virus Type 3 (PIV3), in Healthy 6 to < 24 Month-Old Children and in 2 Month Old Infants*. Available at: <http://clinicaltrials.gov/ct2/show/NCT00686075> (Accessed: 7 May 2012).

Mekseepalard, C., Toms, G.L. and Routledge, E.G. (2006) 'Protection of mice against Human respiratory syncytial virus by wild-type and aglycosyl mouse-human chimaeric IgG antibodies to subgroup-conserved epitopes on the G glycoprotein', *J Gen Virol*, 87(Pt 5), pp. 1267-73.

Melero, J.A. (2007) 'Molecular biology of human respiratory syncytial virus', in P. A., Cane (ed.) *Perspectives in medical virology: respiratory syncytial virus*. 1st edn. Oxford, United Kingdom: Elsevier, pp. 1-42.

- Melero, J.A., Garcia-Barreno, B., Martinez, I., Pringle, C.R. and Cane, P.A. (1997) 'Antigenic structure, evolution and immunobiology of human respiratory syncytial virus attachment (G) protein', *J Gen Virol*, 78 (Pt 10), pp. 2411-8.
- Mellman, I. (1996) 'Endocytosis and molecular sorting', *Annu Rev Cell Dev Biol*, 12, pp. 575-625.
- Mercer, J. and Helenius, A. (2009) 'Virus entry by macropinocytosis', *Nat Cell Biol*, 11(5), pp. 510-20.
- Mercer, J., Schelhaas, M. and Helenius, A. (2010) 'Virus entry by endocytosis', *Annu Rev Biochem*, 79, pp. 803-33.
- Merolla, R., Rebert, N.A., Tsiviste, P.T., Hoffmann, S.P. and Panuska, J.R. (1995) 'Respiratory syncytial virus replication in human lung epithelial cells: inhibition by tumor necrosis factor alpha and interferon beta', *Am J Respir Crit Care Med*, 152(4 Pt 1), pp. 1358-66.
- Merz, D.C., Scheid, A. and Choppin, P.W. (1980) 'Importance of antibodies to the fusion glycoprotein of paramyxoviruses in the prevention of spread of infection', *J Exp Med*, 151(2), pp. 275-88.
- Meurman, O., Ruuskanen, O., Sarkkinen, H., Hanninen, P. and Halonen, P. (1984) 'Immunoglobulin class-specific antibody response in respiratory syncytial virus infection measured by enzyme immunoassay', *J Med Virol*, 14(1), pp. 67-72.
- Mills, J.t., Van Kirk, J.E., Wright, P.F. and Chanock, R.M. (1971) 'Experimental respiratory syncytial virus infection of adults. Possible mechanisms of resistance to infection and illness', *J Immunol*, 107(1), pp. 123-30.
- Mink, M.A., Stec, D.S. and Collins, P.L. (1991) 'Nucleotide sequences of the 3' leader and 5' trailer regions of human respiratory syncytial virus genomic RNA', *Virology*, 185(2), pp. 615-24.
- Moler, F.W., Steinhart, C.M., Ohmit, S.E. and Stidham, G.L. (1996) 'Effectiveness of ribavirin in otherwise well infants with respiratory syncytial virus-associated respiratory failure. Pediatric Critical Study Group', *J Pediatr*, 128(3), pp. 422-8.
- Money, V.A., McPhee, H.K., Mosely, J.A., Sanderson, J.M. and Yeo, R.P. (2009) 'Surface features of a Mononegavirales matrix protein indicate sites of membrane interaction', *Proc Natl Acad Sci U S A*, 106(11), pp. 4441-6.
- Morgan, L.A., Routledge, E.G., Willcocks, M.M., Samson, A.C., Scott, R. and Toms, G.L. (1987) 'Strain variation of respiratory syncytial virus', *J Gen Virol*, 68 (Pt 11), pp. 2781-8.

Morris, J.A., Blount, R.E., Jr. and Savage, R.E. (1956) 'Recovery of cytopathogenic agent from chimpanzees with coryza', *Proc Soc Exp Biol Med*, 92(3), pp. 544-9.

Morton, C.J., Cameron, R., Lawrence, L.J., Lin, B., Lowe, M., Luttick, A., Mason, A., McKimm-Breschkin, J., Parker, M.W., Ryan, J., Smout, M., Sullivan, J., Tucker, S.P. and Young, P.R. (2003) 'Structural characterization of respiratory syncytial virus fusion inhibitor escape mutants: homology model of the F protein and a syncytium formation assay', *Virology*, 311(2), pp. 275-88.

Moudy, R.M., Harmon, S.B., Sullender, W.M. and Wertz, G.W. (2003) 'Variations in transcription termination signals of human respiratory syncytial virus clinical isolates affect gene expression', *Virology*, 313(1), pp. 250-60.

Moudy, R.M., Sullender, W.M. and Wertz, G.W. (2004) 'Variations in intergenic region sequences of Human respiratory syncytial virus clinical isolates: analysis of effects on transcriptional regulation', *Virology*, 327(1), pp. 121-33.

Mufson, M.A., Levine, H.D., Wasil, R.E., Mocega-Gonzalez, H.E. and Krause, H.E. (1973) 'Epidemiology of respiratory syncytial virus infection among infants and children in Chicago', *Am J Epidemiol*, 98(2), pp. 88-95.

Mufson, M.A., Orvell, C., Rafnar, B. and Norrby, E. (1985) 'Two distinct subtypes of human respiratory syncytial virus', *J Gen Virol*, 66 (Pt 10), pp. 2111-24.

Munoz, F.M., Piedra, P.A. and Glezen, W.P. (2003) 'Safety and immunogenicity of respiratory syncytial virus purified fusion protein-2 vaccine in pregnant women', *Vaccine*, 21(24), pp. 3465-7.

Munoz, J.L., McCarthy, C.A., Clark, M.E. and Hall, C.B. (1991) 'Respiratory syncytial virus infection in C57BL/6 mice: clearance of virus from the lungs with virus-specific cytotoxic T cells', *J Virol*, 65(8), pp. 4494-7.

Murawski, M.R., McGinnes, L.W., Finberg, R.W., Kurt-Jones, E.A., Massare, M.J., Smith, G., Heaton, P.M., Fraire, A.E. and Morrison, T.G. (2010) 'Newcastle disease virus-like particles containing respiratory syncytial virus G protein induced protection in BALB/c mice, with no evidence of immunopathology', *J Virol*, 84(2), pp. 1110-23.

Murphy, B.R., Alling, D.W., Snyder, M.H., Walsh, E.E., Prince, G.A., Chanock, R.M., Hemming, V.G., Rodriguez, W.J., Kim, H.W., Graham, B.S. and et al. (1986) 'Effect of age and preexisting antibody on serum antibody response of infants and children to the F and G glycoproteins during respiratory syncytial virus infection', *J Clin Microbiol*, 24(5), pp. 894-8.

Murphy, B.R., Olmsted, R.A., Collins, P.L., Chanock, R.M. and Prince, G.A. (1988) 'Passive transfer of respiratory syncytial virus (RSV) antiserum suppresses the immune

response to the RSV fusion (F) and large (G) glycoproteins expressed by recombinant vaccinia viruses', *J Virol*, 62(10), pp. 3907-10.

Murphy, L.B., Loney, C., Murray, J., Bhella, D., Ashton, P. and Yeo, R.P. (2003) 'Investigations into the amino-terminal domain of the respiratory syncytial virus nucleocapsid protein reveal elements important for nucleocapsid formation and interaction with the phosphoprotein', *Virology*, 307(1), pp. 143-53.

Musiyenko, A., Bitko, V. and Barik, S. (2007) 'RNAi-dependent and -independent antiviral phenotypes of chromosomally integrated shRNA clones: role of VASP in respiratory syncytial virus growth', *J Mol Med (Berl)*, 85(7), pp. 745-52.

Nair, H., Nokes, D.J., Gessner, B.D., Dherani, M., Madhi, S.A., Singleton, R.J., O'Brien, K.L., Roca, A., Wright, P.F., Bruce, N., Chandran, A., Theodoratou, E., Sutanto, A., Sedyaningsih, E.R., Ngama, M., Munywoki, P.K., Kartasasmita, C., Simoes, E.A., Rudan, I., Weber, M.W. and Campbell, H. (2010) 'Global burden of acute lower respiratory infections due to respiratory syncytial virus in young children: a systematic review and meta-analysis', *Lancet*, 375(9725), pp. 1545-55.

Nandi, P.K., Van Jaarsveld, P.P., Lippoldt, R.E. and Edelhoch, H. (1981) 'Effect of basic compounds on the polymerization of clathrin', *Biochemistry*, 20(23), pp. 6706-10.

Naval, J., Pinol, J., Rebordosa, X., Serra-Hartmann, X., Perez-Pons, J.A. and Querol, E. (1997) 'Expression in Escherichia coli and purification of soluble forms of the F protein of bovine respiratory syncytial virus', *Protein Expr Purif*, 9(2), pp. 288-94.

Navas, L., Wang, E., de Carvalho, V. and Robinson, J. (1992) 'Improved outcome of respiratory syncytial virus infection in a high-risk hospitalized population of Canadian children. Pediatric Investigators Collaborative Network on Infections in Canada', *J Pediatr*, 121(3), pp. 348-54.

Neilson, K.A. and Yunis, E.J. (1990) 'Demonstration of respiratory syncytial virus in an autopsy series', *Pediatr Pathol*, 10(4), pp. 491-502.

Nguyen, T.N., Power, U.F., Robert, A., Haeuw, J.F., Helffer, K., Perez, A., Asin, M.A., Corvaia, N. and Libon, C. (2012) 'The respiratory syncytial virus g protein conserved domain induces a persistent and protective antibody response in rodents', *PLoS ONE*, 7(3), p. e34331.

Nichols, B. (2003) 'Caveosomes and endocytosis of lipid rafts', *J Cell Sci*, 116(Pt 23), pp. 4707-14.

Noad, R. and Roy, P. (2003) 'Virus-like particles as immunogens', *Trends Microbiol*, 11(9), pp. 438-44.

Norrby, E., Marusyk, H. and Orvell, C. (1970) 'Morphogenesis of respiratory syncytial virus in a green monkey kidney cell line (Vero)', *J Virol*, 6(2), pp. 237-42.

Nussbaum, O. and Loyter, A. (1987) 'Quantitative determination of virus-membrane fusion events. Fusion of influenza virions with plasma membranes and membranes of endocytic vesicles in living cultured cells', *FEBS Lett*, 221(1), pp. 61-7.

Nygren, P.A., Eliasson, M., Abrahmsén, L., Uhlén, M. and Palmcrantz, E. (1988) 'Analysis and use of the serum albumin binding domains of streptococcal protein G', *Journal of molecular recognition : JMR*, 1(2), pp. 69-74.

O'Brien, W.A., Mao, S.H., Cao, Y. and Moore, J.P. (1994) 'Macrophage-tropic and T-cell line-adapted chimeric strains of human immunodeficiency virus type 1 differ in their susceptibilities to neutralization by soluble CD4 at different temperatures', *J Virol*, 68(8), pp. 5264-9.

O'Donnell, R. (2009) 'Features of respiratory syncytial virus', *Paediatrics and Child Health*, 19(1), pp. 43-47.

Ogilvie, M.M., Vathenen, A.S., Radford, M., Codd, J. and Key, S. (1981) 'Maternal antibody and respiratory syncytial virus infection in infancy', *J Med Virol*, 7(4), pp. 263-71.

Ogino, T., Kobayashi, M., Iwama, M. and Mizumoto, K. (2005) 'Sendai virus RNA-dependent RNA polymerase L protein catalyzes cap methylation of virus-specific mRNA', *J Biol Chem*, 280(6), pp. 4429-35.

Ogra, P.L. (2004) 'Respiratory syncytial virus: the virus, the disease and the immune response', *Paediatr Respir Rev*, 5 Suppl A, pp. S119-26.

Okiro, E.A., White, L.J., Ngama, M., Cane, P.A., Medley, G.F. and Nokes, D.J. (2010) 'Duration of shedding of respiratory syncytial virus in a community study of Kenyan children', *BMC Infect Dis*, 10, p. 15.

Olmsted, R.A., Elango, N., Prince, G.A., Murphy, B.R., Johnson, P.R., Moss, B., Chanock, R.M. and Collins, P.L. (1986) 'Expression of the F glycoprotein of respiratory syncytial virus by a recombinant vaccinia virus: comparison of the individual contributions of the F and G glycoproteins to host immunity', *Proc Natl Acad Sci U S A*, 83(19), pp. 7462-6.

Olszewska, W. and Openshaw, P. (2009) 'Emerging drugs for respiratory syncytial virus infection', *Expert Opin Emerg Drugs*, 14(2), pp. 207-17.

Oomens, A.G., Bevis, K.P. and Wertz, G.W. (2006) 'The cytoplasmic tail of the human respiratory syncytial virus F protein plays critical roles in cellular localization of the F protein and infectious progeny production', *J Virol*, 80(21), pp. 10465-77.

Ostlund, M.R., Lindell, A.T., Stenler, S., Riedel, H.M., Wirtgart, B.Z. and Grillner, L. (2008) 'Molecular epidemiology and genetic variability of respiratory syncytial virus (RSV) in Stockholm, 2002-2003', *J Med Virol*, 80(1), pp. 159-67.

Outlaw, M.C. and Dimmock, N.J. (1990) 'Mechanisms of neutralization of influenza virus on mouse tracheal epithelial cells by mouse monoclonal polymeric IgA and polyclonal IgM directed against the viral haemagglutinin', *J Gen Virol*, 71 (Pt 1), pp. 69-76.

Panuska, J.R., Hertz, M.I., Taraf, H., Villani, A. and Cirino, N.M. (1992) 'Respiratory syncytial virus infection of alveolar macrophages in adult transplant patients', *Am Rev Respir Dis*, 145(4 Pt 1), pp. 934-9.

Panuska, J.R., Merolla, R., Rebert, N.A., Hoffmann, S.P., Tsivitse, P., Cirino, N.M., Silverman, R.H. and Rankin, J.A. (1995) 'Respiratory syncytial virus induces interleukin-10 by human alveolar macrophages. Suppression of early cytokine production and implications for incomplete immunity', *J Clin Invest*, 96(5), pp. 2445-53.

Paradiso, P.R., Hildreth, S.W., Hogerman, D.A., Speelman, D.J., Lewin, E.B., Oren, J. and Smith, D.H. (1994) 'Safety and immunogenicity of a subunit respiratory syncytial virus vaccine in children 24 to 48 months old', *Pediatr Infect Dis J*, 13(9), pp. 792-8.

Parton, R.G. and Simons, K. (2007) 'The multiple faces of caveolae', *Nat Rev Mol Cell Biol*, 8(3), pp. 185-94.

Parton, R.G., Way, M., Zorzi, N. and Stang, E. (1997) 'Caveolin-3 associates with developing T-tubules during muscle differentiation', *J Cell Biol*, 136(1), pp. 137-54.

Parveen, S., Sullender, W.M., Fowler, K., Lefkowitz, E.J., Kapoor, S.K. and Broor, S. (2006) 'Genetic variability in the G protein gene of group A and B respiratory syncytial viruses from India', *J Clin Microbiol*, 44(9), pp. 3055-64.

Pasonen-Seppanen, S., Hyttinen, J.M., Rilla, K., Jokela, T., Noble, P.W., Tammi, M. and Tammi, R. (2012) 'Role of CD44 in the organization of keratinocyte pericellular hyaluronan', *Histochem Cell Biol*, 137(1), pp. 107-20.

Patel, H., Platt, R., Lozano, J.M. and Wang, E.E. (2004) 'Glucocorticoids for acute viral bronchiolitis in infants and young children', *Cochrane Database Syst Rev*, (3), p. CD004878.

Pelkmans, L. and Helenius, A. (2002) 'Endocytosis via caveolae', *Traffic*, 3(5), pp. 311-20.

Peret, T.C., Hall, C.B., Hammond, G.W., Piedra, P.A., Storch, G.A., Sullender, W.M., Tsou, C. and Anderson, L.J. (2000) 'Circulation patterns of group A and B human

respiratory syncytial virus genotypes in 5 communities in North America', *J Infect Dis*, 181(6), pp. 1891-6.

Perez, M., Garcia-Barreno, B., Melero, J.A., Carrasco, L. and Guinea, R. (1997) 'Membrane permeability changes induced in *Escherichia coli* by the SH protein of human respiratory syncytial virus', *Virology*, 235(2), pp. 342-51.

Perkins, S.M., Webb, D.L., Torrance, S.A., El Saleeby, C., Harrison, L.M., Aitken, J.A., Patel, A. and DeVincenzo, J.P. (2005) 'Comparison of a real-time reverse transcriptase PCR assay and a culture technique for quantitative assessment of viral load in children naturally infected with respiratory syncytial virus', *J Clin Microbiol*, 43(5), pp. 2356-62.

Piedra, P.A., Cron, S.G., Jewell, A., Hamblett, N., McBride, R., Palacio, M.A., Ginsberg, R., Oermann, C.M. and Hiatt, P.W. (2003) 'Immunogenicity of a new purified fusion protein vaccine to respiratory syncytial virus: a multi-center trial in children with cystic fibrosis', *Vaccine*, 21(19-20), pp. 2448-60.

Piedra, P.A., Glezen, W.P., Kasel, J.A., Welliver, R.C., Jewel, A.M., Rayford, Y., Hogerman, D.A., Hildreth, S.W. and Paradiso, P.R. (1995) 'Safety and immunogenicity of the PFP vaccine against respiratory syncytial virus (RSV): the western blot assay aids in distinguishing immune responses of the PFP vaccine from RSV infection', *Vaccine*, 13(12), pp. 1095-101.

Piedra, P.A., Grace, S., Jewell, A., Spinelli, S., Bunting, D., Hogerman, D.A., Malinoski, F. and Hiatt, P.W. (1996) 'Purified fusion protein vaccine protects against lower respiratory tract illness during respiratory syncytial virus season in children with cystic fibrosis', *Pediatr Infect Dis J*, 15(1), pp. 23-31.

Platt, J. and Bucknall, R.A. (1985) 'The disinfection of respiratory syncytial virus by isopropanol and a chlorhexidine-detergent handwash', *J Hosp Infect*, 6(1), pp. 89-94.

Poch, O., Blumberg, B.M., Bougueleret, L. and Tordo, N. (1990) 'Sequence comparison of five polymerases (L proteins) of unsegmented negative-strand RNA viruses: theoretical assignment of functional domains', *J Gen Virol*, 71 (Pt 5), pp. 1153-62.

Polack, F.P., Irusta, P.M., Hoffman, S.J., Schiatti, M.P., Melendi, G.A., Delgado, M.F., Laham, F.R., Thumar, B., Hendry, R.M., Melero, J.A., Karron, R.A., Collins, P.L. and Kleeberger, S.R. (2005) 'The cysteine-rich region of respiratory syncytial virus attachment protein inhibits innate immunity elicited by the virus and endotoxin', *Proc Natl Acad Sci U S A*, 102(25), pp. 8996-9001.

Possee, R.D., Schild, G.C. and Dimmock, N.J. (1982) 'Studies on the mechanism of neutralization of influenza virus by antibody: evidence that neutralizing antibody (anti-haemagglutinin) inactivates influenza virus in vivo by inhibiting virion transcriptase activity', *J Gen Virol*, 58(Pt 2), pp. 373-86.

Powell, A.K., Yates, E.A., Fernig, D.G. and Turnbull, J.E. (2004) 'Interactions of heparin/heparan sulfate with proteins: appraisal of structural factors and experimental approaches', *Glycobiology*, 14(4), pp. 17R-30R.

Powell, M.F. 28 (1993) 'Chapter 30. Peptide Stability in Drug Development: in vitro Peptide Degradation in Plasma and Serum' *Annual Reports in Medicinal Chemistry*. pp. 285-294. Available at: <http://www.scopus.com/inward/record.url?eid=2-s2.0-77956836899&partnerID=40&md5=e6c245b4bc3c02a2ae22a8491d2c75ff>

Power, U.F., Nguyen, T.N., Rietveld, E., de Swart, R.L., Groen, J., Osterhaus, A.D., de Groot, R., Corvaia, N., Beck, A., Bouveret-Le-Cam, N. and Bonnefoy, J.Y. (2001) 'Safety and immunogenicity of a novel recombinant subunit respiratory syncytial virus vaccine (BBG2Na) in healthy young adults', *J Infect Dis*, 184(11), pp. 1456-60.

Power, U.F., Plotnicky-Gilquin, H., Huss, T., Robert, A., Trudel, M., Stahl, S., Uhlen, M., Nguyen, T.N. and Binz, H. (1997) 'Induction of protective immunity in rodents by vaccination with a prokaryotically expressed recombinant fusion protein containing a respiratory syncytial virus G protein fragment', *Virology*, 230(2), pp. 155-66.

Pribul, P.K., Harker, J., Wang, B., Wang, H., Tregoning, J.S., Schwarze, J. and Openshaw, P.J. (2008) 'Alveolar macrophages are a major determinant of early responses to viral lung infection but do not influence subsequent disease development', *J Virol*, 82(9), pp. 4441-8.

Punnonen, E.L., Ryhanen, K. and Marjomaki, V.S. (1998) 'At reduced temperature, endocytic membrane traffic is blocked in multivesicular carrier endosomes in rat cardiac myocytes', *Eur J Cell Biol*, 75(4), pp. 344-52.

Ramaswamy, M., Shi, L., Monick, M.M., Hunninghake, G.W. and Look, D.C. (2004) 'Specific inhibition of type I interferon signal transduction by respiratory syncytial virus', *Am J Respir Cell Mol Biol*, 30(6), pp. 893-900.

Randolph, A.G. and Wang, E.E. (1996) 'Ribavirin for respiratory syncytial virus lower respiratory tract infection. A systematic overview', *Arch Pediatr Adolesc Med*, 150(9), pp. 942-7.

Rassa, J.C., Wilson, G.M., Brewer, G.A. and Parks, G.D. (2000) 'Spacing constraints on reinitiation of paramyxovirus transcription: the gene end U tract acts as a spacer to separate gene end from gene start sites', *Virology*, 274(2), pp. 438-49.

Rebuffo-Scheer, C., Bose, M., He, J., Khaja, S., Ulatowski, M., Beck, E.T., Fan, J., Kumar, S., Nelson, M.I. and Henrickson, K.J. (2011) 'Whole genome sequencing and evolutionary analysis of human respiratory syncytial virus A and B from Milwaukee, WI 1998-2010', *PLoS ONE*, 6(10), p. e25468.

Reed, L.J. and Muench, H. (1938) 'A simple method of estimating fifty percent endpoints', *Am. J. Hygiene*, 27, pp. 493-497.

Reeves, J.D., Gallo, S.A., Ahmad, N., Miamidian, J.L., Harvey, P.E., Sharron, M., Pohlmann, S., Sfakianos, J.N., Derdeyn, C.A., Blumenthal, R., Hunter, E. and Doms, R.W. (2002) 'Sensitivity of HIV-1 to entry inhibitors correlates with envelope/coreceptor affinity, receptor density, and fusion kinetics', *Proc Natl Acad Sci U S A*, 99(25), pp. 16249-54.

Reiche, J. and Schweiger, B. (2009) 'Genetic variability of group A human respiratory syncytial virus strains circulating in Germany from 1998 to 2007', *J Clin Microbiol*, 47(6), pp. 1800-10.

Reimers, K., Buchholz, K. and Werchau, H. (2005) 'Respiratory syncytial virus M2-1 protein induces the activation of nuclear factor kappa B', *Virology*, 331(2), pp. 260-8.

Ren, J., Liu, T., Pang, L., Li, K., Garofalo, R.P., Casola, A. and Bao, X. (2011) 'A novel mechanism for the inhibition of interferon regulatory factor-3-dependent gene expression by human respiratory syncytial virus NS1 protein', *J Gen Virol*, 92(Pt 9), pp. 2153-9.

Resch, B. and Paes, B. (2011) 'Are late preterm infants as susceptible to RSV infection as full term infants?', *Early Human Development*, 87(SUPPL.), pp. S47-S49.

Rixon, H.W., Brown, C., Brown, G. and Sugrue, R.J. (2002) 'Multiple glycosylated forms of the respiratory syncytial virus fusion protein are expressed in virus-infected cells', *J Gen Virol*, 83(Pt 1), pp. 61-6.

Roberts, N.J., Jr., Hiscott, J. and Signs, D.J. (1992) 'The limited role of the human interferon system response to respiratory syncytial virus challenge: analysis and comparison to influenza virus challenge', *Microb Pathog*, 12(6), pp. 409-14.

Roberts, S.R., Compans, R.W. and Wertz, G.W. (1995) 'Respiratory syncytial virus matures at the apical surfaces of polarized epithelial cells', *J Virol*, 69(4), pp. 2667-73.

Roberts, S.R., Lichtenstein, D., Ball, L.A. and Wertz, G.W. (1994) 'The membrane-associated and secreted forms of the respiratory syncytial virus attachment glycoprotein G are synthesized from alternative initiation codons', *J Virol*, 68(7), pp. 4538-46.

Roca, A., Abacassamo, F., Loscertales, M.P., Quinto, L., Gomez-Olive, X., Fenwick, F., Saiz, J.C., Toms, G. and Alonso, P.L. (2002) 'Prevalence of respiratory syncytial virus IgG antibodies in infants living in a rural area of Mozambique', *J Med Virol*, 67(4), pp. 616-23.

Roca, A., Loscertales, M.P., Quinto, L., Perez-Brena, P., Vaz, N., Alonso, P.L. and Saiz, J.C. (2001) 'Genetic variability among group A and B respiratory syncytial viruses

in Mozambique: identification of a new cluster of group B isolates', *J Gen Virol*, 82(Pt 1), pp. 103-11.

Rodriguez, L., Cuesta, I., Asenjo, A. and Villanueva, N. (2004) 'Human respiratory syncytial virus matrix protein is an RNA-binding protein: binding properties, location and identity of the RNA contact residues', *J Gen Virol*, 85(Pt 3), pp. 709-19.

Romagnani, S. (1992) 'Induction of TH1 and TH2 responses: a key role for the 'natural' immune response?', *Immunol Today*, 13(10), pp. 379-81.

Roman, M., Calhoun, W.J., Hinton, K.L., Avendano, L.F., Simon, V., Escobar, A.M., Gaggero, A. and Diaz, P.V. (1997) 'Respiratory syncytial virus infection in infants is associated with predominant Th-2-like response', *Am J Respir Crit Care Med*, 156(1), pp. 190-5.

Roymans, D., De Bondt, H.L., Arnoult, E., Geluykens, P., Gevers, T., Van Ginderen, M., Verheyen, N., Kim, H., Willebrords, R., Bonfanti, J.F., Bruinzeel, W., Cummings, M.D., van Vlijmen, H. and Andries, K. (2010) 'Binding of a potent small-molecule inhibitor of six-helix bundle formation requires interactions with both heptad-repeats of the RSV fusion protein', *Proc Natl Acad Sci U S A*, 107(1), pp. 308-13.

Rozen, S. and Skaletsky, H. (2000) 'Primer3 on the WWW for general users and for biologist programmers', in S., Krawetz and S., Misener (eds.) *Bioinformatics methods and protocols: Methods in molecular biology*. Totowa, NJ: Humana Press, pp. 365-386.

Rueda, P., Delgado, T., Portela, A., Melero, J.A. and Garcia-Barreno, B. (1991) 'Premature stop codons in the G glycoprotein of human respiratory syncytial viruses resistant to neutralization by monoclonal antibodies', *J Virol*, 65(6), pp. 3374-8.

Ruiz-Arguello, M.B., Gonzalez-Reyes, L., Calder, L.J., Palomo, C., Martin, D., Saiz, M.J., Garcia-Barreno, B., Skehel, J.J. and Melero, J.A. (2002) 'Effect of proteolytic processing at two distinct sites on shape and aggregation of an anchorless fusion protein of human respiratory syncytial virus and fate of the intervening segment', *Virology*, 298(2), pp. 317-26.

Ruiz-Arguello, M.B., Martin, D., Wharton, S.A., Calder, L.J., Martin, S.R., Cano, O., Calero, M., Garcia-Barreno, B., Skehel, J.J. and Melero, J.A. (2004) 'Thermostability of the human respiratory syncytial virus fusion protein before and after activation: implications for the membrane-fusion mechanism', *J Gen Virol*, 85(Pt 12), pp. 3677-87.

Russell, C.J., Jardetzky, T.S. and Lamb, R.A. (2001) 'Membrane fusion machines of paramyxoviruses: capture of intermediates of fusion', *Embo J*, 20(15), pp. 4024-34.

Ruuskanen, O. and Ogra, P.L. (1993) 'Respiratory syncytial virus', *Curr Probl Pediatr*, 23(2), pp. 50-79.

Sambrook J, F.E.a.M.T. (1989) *Molecular cloning: A laboratory manual*. New York: Cold Spring Harbour Laboratory Press.

Sanchez-Seco, M.P., Navarro, J., Martinez, R. and Villanueva, N. (1995) 'C-terminal phosphorylation of human respiratory syncytial virus P protein occurs mainly at serine residue 232', *J Gen Virol*, 76 (Pt 2), pp. 425-30.

Satake, M., Coligan, J.E., Elango, N., Norrby, E. and Venkatesan, S. (1985) 'Respiratory syncytial virus envelope glycoprotein (G) has a novel structure', *Nucleic Acids Res*, 13(21), pp. 7795-812.

Sato, M., Saito, R., Sakai, T., Sano, Y., Nishikawa, M., Sasaki, A., Shobugawa, Y., Gejyo, F. and Suzuki, H. (2005) 'Molecular epidemiology of respiratory syncytial virus infections among children with acute respiratory symptoms in a community over three seasons', *J Clin Microbiol*, 43(1), pp. 36-40.

Schnell, M.J. and Conzelmann, K.K. (1995) 'Polymerase activity of in vitro mutated rabies virus L protein', *Virology*, 214(2), pp. 522-30.

Schwarze, J. and Schauer, U. (2004) 'Enhanced virulence, airway inflammation and impaired lung function induced by respiratory syncytial virus deficient in secreted G protein', *Thorax*, 59(6), pp. 517-21.

Scopes, G.E., Watt, P.J. and Lambden, P.R. (1990) 'Identification of a linear epitope on the fusion glycoprotein of respiratory syncytial virus', *J Gen Virol*, 71 (Pt 1), pp. 53-9.

Scott, R. and Gardner, P.S. (1974) 'The local antibody response to R.S. virus infection in the respiratory tract', *Journal of Hygiene*, 72(1), pp. 111-120.

Scott, R., Scott, M. and Toms, G.L. (1981) 'Cellular and antibody response to respiratory syncytial (RS) virus in human colostrum, maternal blood, and cord blood', *J Med Virol*, 8(1), pp. 55-66.

Sedlik, C., Dridi, A., Deriaud, E., Saron, M.F., Rueda, P., Sarraseca, J., Casal, J.I. and Leclerc, C. (1999) 'Intranasal delivery of recombinant parvovirus-like particles elicits cytotoxic T-cell and neutralizing antibody responses', *J Virol*, 73(4), pp. 2739-44.

Semple, M.G., Dankert, H.M., Ebrahimi, B., Correia, J.B., Booth, J.A., Stewart, J.P., Smyth, R.L. and Hart, C.A. (2007) 'Severe respiratory syncytial virus bronchiolitis in infants is associated with reduced airway interferon gamma and substance P', *PLoS One*, 2(10), p. e1038.

Siber, G.R., Leombruno, D., Leszczynski, J., McIver, J., Bodkin, D., Gonin, R., Thompson, C.M., Walsh, E.E., Piedra, P.A., Hemming, V.G. and et al. (1994) 'Comparison of antibody concentrations and protective activity of respiratory syncytial

virus immune globulin and conventional immune globulin', *J Infect Dis*, 169(6), pp. 1368-73.

Simoes, E.A. (1999) 'Respiratory syncytial virus infection', *Lancet*, 354(9181), pp. 847-52.

Simoes, E.A., Sondheimer, H.M., Top, F.H., Jr., Meissner, H.C., Welliver, R.C., Kramer, A.A. and Groothuis, J.R. (1998) 'Respiratory syncytial virus immune globulin for prophylaxis against respiratory syncytial virus disease in infants and children with congenital heart disease. The Cardiac Study Group', *J Pediatr*, 133(4), pp. 492-9.

Sjolander, A., Nygren, P.A., Stahl, S., Berzins, K., Uhlen, M., Perlmann, P. and Andersson, R. (1997) 'The serum albumin-binding region of streptococcal protein G: a bacterial fusion partner with carrier-related properties', *J Immunol Methods*, 201(1), pp. 115-23.

Sleat, D.E. and Banerjee, A.K. (1993) 'Transcriptional activity and mutational analysis of recombinant vesicular stomatitis virus RNA polymerase', *J Virol*, 67(3), pp. 1334-9.

Smit, J.J., Lindell, D.M., Boon, L., Kool, M., Lambrecht, B.N. and Lukacs, N.W. (2008) 'The balance between plasmacytoid DC versus conventional DC determines pulmonary immunity to virus infections', *PLoS ONE*, 3(3), p. e1720.

Smit, J.J., Rudd, B.D. and Lukacs, N.W. (2006) 'Plasmacytoid dendritic cells inhibit pulmonary immunopathology and promote clearance of respiratory syncytial virus', *J Exp Med*, 203(5), pp. 1153-9.

Smith, B.J., Lawrence, M.C. and Colman, P.M. (2002) 'Modelling the structure of the fusion protein from human respiratory syncytial virus', *Protein Eng*, 15(5), pp. 365-71.

Smith, E.C., Popa, A., Chang, A., Masante, C. and Dutch, R.E. (2009) 'Viral entry mechanisms: the increasing diversity of paramyxovirus entry', *FEBS J*, 276(24), pp. 7217-27.

Smith, T.J., Olson, N.H., Cheng, R.H., Liu, H., Chase, E.S., Lee, W.M., Leippe, D.M., Mosser, A.G., Rueckert, R.R. and Baker, T.S. (1993) 'Structure of human rhinovirus complexed with Fab fragments from a neutralizing antibody', *J Virol*, 67(3), pp. 1148-58.

Smyth, R.L., Mobbs, K.J., O'Hea, U., Ashby, D. and Hart, C.A. (2002) 'Respiratory syncytial virus bronchiolitis: disease severity, interleukin-8, and virus genotype', *Pediatr Pulmonol*, 33(5), pp. 339-46.

Spann, K.M., Tran, K.C., Chi, B., Rabin, R.L. and Collins, P.L. (2004) 'Suppression of the induction of alpha, beta, and lambda interferons by the NS1 and NS2 proteins of

human respiratory syncytial virus in human epithelial cells and macrophages [corrected]', *J Virol*, 78(8), pp. 4363-9.

Spann, K.M., Tran, K.C. and Collins, P.L. (2005) 'Effects of nonstructural proteins NS1 and NS2 of human respiratory syncytial virus on interferon regulatory factor 3, NF-kappaB, and proinflammatory cytokines', *J Virol*, 79(9), pp. 5353-62.

Spence, L. and Barratt, N. (1968) 'Respiratory syncytial virus associated with acute respiratory infections in Trinidadian patients', *Am J Epidemiol*, 88(2), pp. 257-66.

Spriggs, M.K., Olmsted, R.A., Venkatesan, S., Coligan, J.E. and Collins, P.L. (1986) 'Fusion glycoprotein of human parainfluenza virus type 3: nucleotide sequence of the gene, direct identification of the cleavage-activation site, and comparison with other paramyxoviruses', *Virology*, 152(1), pp. 241-51.

Srinivasakumar, N., Ogra, P.L. and Flanagan, T.D. (1991) 'Characteristics of fusion of respiratory syncytial virus with HEp-2 cells as measured by R18 fluorescence dequenching assay', *J Virol*, 65(8), pp. 4063-9.

Stan, R.V. (2002) 'Structure and function of endothelial caveolae', *Microsc Res Tech*, 57(5), pp. 350-64.

Stensballe, L.G., Ravn, H., Kristensen, K., Meakins, T., Aaby, P. and Simoes, E.A. (2009) 'Seasonal variation of maternally derived respiratory syncytial virus antibodies and association with infant hospitalizations for respiratory syncytial virus', *J Pediatr*, 154(2), pp. 296-8.

Stone-Hulslander, J. and Morrison, T.G. (1997) 'Detection of an interaction between the HN and F proteins in Newcastle disease virus-infected cells', *J Virol*, 71(9), pp. 6287-95.

Subcommittee on diagnosis and management of bronchiolitis (2006) 'Diagnosis and management of bronchiolitis', *Pediatrics*, 118(4), pp. 1774-93.

Sudo, K., Miyazaki, Y., Kojima, N., Kobayashi, M., Suzuki, H., Shintani, M. and Shimizu, Y. (2005) 'YM-53403, a unique anti-respiratory syncytial virus agent with a novel mechanism of action', *Antiviral Res*, 65(2), pp. 125-31.

Sullender, W.M. (2000) 'Respiratory syncytial virus genetic and antigenic diversity', *Clin Microbiol Rev*, 13(1), pp. 1-15.

Sullender, W.M., Anderson, K. and Wertz, G.W. (1990) 'The respiratory syncytial virus subgroup B attachment glycoprotein: analysis of sequence, expression from a recombinant vector, and evaluation as an immunogen against homologous and heterologous subgroup virus challenge', *Virology*, 178(1), pp. 195-203.

- Sullender, W.M., Mufson, M.A., Anderson, L.J. and Wertz, G.W. (1991) 'Genetic diversity of the attachment protein of subgroup B respiratory syncytial viruses', *J Virol*, 65(10), pp. 5425-34.
- Sullender, W.M., Sun, L. and Anderson, L.J. (1993) 'Analysis of respiratory syncytial virus genetic variability with amplified cDNAs', *J Clin Microbiol*, 31(5), pp. 1224-31.
- Sullivan, N., Sun, Y., Li, J., Hofmann, W. and Sodroski, J. (1995) 'Replicative function and neutralization sensitivity of envelope glycoproteins from primary and T-cell line-passaged human immunodeficiency virus type 1 isolates', *J Virol*, 69(7), pp. 4413-22.
- Sung, R.Y., Yin, J., Oppenheimer, S.J., Tam, J.S. and Lau, J. (1993) 'Treatment of respiratory syncytial virus infection with recombinant interferon alfa-2a', *Arch Dis Child*, 69(4), pp. 440-2.
- Sutherland, K.A., Collins, P.L. and Peeples, M.E. (2001) 'Synergistic effects of gene-end signal mutations and the M2-1 protein on transcription termination by respiratory syncytial virus', *Virology*, 288(2), pp. 295-307.
- Svensson, U. and Persson, R. (1984) 'Entry of adenovirus 2 into HeLa cells', *J Virol*, 51(3), pp. 687-94.
- Swanson, K.A., Settembre, E.C., Shaw, C.A., Dey, A.K., Rappuoli, R., Mandl, C.W., Dormitzer, P.R. and Carfi, A. (2011) 'Structural basis for immunization with postfusion respiratory syncytial virus fusion F glycoprotein (RSV F) to elicit high neutralizing antibody titers', *Proc Natl Acad Sci U S A*, 108(23), pp. 9619-24.
- Swedan, S., Andrews, J., Majumdar, T., Musiyenko, A. and Barik, S. (2011) 'Multiple functional domains and complexes of the two nonstructural proteins of human respiratory syncytial virus contribute to interferon suppression and cellular location', *J Virol*, 85(19), pp. 10090-100.
- Swedan, S., Musiyenko, A. and Barik, S. (2009) 'Respiratory syncytial virus nonstructural proteins decrease levels of multiple members of the cellular interferon pathways', *J Virol*, 83(19), pp. 9682-93.
- Swenson, D.L., Warfield, K.L., Negley, D.L., Schmaljohn, A., Aman, M.J. and Bavari, S. (2005) 'Virus-like particles exhibit potential as a pan-filovirus vaccine for both Ebola and Marburg viral infections', *Vaccine*, 23(23), pp. 3033-42.
- Tal, G., Mandelberg, A., Dalal, I., Cesar, K., Somekh, E., Tal, A., Oron, A., Itskovich, S., Ballin, A., Houry, S., Beigelman, A., Lider, O., Rechavi, G. and Amariglio, N. (2004) 'Association between common Toll-like receptor 4 mutations and severe respiratory syncytial virus disease', *J Infect Dis*, 189(11), pp. 2057-63.

Tang, R.S., MacPhail, M., Schickli, J.H., Kaur, J., Robinson, C.L., Lawlor, H.A., Guzzetta, J.M., Spaete, R.R. and Haller, A.A. (2004) 'Parainfluenza virus type 3 expressing the native or soluble fusion (F) Protein of Respiratory Syncytial Virus (RSV) confers protection from RSV infection in African green monkeys', *J Virol*, 78(20), pp. 11198-207.

Tang, R.S., Nguyen, N., Zhou, H. and Jin, H. (2002) 'Clustered charge-to-alanine mutagenesis of human respiratory syncytial virus L polymerase generates temperature-sensitive viruses', *Virology*, 302(1), pp. 207-16.

Tang, R.S., Schickli, J.H., MacPhail, M., Fernandes, F., Bicha, L., Spaete, J., Fouchier, R.A., Osterhaus, A.D., Spaete, R. and Haller, A.A. (2003) 'Effects of human metapneumovirus and respiratory syncytial virus antigen insertion in two 3' proximal genome positions of bovine/human parainfluenza virus type 3 on virus replication and immunogenicity', *J Virol*, 77(20), pp. 10819-28.

Tawar, R.G., Duquerroy, S., Vonnrhein, C., Varela, P.F., Damier-Piolle, L., Castagne, N., MacLellan, K., Bedouelle, H., Bricogne, G., Bhella, D., Eleouet, J.F. and Rey, F.A. (2009) 'Crystal structure of a nucleocapsid-like nucleoprotein-RNA complex of respiratory syncytial virus', *Science*, 326(5957), pp. 1279-83.

Taylor, G., Stott, E.J., Bew, M., Fernie, B.F., Cote, P.J., Collins, A.P., Hughes, M. and Jebbett, J. (1984) 'Monoclonal antibodies protect against respiratory syncytial virus infection in mice', *Immunology*, 52(1), pp. 137-42.

Taylor, G., Stott, E.J., Furze, J., Ford, J. and Sopp, P. (1992) 'Protective epitopes on the fusion protein of respiratory syncytial virus recognized by murine and bovine monoclonal antibodies', *J Gen Virol*, 73 (Pt 9), pp. 2217-23.

Taylor, G., Thomas, L.H., Furze, J.M., Cook, R.S., Wyld, S.G., Lerch, R., Hardy, R. and Wertz, G.W. (1997) 'Recombinant vaccinia viruses expressing the F, G or N, but not the M2, protein of bovine respiratory syncytial virus (BRSV) induce resistance to BRSV challenge in the calf and protect against the development of pneumonic lesions', *J Gen Virol*, 78 (Pt 12), pp. 3195-206.

Taylor, H.P., Armstrong, S.J. and Dimmock, N.J. (1987) 'Quantitative relationships between an influenza virus and neutralizing antibody', *Virology*, 159(2), pp. 288-98.

Taylor, H.P. and Dimmock, N.J. (1985) 'Mechanisms of neutralization of influenza virus by IgM', *J Gen Virol*, 66 (Pt 4), pp. 903-7.

Tayyari, F., Marchant, D., Moraes, T.J., Duan, W., Mastrangelo, P. and Hegele, R.G. (2011) 'Identification of nucleolin as a cellular receptor for human respiratory syncytial virus', *Nat Med*, 17(9), pp. 1132-5.

Techaarpornkul, S., Barretto, N. and Peeples, M.E. (2001) 'Functional analysis of recombinant respiratory syncytial virus deletion mutants lacking the small hydrophobic and/or attachment glycoprotein gene', *J Virol*, 75(15), pp. 6825-34.

Techaarpornkul, S., Collins, P.L. and Peeples, M.E. (2002) 'Respiratory syncytial virus with the fusion protein as its only viral glycoprotein is less dependent on cellular glycosaminoglycans for attachment than complete virus', *Virology*, 294(2), pp. 296-304.

Teng, M.N. and Collins, P.L. (1998) 'Identification of the respiratory syncytial virus proteins required for formation and passage of helper-dependent infectious particles', *J Virol*, 72(7), pp. 5707-16.

Teng, M.N. and Collins, P.L. (1999) 'Altered growth characteristics of recombinant respiratory syncytial viruses which do not produce NS2 protein', *J Virol*, 73(1), pp. 466-73.

Teng, M.N. and Collins, P.L. (2002) 'The central conserved cystine noose of the attachment G protein of human respiratory syncytial virus is not required for efficient viral infection in vitro or in vivo', *J Virol*, 76(12), pp. 6164-71.

Teng, M.N., Whitehead, S.S., Bermingham, A., St Claire, M., Elkins, W.R., Murphy, B.R. and Collins, P.L. (2000) 'Recombinant respiratory syncytial virus that does not express the NS1 or M2-2 protein is highly attenuated and immunogenic in chimpanzees', *J Virol*, 74(19), pp. 9317-21.

Teng, M.N., Whitehead, S.S. and Collins, P.L. (2001) 'Contribution of the respiratory syncytial virus G glycoprotein and its secreted and membrane-bound forms to virus replication in vitro and in vivo', *Virology*, 289(2), pp. 283-96.

The antiviral drug advisory committee of the Food and Drug Administration (2010) *Summary Minutes of the Antiviral Drugs Advisory Committee*. Silver Spring, Maryland. [Online]. Available at: <http://www.fda.gov/downloads/AdvisoryCommittees/CommitteesMeetingMaterials/Drugs/AntiviralDrugsAdvisoryCommittee/UCM241510.pdf> (Accessed: 17 February 2012).

The IMPact-RSV Study Group (1998) 'Palivizumab, a humanized respiratory syncytial virus monoclonal antibody, reduces hospitalization from respiratory syncytial virus infection in high-risk infants. The IMPact-RSV Study Group', *Pediatrics*, 102(3 Pt 1), pp. 531-7.

The PREVENT Study Group (1997) 'Reduction of respiratory syncytial virus hospitalization among premature infants and infants with bronchopulmonary dysplasia using respiratory syncytial virus immune globulin prophylaxis. The PREVENT Study Group', *Pediatrics*, 99(1), pp. 93-9.

Thomas, S.J., Nisalak, A., Anderson, K.B., Libraty, D.H., Kalayanarooj, S., Vaughn, D.W., Putnak, R., Gibbons, R.V., Jarman, R. and Endy, T.P. (2009) 'Dengue plaque reduction neutralization test (PRNT) in primary and secondary dengue virus infections: How alterations in assay conditions impact performance', *Am J Trop Med Hyg*, 81(5), pp. 825-33.

Tillett, D., Burns, B.P. and Neilan, B.A. (2000) 'Optimized rapid amplification of cDNA ends (RACE) for mapping bacterial mRNA transcripts', *Biotechniques*, 28(3), pp. 448, 450, 452-3, 456.

Toiron, C., Lopez, J.A., Rivas, G., Andreu, D., Melero, J.A. and Bruix, M. (1996) 'Conformational studies of a short linear peptide corresponding to a major conserved neutralizing epitope of human respiratory syncytial virus fusion glycoprotein', *Biopolymers*, 39(4), pp. 537-48.

Toms, G.L., Quinn, R. and Robinson, J.W. (1996) 'Undetectable IgE responses after respiratory syncytial virus infection', *Arch Dis Child*, 74(2), pp. 126-30.

Toms, G.L., Webb, M.S., Milner, P.D., Milner, A.D., Routledge, E.G., Scott, R., Stokes, G.M., Swarbrick, A. and Taylor, C.E. (1989) 'IgG and IgM antibodies to viral glycoproteins in respiratory syncytial virus infections of graded severity', *Arch Dis Child*, 64(12), pp. 1661-5.

Tran, T.L., Castagne, N., Dubosclard, V., Noinville, S., Koch, E., Moudjou, M., Henry, C., Bernard, J., Yeo, R.P. and Eleouet, J.F. (2009) 'The respiratory syncytial virus M2-1 protein forms tetramers and interacts with RNA and P in a competitive manner', *J Virol*, 83(13), pp. 6363-74.

Tripp, R.A., Jones, L.P., Haynes, L.M., Zheng, H., Murphy, P.M. and Anderson, L.J. (2001) 'CX3C chemokine mimicry by respiratory syncytial virus G glycoprotein', *Nat Immunol*, 2(8), pp. 732-8.

Tripp, R.A., Moore, D., Barskey, A.t., Jones, L., Moscattiello, C., Keyserling, H. and Anderson, L.J. (2002) 'Peripheral blood mononuclear cells from infants hospitalized because of respiratory syncytial virus infection express T helper-1 and T helper-2 cytokines and CC chemokine messenger RNA', *J Infect Dis*, 185(10), pp. 1388-94.

Tristram, D.A., Welliver, R.C., Mohar, C.K., Hogerman, D.A., Hildreth, S.W. and Paradiso, P. (1993) 'Immunogenicity and safety of respiratory syncytial virus subunit vaccine in seropositive children 18-36 months old', *J Infect Dis*, 167(1), pp. 191-5.

Trudel, M., Nadon, F., Seguin, C., Dionne, G. and Lacroix, M. (1987a) 'Identification of a synthetic peptide as part of a major neutralization epitope of respiratory syncytial virus', *J Gen Virol*, 68 (Pt 9), pp. 2273-80.

Trudel, M., Nadon, F., Seguin, C., Payment, P. and Talbot, P.J. (1987b) 'Respiratory syncytial virus fusion glycoprotein: further characterization of a major epitope involved in virus neutralization', *Can J Microbiol*, 33(10), pp. 933-8.

Valarcher, J.F., Furze, J., Wyld, S., Cook, R., Conzelmann, K.K. and Taylor, G. (2003) 'Role of alpha/beta interferons in the attenuation and immunogenicity of recombinant bovine respiratory syncytial viruses lacking NS proteins', *J Virol*, 77(15), pp. 8426-39.

Vardas, E., Blaauw, D. and McAnerney, J. (1999) 'The epidemiology of respiratory syncytial virus (RSV) infections in South African children', *S Afr Med J*, 89(10), pp. 1079-84.

Venter, M., Madhi, S.A., Tiemessen, C.T. and Schoub, B.D. (2001) 'Genetic diversity and molecular epidemiology of respiratory syncytial virus over four consecutive seasons in South Africa: identification of new subgroup A and B genotypes', *J Gen Virol*, 82(Pt 9), pp. 2117-24.

Ventre, K. and Randolph, A. (2004) 'Ribavirin for respiratory syncytial virus infection of the lower respiratory tract in infants and young children', *Cochrane Database Syst Rev*, (4), p. CD000181.

Volovitz, B., Welliver, R.C., De Castro, G., Krystofik, D.A. and Ogra, P.L. (1988) 'The release of leukotrienes in the respiratory tract during infection with respiratory syncytial virus: role in obstructive airway disease', *Pediatr Res*, 24(4), pp. 504-7.

Walsh, E.E., Cote, P.J., Fernie, B.F., Schlesinger, J.J. and Brandriss, M.W. (1986) 'Analysis of the respiratory syncytial virus fusion protein using monoclonal and polyclonal antibodies', *J Gen Virol*, 67 (Pt 3), pp. 505-13.

Walsh, E.E. and Hruska, J. (1983) 'Monoclonal antibodies to respiratory syncytial virus proteins: identification of the fusion protein', *J Virol*, 47(1), pp. 171-7.

Walsh, E.E., Schlesinger, J.J. and Brandriss, M.W. (1984) 'Protection from respiratory syncytial virus infection in cotton rats by passive transfer of monoclonal antibodies', *Infect Immun*, 43(2), pp. 756-8.

Wang, H., Peters, N. and Schwarze, J. (2006) 'Plasmacytoid dendritic cells limit viral replication, pulmonary inflammation, and airway hyperresponsiveness in respiratory syncytial virus infection', *J Immunol*, 177(9), pp. 6263-70.

Wang, L.H., Rothberg, K.G. and Anderson, R.G. (1993) 'Mis-assembly of clathrin lattices on endosomes reveals a regulatory switch for coated pit formation', *J Cell Biol*, 123(5), pp. 1107-17.

Weber, E., Humbert, B., Streckert, H.J. and Werchau, H. (1995) 'Nonstructural protein 2 (NS2) of respiratory syncytial virus (RSV) detected by an antipeptide serum', *Respiration*, 62(1), pp. 27-33.

Welliver, R.C., Kaul, T.N., Putnam, T.I., Sun, M., Riddlesberger, K. and Ogra, P.L. (1980) 'The antibody response to primary and secondary infection with respiratory syncytial virus: kinetics of class-specific responses', *J Pediatr*, 96(5), pp. 808-13.

Welliver, R.C., Sr. (2008) 'The immune response to respiratory syncytial virus infection: friend or foe?', *Clin Rev Allergy Immunol*, 34(2), pp. 163-73.

Welliver, R.C., Wong, D.T., Sun, M., Middleton, E., Jr., Vaughan, R.S. and Ogra, P.L. (1981) 'The development of respiratory syncytial virus-specific IgE and the release of histamine in nasopharyngeal secretions after infection', *N Engl J Med*, 305(15), pp. 841-6.

Welliver, T.P., Garofalo, R.P., Hosakote, Y., Hintz, K.H., Avendano, L., Sanchez, K., Velozo, L., Jafri, H., Chavez-Bueno, S., Ogra, P.L., McKinney, L., Reed, J.L. and Welliver, R.C., Sr. (2007) 'Severe human lower respiratory tract illness caused by respiratory syncytial virus and influenza virus is characterized by the absence of pulmonary cytotoxic lymphocyte responses', *J Infect Dis*, 195(8), pp. 1126-36.

Welsh, S.H. (2010) *Mechanisms of human respiratory syncytial virus (hRSV) resistance to Palivizumab*. PhD thesis. University of Newcastle upon Tyne.

Werling, D., Hope, J.C., Chaplin, P., Collins, R.A., Taylor, G. and Howard, C.J. (1999) 'Involvement of caveolae in the uptake of respiratory syncytial virus antigen by dendritic cells', *J Leukoc Biol*, 66(1), pp. 50-8.

Wertz, G.W., Collins, P.L., Huang, Y., Gruber, C., Levine, S. and Ball, L.A. (1985) 'Nucleotide sequence of the G protein gene of human respiratory syncytial virus reveals an unusual type of viral membrane protein', *Proc Natl Acad Sci U S A*, 82(12), pp. 4075-9.

Wertz, G.W., Krieger, M. and Ball, L.A. (1989) 'Structure and cell surface maturation of the attachment glycoprotein of human respiratory syncytial virus in a cell line deficient in O glycosylation', *J Virol*, 63(11), pp. 4767-76.

Wertz, G.W. and Moudy, R.M. (2004) 'Antigenic and genetic variation in human respiratory syncytial virus', *Pediatr Infect Dis J*, 23(1 Suppl), pp. S19-24.

West, W.H., Lounsbach, G.R., Bourgeois, C., Robinson, J.W., Carter, M.J., Crompton, S., Duhindan, N., Yazici, Z.A. and Toms, G.L. (1994) 'Biological activity, binding site and affinity of monoclonal antibodies to the fusion protein of respiratory syncytial virus', *J Gen Virol*, 75 (Pt 10), pp. 2813-9.

Whimbey, E., Couch, R.B., Englund, J.A., Andreeff, M., Goodrich, J.M., Raad, II, Lewis, V., Mirza, N., Luna, M.A., Baxter, B. and et al. (1995) 'Respiratory syncytial virus pneumonia in hospitalized adult patients with leukemia', *Clin Infect Dis*, 21(2), pp. 376-9.

Whitehead, S.S., Bukreyev, A., Teng, M.N., Firestone, C.Y., St Claire, M., Elkins, W.R., Collins, P.L. and Murphy, B.R. (1999a) 'Recombinant respiratory syncytial virus bearing a deletion of either the NS2 or SH gene is attenuated in chimpanzees', *J Virol*, 73(4), pp. 3438-42.

Whitehead, S.S., Firestone, C.Y., Karron, R.A., Crowe, J.E., Jr., Elkins, W.R., Collins, P.L. and Murphy, B.R. (1999b) 'Addition of a missense mutation present in the L gene of respiratory syncytial virus (RSV) cpts530/1030 to RSV vaccine candidate cpts248/404 increases its attenuation and temperature sensitivity', *J Virol*, 73(2), pp. 871-7.

WHO (2009) *Acute respiratory infections*. Available at: http://www.who.int/vaccine_research/diseases/ari/en/index2.html (Accessed: 1 June 2012).

Wild, C., Greenwell, T. and Matthews, T. (1993) 'A synthetic peptide from HIV-1 gp41 is a potent inhibitor of virus-mediated cell-cell fusion', *AIDS Res Hum Retroviruses*, 9(11), pp. 1051-3.

Wild, C., Oas, T., McDanal, C., Bolognesi, D. and Matthews, T. (1992) 'A synthetic peptide inhibitor of human immunodeficiency virus replication: correlation between solution structure and viral inhibition', *Proc Natl Acad Sci U S A*, 89(21), pp. 10537-41.

Wilson, R.L., Fuentes, S.M., Wang, P., Taddeo, E.C., Klatt, A., Henderson, A.J. and He, B. (2006) 'Function of small hydrophobic proteins of paramyxovirus', *J Virol*, 80(4), pp. 1700-9.

Worthington, M.T., Amann, B.T., Nathans, D. and Berg, J.M. (1996) 'Metal binding properties and secondary structure of the zinc-binding domain of Nup475', *Proc Natl Acad Sci U S A*, 93(24), pp. 13754-9.

Wright, P.F., Belshe, R.B., Kim, H.W., Van Voris, L.P. and Chanock, R.M. (1982) 'Administration of a highly attenuated, live respiratory syncytial virus vaccine to adults and children', *Infect Immun*, 37(1), pp. 397-400.

Wright, P.F., Gruber, W.C., Peters, M., Reed, G., Zhu, Y., Robinson, F., Coleman-Dockery, S. and Graham, B.S. (2002) 'Illness severity, viral shedding, and antibody responses in infants hospitalized with bronchiolitis caused by respiratory syncytial virus', *J Infect Dis*, 185(8), pp. 1011-8.

Wright, P.F., Karron, R.A., Belshe, R.B., Shi, J.R., Randolph, V.B., Collins, P.L., O'Shea, A.F., Gruber, W.C. and Murphy, B.R. (2007) 'The absence of enhanced disease with wild type respiratory syncytial virus infection occurring after receipt of live, attenuated, respiratory syncytial virus vaccines', *Vaccine*, 25(42), pp. 7372-8.

Wright, P.F., Karron, R.A., Belshe, R.B., Thompson, J., Crowe, J.E., Jr., Boyce, T.G., Halburnt, L.L., Reed, G.W., Whitehead, S.S., Anderson, E.L., Wittek, A.E., Casey, R., Eichelberger, M., Thumar, B., Randolph, V.B., Udem, S.A., Chanock, R.M. and Murphy, B.R. (2000) 'Evaluation of a live, cold-passaged, temperature-sensitive, respiratory syncytial virus vaccine candidate in infancy', *J Infect Dis*, 182(5), pp. 1331-42.

Wright, P.F., Shinozaki, T., Fleet, W., Sell, S.H., Thompson, J. and Karzon, D.T. (1976) 'Evaluation of a live, attenuated respiratory syncytial virus vaccine in infants', *J Pediatr*, 88(6), pp. 931-6.

Wrin, T., Loh, T.P., Vennari, J.C., Schuitemaker, H. and Nunberg, J.H. (1995) 'Adaptation to persistent growth in the H9 cell line renders a primary isolate of human immunodeficiency virus type 1 sensitive to neutralization by vaccine sera', *J Virol*, 69(1), pp. 39-48.

Wu, H., Pfarr, D.S., Johnson, S., Brewah, Y.A., Woods, R.M., Patel, N.K., White, W.I., Young, J.F. and Kiener, P.A. (2007) 'Development of motavizumab, an ultra-potent antibody for the prevention of respiratory syncytial virus infection in the upper and lower respiratory tract', *J Mol Biol*, 368(3), pp. 652-65.

Wu, H., Pfarr, D.S., Losonsky, G.A. and Kiener, P.A. (2008) 'Immunoprophylaxis of RSV infection: advancing from RSV-IGIV to palivizumab and motavizumab', *Curr Top Microbiol Immunol*, 317, pp. 103-23.

Wu, H., Pfarr, D.S., Tang, Y., An, L.L., Patel, N.K., Watkins, J.D., Huse, W.D., Kiener, P.A. and Young, J.F. (2005) 'Ultra-potent antibodies against respiratory syncytial virus: effects of binding kinetics and binding valence on viral neutralization', *J Mol Biol*, 350(1), pp. 126-44.

Yu, Q., Hardy, R.W. and Wertz, G.W. (1995) 'Functional cDNA clones of the human respiratory syncytial (RS) virus N, P, and L proteins support replication of RS virus genomic RNA analogs and define minimal trans-acting requirements for RNA replication', *J Virol*, 69(4), pp. 2412-9.

Yunus, A.S., Jackson, T.P., Crisafi, K., Burimski, I., Kilgore, N.R., Zoumplis, D., Allaway, G.P., Wild, C.T. and Salzwedel, K. (2010) 'Elevated temperature triggers human respiratory syncytial virus F protein six-helix bundle formation', *Virology*, 396(2), pp. 226-37.

Zhang, L., Peeples, M.E., Boucher, R.C., Collins, P.L. and Pickles, R.J. (2002) 'Respiratory syncytial virus infection of human airway epithelial cells is polarized,

specific to ciliated cells, and without obvious cytopathology', *J Virol*, 76(11), pp. 5654-66.

Zhao, X., Chen, F.P., Megaw, A.G. and Sullender, W.M. (2004a) 'Variable resistance to palivizumab in cotton rats by respiratory syncytial virus mutants', *Journal of Infectious Diseases*, 190(11), pp. 1941-1946.

Zhao, X., Chen, F.P. and Sullender, W.M. (2004b) 'Respiratory syncytial virus escape mutant derived in vitro resists palivizumab prophylaxis in cotton rats', *Virology*, 318(2), pp. 608-612.

Zhao, X., Singh, M., Malashkevich, V.N. and Kim, P.S. (2000) 'Structural characterization of the human respiratory syncytial virus fusion protein core', *Proc Natl Acad Sci U S A*, 97(26), pp. 14172-7.

Zhu, Q., McAuliffe, J.M., Patel, N.K., Palmer-Hill, F.J., Yang, C.F., Liang, B., Su, L., Zhu, W., Wachter, L., Wilson, S., MacGill, R.S., Krishnan, S., McCarthy, M.P., Losonsky, G.A. and Suzich, J.A. (2011) 'Analysis of respiratory syncytial virus preclinical and clinical variants resistant to neutralization by monoclonal antibodies palivizumab and/or motavizumab', *J Infect Dis*, 203(5), pp. 674-82.

Zimmer, G., Budz, L. and Herrler, G. (2001) 'Proteolytic activation of respiratory syncytial virus fusion protein. Cleavage at two furin consensus sequences', *J Biol Chem*, 276(34), pp. 31642-50.